THE MINOR PLANET BULLETIN

BULLETIN OF THE MINOR PLANETS SECTION OF THE ASSOCIATION OF LUNAR AND PLANETARY OBSERVERS

VOLUME 48, NUMBER 2, A.D. 2021 APRIL-JUNE 99.

ROTATION PERIOD DETERMINATION FOR ASTEROID 665 SABINE

Nick Sioulas
NOAK Observatory (L02)
Stavraki Ioannina, Greece
nsioulas@hotmail.com

(Received: 2020 Dec 7)

Photometric observations of the main-belt asteroid 665 Sabine were conducted from the NOAK Observatory, in Greece in order to determine its synodic rotation period. The results are: P = 4.299 ± 0.004 h, A = 0.33 mag.

All observations were performed at the NOAK Observatory, Ioannina Greece (MPC-International Astronomical Union code L02), using a 0.25-m Newtonian Skywatcher optical tube operating at f/4.7. The optical tube is mounted on NEQ6 Skywatcher robotic mount and equipped with ATIK 460exm CCD camera. It is a high Quantum Efficiency CCD. No filters used so as to optimize the signal-to-noise. Exposure time for all the images was 2 minutes. The camera was binned at 1×1. The image scale after 1×1 binning was 0.78 arcsec/pixel and the field of view 35.77 × 28.61 arcmin. In these fields, the asteroid and five comparison stars were measured for differential photometry.

All images were reduced in the standard manner using nightly flatfield files as well as dark-current and bias images. Photometric measurements and lightcurve analysis were performed using *MPO Canopus* (version 10.8.1.1; Warner, 2019). The Cartes Du Ciel was used as the planetarium software with the most recent ephemerides downloaded from the Minor Planet Center (2020) and Artemis Capture was used for image capture.

665 Sabine (A908 OE) was discovered by German astronomer Wilhelm Lorenz on July 22, 1908 at Heidelberg. It is an outer main-belt asteroid with a semi-major axis of 3.144 AU, eccentricity 0.172, inclination 14.753°, and an orbital period of 5.58 years. Its absolute magnitude is H = 8.7 (JPL, 2020). The period analysis shows a solution for the rotational period of P = 4.299 ± 0.004 h with an amplitude A = 0.33 ± 0.03 mag, which is close to previously published results in the asteroid lightcurve database of 4.294 h (LCDB; Warner et al., 2009).

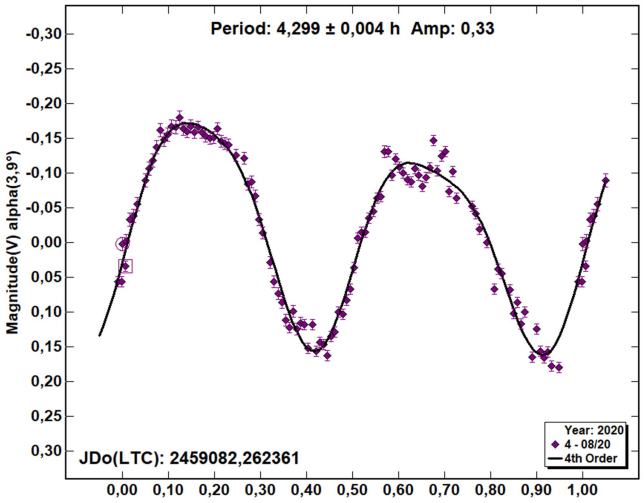

References

Harris, A.W.; Young, J.W.; Scaltriti, F.; Zappala, V. (1984). "Lightcurves and phase relations of the asteroids 82 Alkmene and 444 Gyptis." *Icarus* **57**, 251-258.

JPL (2020). Small Body Database Browser. *https://ssd.jpl.nasa.gov*

MPC (2020). Database Search. *https://minorplanetcenter.net/db_search/*

Warner, B.D.; Harris, A.W.; Pravec, P. (2009). "The Asteroid Lightcurve Database." *Icarus* **202**, 134-146. Updated 2019 Aug. *http://www.minorplanet.info/lightcurvedatabase.html*

Warner, B.D. (2019). MPO Software, MPO Canopus v10.8.1.1. Bdw Publishing. *http://minorplanetobserver.com*

Number	Name	yyyy mm/dd	Phase	L_{PAB}	B_{PAB}	Period(h)	P.E.	Amp	A.E.	Grp
665	Sabine	2020 08/20	3.8	326	9	4.299	0.004	0.33	0.02	MB-O

Table I. Observing circumstances and results. The phase angle is given for the first and last date. If preceded by an asterisk, the phase angle reached an extrema during the period. L_{PAB} and B_{PAB} are the approximate phase angle bisector longitude/latitude at mid-date range (see Harris et al., 1984). Grp is the asteroid family/group (Warner et al., 2009).

FAST ROTATOR MINOR PLANET 2020 UA FROM CLUJ AND BERTHELOT OBSERVATORY

Adrian Bruno Sonka
Astronomical Institute of the Romanian Academy, 5 Cuţitul de Argint, 040557 Bucharest, ROMANIA
sonka@astro.ro

Vlad Turcu
Romanian Academy Cluj-Napoca Branch, Astronomical Observatory Cluj-Napoca, 19 Cireșilor, 400487 Cluj-Napoca, Romania

Alin Nedelcu
Astronomical Institute of the Romanian Academy Bucharest, Romania

Mirel Birlan
Astronomical Institute of the Romanian Academy Bucharest, Romania
IMCCE, Observatoire de Paris77 av Denfert Rochereau, 75014 Paris cedex, France

Dan Moldovan
Romanian Academy Cluj-Napoca Branch, Astronomical Observatory Cluj-Napoca

(Received: 2020 Nov 6, Revised: 2021 Mar 5)

We have observed minor planet 2020 UA during an exceptional close approach and determined that it is a fast rotator. For two data sets, taken 2 hours apart, our measurements suggest two different rotational periods: 0.0440 ± 0.0006 h and 0.0293 ± 0.0002 h.

Small (H = 28.44) minor planet 2020 UA, discovered on 16 October 2020 at G96 Mt. Lemmon Survey, had an extremely close approach on 21 October, 02 UT, at 0.000297 AU (44.498 km). It was shown (Thirouin et al., 2016; Kwiatkowski et al., 2010) that very small asteroids usually have elongated shapes (i.e., large brightness variations), very fast rotations and tumbling states, which made 2020 UA an interesting object to observe, with unknown rotational parameters.

As small minor planets in the vicinity of Earth are rarely observable, and because the observing circumstances were favorable, we undertook the observation of the object, with the goal of determining the rotational period and other characteristics regarding the rotation.

Observations were made from Cluj-Napoca and Berthelot Observatory (IAU MPC L54 code), branches of The Astronomical Institute of the Romanian Academy. Cluj-Napoca Feleacu Observatory operated a Plane Wave CDK24, f/6.5 telescope equipped with the SBIG STL-6303 CCD Camera (23.9×15.9 arcmin field of view) operating at bin 2×2. Berthelot Observatory operated the OGS RC 14.5, f/8 telescope equipped with a SBIG STL-11000M CCD Camera (44×30 arcmin of field of view), operating in binning 2×2.

We observed the asteroid on the night of 20/21 Oct. 2020, for 30 minutes, starting with 20:30 UT, from Cluj, and for 36 minutes starting at 22:24 UT, from Berthelot. The exposure time was 2 sec for Berthelot. The exposure time of 5 sec was used by Cluj Observatory, which recorded the asteroid as a trail. Observing circumstances are presented in Table 1.

The raw images were calibrated with bias, flats, and darks using the standard procedures of *Maxim DL* (2016) software. Data processing and period analysis were made using *MPO Canopus* software (Warner, 2015). Differential photometric measurements were performed using the Comp Star Selector (CSS) procedure in *MPO Canopus*, which allowed selecting three reference stars with a near solar color. The comp star magnitudes were taken from the CMC-15 catalog (*http://svo2.cab.inta-csic.es/vocats/cmc15/)*.

The sky motion of 2020 UA during the observations spans the interval between 203 arcsec/min and 563 arcsec/min. Thus, during the observations the asteroid crossed several CCD fields. We organized the images and performed photometry in each field, were we identified the solar type reference stars, being able to combine the photometric measurements. Elliptical apertures were used to measure the brightness of the asteroid and circular ones for reference stars.

In every set of observations, the asteroid presented brightness variations of over 1 magnitude, as can be seen below, in the raw data plots made with data from both observatories.

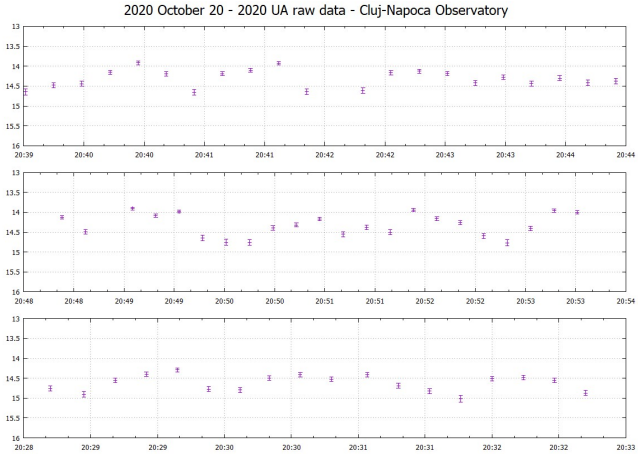

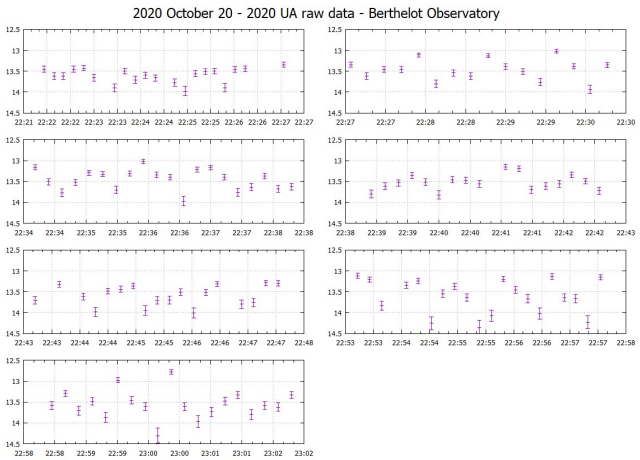

Number	Name	yyyy mm/dd	Phase	L_{PAB}	B_{PAB}	Period(h)	P.E.	Amp	A.E.	Grp
	2020 UA - Cluj-Napoca	2020 10/20	33	43.5	-4.9	0.0440	0.0006	0.61	0.2	ATEN
	2020 UA - Berthelot	2020 10/20	42	47.9	-4.0	0.0293	0.0002	0.47	0.15	ATEN

Table I. Observing circumstances and results for Cluj-Napoca Feleacu Observatory (first line) and Berthelot Observatory (second line). The phase angle is given for the first and last date. If preceded by an asterisk, the phase angle reached an extremum during the period. L_{PAB} and B_{PAB} are the approximate phase angle bisector longitude/latitude at mid-date range (see Harris et al., 1984). Grp is the asteroid family/group (Warner et al., 2009).

We used the period finding tool included in MPO Canopus, in order to find the rotational period of the asteroid. We found that the s form Berthelot and Cluj-Napoca could not be fitted with the same period, although we could find a common period for sessions from the same observatory. For Berthelot we found a period of 0.0293 ± 0.0002 h with an amplitude of the Fourier fit of 0.47 mag. We mention that the real amplitude is variable from one cycle of rotation to another. For Cluj-Napoca data we found a rotational period of 0.0440 ± 0.0006 h with an amplitude of 0.61 mag. We noticed that for Cluj-Napoca data another solution of 0.022 hours is available, but for a monomodal lightcurve, and the result was discarded.

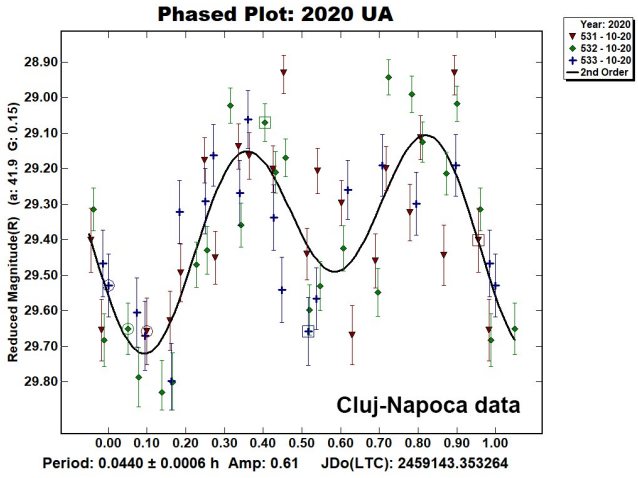

The discrepancy between the two periods found is 0.0147 hours, over 66% of the shortest period found. Although our data show a decrease in the rotational period, we need to verify if the change is real, which if correct, indicates a tumbling asteroid.

The lightcurve amplitude roughly of half magnitude suggest an elongated body. Also, for such a short period lightcurve internal strength is necessary and usually interpreted as a monolithic object.

Cluj-Napoca data were taken two hours earlier than Berthelot's, a time period during which the asteroid made 45 rotations (computed using the period 0.044 h). We can verify if the period found at Cluj-Napoca can be used to fit the data from Berthelot by propagating a calculated period and its associated error to the time of the second observation (Berthelot), using Eq. 3 in (Kwiatkowski, T., 2010), where the parameter ΔN, computed using the found period, it's error and the time difference between observations must be lower than 0.25 for a match between lightcurves. For our data we found that ΔN = 0.0012, which means that the period of 0.044 h could be a good match for data taken 2 hours later. This period enforced on Berthelot data showed no meaningful result, and therefore we conclude that a change in the rotational period is possible.

We also checked for a secondary period, using Dual Period tool in MPO Canopus, but we could not find a significant result. But, when taking in consideration the shape and the variable amplitude of the light curve, we could not exclude a tumbling solution for this asteroid. search of the Asteroid Lightcurve Database did not find any previously reported results for asteroid.

Acknowledgements

This work was supported by a grant of the Ministry of National Education and Scientific Research, RDI Programe for Space Technology and Advanced Research - STAR, project number 513 This work was supported by a grant of the Romanian Ministry of Research and Innovation, CCCDI-UEFISCDI, project number PN-III-P1-1.2-PCCDI-2017-0266, contract number 16 PCCDI/2018, within PNCDI III.

References

Harris, A.W.; Young, J.W.; Scaltriti, F.; Zappala, V. (1984). "Lightcurves and phase relations of the asteroids 82 Alkmene and 444 Gyptis." *Icarus* 57, 251-258.

Kwiatkowski, T.; Buckley, D.A.H.; O'Donoghue, D.; Crause, L.; Crawford, S.; Hashimoto, Y.; Kniazev, A.; Loaring, N.; Romero Colmenero, E.; Sefako, R.; Still, M.; Vaisanen, P. (2010). "Photometric survey of the very small near-Earth asteroids with the SALT telescope I. Lightcurves and periods for 14 objects." *Astronomy & Astrophysics* **509**, A94.

MaxIm DL (2016). *Maxim DL* software manual. *https://diffractionlimited.com/help/maximdl/MaxIm-DL.htm*

Thirouin, A.; Moskovitz, N.; Binzel, R.P.; Christensen, E.; DeMeo, F.E.; Person, M.J.; Polishook, D.; Thomas, C.A.; Trilling, D.; Willman, M.; Hinkle, M.; Burt, B.; Avner, D.; Aceituno, F.J. (2016). "The mission accessible near-earth objects survey (MANOS): first photometric results." *The Astronomical Journal* **152.6**, 163.

Warner, B.D.; Harris, A.W.; Pravec, P. (2009). "The Asteroid Lightcurve Database." *Icarus* **202**, 134-146. Updated 2016 Sep. *http://www.minorplanet.info/lightcurvedatabase.html*

Warner, B.D. (2015). *MPO Canopus* software v10.7.0.6. Bdw Publishing. *http//www.MinorPlanetObserver.com*

THE ELUSIVE PERIOD OF THE HILDA 1269 ROLLANDIA

W. Romanishin
1933 Whispering Pines Cir, Norman, OK 73072
wromanishin@ou.edu

(Received: 2021 Jan 15, Revised: 2021 Mar 5)

I present high quality lightcurve data on the large Hilda 1269 Rollandia. The data were obtained using a 0.9m telescope at Cerro Tololo Interamerican Observatory in Chile in May 2013 and cover over 17 hours split over two consecutive nights. This data is not sufficient to find a reliable rotation period for Rollandia. However, the data it is sufficient to rule out most of the published periods for this object.

1269 Rollandia is a member of the Hilda group discovered in 1930 by G. Neujmin at Simeiz, in the Crimean Peninsula. Rollandia is the fifth largest Hilda, with a diameter of about 105 km (Mainzer et al., 2019).

I observed Rollandia using the 0.9-m SMARTS telescope at Cerro Tololo Observatory in Chile on two night in May of 2013, using 100 s long exposures. I obtained interleaved V and R sequences of images to search for any color variation with phase. When planning the run, I thought the period for Rollandia was ~15.3 h. This period would have allowed a complete lightcurve to be obtained using long sequences (>8 hours) on two consecutive nights. The object was ideally placed and was in a dark sky and at airmass less than 2 for almost 9 hours each night. On 2013 May 6, I obtained 108 R and 107 V exposures spanning 8.6 h, and on 2013 May 7, 114 R and 113 V exposures spanning 8.8 h. The observing conditions were superb.

All CCD images were reduced and measured using custom scripts using the IRAF software package. Reduction steps included subtraction of background images to reduce the effects of contaminating stars and galaxies, and pairwise comparison of seeing and transparency monitoring stars to look for stellar variations during the night.

Photometric calibration in the Landolt VR magnitude system was made using observations of several Landolt standard fields each night (Clem and Landolt, 2013). On both nights the V and R lightcurves of Rollandia were visually indistinguishable in shape. The color computed from adjacent V and R images showed no noticeable change with time over the course of either night. The average color was V-R = 0.486 on 6 May and 0.477 on 7 May. The color calibrations were independently derived each night and have estimated uncertainties of about 0.01 mag. Thus, the two color determinations agree well, given the calibration uncertainty, and the overall average V-R color of Rollandia is 0.482.

Magnitudes were reduced to absolute (r = 1 au, Δ = 1 au, phase = 0°) R band magnitudes (H(R)) using the Bowell et al. (1989) H, G formalism with $G = 0.15$. The H(R) magnitudes are plotted as a function of the observation midpoint time, with the x-axis starting at 0:00 UT on 6 May 2013. The random photometric error bars are about 0.007 mag and are not shown on the plot as they are only a little larger than the symbol size.

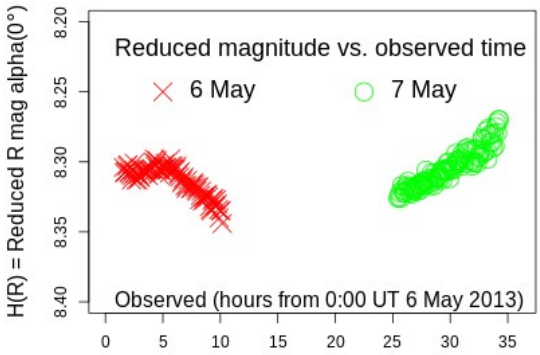

There have been a number of periods published for Rollandia. Fauvaud and Fauvaud (2013) quote a period of 15.32 h. Warner et al. (2017) quote 19.98 h. Warner and Stephens (2019) discuss several possible periods and adopt 17.36 h, while Polakis (2019) gives a period of 28.277 h. Slyusarev et al. (2013) give a lower limit to the period of 36 h. (This value replaces the preliminary period of 30.98 h in Slyusarev et al. (2012) (personal communication, Slyusarev). Behrend (2019web) gives a period estimate of 72 h, but this is based only on a small fragment of a period, about 6 hours of data. Colazo et al. (2021) present a period of 39.81 h.

To check the consistency of these periods with my data, I phased the CTIO data to the various periods, as shown in the figures below. My data covers a time span of about 32.7 h from the first observation on 6 May to the last on 7 May. Thus, if the correct period is less than 32.7 hours, the data should repeat itself for a portion of the lightcurve. In my opinion, none of the four phased plots produce an acceptable repeating lightcurve. Thus, these four periods are inconsistent with the CTIO data.

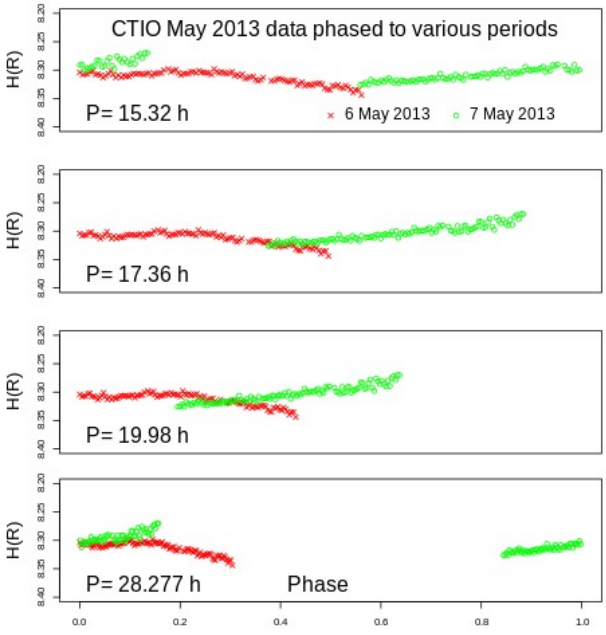

Number	Name	yyyy mm/dd	Phase	L_{PAB}	B_{PAB}	Period(h)	P.E.	Amp	A.E.
1269	Rollandia	2013 05/06-05/07	5.1,4.	24	3	unknown	unknown	0.07	0.01

Table I. Observing circumstances and results. The phase angle is given for the first and last date. If preceded by an asterisk, the phase angle reached an extrema during the period. L_{PAB} and B_{PAB} are the approximate phase angle bisector longitude/latitude at mid-date range (see Harris et al., 1984).

For the Colazo et al. (2021) period, 39.81 h, the CTIO data would not span a full period. The Colazo et al. (2021) lightcurve shows a two peaked curve, with the two maxima separated by 0.44 or 0.56 of a period, corresponding to 17.5 or 22.3 h. The CTIO data might show a broad maximum at about 4 h UT on 6 May and another maximum at or somewhat past 35 h after 0:00 UT on 6 May. I tried to fit the CTIO data to the Colazo two peaked 39.81 h period lightcurve by shifting the phase and magnitude of the Colazo et al. lightcurve. Of course, the two lightcurves would not be expected to match in detail as the observing geometries were different. However, if the correct period is 39.81 h, the time difference between lightcurve peaks in the CTIO data should line up pretty well with those in the Colazo data. The top two panels of the last figure show four (of many) attempts to align the peak times. Clearly, the CTIO data is inconsistent with any such match, indicating that the rotational period of Rollandia is not 39.81 h.

In the bottom panel of the figure, I show the CTIO data phased to a period of 65 h, and a simple sinewave lightcurve of 65 h rotational period. This is obviously not meant to be a proper fit to the period, but does suggest that much longer periods than those published so far should be considered, as suggested by Behrend (2019web).

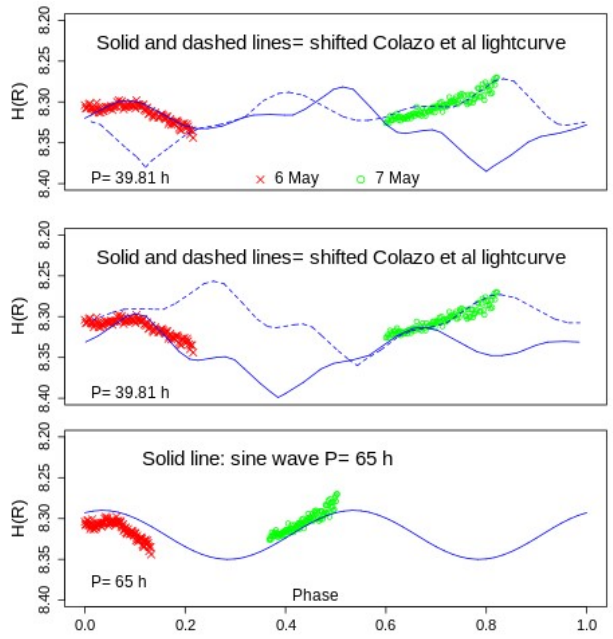

In summary, I believe the rotational period of Rollandia must be considered unknown at present. As a period of several days is quite possible, finding the correct period might well require a lot of time coverage from a number of telescopes at different longitudes. At the next few oppositions of Rollandia (June 2021 and July 2022), the object will be at a declination near -20°, so will be extremely difficult for northern hemisphere observers, but will be ideally places for long sequences from southern hemisphere observatories.

One possible explanation for the disparate published periods is that Rollandia is a tumbling object. If it is, it would be the largest known tumbling minor planet. Plots were produced with the freely available R software package (R Core Team 2020).

References

Behrend, R. (2019). Observatiore de Geneve web site. *http://obswww.unige.ch/~behrend/page_cou.html*

Bowell, E.; Hapke, E.B.; Domingue, D.; Lumme, K.; Peltoniemi, J.; Harris, A.W. (1989). "Application of Photometric Models to Asteroids." In *Asteroids II* (R.P. Binzel, R. Gehrels, M.S. Matthews, eds.) pp 524-556. Univ of Arizona Press, Tucson.

Clem, J.L.; Landolt, A.U. (2013). "Faint UBVR Standard Star Fields." *Astronomical Journal*, **146**, A88.

Colazo, M.; Stechina, A.; Fornari, C.; Santucho, M.; Mottino, A.; and 19 colleagues (2021). "Asteroid Photometry and Lightcurve Analysis at GORA Observatories." *Minor Planet Bull*. **48**, 50**.**

Fauvaud, S.; Fauvaud, M. (2013). "Photometry of Minor Planets. I. Rotation Periods from Lightcurve Analysis for Seven Main-Belt Asteroids." *Minor Planet Bull*. **40**, 226.

Harris, A.W.; Young, J.W.; Scaltriti, F.; Zappala, V. (1984). "Lightcurves and phase relations of the asteroids 82 Alkmene and 444 Gyptis." *Icarus* **57**, 251-258.

Mainzer, A.; Bauer, J.; Cutri, R.; Grav, T.; Kramer, E.; Masiero, J.; Sonnett, S.; Wright, E.; Eds. (2019). NEOWISE Diameters and Albedos V2.0. urn:nasa:pds:neowise_diameters_albedos::2.0. NASA Planetary Data System. *https://doi.org/10.26033/18S3-2Z54*

Polakis, T. (2019). "Lightcurves of Twelve Main-Belt Minor Planets." *Minor Planet Bull*. **46**, 287.

R Core Team (2020). R: A language and environment for statistical computing. R Foundation for Statistical Computing. Vienna, Austria. *https://www.R-project.org/*.

Slyusarev, I.G.; Shevchenko, V.G.; Belskaya, I.N.; Krugly, Yu.N.; Chiorny, V.G. (2012). ACM 2012, #6398.

Slyusarev, I.G.; Shevchenko, V.G.; Belskaya, I.N.; Krugly, Yu.N.; Chiorny,V.G. (2013). "Results of photometry of selected asteroids from the Hilda group." *Astronomical School's Report*, **9**, 75.

Warner, B.D.; Stephens, R.D.; Coley, D.R. (2017). "Lightcurve Analysis of Hilda Asteroids at the Center for Solar System Studies: 2016 June - September." *Minor Planet Bull*. **44**, 36.

Warner, B.D.; Stephens, R.D. (2019). "Lightcurve Analysis of Hilda Asteroids at the Center for Solar System Studies: 2019 April - June." *Minor Planet Bull*. **46**, 406.

PHOTOMETRIC ANALYSIS AND ROTATION PERIOD DETERMINATION OF THE POTENTIALLY HAZARDOUS ASTEROID 2020 WU5

Alessandro Marchini
Astronomical Observatory, DSFTA - University of Siena (K54)
Via Roma 56, 53100 - Siena, ITALY
marchini@unisi.it

Riccardo Papini
Wild Boar Remote Observatory (K49)
San Casciano in Val di Pesa (FI), ITALY

Giorgio Baj
M57 Observatory (K38), Saltrio, ITALY

Gianni Galli
GiaGa Observatory (203), Pogliano Milanese, ITALY

Paolo Bacci
GAMP - San Marcello Pistoiese (104), Pistoia, ITALY

Lorenzo Franco
Balzaretto Observatory (A81), Rome, ITALY

(Received: 15 Jan 2021 - Revised: 22 Jan 2021)

Photometric observations of 2020 WU5 were conducted in 2021 January in order to determine its synodic rotation period and revealed a bimodal solution with P = 5.574 ± 0.002 h and an amplitude A = 0.84 ± 0.08 mag.

CCD photometric observations of the Potentially Hazardous Asteroid (PHA) 2020 WU5 were carried out in 2021 January 12-19 at the Astronomical Observatory of the University of Siena (K54), a facility inside the Department of Physical Sciences, Earth and Environment (DSFTA, 2021), and at three other Italian observatories inside the Italian Amateur Astronomers Union (UAI, 2021) group. Table I shows the observing circumstances and results, Table II describes the instrumentation used in each observatory.

Data processing and lightcurve analysis were performed with *MPO Canopus* (Warner, 2018). All images were calibrated with dark and flat-field frames and the instrumental magnitudes converted to R magnitudes using solar-colored field stars from the catalogues distributed with *MPO Canopus*.

2020 WU5 was observed for the first time on 2020 November 29 by WISE (WISE, 2021). It belongs to the Apollo family and is a PHA with a semi-major axis of 1.059 AU, eccentricity 0.102, inclination 41.484°, an orbital period of 1.09 years and an absolute magnitude H = 18.651 (JPL, 2021). Its Earth MOID (Minimum Orbit Intersection Distance) is of 0.041 AU (NEODyS-2, 2021).

Observations were intensively conducted over six nights and collected 4,560 data points. The asteroid moved across the sky very quickly (about 27 arcmin per hour on January 15) challenging the observers who had to re-point their telescopes every 30-60 minutes to keep it in the frame. The period analysis shows a bimodal solution for the rotational period of P = 5.574 ± 0.002 h with an amplitude A = 0.84 ± 0.08 mag. The large amplitude suggests that the shape is quite elongated. The large dispersion and subtle variations in the light curve are likely effects of the large variation of the phase angle, which changed more than 40 degrees during the observations (see table I for details).

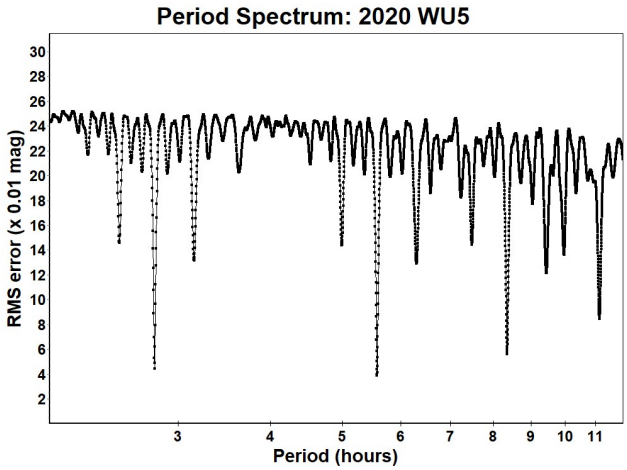

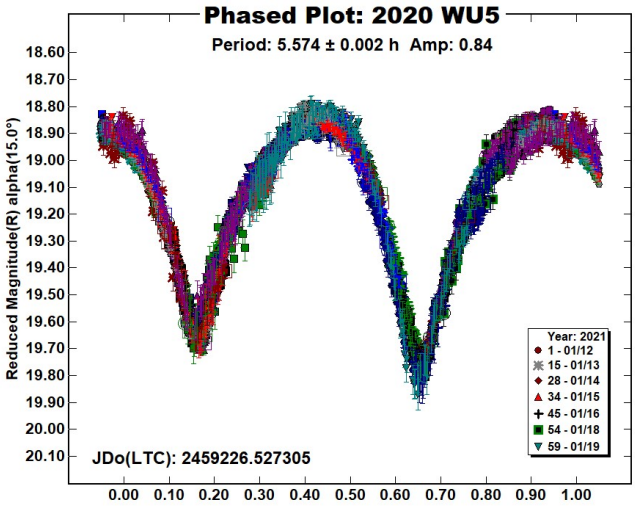

Number	Name	2021/mm/dd	Phase	L_{PAB}	B_{PAB}	Period(h)	P.E.	Amp	A.E.	Grp
	2000 WU5	01/12-01/19	*14.9,56.6	105	13	5.574	0.002	0.84	0.08	PHA

Table I. Observing circumstances and results. The phase angle is given for the first and last date. If preceded by an asterisk, the phase angle reached an extrema during the period. L_{PAB} and B_{PAB} are the approximate phase angle bisector longitude/latitude at mid-date range (see Harris *et al.*, 1984). Grp is the asteroid family/group (Warner *et al.*, 2009).

Observatory (IAU code)	Instrumentation
Astronomical Observatory, University of Siena (K54)	0.30-m MCT f/5.6 telescope, SBIG STL-6303e CCD, Clear filter
M57 Observatory (K38)	0.30-m RCT f/5.5 telescope, SBIG STT-1603 CCD camera, Clear filter
GiaGa Observatory (203)	0.36-m SCT f/5.8 telescope, Moravian G2-3200 CCD, Clear filter
GAMP - San Marcello Pistoiese (104)	0.60-m NRT f/4.0 telescope, Apogee Alta CCD, Clear filter

Table II. Observing Instrumentations. MCT: Maksutov-Cassegrain, NRT: Newtonian Reflector, RCT: Ritchey-Chretien, SCT: Schmidt-Cassegrain.

References

DSFTA (2021). Dipartimento di Scienze Fisiche, della Terra e dell'Ambiente – Astronomical Observatory. *https://www.dsfta.unisi.it/en/research/labs/astronomical-observatory*

Harris, A.W.; Young, J.W.; Scaltriti, F.; Zappala, V. (1984). "Lightcurves and phase relations of the asteroids 82 Alkmene and 444 Gyptis." *Icarus* **57**, 251-258.

JPL (2021). Small-Body Database Browser. *http://ssd.jpl.nasa.gov/sbdb.cgi#top*

NEODyS-2 (2021). Near Earth Objects - Dynamic Site 2 web site. *https://newton.spacedys.com/neodys/index.php*

UAI (2021). "Unione Astrofili Italiani" web site. *https://www.uai.it*

Warner, B.D.; Harris, A.W.; Pravec, P. (2009). "The Asteroid Lightcurve Database." *Icarus* **202**, 134-146. Updated 2020 Oct. *http://www.minorplanet.info/lightcurvedatabase.html*

Warner, B.D. (2018). MPO Software, MPO Canopus v10.7.7.0. Bdw Publishing. *http://minorplanetobserver.com*

WISE (2021). Wide-field Infrared Survey Explorer web site. *https://www.jpl.nasa.gov/missions/wide-field-infrared-survey-explorer-wise/*

ROTATIONAL PERIOD AND LIGHTCURVE DETERMINATION OF 2020 UQ6: A SUPER FAST ROTATOR

Ernesto Guido
AstroCampania ETS, Naples, Italy
Osservatorio Salvatore Di Giacomo (L07)
Via Salvatore Di Giacomo 7b
Agerola (Na) Italy
comets77@astrocampania.it

Antonio Catapano, Alfonso Noschese, Antonio Vecchione
AstroCampania ETS, Naples, Italy
Osservatorio Salvatore Di Giacomo (L07)
Via Salvatore Di Giacomo 7b, 80051
Agerola (Na) Italy

(Received: 2020 Nov 3)

The lightcurve and rotation period determination for 2020 UQ6 are reported based on observations made in late October 2020. 2020 UQ6 is a super-fast rotator with a period of 0.04521 +/- 0.000001 h.

The aim of this research was to find the rotational period and lightcurve of 2020 UQ6. This asteroid is a Near-Earth object belonging to the Apollo group discovered at Tokyo-Kiso Observatory (MPC code 381) on 2020 October 27. Based on the latest orbit computations performed by the Jet Propulsion Laboratory (JPL, 2020), it is confirmed that 2020 UQ6 is not going to impact Earth in the near future (it is not a potentially hazardous asteroid).

It has a semi-major axis of 2.352 AU, orbital period of 3.62 years, eccentricity of 0.760°, and inclination of 4.516°. JPL Small-Body Database Browser reports an absolute magnitude H = 22.6, with an estimated diameter of 80 to 180 meters, respectively for medium and low albedo object type (JPL, 2020).

CCD photometric observation of 2020 UQ6 were carried out in 2×2 binned format during the night between 2020 October 28 and 29 by using the main telescope of the Osservatorio Salvatore di Giacomo, Agerola (MPC code L07). It is a 0.50-m Ritchey-Chretien operating at *f*/8 equipped with an unfiltered FLI-PL4240 CCD camera (2048×2048array of 13.5-micron pixels).

All images were astrometrically aligned, dark and flat-field corrected using *Maxim DL* software. *MPO Canopus* (Warner, 2017) was used to measure the magnitudes, perform Fourier analysis, and produce the final lightcurve. In particular, data were reduced in *MPO Canopus* using differential photometry. Night-to-night zero-point calibration was accomplished by selecting up to five comparison stars with near-solar colors using the "comp star selector" feature.

To analyze the data points, the ATLAS star catalog (Torny 2018) was used for determining the comparison star magnitudes. The "StarBGone" routine within *MPO Canopus* was used to subtract stars that occasionally merged with the asteroid during the observations. *MPO Canopus* was also used for rotation period analysis. The software employs a FALC Fourier analysis algorithm developed by Harris (Harris et al., 1989).

Number	Name	2020 mm/dd	Phase	L_{PAB}	B_{PAB}	Period(h)	P.E.	Amp	A.E.	Grp
	2020 UQ6	10/28-10/29	15.39,13.25	43	-1	0.04521	0.0001	0.57	0.02	NEA

Table I. Observing circumstances and results. The phase angle is given for the first and last date. L_{PAB} and B_{PAB} are the approximate phase angle bisector longitude and latitude at mid-date range (Harris et al., 1984). Grp is the asteroid family/group (Warner et al., 2009).

2020 UQ6 proved to be challenging since the rate of sky motion and potentially fast rotation required using short exposures and dealing with the subsequent low (but useful) SNR values. In order to take in account both the high speed of the object (ranging from 21.48 arcec/min to 17.46 arcsec/min during the measurements) and to avoid rotational smearing (Pravec, 2000), which typically leading to a loss of rotation information or to an amplitude significantly underestimated, exposure times were kept to 4 s for all sessions.

Eight observation sessions collected 1373 data points for lightcurve analysis. This led to a bimodal lightcurve with a period of 0.04521 h (162.76 s), or a frequency of 530.84 rev/d, and an amplitude of 0.57 magnitudes. This finding identifies this object as a super-fast rotator asteroid (P << 2 h). This puts it beyond the rotation rate barrier of 11 rev/d for rubble piles.

It can be speculated that the asteroid is most likely strength-bound rather than gravity-bound. Moreover, from the absolute magnitude value of H = 22.6 and assuming the asteroid to be a spherical object with a uniform surface and albedo ranging from 0.05 and 0.30, one can gets an estimated diameter ranging from 80 and 180 m. From this, it is possible to add the average value of the estimated diameter, D = 130 m, to the frequency vs diameter plot from LCDB. As it can be observed, 2020 UQ6 is located in an uncrowded region of the graph (identified by a yellow point), making this object particularly noteworthy.

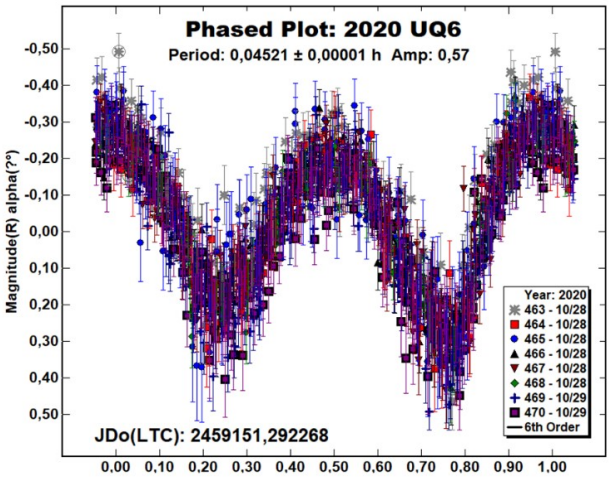

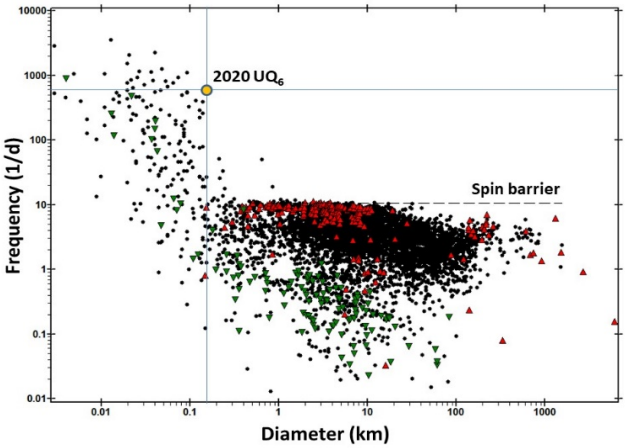

Acknowledgements

The authors gratefully acknowledge Lorenzo Franco for his valuable discussions and suggestions.

References

JPL (2020). Small-Body Database Browser. *https://ssd.jpl.nasa.gov/sbdb.cgi*

Harris, A.W.; Young, J.W.; Scaltriti, F.; Zappala, V. (1984). "Lightcurves and phase relations of the asteroids 82 Alkmene and 444 Gyptis." *Icarus* **57**, 251-258.

Harris, A.W.; Young, J.W.; Bowell, E.; Martin, L.J.; Millis, R.L.; Poutanen, M.; Scaltriti, F.; Zappala, V.; Schober, H.J.; Debehogne, H.; Zeigler, K.W. (1989). "Photoelectric Observations of Asteroids" 3, 24, 60, 261, and 863." *Icarus* **77**, 171-186.

Pravec, P.; Hergenrother, C.; Whiteley, R.; Sarounova, L.; Kusnirak, P. (2000). "Fast Rotating Asteroids 1999 TY2, 1999 SF10, and 1998 WB2." *Icarus* **147**, 477-486.

Tonry, J.L.; Denneau, L.; Flewelling, H.; Heinze, A.N.; Onken, C.A.; Smartt, S.J.; Stalder, B.; Weiland, H.J.; Wolf, C. (2018). "The ATLAS All-Sky Stellar Reference Catalog." *Astrophys. J.* **867**, A105.

Warner, B.D.; Harris, A.W.; Pravec, P. (2009). "The Asteroid Lightcurve Database." *Icarus* **202**, 134-146. Updated 2020 Aug. *http://www.minorplanet.info/lightcurvedatabase.html*

Warner, B.D. (2017). MPO Software, *MPO Canopus* version 10.7.11.1 Bdw Publishing. *http://minorplanetobserver.com*

LIGHTCURVE ANALYSIS FOR TWO MAIN BELT ASTEROIDS

Giovanni Battista Casalnuovo,
Filzi School Observatory D12
Laives, ITALY
gb.minorplanet@gmail.com

(Received: 2020 Oct 26)

Photometric observations of two main-belt asteroids, (11894) 1991 GW, 19120 Doronina (1983 PM1), were made at the Filzi School Observatory (School in country Laives - Italy) MPC code D12.

CCD photometric observations, were made at the Filzi School Observatory, all are without filter (clear). All images were obtained with a 0.35-m reflector telescope reduced to *f*/8.0, a QHY9 CCD camera, and then calibrated with dark and flat-field frames. The pixel scale was 1.56 arcsec when binned at 4×4 pixels. All exposures were 120 seconds. The computer clock was synchronized with an internet time server before each session. Differential photometry and period analysis were done using *MPO Canopus* version 10.7.12.9 (Warner, 2018). Solar type stars from CMC15 catalog in R band were used as comparison stars.

(11894) 1991 GW. This main-belt asteroid was reported as a lightcurve photometry opportunity for 2020 April on the MinorPlanet.Info Gateway web site (*http://www.MinorPlanet.info*; hereafter referenced as MPI). (11894) 1991 GW was discovered in the year 1991 by Kawasato, N. at Uenohara. It is a main-belt asteroid with a semi-major axis of 2.35 AU, eccentricity 0.188, inclination 7.95°, and orbital period of 3.62 yr. Its absolute magnitude is H = 14.20. It was studied for four nights. The derived synodic period was P = 3.331 ± 0.002 h with an amplitude of A = 0.27 ± 0.07 mag. There were no entries in the LCDB (Warner et al., 2009) for this asteroid.

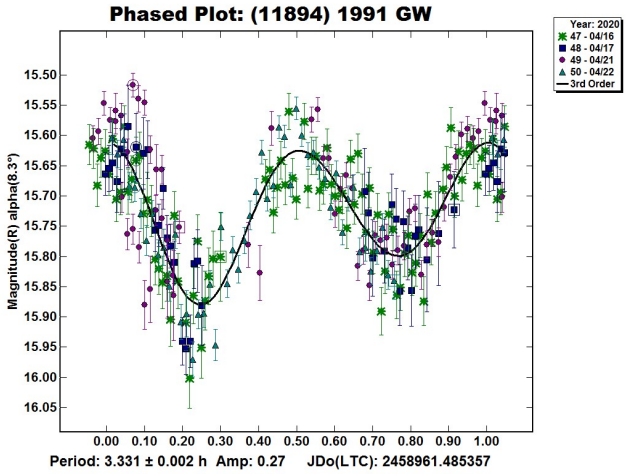

19120 Doronina (1983 PM1). This main-belt asteroid was reported as a lightcurve photometry opportunity for 2020 August on the MPI web site. 19120 Doronina was discovered in the year 1983 by L. G. Karachkina at the Crimean Astrophysical Observatory. It is a main-belt asteroid with a semi-major axis of 2.56 AU, eccentricity 0.215, inclination 7.98°, and orbital period of 4.12 yr. Its absolute magnitude is H = 13.8 It was studied for seven nights. The derived synodic period was P = 5.395 ± 0.001 h with an amplitude of A = 0.56 ± 0.10 mag. Pál et al. (2020) reported a period of 5.39151 h., which is in very close agreement with the result given here.

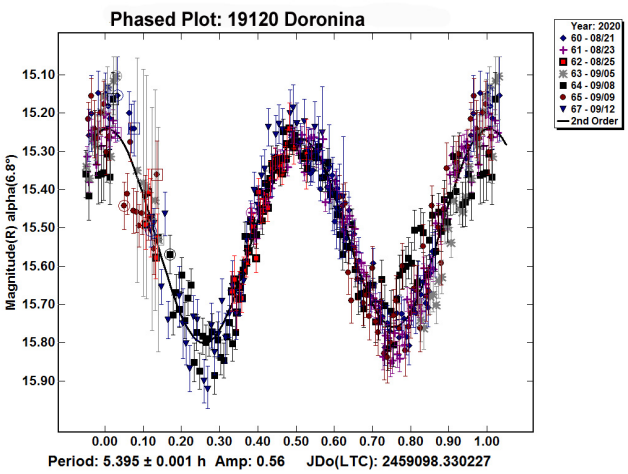

References

Harris, A.W.; Young, J.W.; Scaltriti, F.; Zappala, V. (1984). "Lightcurves and phase relations of the asteroids 82 Alkmene and 444 Gyptis." *Icarus* **57**, 251-258.

Pál, A.; Szakats, R.; Kiss, C.; Bódi, A.; Bognár, Z.; Kalup, C.; Kiss, L.L.; Marton, G.; Molnár, L.; Plachy, E.; Sárneczky, K.; Szabó, G.; Szabó, R (2020). "Solar system objects observed with TESS - First data release: Bright main-belt and Trojan asteroids from the southern survey." *Astrophys. J. Suppl. Ser.* **247**, id.26.

Warner, B.D.; Harris, A.W.; Pravec, P. (2009). "The Asteroid Lightcurve Database." *Icarus* **202**, 134-146. Updated 2020 June. *http://www.minorplanet.info/lightcurvedatabase.html*

Warner, B.D. (2018). MPO Software Canopus, version 10.7.12.9. Bdw Publishing, Colorado Springs, CO.

Number	Name	yyyy mm/dd	Phase	L_{PAB}	B_{PAB}	Period(h)	P.E.	Amp	A.E.	Grp
11894	1991 GW	2020 04/16-04/22	7.7 11.0	196.1	3.6	3.331	0.002	0.27	0.07	MB
19120	Doronina	2020 08/21-09/12	6.7 14.3	327.8	-10.4	5.395	0.001	0.56	0.10	MB

Table I. Observing circumstances and results. The phase angle is given for the first and last date. If preceded by an asterisk, the phase angle reached an extrema during the period. L_{PAB} and B_{PAB} are the approximate phase angle bisector longitude/latitude at mid-date range (see Harris et al. 1984). Grp is the asteroid family/group (Warner et al. 2009).

LIGHTCURVE ANALYSIS FOR THREE MAIN BELT ASTEROIDS

Giovanni Battista Casalnuovo
Filzi School Observatory D12
Laives, ITALY
gb.minorplanet@gmail.com

(Received: 2021 Jan 15)

Photometric observations of three main-belt asteroids, (18640) 1998 EF9, (41331) 1999 XB232, (50713) 2000 EZ135, were made at the Filzi School Observatory (School in country Laives - Italy) MPC code D12.

CCD photometric observations, were made at the Filzi School Observatory, all are without filter (clear). All images were obtained with a 0.35-m reflector telescope reduced to *f*/8.0, a QHY9 CCD camera, and then calibrated with dark and flat-field frames. The pixel scale was 1.56 arcsec when binned at 4×4 pixels. All exposures were 120 seconds. The computer clock was synchronized with an Internet time server before each session. Differential photometry and period analysis were done using *MPO Canopus* version 10.7.12.9 (Warner, 2018). Solar type stars from CMC15 catalog in R band were used as comparison stars.

(18640) 1998 EF9. This main-belt asteroid was reported as a lightcurve photometry opportunity for 2020 October on the MinorPlanet.info web site (*http://www.MinorPlanet.info/lightcurvedatabase.html*; hereafter referenced as MPI). It was discovered in the year 2000 by *Loneos* at Anderson Mesa. It is a main belt asteroid with a semi-major axis of 2.42 AU, eccentricity 0.29, inclination 20.37°, and orbital period of 3.78 yr. Its absolute magnitude is H = 13.20. This asteroid was studied for three nights (for a total of 230 images), the derived synodic period was P = 3.630 ± 0.001 h with an amplitude of A = 0.50 ± 0.08 mag. There were no entries in the LCDB (Warner et al., 2009) for this asteroid.

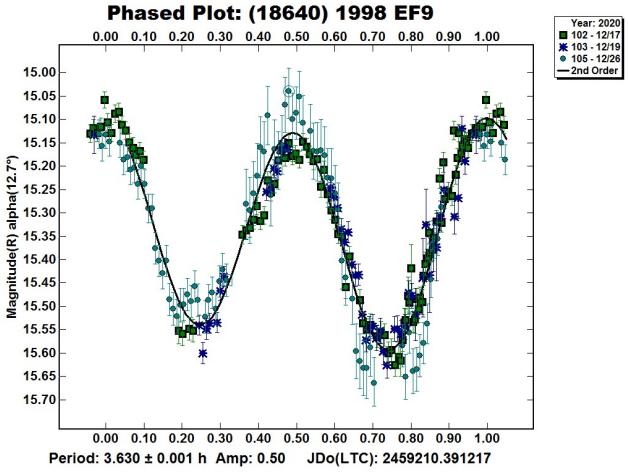

(41331) 1999 XB232. This main-belt asteroid was reported as a lightcurve photometry opportunity for 2020 November on the MPI. It was discovered in the year 1999 by *Linear* at Socorro. It is a main belt asteroid with a semi-major axis of 2.34 AU, eccentricity 0.17, inclination 23.53° and orbital period of 3.58 yr. Its absolute magnitude is H = 13.50. This asteroid was studied for four nights (for a total of 353 images), The derived synodic period was P = 3.296 ± 0.001 h with an amplitude of A = 0.42 ± 0.07 mag. The V and R band frames were acquired in sequence changing alternatively the filters (VR VR VR). This allowed us to find the color index of V-R = 0.54+-0.05 There were no entries in the LCDB (Warner et al., 2009) for this asteroid.

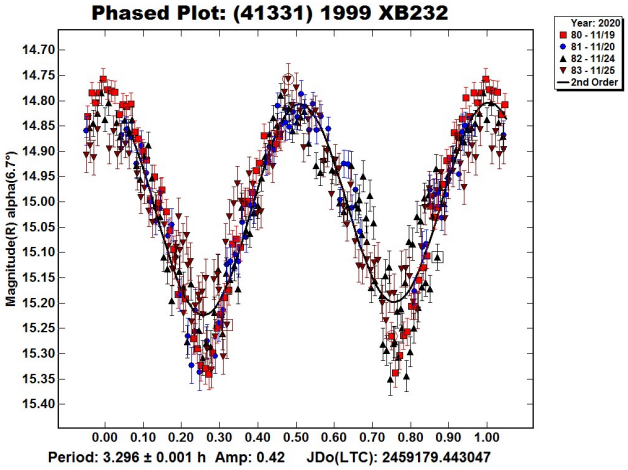

(50713) 2000 EZ135. This main-belt asteroid was reported as a lightcurve photometry opportunity for 2020 November on the MPI. It was discovered in the year 2000 by *Loneos* at Anderson Mesa. It is a main belt asteroid with a semi-major axis of 2.36 AU, eccentricity 0.24, inclination 26.07°, and orbital period of 3.65 yr; absolute magnitude is H = 14.00. It was studied for six nights (for a total of 510 images). The derived synodic period was P = 10.816 ± 0.002 h with an amplitude of A = 0.29 ± 0.08 mag. There were no entries in the LCDB (Warner et al., 2009) for this asteroid.

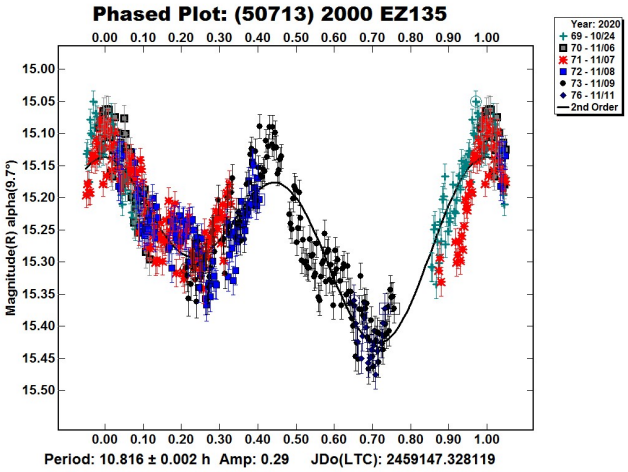

Number	Name	yyyy mm/dd	Phase	L_{PAB}	B_{PAB}	Period(h)	P.E.	Amp	A.E.	Grp
18640	1998 EF9	2020 12/17-12/26	13.0 9.5	103.7	-8.9	3.630	0.001	0.50	0.08	MB
41331	1999 XB232	2020 11/19-11/25	6.6 3.6	66.5	-3.5	3.296	0.001	0.42	0.07	MB
50713	2000 EZ135	2020 10/24-11/11	9.7 13.9	38.2	13.7	10.816	0.002	0.29	0.08	MB

Table I. Observing circumstances and results. The phase angle is given for the first and last date. If preceded by an asterisk, the phase angle reached an extrema during the period. L_{PAB} and B_{PAB} are the approximate phase angle bisector longitude/latitude at mid-date range (see Harris et al., 1984). Grp is the asteroid family/group (Warner et al., 2009).

References

Harris, A.W.; Young, J.W.; Scaltriti, F.; Zappala, V. (1984). "Lightcurves and phase relations of the asteroids 82 Alkmene and 444 Gyptis." *Icarus* **57**, 251-258.

Warner, B.D.; Harris, A.W.; Pravec, P. (2009). "The Asteroid Lightcurve Database." *Icarus* **202**, 134-146. Updated 2018 June. *http://www.minorplanet.info/lightcurvedatabase.html*

Warner, B.D. (2014). MPO Software Canopus, version 10.7.12.9. Bdw Publishing, Colorado Springs, CO. *http://minorplanetobserver.com*

ROTATIONAL PERIOD DETERMINATION OF 1526 MIKKELI

Maurizio Scardella, Federico Badoni,
Angelo Tomassini, Fernando Pierri
ATA (Associazione Tuscolana di Astronomia)
"F. Fuligni" Observatory (MPC code D06)
Via Lazio, 14 - Rocca di Papa (RM) - 00040– ITALY
nikkor5@gmail.com

(Received: 2020 Dec 16)

The main-belt asteroid 1526 Mikkeli was observed over seven nights throughout 2020 October-November in order to determine its synodic rotational period. Lightcurve analysis was done using differential photometry technique using MPO Canopus (Warner, 2012). The observations were carried out from "F. Fuligni" Observatory using a 0.35-m f/10 ACF telescope and SBIG ST8-XE CCD camera unfiltered. All images were dark and flat-field calibrated with Maxim DL.

Asteroid 1526 Mikkeli was discovered in 1939 by the Finnish astronomer Yrjö Väisälä. This main-belt asteroid was selected from Warner et al. (2020). The name of the asteroid is derived from the Finnish city of Mikkeli. The observations were carried out from "*F. Fuligni*" Observatory during seven nights throughout 2020 October-November. All the images were calibrated with dark and flat frames. Differential photometry and period analysis has been performed using *MPO Canopus* (Warner, 2012). The derived synodic period is P = 2.934 ± 0.001 h with an amplitude of A = 0.25 mag.

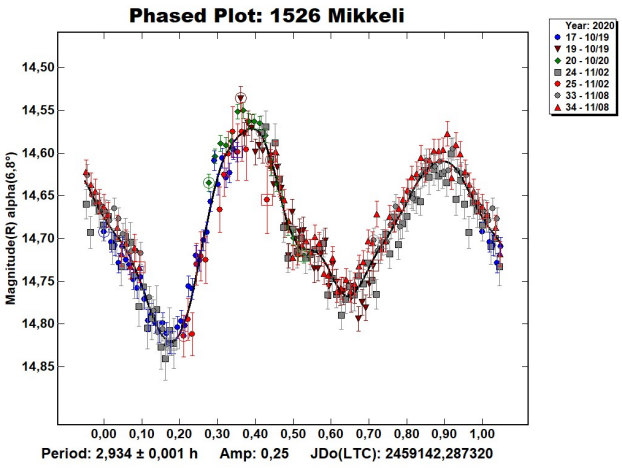

Acknowledgement

We would like to thank Samuele Piscitello for his help in taking the frames and maintaining the instruments of the ATA observatory.

References

Harris, A.W.; Young, J.W.; Scaltriti, F.; Zappala, V. (1984). "Lightcurves and phase relations of the asteroids 82 Alkmene and 444 Gyptis." *Icarus* **57**, 251-258.

Warner, B.D.; Harris, A.W.; Pravec, P. (2009). "The Asteroid Lightcurve Database." *Icarus* **202**, 134-146. Updated 2020 Aug. *http://www.minorplanet.info/lightcurvedatabase.html*

Warner, B.D. (2012). MPO Software, MPO Canopus v10.4.1.9. Bdw Publishing. *http://minorplanetobserver.com/*

Warner, B.D.; Harris, A.W.; Ďurech, J.; Benner, L.A.M. (2020). "Lightcurve Photometry Opportunities: October-December 2020." *The Minor Planet Bulletin* **47**, 330-335.

Number	Name	yyyy mm/dd	Pts	Phase	L_{PAB}	B_{PAB}	Period(h)	P.E.	Amp	A.E.	Grp
1526	Mikkeli	2020 10/19-11/08	264	6.8,17.1	20.4	7.1	2.934	0.001	0.25	0.1	FLOR

Table I. Observing circumstances and results. Pts is the number of data points. The phase angle is given for the first and last date. L_{PAB} and B_{PAB} are the approximate phase angle bisector longitude and latitude at mid-date range (see Harris *et al.*, 1984). Grp is the asteroid family/group (Warner *et al.*, 2009). FLOR = Flora.

PHOTOMETRIC ANALYSIS AND ROTATION PERIOD DETERMINATION FOR ASTEROIDS 5445 WILLIWAW, (8823) 1987 WS3 AND (26568) 2000 ET49

Alessandro Marchini
Astronomical Observatory, DSFTA - University of Siena (K54)
Via Roma 56, 53100 - Siena, ITALY
marchini@unisi.it

Riccardo Papini
Wild Boar Remote Observatory (K49)
San Casciano in Val di Pesa (FI), ITALY

Giulio Scarfi
Iota Scorpii Observatory (K78), La Spezia, ITALY

(Received: 2021 Jan 15)

Photometric observations of three main-belt asteroids were conducted in order to determine their synodic rotation periods. For 5445 Williwaw we found P = 10.65 ± 0.02 h, A = 0.29 ± 0.05 mag; for (8823) 1987 WS3, a slow rotator, we found a rough period of P = 86.0 ± 1.0 h, A = 0.24 ± 0.02 mag; for (26568) 2000 ET49 we found P = 7.171 ± 0.003 h, A = 0.71 ± 0.04 mag

CCD photometric observations of three main-belt asteroids were carried out in 2020 October - December at three Italian observatories. At the Astronomical Observatory of the University of Siena (K54), a facility inside the Department of Physical Sciences, Earth and Environment (DSFTA, 2020), we used a 0.30-m *f*/5.6 Maksutov-Cassegrain telescope, SBIG STL-6303E NABG CCD camera, and clear filter; the pixel scale was 2.30 arcsec when binned at 2×2 pixels and all exposures were 300 seconds. At the Wild Boar Remote Observatory (K49) data were obtained with a 0.235-m f/10 (SCT) telescope, a SBIG ST8-XME NABG CCD camera unfiltered; the pixel scale was 1.60 arcsec in binning 2×2 and all exposures were 300 seconds. At the Iota Scorpii Observatory (K78) we used a 0.40-m f/6 Ritchey- Chretién telescope, SBIG STXL 6303E NABG CCD camera, and R filter; the pixel scale was 1.55 when binned 2×2 and all exposures were 180 seconds.

Data processing and analysis were done with *MPO Canopus* (Warner, 2018). All images were calibrated with dark and flat-field frames and the instrumental magnitudes converted to R magnitudes using solar-colored field stars from a version of the CMC-15 catalogue distributed with *MPO Canopus*. Table I shows the observing circumstances and results.

A search through the asteroid lightcurve database (LCDB; Warner et al., 2009) indicates that our results may be the first reported lightcurve observations and results for these asteroids.

5445 Williwaw. (1991 PA12) was discovered on 1991 August 7 by H.E. Holt at Mount Palomar and named after a dramatic mountain on the skyline of Anchorage. Mount Williwaw stands 5445 feet above sea level and it's the highest point in the Campbell Creek drainage. [Ref: Minor Planet Circ. 34341] It is a main-belt asteroid with a semi-major axis of 2.552 AU, eccentricity 0.223, inclination 6.115°, and an orbital period of 4.08 years. Its absolute magnitude is H = 12.4 (JPL, 2020). The WISE/NEOWISE satellite infrared radiometry survey (Masiero et al., 2014) found a diameter D = 8.797 ± 0.107 km using an absolute magnitude H = 12.2.

Observations were conducted over three nights and collected 213 data points. The period analysis shows a solution for the rotational period of P = 10.65 ± 0.02 h with an amplitude A = 0.29 ± 0.05 mag.

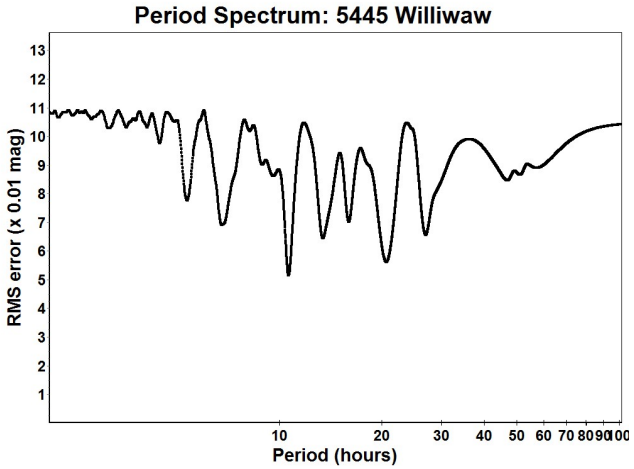

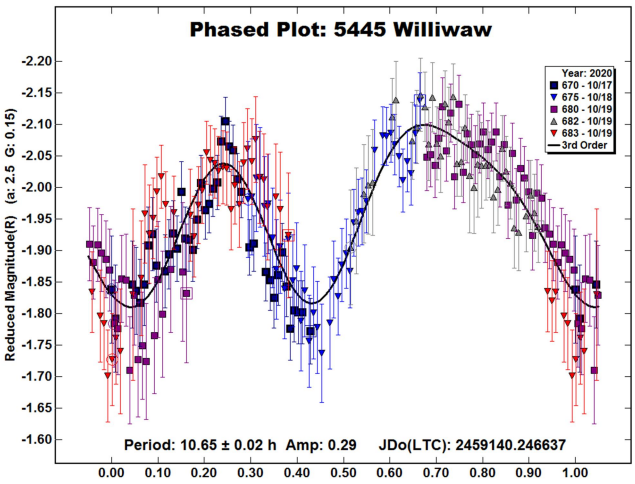

Number	Name	2020/mm/dd	Phase	L_{PAB}	B_{PAB}	Period(h)	P.E.	Amp	A.E.	Grp
5445	Williwaw	10/17-10/20	2.4,2.6	24	6	10.65	0.02	0.29	0.05	MB
8823	1987 WS3	11/18-12/15	*6.8,10.0	68	-2	86.0	1.0	0.24	0.02	MB
26568	2000 ET49	11/06-11/10	4.4,5.3	41	-8	7.171	0.003	0.71	0.04	MB

Table I. Observing circumstances and results. The first line gives the results for the primary of a binary system. The second line gives the orbital period of the satellite and the maximum attenuation. The phase angle is given for the first and last date. If preceded by an asterisk, the phase angle reached an extrema during the period. L_{PAB} and B_{PAB} are the approximate phase angle bisector longitude/latitude at mid-date range (see Harris *et al*., 1984). Grp is the asteroid family/group (Warner *et al*., 2009).

(8823) 1987 WS3. (1981 QC1) was discovered on 1987 November 24 by S. McDonald at Anderson Mesa. It is a main-belt asteroid with a semi-major axis of 2.570 AU, eccentricity 0.240, inclination 13.557°, and an orbital period of 4.12 years. Its absolute magnitude is H = 12.8 (JPL, 2020). The WISE/NEOWISE satellite infrared radiometry survey (Masiero et al., 2011) found a diameter D = 10.652 ± 0.108 km using an absolute magnitude H = 12.6.

Observations over seven nights collected 351 data points. The period analysis shows a possible bimodal solution for the rotational period of P = 86.0 ± 1.0 h with an amplitude A = 0.24 ± 0.02 mag. This target revealed to be a very slow rotator and the result is based on less than full coverage, so that the true period may differ a few hours.

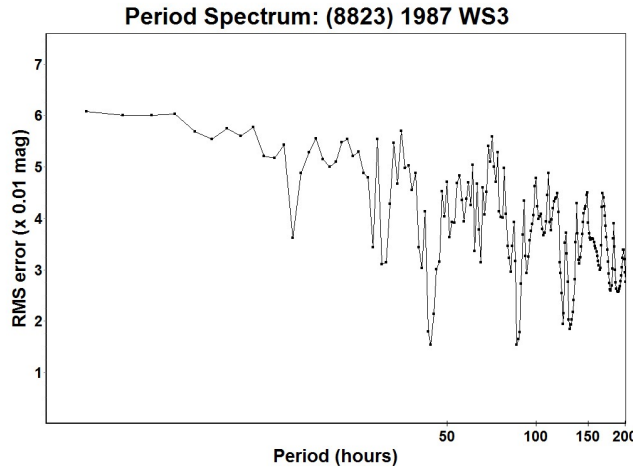

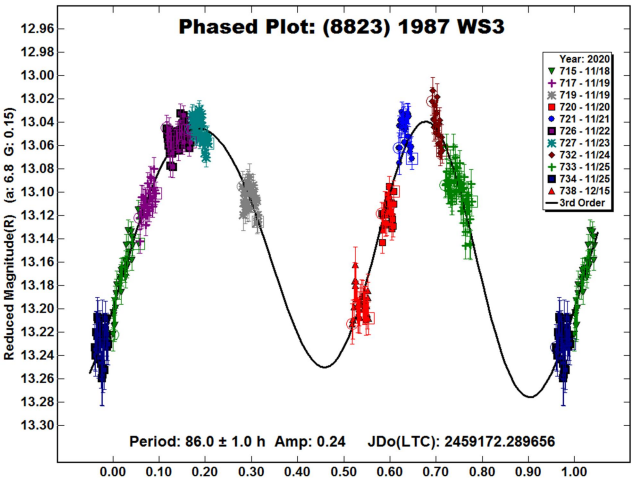

(26568) 2000 ET49 was discovered on 2000 March 9 by LINEAR at Socorro. It is a main-belt asteroid with a semi-major axis of 3.155 AU, eccentricity 0.208, inclination 14.842°, and an orbital period of 5.60 years. Its absolute magnitude is H = 13.0 (JPL, 2020). The WISE/NEOWISE satellite infrared radiometry survey (Masiero et al., 2011) found a diameter D = 16.708 ± 0.160 km using an absolute magnitude H = 13.0.

Observations were conducted over three nights and collected 245 data points. The period analysis shows a result for the rotational period of P = 7.171 ± 0.003 h with an amplitude A = 0.71 ± 0.04 mag as the most likely bimodal solution for this asteroid.

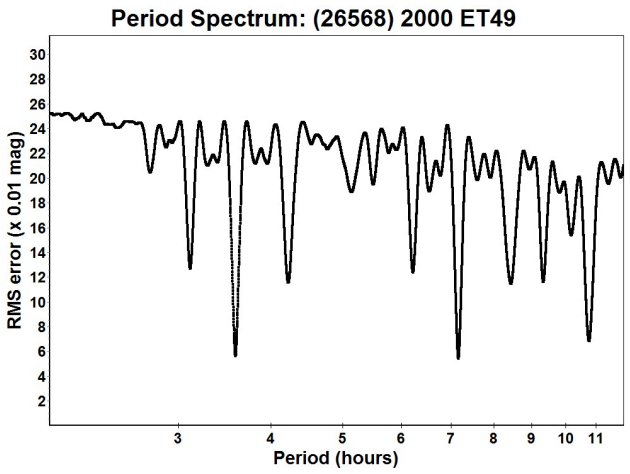

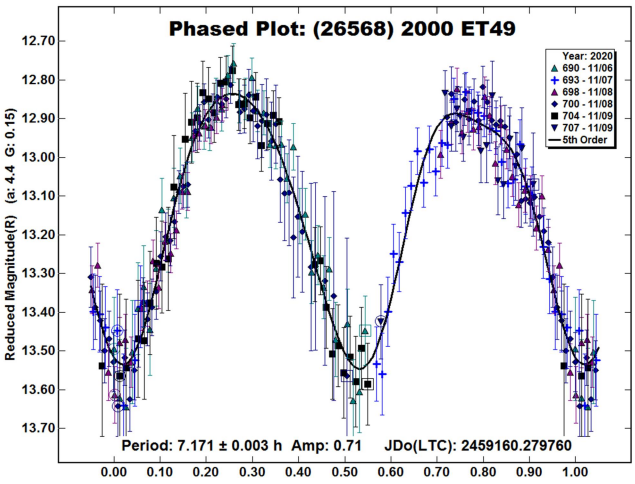

Acknowledgements

Minor Planet Circulars (MPCs) are published by the International Astronomical Union's Minor Planet Center.
https://www.minorplanetcenter.net/iau/ECS/MPCArchive/MPCArchive_TBL.html

References

DSFTA (2020). Dipartimento di Scienze Fisiche, della Terra e dell'Ambiente - Astronomical Observatory.
https://www.dsfta.unisi.it/en/research/labs/astronomical-observatory

Harris, A.W.; Young, J.W.; Scaltriti, F.; Zappala, V. (1984). "Lightcurves and phase relations of the asteroids 82 Alkmene and 444 Gyptis." *Icarus* **57**, 251-258.

JPL (2020). Small-Body Database Browser.
http://ssd.jpl.nasa.gov/sbdb.cgi#top

Masiero, J.R.; Mainzer, A.K.; Grav, T.; Bauer, J.M.; Cutri, R.M.; Dailey, J.; Eisenhardt, P.R.M.; McMillan, R.S.; Spahr, T.B.; Skrutskie, M.F.; Tholen, D.; Walker, R.G.; Wright, E.L.; DeBaun, E.; Elsbury, D.; Gautier IV, T.; Gomillion, S.; Wilkins, A. (2011). "Main Belt Asteroids with WISE/NEOWISE. I. Preliminary Albedos and Diameters." *Astrophys. J.* **741**, A68.

Masiero, J.R.; Grav, T.; Mainzer, A.K.; Nugent, C.R.; Bauer, J.M.; Stevenson, R.; Sonnett, S. (2014). "Main-belt Asteroids with WISE/NEOWISE: Near-infrared Albedos." *Astrophys. J.* **791**, 121.

Warner, B.D.; Harris, A.W.; Pravec, P. (2009). "The Asteroid Lightcurve Database." *Icarus* **202**, 134-146. Updated 2020 Oct. *http://www.minorplanet.info/lightcurvedatabase.html*

Warner, B.D. (2018). MPO Software, MPO Canopus v10.7.7.0. Bdw Publishing. *http://minorplanetobserver.com*

ROTATION PERIOD OF KORONIS FAMILY MEMBER 1840 HUS

Stephen M. Slivan, Claire McLellan-Cassivi,
Rila Shishido, Nieky Wang
Massachusetts Institute of Technology,
Dept. of Earth, Atmospheric, and Planetary Sciences
77 Mass. Ave. Rm. 54-410, Cambridge, MA 02139
slivan@mit.edu

(Received: 2021 Jan 7)

We report rotation lightcurves of 1840 Hus observed during its apparition in 2020. The constraints from our data, combined with a reanalysis of published lightcurves recorded in 2009, yield a secure rotation period of 4.7483 ± 0.0008 h.

Koronis family member 1840 Hus was observed in 2020 as a "target of opportunity" during an ongoing observing program to study rotation properties of the family's brighter objects (Slivan et al., 2008). In the literature we find lightcurves of Hus from only a single previous apparition in 2009, with considerable noise in the data and an uncertain derived rotation period of 4.780 h (Clark, 2010). Subsequent statistical analyses of "sparse data" from photometric surveys suggest a slightly shorter period of 4.749 h (Erasmus et al., 2020) and report a sidereal period and spin vector (Durech et al., 2016).

Observations were made on 14 nights over a 34-night interval in 2020 (Table I) using 0.36-m telescopes at the Wallace Astrophysical Observatory in Westford, MA. Each system imaged a 22 arcmin square field of view at a resolution of 1.3 arcsec per pixel, using an SBIG STL-1001 CCD camera and *R* filter. Image processing and measurement were as described by Slivan et al. (2008), except that for Hus as a fainter object observed with smaller telescopes, we chose synthetic aperture sizes guided by the experience of Howell (1989) for the on-chip relative photometry.

The lightcurves show that Hus completes either four, five, or six rotations in about 23.7 hours; all three candidate periods yield credible doubly-periodic composites. However, these data cannot further distinguish the true period from the aliases because the individual unbroken spans of lightcurve are too short relative to the periods, a consequence of Hus's southern declination in 2020 during northern hemisphere summer, combined with a zone of obstructed telescope view across the meridian at low altitudes.

To resolve the ambiguity, we reanalyzed the published lightcurves from the 2009 apparition, which include spans of nightly coverage that are longer than the candidate periods. Given the noise in these data we used a "noise spectrum" approach, fitting a Fourier series model including through the 2nd harmonic to the lightcurves in order to test a range of trial rotation periods that includes the three candidates. The resulting graph (Fig. 1) shows that 4.748 h is the only period that is consistent with the lightcurves from both 2009 and 2020. Our final result of 4.7483 ± 0.0008 h (Fig. 2) is consistent with the published periods based on "sparse" data.

Acknowledgments

We thank Dr. Michael Person and Timothy Brothers for allocation of telescope time and for observer instruction and support, and especially for retooling to enable summer research at Wallace to happen remotely. The student observers were supported by a grant from MIT's Undergraduate Research Opportunities Program. We thank Dr. Maurice Clark for providing to us his data from 2009.

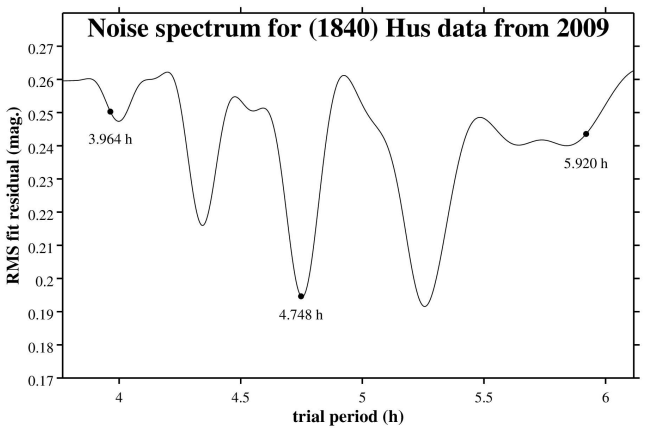

Figure 1. "Noise spectrum" graph for the lightcurves of (1840) Hus recorded during the 2009 apparition by Clark (2010). The candidate periods allowed by the 2020 lightcurves are highlighted; only 4.748 h is consistent with the data from both apparitions.

Number	Name	yyyy mm/dd	Phase	L_{PAB}	B_{PAB}	Period(h)	P.E.	Amp	A.E.
1840	Hus	2020 07/21-08/23	*9.1,4.0	321	-3	4.7483	0.0008	0.42	0.05

Table I. Observing circumstances and results. Solar phase angle is given for the first and last dates; the asterisk indicates that the phase angle reached a minimum within that interval. L_{PAB} and B_{PAB} are the phase angle bisector longitude and latitude at mid-date range.

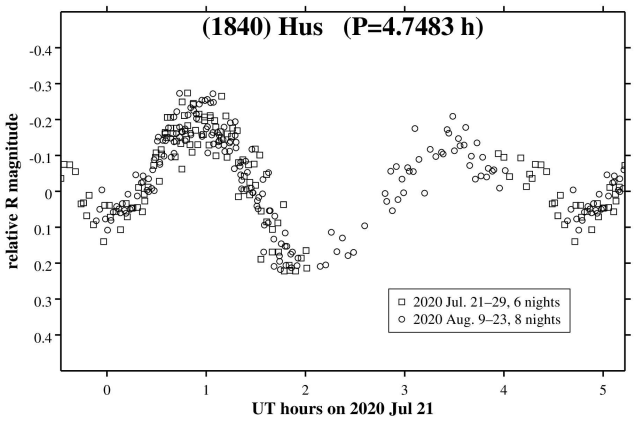

Figure 2. Folded composite lightcurve of (1840) Hus during its 2020 apparition, showing one rotation period plus the earliest and latest 10% repeated. The data are relative photometry only, and have been shifted in brightness to form a self-consistent composite.

References

Clark, M. (2010). "Asteroid Lightcurves from the Chiro Observatory." *Minor Planet Bull.* **37**, 89–92.

Durech, J.; Hanus, J.; Oszkiewicz, D.; Vanco, R. (2016). "Asteroid Models from the Lowell Photometric Database." *Astron. Astrophys.* **587**, A48.

Erasmus, N.; Navarro-Meza, S.; McNeill, A.; Trilling, D.E.; Sickafoose, A.A.; Denneau, L.; Flewelling, H.; Heinze, A.; Tonry, J.L. (2020). "Investigating Taxonomic Diversity within Asteroid Families through ATLAS Dual-band Photometry." *Ap. J. Suppl. Ser.* **247**, A13.

Howell, S.B. (1989). "Two-dimensional Aperture Photometry: Signal-to-noise Ratio of Point-source Observations and Optimal Data-extraction Techniques." *PASP* **101**, 616–622.

Slivan, S.M.; Binzel, R.P.; Boroumand, S.C.; Pan, M.W.; Simpson, C.M.; Tanabe, J.T.; Villastrigo, R.M.; Yen, L.L.; Ditteon, R.P.; Pray, D.P.; Stephens, R.D. (2008). "Rotation Rates in the Koronis Family, Complete to $H \approx 11.2$." *Icarus* **195**, 226–276.

VISUAL OBSERVATION OF 3000+ MINOR PLANETS

Andrew Salthouse
560 Heritage Road, Millington NJ 07946 USA
asalthouse@hotmail.com

(Received: 2020 Feb 21)

The author describes the results of visually observing 3,028 distinct minor planets over a 54-year period.

Unlike most celestial objects, the minor planets of our Solar System are both faint and constantly on the move, so that finding them is a challenge to the skill of visual observers. Tracking these small objects requires planning and perseverance.

The methods used to plan, prepare, observe, confirm, and record the author's observations of minor planets are described in Salthouse (2019). He started observing the major planets as a teenager in 1965, beginning with Jupiter and Saturn in a small refractor. His first minor planet observations began in late 1966 with a 4-inch reflector, and by the spring of 1967 he had captured 1 Ceres, 2 Pallas, 3 Juno, and 4 Vesta. These observations were enabled by charts in *Sky & Telescope* magazine (2020). Over the ensuing decades the author observed these four objects about one hundred times each.

Note that the author started this process before the internet, personal computers, spreadsheets, or even calculators. He performed all his calculations on blue-lined paper with a slide rule. Today, when he shows the latter to his colleagues, they have no idea how it works, but it is one of his favorite reminders of those days.

The process of tracking down minor planets was very haphazard for the next couple of decades, as the author was hampered by two key factors: a lack of information about where to locate many asteroids, and a lack of sufficient aperture to observe most of them.

Fortunately, the *RASC Observer's Handbook* (2020) and *Sky & Telescope* (2020) provided just enough information to track down a handful of bright asteroids over the years. Consequently, by 1990 the author had observed 35 distinct minor planets, a rather unimpressive result after 24 years of effort.

As with many amateurs, the author caught "aperture fever" and continually upgraded the size of his telescopes. He used a 10-inch equatorial reflector throughout the 1970s and 1980s but eventually purchased a 17-inch Dobsonian reflector in 1989. This was donated to a local community college and replaced by an 18-inch Dobsonian in 2007. Thus, all searching and tracking operations were fully manual.

Commencing in August 1990, the author had a private observatory to house his new reflector. Up to that point he had made only 190 observations of 35 different objects, but he used his new facilities to systematically re-observe every asteroid that he had seen before. More than 99% of all minor planet observations were made from this home observatory in central New Jersey.

Also, in 1990, the author was directed to Brian Warner, who was publishing the *Minor Planet Observer* print edition, which replaced by a web-only version in 2000 (Warner, 2020). This finally gave the author the means to begin a thorough and systematic search for every minor planet within the magnitude limit of his telescopes.

The combination of a new observatory with a large reflector and the *Minor Planet Observer* monthly publication and then web site was the impetus the author needed to initiate a serious search for minor planets. Over the 30-year period from 1990 August through 2020 August, the author visually observed more than 3,000 distinct objects.

The author quickly realized that visual identification of faint targets had its pitfalls, as each object had to be unambiguously identified from drawings of the star field made at the eyepiece. He then developed the "three observations rule", which requires each object to be seen on at least two different nights *and* at least twice on the same night, confirming the motion against the stellar background. Objects that did not meet these criteria had to be rejected as unconfirmed.

This rule was always employed when searching for a minor planet for the first time, but it was relaxed somewhat when observing brighter objects at 2nd and subsequent oppositions.

Results

Between 1966 December and 2020 December, the author visually observed 3,028 distinct minor planets. All of the objects observed prior to 1990 August were subsequently re-observed.

Table I shows the entire set of observations arranged by the number of oppositions; 30% were observed at a single opposition, 38% were seen at two different oppositions, and the rest were seen at three or more. The dwarf planets Ceres and Pluto are excluded from the minor planet totals.

Oppositions	Observed
1	920
2	1,161
3-4	425
5-6	200
7-8	120
9-10	78
11+	124
Total	**3,028**

Table I. Number of minor planets observed vs number of oppositions.

Table II shows the distribution of observations arranged by minor planet number. The lowest numbered minor planet *not* seen was 452 Hamiltonia. Out of the first 1,000 numbered objects, sixteen were never seen.

Asteroid Number	Total Seen	Total Oppositions	Total Observations
2 - 1000	983	5,903	17,653
1001 - 2000	761	1,667	5,195
2001 - 3000	400	656	2,171
3001 - 4000	248	368	1,252
4001 - 5000	156	213	758
5001+	480	554	2,134
Minor Planets	**3,028**	**9,361**	**29,163**

Table II. Number of minor planets observed vs assigned number.

The median minor planet number observed was 1625. The author averaged 3.1 oppositions per minor planet, and 3.1 observations per opposition. Thus, the average number of observations per object was 9.6, but the median number was only 6. As one might expect, the distribution of observations per minor planet was highly skewed, with lower numbered objects being observed far more frequently than the higher numbered ones. Objects numbered 500 or less were observed 24.5 times on average whereas those numbered over 5000 were observed only 4.5 times each.

In addition to the minor planets, the author also made 450 observations of 64 comets, 294 of the dwarf planets Ceres and Pluto, 2,761 of the three rocky planets, and 7,663 of the four gas giant planets, for a total in excess of 40,000 logged Solar System observations.

There were roughly 4,300 known minor planets when the author began observing them in 1966. That number has grown more than a hundred-fold since, but the author at least has the satisfaction of having observed most of the objects known to exist at the time he started, plus several hundred more discovered after he began.

Acknowledgements

The author thanks Mr. Brian Warner for providing the *Minor Planet Observer* (2020) suite of products and services, without which this work would have been impossible. He also thanks Ms. Mary Ellen Salthouse for the gift of an 18-inch reflector in the summer of 2007. He is especially grateful for the encouragement of his colleagues Mr. Frederick Pilcher, Mr. Roger Harvey, Mr. Lawrence Garrett, Mr. Gerard Faure, and Mr. Brian Warner over many years. It is only fair to point out that Mr. Harvey achieved this milestone long before the author.

References

Salthouse, A. (2019). "Visual Observation of Minor Planets." *Minor Planet Bulletin* **46**, 5-7.

Sky & Telescope (2020). AAS Sky Publishing LLC. *https://skyandtelescope.org/*

RASC (2020). *Royal Astronomical Society of Canada Observer's Handbook*. Royal Astronomical Society of Canada. *https://www.rasc.ca/*

Warner, B. (2020). Minor Planet info website. *www.MinorPlanet.Info*

LIGHTCURVES OF SIX ASTEROIDS

Andrea Ferrero
Bigmuskie Observatory (B88)
via Italo Aresca 12
14047 Mombercelli, Asti, ITALY
bigmuskie@outlook.com

(Received: 2021 Jan 15)

In the following paper we present the result of a photometric survey on six asteroids: 2262 Mitidika, P = 28.257 ± 0.004 h, A = 0.26 mag; 3955 Bruckner, P = 7.549 ± 0.002 h, A = 0.25 mag; (16559) 1991 VA3, P = 473.34 ± 0.27 h, A = 1.17 mag; (21182) 1994 EC2, P = 12.981 ± 0.002 h, A = 0.10 mag; (22393) 1994 QV, P = 3.419 ± 0.001 h, A = 0.23 mag; (43028) 1999 VE23, P = 3.940 ± 0.002 h, A = 0.36 mag.

From 2020 September to 2021 January, the Bigmuskie Observatory worked on six asteroids to determinate their rotational periods. Unfortunately observations during 2020 December and the first days of 2021 January were almost impossibile due to bad weather and so the work on some targets was interrupted and restarted when the brightness was very low All targets were found on the CALL website ephemeris generator (Warner, 2020).

All targets were worked with the same setup: a Marcon 0.30-m *f*/8 Ritchey-Chretién telescope coupled with a Moravian G3 01000 camera equipped with a KAF-1001E CCD with a pixel array of 1024 ×1024 × 24 microns. This provided a pixel scale of exactly 2 arcsec/pixel and a field of view of 36×36 arcmin. Exposures were unguided and taken through a Toptec R filter to reduce light pollution as much as possible. The telescope and camera were under the control of *Maxim DL* (Diffraction Limited, 2020) and *The Sky 6 Pro* (Bisque, 2020). *Voyager* (Starkeeper, 2020) controlled the entire observatory. All photometric reductions were done with *MPO Canopus* v10.7.12.9 (Warner, 2018), which permits obtaining precise night-to-night zero point calibration using the Comparison Star Selector utility.

2262 Mitidika: A previous period of 28.0933 ± 0.0005 h measured by Pál et al. (2020) is reported in the LCDB (Warner et al., 2009).

Observed over a period of forty days and eight sessions showed a slightly different rotational period of P = 28.257 ± 0.004 h with an amplitude of A = 0.26 mag. An attempt to fit the sessions at the previously reported period produced poor results.

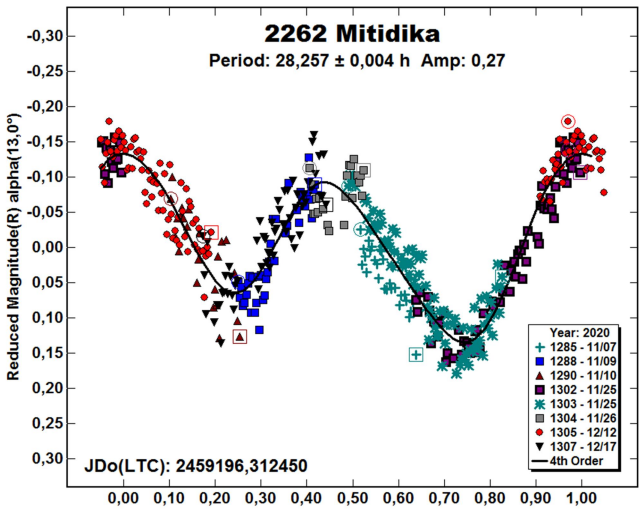

3955 Bruckner was observed on three nights from 2020 December 13 to 2021 January 10. The final result is a period of P = 7.549 ± 0.002 h, A = 0.25 mag.

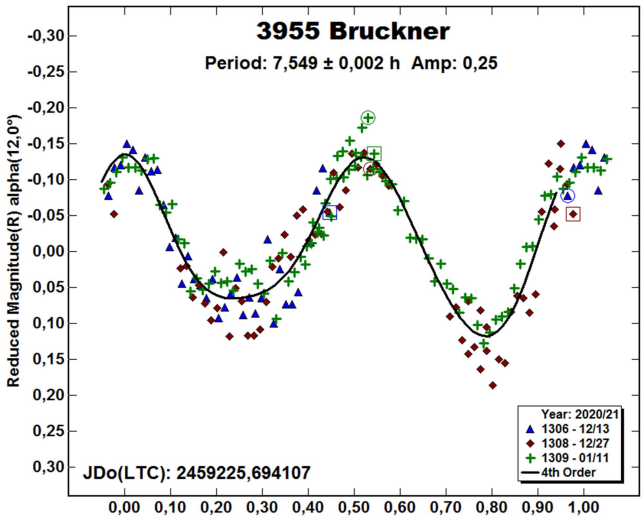

(16559) 1991 VA3. This target required about two months of work and eighteen sessions due to its very long period. The previous period of 435.193 ± 0.005 h found in the LCDB Database was measured by Pál et al. (2020). The period found at the Bigmuskie Observatory is P = 437.34 ± 0.27 h, A = 1.17 mag but a solution at 435 h is also possible, even if *MPO Canopus* prefers the longer one.

Number	Name	yyyy mm/dd	Phase	L_{PAB}	B_{PAB}	Period(h)	P.E.	Amp	A.E.	Grp
2262	Mitidika	2020 11/07-12/18	13,14.3	62	16	28.257	0.004	0.26	0.05	MB-I
3955	Bruckner	2020 12/13-01/11	12.03,5.6	110	13	7.549	0.002	0.25	0.05	EOS
16559	1991 VA3	2020 09/16-11/07	10.6,24.9	353	15	437.34	0.27	1.17	0.05	EUN
21182	1994 EC2	2020 10/13-11/21	3.7,27.4	18	9	12.981	0.002	0.10	0.05	PHO
22393	1994 QV	2020 09/30-11/22	14,18.7	26	9	3.419	0.001	0.23	0.05	MB
43028	1999 VE23	2020 11/19-11/23	9.7,7.5	73	1	3.940	0.002	0.36	0.05	MB-I

Table I. Observing circumstances and results. The phase angle is given for the first and last date. If preceded by an asterisk, the phase angle reached an extremum during the period. L_{PAB} and B_{PAB} are the approximate phase angle bisector longitude/latitude at mid-date range (see Harris et al., 1984). Grp is the asteroid family/group (Warner et al., 2009).

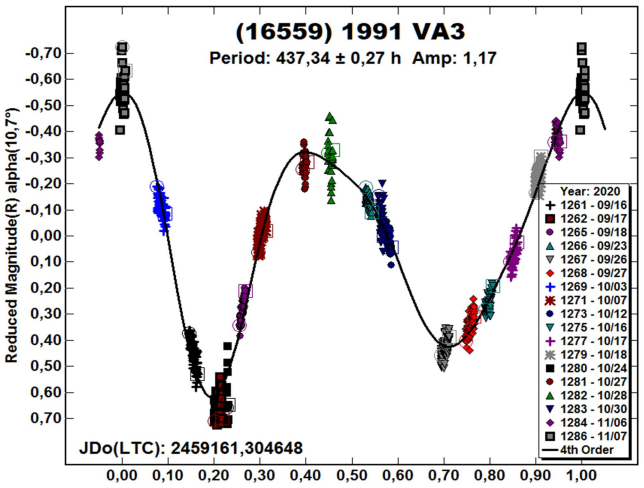

(21182) 1994 EC2. Due to the very low amplitude and a period close to half an Earth day, it took a month of observations and ten sessions to reach the final result of P = 12.981 ± 0.002 h and A = 0.10 mag.

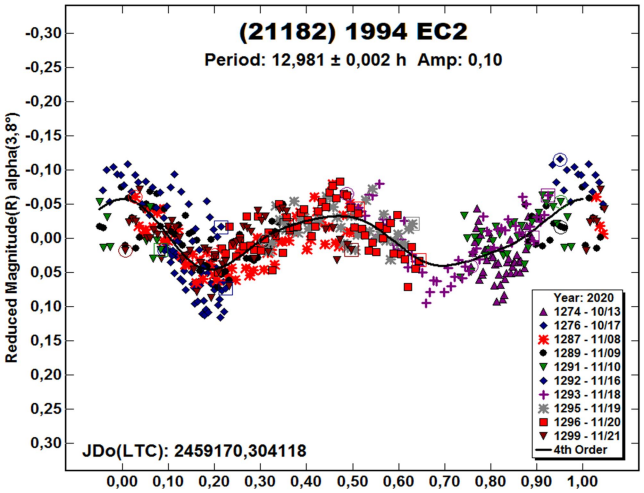

(22393) 1994 QV. This target was observed in three sessions but separated by a fairly long period of time. The first one on 30 September was worked in the second part of the night after the work on another asteroid ended. Observations continued on 5 October and then, after a long period of bad weather, on 22 November. The period found is P = 3.419 ± 0.001 h and A = 0.23 mag.

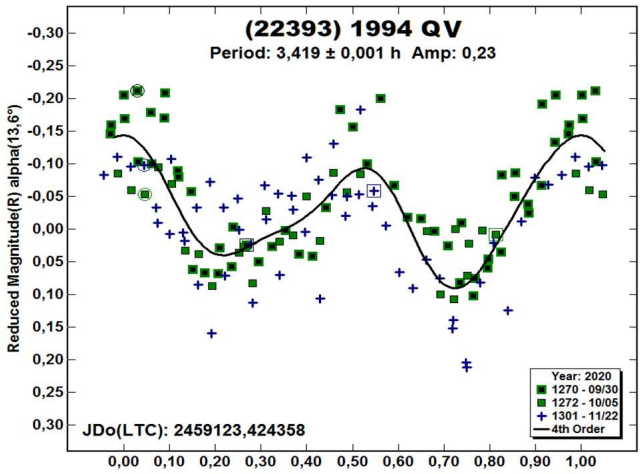

(43028) 1999 VE23. After four sessions, the period was found to be P = 3.940 ± 0.002 h and A = 0.36 mag.

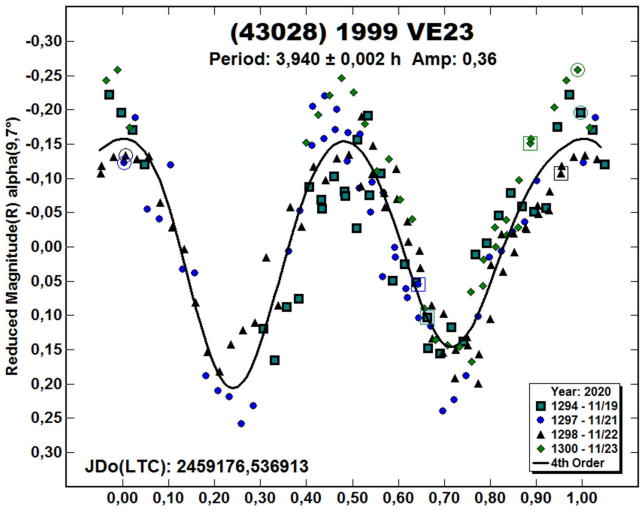

References

Bisque (2020). Software Bisque. *The Sky Pro 6*. *http://www.bisque.com*

Diffraction Limited (2020). *Maxim DL* software. *http://diffractionlimited.com/product/maxim-dl/*

Harris, A.W.; Young, J.W.; Scaltriti, F.; Zappala, V. (1984). "Lightcurves and phase relations of the asteroids 82 Alkmene and 444 Gyptis." *Icarus* **57**, 251-258.

Pál, A.; Szakáts, R.; Kiss, C.; Bódi, A.; Bognár, Z.; Kalup, C.; Kiss, L.; Marton, G.; Molnár, L.; Plachy, E.; Sárneczky, K.; Szabó, G.; Szabó, R. (2020). "Solar System Objects Observed with TESS - First Data Release: Bright Main-belt and Trojan Asteroids from the Southern Survey." *Ap. J. Supl. Ser.* **247**, 26-34.

Voyager (2020). Observatory control software. *http://software.starkeeper.it*

Warner, B.D.; Harris, A.W.; Pravec, P. (2009). "The Asteroid Lightcurve Database." *Icarus* **202**, 134-146. Updated 2021 Jan. *http://www.minorplanet.info/lightcurvedatabase.html*

Warner, B.D. (2018). *MPO Canopus* software. *http://bdwpublishing.com*

Warner, B.D. (2020). CALL website ephemeris generator. *http://www.minorplanet.info/PHP/call_OppLCDBQuery.php*

PHOTOMETRY OF 12 ASTEROIDS FROM SOPOT ASTRONOMICAL OBSERVATORY: 2020 OCTOBER- DECEMBER

Vladimir Benishek
Belgrade Astronomical Observatory
Volgina 7, 11060 Belgrade 38, SERBIA
vlaben@yahoo.com

(Received: 2021 Jan 15, Revised: 2021 Mar 5)

A brief overview of the lightcurve and synodic rotation period determination for 12 asteroids from CCD photometric observations conducted at Sopot Astronomical Observatory (SAO) in the time span 2020 October - December is presented in this paper.

Photometric observations of 12 asteroids were conducted at Sopot Astronomical Observatory (SAO) from 2020 October through 2020 December in order to determine the asteroids' synodic rotation periods. For this purpose, two 0.35-m *f*/6.3 Meade LX200GPS Schmidt-Cassegrain telescopes were employed. The telescopes are equipped with a SBIG ST-8 XME and a SBIG ST-10 XME CCD cameras. The exposures were unfiltered and unguided for all targets. Both cameras were operated in 2×2 binning mode, which produces image scales of 1.66 arcsec/pixel and 1.25 arcsec/pixel for ST-8 XME and ST-10 XME cameras, respectively. Prior to measurements, all images were corrected using dark and flat field frames.

Photometric reduction was conducted using *MPO Canopus* (Warner, 2018). Differential photometry with up to five comparison stars of near solar color ($0.5 \leq$ B-V ≤ 0.9) was performed using the Comparison Star Selector (CSS) utility. This helped ensure a satisfactory quality level of night-to-night zero-point calibrations and correlation of the measurements within the standard magnitude framework. Field comparison stars were calibrated using standard Cousins R magnitudes derived from the Carlsberg Meridian Catalog 15 (VizieR, 2020) Sloan r' magnitudes using the formula: R = r' - 0.22 in all cases presented in this paper. In some instances, small zero-point adjustments were necessary in order to achieve the best match between individual data sets in terms of achieving the most favorable statistical indicators of Fourier fit goodness.

Lightcurve construction and period analysis was performed using *Perfindia* custom-made software developed in the R statistical programming language (R Core Team, 2020) by the author of this paper. The essence of its algorithm is reflected in finding the most favorable solution for rotational period by minimizing the *residual standard error* of the lightcurve Fourier fit.

The lightcurve plots presented here show so-called 2% error for rotational periods, i.e., an error that would cause the last data point in a combined data set by date order to be shifted by 2% (Warner, 2012) and which is represented by the following formula: $\Delta P = (0.02 * P^2) / T$, where P and T are the rotational period and the total time span of observations, respectively. Both of these quantities must be expressed in the same units.

Some of the targets presented in this paper were observed within the Photometric Survey for Asynchronous Binary Asteroids (*BinAstPhot Survey*) under the leadership of Dr Petr Pravec from Ondřejov Observatory, Czech Republic.

Table I gives the observing circumstances and summarizes results.

Observations and Results

1165 Imprinetta. In reviewing previous findings, multiple rotation period determinations were reported and all yielded inconsistent results: 7.9374 h (Monson and Kipp, 2004), 8.107 h (Menke, 2005), 3.66 h (Behrend, 2018web) and a sidereal period of 10.8087 h found by Ďurech and Hanuš (2018). In an attempt to contribute to resolving this rotation period confusion, photometric observations were carried out at SAO in 2020 November-December over only 4 nights due to bad weather conditions. Nevertheless, the data collected were sufficient to unambiguously establish a value for period of $P = 10.797 \pm 0.006$ h, which is closest to the result found by Ďurech and Hanuš.

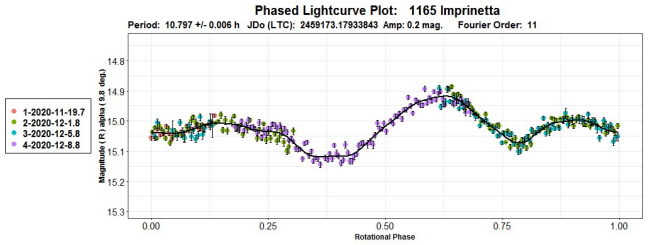

Number	Name	2020/mm/dd	Phase	L_{PAB}	B_{PAB}	Period (h)	P.E.	Amp	A.E.	Grp
1165	Imprinetta	11/19-12/08	9.8,14.7	31	-4	10.797	0.006	0.20	0.02	MB-O
2424	Tautenburg	10/18-10/23	13.8,12.0	51	3	5.469	0.006	0.15	0.02	MB-I
3001	Michelangelo	10/21-10/31	15.1,17.5	13	24	8.345	0.006	0.28	0.03	MB-I
3048	Guangzhou	10/25-10/28	13.8,12.8	58	-1	3.811	0.006	0.18	0.03	MB-I
3133	Sendai	11/30-12/02	23.2,22.8	109	8	5.75	0.03	0.75	0.02	FLOR
5111	Jacliff	11/22-12/17	*12.1,1.5	85	-2	2.8400	0.0003	0.24	0.01	V
6701	Warhol	11/25-12/10	*7.7,9.2	67	15	3.5230	0.0007	0.23	0.01	EUN
17312	7622 P-L	10/11-10/18	14.5,10.3	39	-2	2.5790	0.0009	0.11	0.03	FLOR
18418	Ujibe	10/16-10/27	12.1,4.8	40	-2	3.470	0.001	0.28	0.02	MB-I
21242	1995 WZ41	10/18-10/21	22.2,20.9	53	9	5.45	0.02	0.55	0.01	PHO
24038	1999 SL8	11/06-11/08	8.1,7.3	55	2	2.877	0.006	0.10	0.03	MB-I
137311	1999 TX9	10/27-11/09	18.4,10.2	58	1	9.926	0.007	0.17	0.03	PHO

Table I. Observing circumstances and results. Phase is the solar phase angle given at the start and end of the date range. If preceded by an asterisk, the phase angle reached an extrema during the period. L_{PAB} and B_{PAB} are the average phase angle bisector longitude and latitude. Grp is the asteroid family/group (Warner *et al.*, 2009): EUN = Eunomia, FLOR = Flora, MB-I/O = main-belt inner/outer, PHO = Phocaea, V = Vestoid.

2424 Tautenburg. Interestingly, despite being a relatively low numbered asteroid its rotation period has not yet been established. The 2020 October SAO data led to an unequivocal synodic rotation period result of $P = 5.469 \pm 0.006$ h.

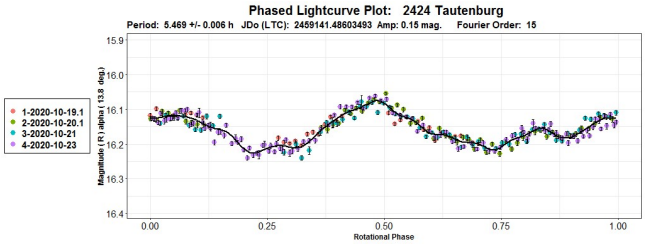

3001 Michelangelo. Previous consistent rotation period results were found by Ditteon and West (2011, 8.338 h), Waszczak et al. (2015, 8.343 h) and by Pál et al. (2020, 8.35088 h). Period analysis of the 2020 October SAO data collected over 6 nights shows a similar period result: $P = 8.345 \pm 0.006$ h.

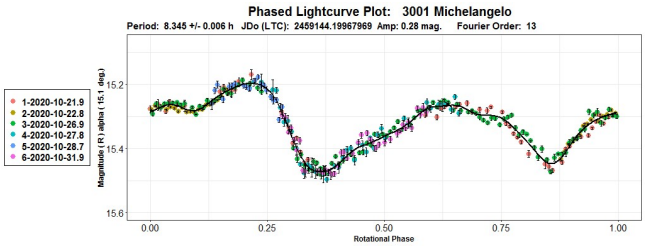

3048 Guangzhou. Previously established rotation period results by Chang et al. (2015, 3.81 h) and Waszczak et al. (2015, 3.808 h) are fully consistent with the rotation period of $P = 3.811 \pm 0.006$ h, found analyzing the 2020 October SAO data obtained over 3 nights.

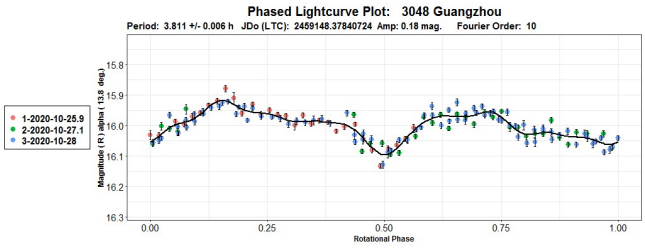

3133 Sendai. A synodic rotation period found from the SAO data obtained over only two consecutive nights in early 2020 December ($P = 5.75 \pm 0.03$ h) is in good agreement with the previously established values by Waszczak et al. (2015, 5.749 h), Erasmus et al. (2020, 5.749 h) and Pál et al. (2020, 5.75011 h).

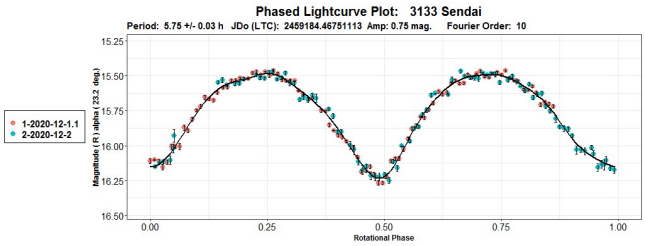

5111 Jacliff. Data taken on two nights in late 2020 November and early 2020 December led to a rotation period of $P = 2.8400 \pm 0.0003$ h, a value in very good agreement with the previous rotation period determination results by Behrend (2005web, 2.839 h), Erasmus et al. (2020, 2.840 h), and sidereal period found by Hanuš et al. (2016, 2.83990 h).

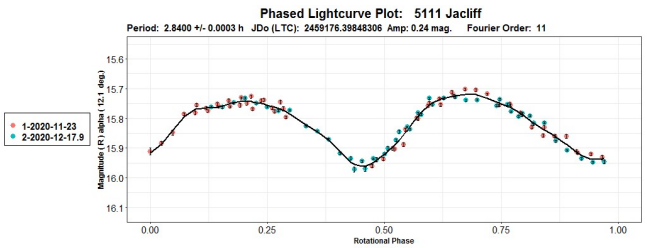

6701 Warhol. A rotation period of 3.52157 h was recently found by Pál et al. (2020) for this Eunomia family asteroid. Period analysis conducted upon the 2020 November-December SAO data obtained on two nights confirms the previously found result indicating a bimodal solution for period of $P = 3.5230 \pm 0.0007$ h as an equivocally most favorable one.

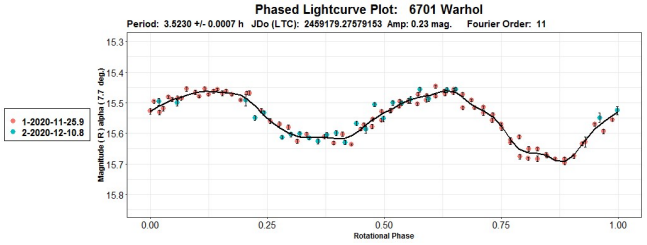

(17312) 7622 P-L. A check for previous rotation period determination reports shows no results. An analysis conducted on the 2020 October SAO data finds a rotation period of $P = 2.5790 \pm 0.0009$ h to be statistically the most plausible solution.

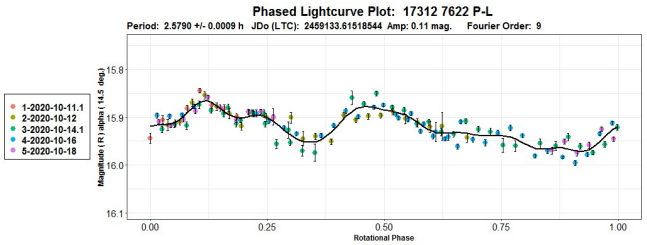

18418 Ujibe. Waszczak et al. (2015) found a rotation period of 3.470 h for this asteroid. Exactly the same value ($P = 3.470 \pm 0.001$ h) associated with a bimodal lightcurve was obtained from the SAO observations carried out on 5 nights in 2020 October.

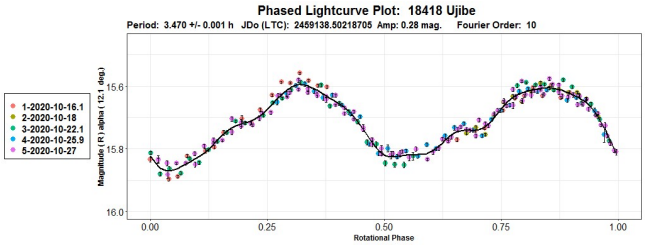

(21242) 1995 WZ41. A Phocaea family asteroid with a previously unknown rotation period observed at the SAO as a program target within the *BinAstPhot Survey* over 3 consecutive nights in 2020 October. A bimodal lightcurve phased to a period of $P = 5.45 \pm 0.02$ h was found as the most plausible solution from the collected data. A rotation period of 5.4535 h was derived by Pravec (2020) by pooling the SAO data with the single-night observations obtained by Marc Deldem in 2020 October.

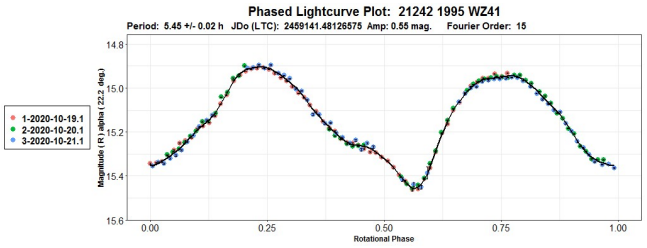

(24038) 1999 SL8. Another *BinAstPhot Survey* target observed on two consecutive nights at the SAO in early 2020 November. Period analysis performed upon the collected data shows a period of P = 2.877 ± 0.006 h. Using the same dataset Pravec (2020) finds a period value of 2.873 ±0.003 h. These results are in good agreement with what was previously established by Waszczak et al. (2015, 2.880 h).

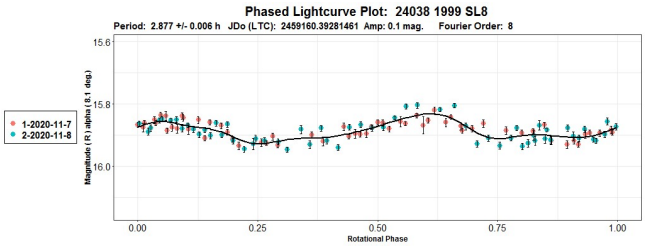

(137311) 1999 TX9. A Phocaea family asteroid and another *BinAstPhot Survey* target with no previously known rotation period. Photometric observations conducted at the SAO in 2020 October-November on 5 nights indicate a value of P = 9.926 ± 0.007 h as an unambiguous synodic rotation period solution. Pravec (2020) finds a value of 9.921 ± 0.005 h analyzing exactly the same dataset.

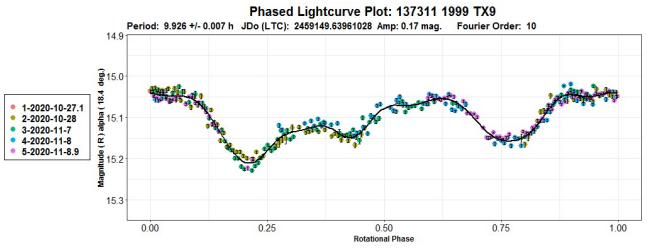

Acknowledgements

Observational work at Sopot Astronomical Observatory is supported by a 2018 Gene Shoemaker NEO Grant from The Planetary Society.

References

Behrend, R. (2005, 2018). Observatoire de Geneve web site. *http://obswww.unige.ch/~behrend/page_cou.html*

Chang, C.-K.; Ip W.-H.; Lin, H.-W.; Cheng, Y.-C.; Ngeow, C.-C.; Yang, T.-C.; Waszczak, A.; Kulkarni, S.R.; Levitan, D.; Sesar, B.; Laher, R.; Surace, J.; Prince, T.A. (2015). "Asteroid Spin-Rate Study Using the Intermediate Palomar Transient Factory." *Ap. J. Suppl. Ser.* **219**, Issue 2, id. 27.

Ditteon, R.; West, J. (2011). "Asteroid Lightcurve Analysis at the Oakley Southern Observatory: 2011 January thru April." *Minor Planet Bull.* **38**, 214-217.

Ďurech, J.; Hanuš, J. (2018). "Reconstruction of Asteroid Spin States from Gaia DR2 Photometry." *Astron. Astrophys.* **620**, id. A91.

Erasmus, N.; Navarro-Meza, S.; McNeill, A.; Trilling, D.E.; Sickafoose, A.; Denneau, L.; Flewelling, H.; Heinze, A.; Tonry, J.L. (2020). "Investigating Taxonomic Diversity within Asteroid Families through ATLAS Dual-band Photometry." *Ap. J. Suppl. Ser*. **247**, A13.

Hanuš, J.; Ďurech, J.; Oszkiewicz, D.A.; Behrend, R.; Carry, B.; Delbo, M.; Adam, O.; Afonina, V.; Anquetin, R.; Antonini, P.; and 159 colleagues. (2016). "New and updated convex shape models of asteroids based on optical data from a large collaboration network." *Astron. Astrophys.* **586**, A108.

Menke, J.L. (2005). "Lightcurves and Periods for Asteroids 471 Papagena, 675 Ludmilla, 1016 Anitra, 1127 Mimi, 1165 Imprinetta, 1171 Rustahawelia, and 2283 Bunke." *Minor Planet Bull.* **32**, 64-66.

Monson, A.; Kipp, S. (2004). "Rotational Periods of Asteroids 1165 Imprinetta, 1299 Mertona, 1645 Waterfield, 1833 Shmakova, 2313 Aruna, and (13856) 1999 XZ105." *Minor Planet Bull.* **31**, 71-73.

Pál, A.; Szakáts, R; Kiss, C.; Bódi, A.; Bognár, Z.; Kalup, C.; Kiss, L.; Marton, G.; Molnár, L.; Plachy, E.; Sárneczky, K.; Szabó, G.; Szabó, R. (2020). "Solar System Objects Observed with TESS - First Data Release: Bright Main-belt and Trojan Asteroids from the Southern Survey." *Astron. J.* **247**, id 26.

Pravec, P. (2020). Photometric Survey for Asynchronous Binary Asteroids web site. *http://www.asu.cas.cz/~ppravec/newres.txt*

R Core Team (2020). R: A language and environment for statistical computing. R Foundation for Statistical Computing. Vienna, Austria. *https://www.R-project.org/*

VizieR (2020). *http://vizier.u-strasbg.fr/viz-bin/VizieR.*

Warner, B.D.; Harris, A.W.; Pravec, P. (2009). "The Asteroid Lightcurve Database." *Icarus* **202**, 134-146. Updated 2020 Aug. *http://www.minorplanet.info/lightcurvedatabase.html*

Warner, B.D. (2012). *The MPO Users Guide: A Companion Guide to the MPO Canopus/PhotoRed Reference Manuals*. BDW Publishing, Colorado Springs, CO.

Warner, B.D. (2018). MPO Canopus software, version 10.7.11.3. *http://www.bdwpublishing.com*

Waszczak, A.; Chang, C.-K.; Ofek, E.O.; Laher, R.; Masci, F.; Levitan, D.; Surace, J.; Cheng, Y.-C.; Ip, W.-H.; Kinoshita, D.; Helou, G.; Prince, T.A.; Kulkarni, S. (2015). "Asteroid Light Curves from the Palomar Transient Factory Survey: Rotation Periods and Phase Functions from Sparse Photometry." *Astron. J.* **150**, A75.

COLLABORATIVE ASTEROID PHOTOMETRY FROM UAI: 2020 OCTOBER-DECEMBER

Lorenzo Franco
Balzaretto Observatory (A81), Rome, ITALY
lor_franco@libero.it

Antonio De Pieri, Antonino Brosio
Parco Astronomico Lilio (K96), Savelli (KR), ITALY

Riccardo Papini, Fabio Salvaggio
Wild Boar Remote Observatory (K49)
San Casciano in Val di Pesa (FI), ITALY

Giulio Scarfi
Iota Scorpii Observatory (K78), La Spezia, ITALY

Alessandro Marchini
Astronomical Observatory, DSFTA - University of Siena (K54)
Via Roma 56, 53100 - Siena, ITALY

Nello Ruocco
Osservatorio Astronomico Nastro Verde (C82), Sorrento, ITALY

Gianni Galli
GiaGa Observatory (203), Pogliano Milanese, ITALY

Massimiliano Mannucci, Nico Montigiani
Osservatorio Astronomico Margherita Hack (A57)
Florence, ITALY

Luciano Tinelli
GAV (Gruppo Astrofili Villasanta), Villasanta, ITALY

Pietro Aceti, Massimo Banfi
Seveso Observatory (C24), Seveso, ITALY

Giorgio Baj
M57 Observatory (K38), Saltrio, ITALY

Giovanni Battista Casalnuovo, Benedetto Chinaglia
Filzi School Observatory (D12), Laives, ITALY

Paolo Bacci, Martina Maestripieri
GAMP - San Marcello Pistoiese (104), Pistoia, ITALY

Alessandro Coffano, Wladimiro Marinello
UAB - Unione Astrofili Bresciani
Osservatorio Serafino Zani (130), Lumezzane, ITALY

Liviano Betti, Fabio Mortari
Gruppo Astrofili DLF Rimini
Osservatorio Astronomico Monte San Lorenzo, Monte Grimano Terme, ITALY

(Received: 2021 Jan 13)

Photometric observations of five asteroids were made in order to acquire lightcurves for shape/spin axis modeling. The synodic period and lightcurve amplitude were found for 102 Miriam: 23.63 ± 0.01 h, 0.14 mag; 635 Vundtia: 11.784 ± 0.004 h, 0.20 mag; 1342 Brabantia: 4.175 ± 0.001 h, 0.13 mag; 2346 Lilio: 3.0290 ± 0.0005 h, 0.18 mag; (153201) 2000 WO107: 5.026 ± 0.001 h, 1.14 mag.

Collaborative asteroid photometry was done inside the Italian Amateur Astronomers Union (UAI; 2020) group. The targets were selected mainly in order to acquire lightcurves for shape/spin axis modeling. Table I shows the observing circumstances and results.

The CCD observations were made in 2020 October-December using the instrumentation described in the Table II. Lightcurve analysis was performed at the Balzaretto Observatory with *MPO Canopus* (Warner, 2019). All the images were calibrated with dark and flat frames and converted to R magnitudes using solar colored field stars from CMC15 catalogue, distributed with *MPO Canopus*. For brevity, the following citations to the asteroid lightcurve database (LCDB; Warner et al., 2009) will be summarized only as "LCDB".

102 Miriam is a C-type (Bus & Binzel, 2002) middle main-belt asteroid discovered on 1868 August 22 by C.H.F. Peters at Clinton. Collaborative observations were made over eleven nights. The period analysis shows a synodic period of P = 23.63 ± 0.01 h with an amplitude A = 0.14 ± 0.02 mag. The period is close to the previously published results by Pilcher (2008, 2013).

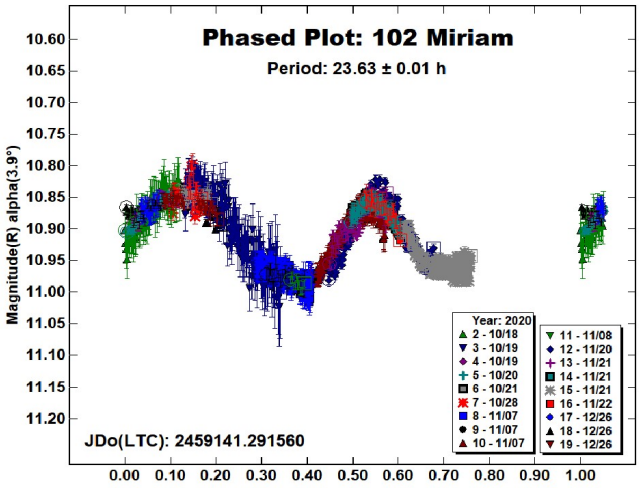

635 Vundtia is a C-type (Bus & Binzel, 2002) outer main-belt asteroid discovered on 1907 June 9 by K. Lohnert at Heidelberg. Collaborative observations were made over six nights. The period analysis shows a synodic period of P = 11.784 ± 0.004 h with an amplitude A = 0.20 ± 0.02 mag. The period is close to the previously published results in the LCDB.

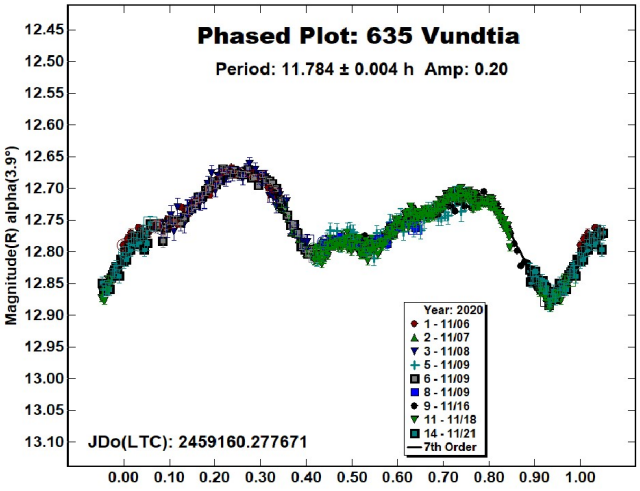

1342 Brabantia is an X-type (Tholen, 1984) inner main-belt asteroid discovered on 1935 February 13 by H. Van Gent at Johannesburg. Collaborative observations were made over eight nights. We found a synodic period of P = 4.175 ± 0.001 h with an amplitude A = 0.13 ± 0.03 mag. The period is close to the previously published results in the LCDB.

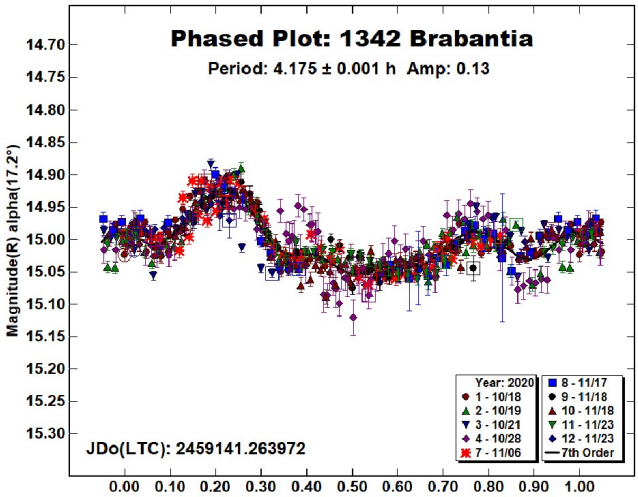

2346 Lilio is a C-type (Bus & Binzel, 2002) inner main-belt asteroid discovered on 1934 February 5 by K. Reinmuth at Heidelberg. Collaborative observations were made over six nights. We found a synodic period of P = 3.0290 ± 0.0005 h with an amplitude A = 0.18 ± 0.04 mag. The period is close to the previously published results in the LCDB.

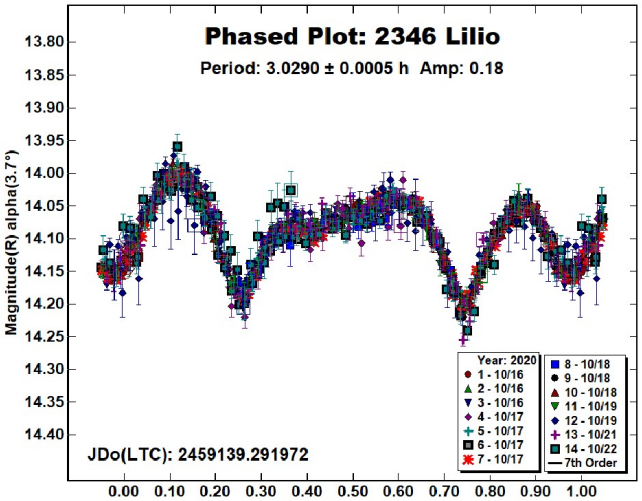

(153201) 2000 WO107 is an X-type (Bus & Binzel, 2002) Aten near-Earth asteroid discovered on 2000 November 29 by LINEAR at Socorro. Observations were made at Filzi School Observatory (D12) during the close approach to Earth and at GAMP (104) Observatory in the following days. We found a bimodal solution with a synodic period of P = 5.026 ± 0.001 h and an amplitude A = 1.14 ± 0.16 mag. Radar images from Goldstone radio telescope revealed that it is a contact binary asteroid (Goldstone, 2020)

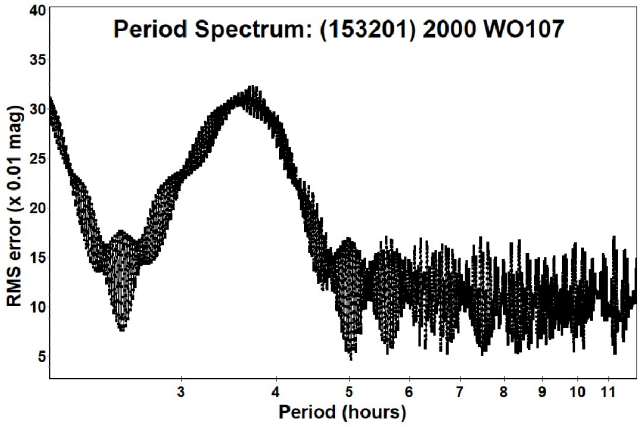

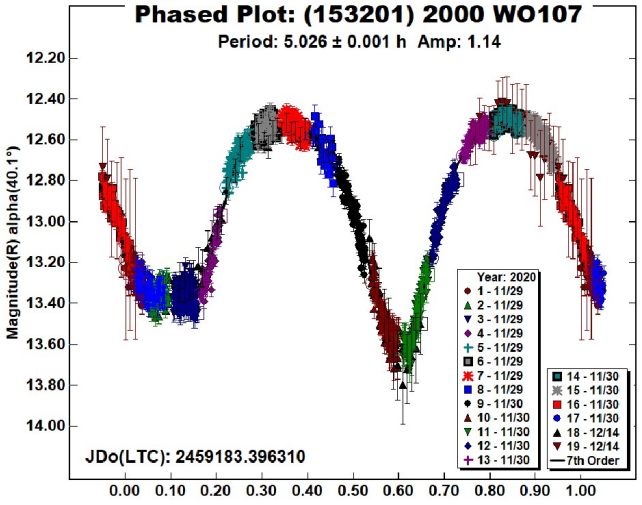

Number	Name	2020 mm/dd	Phase	L_{PAB}	B_{PAB}	Period(h)	P.E.	Amp	A.E.	Grp
102	Miriam	10/18-12/26	3.9,26.3	24	0	23.63	0.01	0.14	0.02	MB-M
635	Vundtia	11/06-11/21	3.9,8.3	41	-9	11.784	0.004	0.20	0.02	MB-O
1342	Brabantia	10/18-11/23	17.1,12.4	58	26	4.175	0.001	0.13	0.03	MB-I
2346	Lilio	10/16-10/22	3.6,4.7	24	6	3.0290	0.0005	0.18	0.04	MB-I
153201	2000 WO107	11/29-12/14	*37.8,30.3	63	3	5.026	0.001	1.14	0.16	NEA

Table I. Observing circumstances and results. The first line gives the results for the primary of a binary system. The second line gives the orbital period of the satellite and the maximum attenuation. The phase angle is given for the first and last date. If preceded by an asterisk, the phase angle reached an extrema during the period. L_{PAB} and B_{PAB} are the approximate phase angle bisector longitude/latitude at mid-date range (see Harris et al., 1984). Grp is the asteroid family/group (Warner et al., 2009).

Observatory (MPC code)	Telescope	CCD	Filter	Observed Asteroids (#Sessions)
Balzaretto Observatory (A81)	0.20-m SCT f/5.0	SBIG ST7-XME	Rc	102(3)
Parco Astronomico Lilio (K96)	0.50-m RCT f/8.0	FLI PL1001	r'	102(3),2346(2)
WBRO (K49)	0.235-m SCT f/10	SBIG ST8-XME	Rc	102(1),635(1),1342(2), 2346(1)
Iota Scorpii(K78)	0.40-m RCT f/8.0	SBIG STXL-6303e(bin 2x2)	Rc	102(1),635(1),1342(1), 2346(1)
Astronomical Observatory of the University of Siena(K54)	0.30-m MCT f/5.6	SBIG STL-6303e(bin 2x2)	Rc	635(2),2346(2)
Osservatorio Astronomico Nastro Verde (C82)	0.35-m SCT f/6.3	SBIG ST10XME (bin 2x2)	C	1342(2),2346(2)
GiaGa Observatory (203)	0.36-m SCT f/5.8	Moravian G2-3200	Rc	102(3)
Osservatorio Astronomico Margherita Hack (A57)	0.35-m SCT f/8.3	SBIG ST10XME (bin 2x2)	Rc	1342(2)
GAV	0.20-m SCT f/6.3	SXV-H9	Rc	102(2)
Seveso Observatory (C24)	0.30-m SCT f/6.3	SBIG ST9	Rc	102(1)
M57 (K38)	0.30-m RCT f/5.5	SBIG STT-1603	C	635(1)
Filzi School Observatory (D12)	0.35-m RCT f/8.0	QHY9 (KAF8300)	C	153201(1)
GAMP (104)	0.60-m NRT f/4.0	Apogee Alta	C	153201(1)
Serafino Zani (130)	0.40-m RCT f/5.8	SBIG ST8 XME (bin 2x2)	C	635(1)
Osservatorio Astronomico Monte San Lorenzo	0.53-m RCT f/6.7	SBIG ST8 XME (bin 2x2)	C	1342(1)

Table II. Observing Instrumentations. MCT: Maksutov-Cassegrain, NRT: Newtonian Reflector, RCT: Ritchey-Chretien, SCT: Schmidt-Cassegrain.

References

Bus, S.J.; Binzel, R.P. (2002). "Phase II of the Small Main-Belt Asteroid Spectroscopic Survey - A Feature-Based Taxonomy." *Icarus* **158**, 146-177.

DSFTA (2020), Dipartimento di Scienze Fisiche, della Terra e dell'Ambiente – Astronomical Observatory , University of Siena. *https://www.dsfta.unisi.it/en/research/labs/astronomical-observatory*

Goldstone (2020). Goldstone Radar Observations Planning: (7753) 1988 XB, 2017 WJ16, and 2000 WO107. *https://echo.jpl.nasa.gov/asteroids/1988XB/1988xb.2020.goldstone.planning.html*

Harris, A.W.; Young, J.W.; Scaltriti, F.; Zappala, V. (1984). "Lightcurves and phase relations of the asteroids 82 Alkmene and 444 Gyptis." *Icarus* **57**, 251-258.

Pilcher, F. (2008). "Period Determination for 84 Klio, 98 Ianthe, 102 Miriam 112 Iphigenia, 131 Vala, and 650 Amalasuntha." *Minor Planet Bulletin* **35**, 71-72.

Pilcher, F. (2013). "Rotation Period Determinations for 102 Miriam, 108 Hecuba, 221 Eos 225 Oppavia, and 745 Mauritia, and a Note on 871 Amneris." *Minor Planet Bulletin* **40**, 158-160.

Tholen, D.J. (1984). "Asteroid taxonomy from cluster analysis of Photometry." Doctoral Thesis. University Arizona, Tucson.

UAI (2020), "Unione Astrofili Italiani" web site. *https://www.uai.it*

Warner, B.D.; Harris, A.W.; Pravec, P. (2009). "The asteroid lightcurve database." *Icarus* **202**, 134-146. Updated 2020 Oct. *http://www.minorplanet.info/lightcurvedatabase.html*

Warner, B.D. (2019). MPO Software, MPO Canopus v10.8.1.1. Bdw Publishing. *http://minorplanetobserver.com*

CCD PHOTOMETRIC OBSERVATIONS OF ASTEROIDS 4493 NAITOMITSU, (21242) 1995 WZ41, (68130) 2001 AO17, AND (183230) 2002 TC58

Kenneth Zeigler
Star Z Research Ranch
PO Box 1464, George West, Texas 78022 USA
Dylan_lucard@yahoo.com

(Received: 2021 Jan 5)

CCD Photometric observations of asteroids 4493 Naitomitsu, (21242) 1995 WZ41, (68130) 2001 AO17, and (183230) 2002 TC58 were conducted from the Star Z Research Ranch in South Texas. The results found are 4493 Naitomitsu 7.423 ± 0.01 hr, amplitude 0.22 mag.; 1995 WZ41 5.456 ± 0.01 hr, amplitude 0.47 mag.; 2001 AO17 10.515 ± 0.01 hr, amplitude 0.34 mag.; 2002 TC58 3.616 ± 0.01 hr, amplitude 0.14 mag.

The photometric observations described in this paper were conducted from the Star Z Research Ranch, which is located at a dark sky site, 19 kilometers south of the Town of George West, Texas. Throughout this research program, a Meade 0.35-m LX600 Schmidt Cassegrain telescope was used. The telescope is housed within a converted eight by sixteen-foot Wells Cargo trailer with a hinged roof, which in turn sets upon four steel jacks resting on a concrete slab. The telescope pier itself rests upon a heavy steel tripod, independent of the trailer, to minimize vibrations. An SBIG STXL 6303 camera thermoelectrically cooled to -35°C was used to make the photometric observations. The photometric exposures were all 120 seconds in length and were dark subtracted and flat-fielded. To preserve the maximum light intensity of the objects observed, no filters were placed in the optical path during the observations.

The brightness of the asteroid was compared to that of three comparison stars in the same CCD frame. The average instrumental magnitude of the three stars was determined and this average was subtracted from the instrumental magnitude of the asteroid. A constant was then added to approximate the visual magnitude. The instrumental magnitude of the three comparison stars with respect to one another was continuously monitored in the event that one of them was determined to be a short period variable star. The target brightness was determined by measuring a 121-pixel (11×11 pixel) sample surrounding the asteroid or star in question. This corresponds to a 7.15×7.15 arcsec box. When possible, the same comparison stars were used during consecutive nights of observation. The coordinates of the asteroid and its approximate visual magnitude on any specific night were obtained from the online Lowell Minor Planet Services. This information was also used to compensate for the effect of the asteroid's changing distance from the sun and earth on its visual magnitude when vertically aligning the photometric data points from different nights in the construction of a composite lightcurve.

4493 Naitomitsu was discovered on October 14, 1988 by T. Kojima in Chiyoda, Japan. It was named for is the mother of the first female Japanese astronaut, Chiaki Mukai. The orbit of the asteroid has a semi-major axis of 3.22 astronomical units with an orbital period of 5.25 years. This asteroid was observed by Behrend (2009web), who determined a 5.04-hour rotational period based upon a partial lightcurve. This asteroid was observed from the Star Z Research Ranch on three separate nights between December 16 and December 20, 2020. On two of these nights, the asteroid was observed long enough to obtain a complete rotational cycle. On each of these nights, measurements were taken once every 5 minutes. The lightcurve of the asteroid is very atypical, displaying four distinct maxima and minima per rotational cycle. One of the minima is twice as deep as any of the others. This characteristic was observed on each of the three nights of observation. A composite lightcurve with a period of 7.423 ± 0.01 hours best fits the available data. The lightcurve has an amplitude of 0.22 magnitudes, as shown in the accompanying figure.

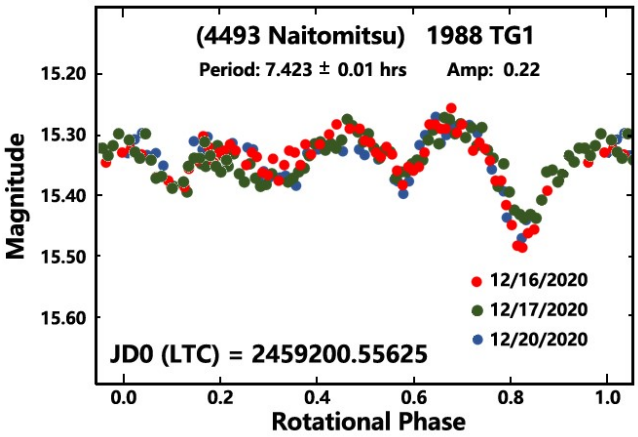

(21242) 1995 WZ41 was discovered by S. Uedav and H. Kaneda, at Kushiro, Japan on November 25, 1995. With a semi-major axis of 2.34 astronomical units, and an eccentricity of 0.281, it is located in the inner region of the main belt and at perihelion, approaches the orbit of Mars. According to the Lightcurve Data Base (Warner et al. 2009), as of October 2020, a rotational period for this asteroid has not yet been determined. This asteroid was observed from the Star Z Research Ranch on the nights of November 16, 17, and 18, 2020. The asteroid was determined to have a rotational period of 5.456 ± 0.01 hours, with a lightcurve amplitude of 0.47 magnitudes. The lightcurve is characterized by two maxima and two minima per rotational cycle. The two maxima are virtually identical in shape, and are of equal brightness. The minima are also very similar to each other.

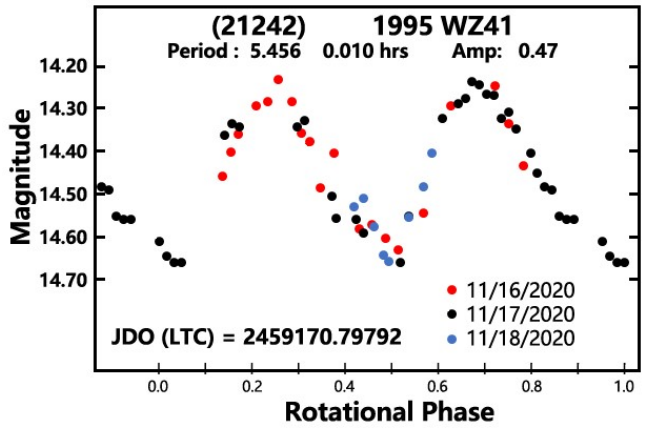

Number	Name	yyyy mm/dd	Phase	L_{PAB}	B_{PAB}	Period(h)	P.E.	Amp	A.E.	Grp
4493	Naitomitsu	2020 12/16-12/20	5.1,6.4	--	--	7.423	0.010	0.22	0.02	
21242	1995 WZ41	2020 11/16-11/18	-2.2,1.0	--	--	5.456	0.010	0.47	0.02	
68130	2001 AO17	2020 08/24-8/27	-2.7,2.8	--	--	10.515	0.010	0.34	0.02	
183230	2002 TC58	2020 08/11-8/13	-7.5,-7.8	--	--	3.616	0.010	0.14	0.02	

Table I. Observing circumstances and results. The phase angle is given for the first and last date. If preceded by an asterisk, the phase angle reached an extrema during the period. L_{PAB} and B_{PAB} are the approximate phase angle bisector longitude/latitude at mid-date range (see Harris et al., 1984). Grp is the asteroid family/group (Warner et al., 2009).

(68130) 2001 AO17 was discovered on January 2, 2001 by the LINEAR Survey at Socorro, New Mexico. Its orbit has a semi-major axis of 2.67 astronomical units, placing it at about the middle of the main belt. This asteroid was observed from the Star Z Research Ranch on the nights of August 24, 25, and 27, 2020. The composite lightcurve displays two symmetrical maxima and minima per rotational cycle. A rotational period of 10.515 ± 0.01 hours, with a lightcurve amplitude of 0.34 magnitudes best fits the observations. According to the October 2020 update of the LCDB, Asteroid 68130 had been previously observed by Pál et al. (2020), who determined a rotational period of 10.479 hours. This is close to the value presented here.

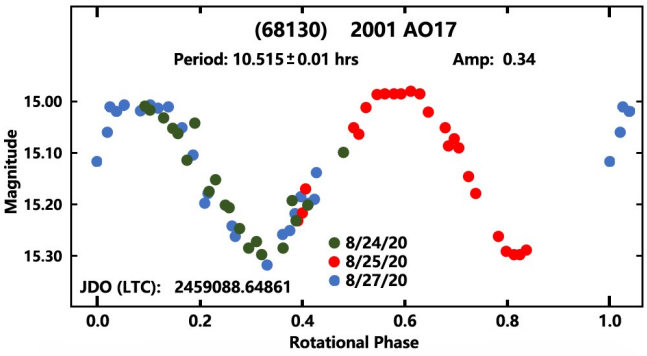

(183230) 2002 TC58 was discovered on January 21, 1990 by T Hioki and S. Hayakawa. It orbits the sun at a distance between 1.81 and 2.90 astronomical units, making it an inner main belt asteroid. This asteroid was observed on August 11, 12, and 13, 2020. A rotational period of 3.616 ± 0.01 hours was determined. The asteroid displays two maxima and minima per rotational cycle. Although the maxima have approximately the same brightness, one minimum is only about 0.05 magnitudes fainter than the two maxima, while the second minimum is about 0.14 magnitudes fainter than the maxima. An examination of the October 2020 update of the Asteroid Lightcurve Database reveals that this asteroid currently has no published lightcurves.

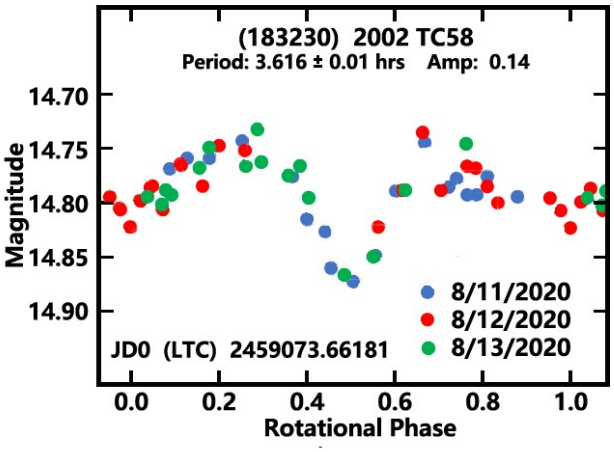

References

Behrend, R. (2009). Observatoire de Geneve web site. *http://obswww.unige.ch/~behrend/page_cou.html*

Harris, A.W.; Young, J.W.; Scaltriti, F.; Zappala, V. (1984). "Lightcurves and phase relations of the asteroids 82 Alkmene and 444 Gyptis." *Icarus* **57**, 251-258.

JPL (2018). Small Body Database Browser. *http://ssd.jpl.nasa.gov/sbdb.cgi*

Lowell Minor Planet Services. *https://asteroid.lowell.edu/gui/*

Pál, A.; Szakáts, R.; Kiss, C.; Bódi, A.; Bognár, Z.; Kalup, C.; Kiss, L.; Marton, G.; Molnár, L.; Plachy, E.; Sárneczky, K.; Szabó, G.; Szabó, R. (2020). "Solar System Objects Observed with TESS - First Data Release: Bright Main-belt and Trojan Asteroids from the Southern Survey." *Ap. J. Supl. Ser.* **247**, 26-34.

Warner, B.D.; Harris, A.W.; Pravec, P. (2009). "The Asteroid Lightcurve Database." *Icarus* **202**, 134-146. Updated 2020 Oct. *http://www.minorplanet.info/lightcurvedatabase.html*

LIGHTCURVES OF EIGHTEEN ASTEROIDS

Eric V. Dose
3167 San Mateo Blvd NE #329
Albuquerque, NM 87110
mp@ericdose.com

(Received: 2021 Jan 13, Revised: 2021 Mar 3)

Using a previously described workflow built on applying to each image dozens of comparison stars from the ATLAS refcat2 catalog, we have obtained and present here lightcurves and synodic rotation periods for eighteen asteroids.

Introduction and Workflow Description

In this paper we present asteroid lightcurve photometry results achieved by following the workflow process described by Dose (2020a). This workflow applies to each image an ensemble of typically 30-150 ATLAS refcat2 catalog (Tonry et al, 2018) comparison ("comp") stars for yielding photometric solutions. Diagnostic plots and this large number of comp stars allow for effective identification and removal of outlier, variable, and poorly measured comp stars. Improved handling of atmospheric extinction was described previously in Dose (2020b).

The present workflow produces a raw lightcurve, that is, the best estimates of asteroid magnitude on catalog basis (here, Sloan r'), unreduced and without H-G adjustment. These magnitudes are imported directly into *MPO Canopus* software (Warner, 2018) where they are adjusted for distances and phase-angle dependence, fit by Fourier analysis including identifying and ruling out of aliases, and plotted. Phase-angle dependence is corrected with a H-G model, using G = 0.15 for each asteroid unless otherwise specified.

No nightly zero-point adjustments (DeltaComps in *MPO Canopus* terminology) were made to any session herein, other from adjusting the G value (H-G). All lightcurve data herein have been submitted to ALCDEF.

Over the past few months, minor improvements have been made to the workflow. In nightly planning, we now superimpose a Digital Sky Survey photo on each asteroid's predicted path; observations are suspended (and imaging time is released to other asteroids) during any time periods where a given asteroid will be too near any background star. We use *TheSkyX* software, build 12868 (Software Bisque) to make these overlays and to predict accurate times of asteroid proximity to background stars. While this practice is laborious, it has practically eliminated rejection of images for background star interference. The occasional fragmentation of sessions is unwelcome, but if stars do lie in the asteroid's path, this fragmentation is already unavoidable, and accounting for this during planning minimizes lost observing time.

When imaging, we now make longer image exposures to improve the resulting lightcurves, even at the cost of lower image frequency. The application of very many comp stars has beaten down errors in comp-star flux and zero-point to the extent that asteroid photometric errors themselves entirely dominate errors in final magnitudes.

For deciding when to close a given asteroid's observing campaign, elimination of need to make nightly zero-point adjustments has reduced the closing criteria to only two: (1) absence of any phase-plot gap significant enough to risk fit by exclusion, and (2) absence of any remaining credible alias in the best period spectrum — or a recognition that aliases cannot be eliminated within the remaining nights of the current apparition.

Lightcurve Results

Eighteen asteroids were observed from Deep Sky West observatory (IAU V28) at 2210 meters elevation in northern New Mexico. Images were acquired with a 0.35-m SCT reduced to f/7.7; a SBIG STXL-6303E camera cooled to -35C and fitted with a Clear filter (Astrodon); and a PlaneWave L-500 direct-drive mount. The equipment was operated remotely via ACP software version 8.3 (DC-3 Dreams), running plan text files generated for each night by the author's python scripts (Dose, 2020a). Observations often cycled between 2-4 asteroids, as facilitated by the mount's rapid slews. Exposure times targeted 5-8 millimagnitudes uncertainty in asteroid raw magnitude, subject to a maximum of 900 seconds and a minimum of 90 seconds to ensure suitable comp-star photometry. All exposures were autoguided.

FITS images were plate-solved by *PinPoint* (DC-3 Dreams) or *TheSkyX* and were calibrated using temperature-matched, median-averaged dark images and recent flat images of a flux-adjustable flat panel. Every photometric image was visually inspected; all images with poor tracking, obvious interference by cloud or moon, or having stars or other light sources within 10 arcseconds of the target asteroid were excluded. Photometry-ready images that pass these screens were submitted to the workflow, which applies separately measured second-order transforms from Clear filter to deliver asteroid magnitudes in Sloan r' passband.

Errors are given in parentheses after the value and are in units of the last decimal place.

589 Croatia. Aliases have afflicted previous synodic period determinations for this bright outer main-belt asteroid. Reports of 11.7 h (Warner, 2008), 16.384 h (Waszczak et al, 2015), 24.821 h (Behrend, 2013web) and 24.734 h (Mas et al, 2018) have LCDB quality codes of 2+ or lower; the two phase plots in these reports contain significant gaps.

We report a period of 24.933(2) h from a clearly bimodal lightcurve taken over eight weeks. The previously reported period of 16.384 h is an alias by one-half period per 24 hours. A G value (H-G phase correction) of 0.10 improved the Fourier fit; our RMS error (observations vs best Fourier fit) is 8 millimagnitudes.

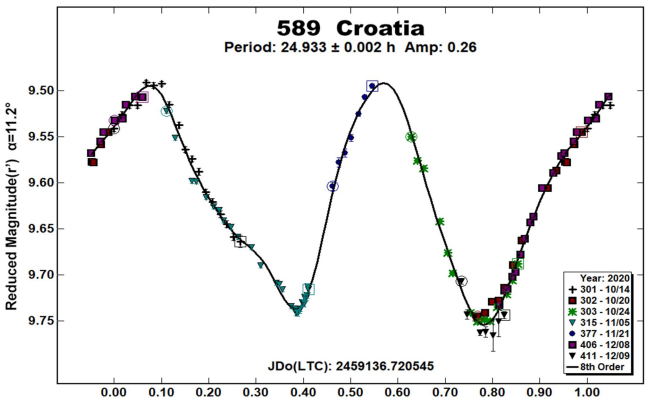

Number	Name	yyyy mm/dd	Phase	L_{PAB}	B_{PAB}	Period(h)	P.E.	Amp	A.E.	Grp
589	Croatia	2020 10/14-12/09	*11.3,10.6	50	-11	24.933	0.002	0.26	0.02	MB-O
722	Frieda	2020 10/30-11/22	12.6,1.1	60	2	128.990	0.176	0.71	0.04	FLOR
805	Hormuthia	2020 10/09-11/14	12.6,19.5	347	-3	11.890	0.002	0.10	0.03	UKN
866	Fatme	2020 11/12-12/23	*6.9,8.9	67	-4	11.600	0.001	0.19	0.03	MB-O
1114	Lorraine	2020 10/20-11/14	3.0,12.1	20	-2	20.680	0.005	0.10	0.02	MB-O
1241	Dysona	2020 10/02-10/16	15.8,14.1	65	26	8.606	0.002	0.36	0.02	MB-O
1721	Wells	2020 10/16-11/06	*8.2,8.1	34	19	11.845	0.001	0.08	0.03	MB-O
2689	Bruxelles	2020 10/18-11/20	*8.2,8.5	41	-4	101.800	0.026	0.80	0.03	FLOR
3001	Michelangelo	2020 10/18-10/23	14.4,15.4	13	24	8.345	0.002	0.26	0.02	MB-I
3600	Archimedes	2020-21 12/24-01/12	18.3,11.3	130	9	5.436	0.001	0.22	0.03	MB-I
4717	Kaneko	2020-21 11/20-01/03	12.4,19.2	28	-8	12.811	0.001	0.23	0.02	EOS
4995	Griffin	2020 10/31-12/06	33.8,24.3	84	30	26.370	0.002	0.74	0.03	MC
5802	Casteldelpiano	2020 11/22-12/06	1.8,9.3	58	2	2.971	0.001	0.18	0.04	FLOR
8078	Carolejordan	2020 10/21-10/24	6.9,8.6	18	-2	3.054	0.001	0.38	0.02	MB-I
10221	Kubrick	2020 10/24-12/22	*12.9,15.1	58	2	11.070	0.002	0.20	0.06	V
21787	1999 SG4	2020-21 12/07-01/08	7.1,18.5	60	4	2.939	0.001	0.20	0.03	EUN
26858	Misterrogers	2020 10/11-11/17	12.8,28.4	2	6	6.054	0.001	0.14	0.03	MC
49125	1998 SB22	2020 11/06-12/04	2.0,13.8	42	-4	5.968	0.001	0.64	0.10	V

Table I. Observing circumstances and results. The phase angle is given for the first and last date. If preceded by an asterisk, the phase angle reached an extrema during the period. L_{PAB} and B_{PAB} are the approximate phase angle bisector longitude/latitude at mid-date range (see Harris et al., 1984). Grp is the asteroid family/group (Warner et al., 2009).

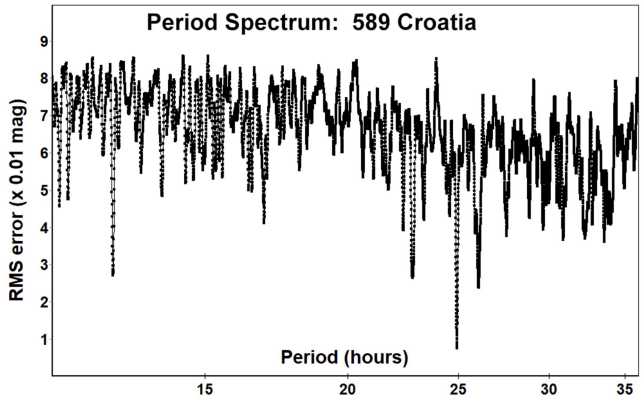

722 Frieda. Two recent previous period determinations for this Flora-family asteroid yielded 131.1 h (Polakis, 2019) and 30.06 h (Olguín et al, 2020). We generally confirm the longer period with a determination of 128.99(18) h, although we observed a much larger amplitude of 0.71 magnitudes than given by either previous report.

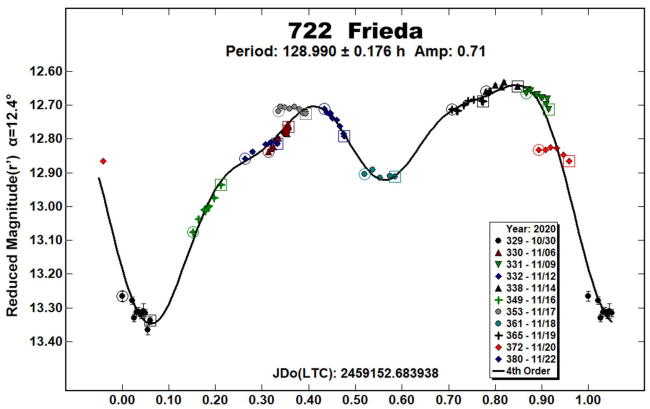

Two nights' observations of 722 Frieda (near phases 0.36 and 0.92) showed small, systematic intra-night deviations from the best Fourier fit, possibly indicating a modest effect from tumbling. The Asteroid Lightcurve Database (LCDB, Warner et al, 2009) entry for 722 Frieda also suggests tumbling, which would not be surprising given the long period. A *G* value of 0.40 markedly improved the Fourier fit vs *G* of 0.15; RMS error is 32 millimagnitudes.

805 Hormuthia. A convincing rotation period for this large (67 km) asteroid of undetermined family has proven difficult to obtain (Polakis, 2019), surely due to its low amplitude, very simple lightcurve shape with only a single broad feature, as well as an orbit of low eccentricity that precludes close approaches to earth. Periods of 9.510 h (Pilcher and Benishek, 2009), 23.76 h (Behrend 2019web), and 35.64 h (Polakis, 2020) have been reported. We find a period of 11.890(2) h from observations assisted by a rather bright 2020 apparition, though the target's declination was unfavorable for the observer's site. RMS error is 8 millimagnitudes.

A small gap in our phase plot was unavoidable as the period is quite close to one-half sidereal day (11.967 h). Its unfavorable declination for the observation site also prevented observing sessions longer than about one-half period. Even so, the present lightcurve shape is clear, when taken on the proposed monomodal basis.

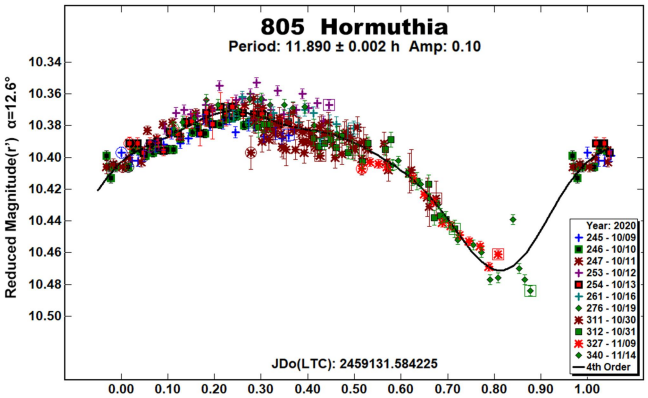

The 9.510 h period listed as favored in the LCDB is an alias of the present result, differing by exactly one-half period per 24 hours; it simply does not appear in our period spectrum. Similarly, the previous report of 23.76 h differs by exactly one period per 24 hours; the reported trimodal period of 35.64 h is quite close to three times the present monomodal solution, and it cannot be ruled out. Our period spectrum does show the expected minor aliases near 6, 8, and 16 h, but these candidate periods give poor Fourier fits to our photometric data, so we exclude them. In the end, we adopt the monomodal 11.890 h solution, though bimodal and even trimodal solutions also possible.

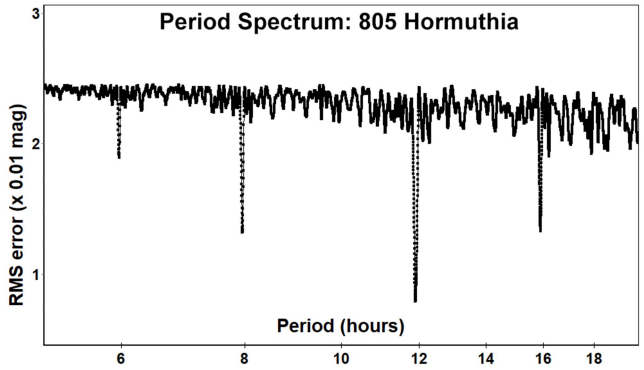

866 Fatme. Our period determination of 10.600(1) h for this outer main-belt asteroid differs from previous reports known to the author: 5.800 h (Polakis, 2018), 9.4 h (Behrend, 2004web), 9.36 h (Behrend, 2012web), 20.03 h (Stephens, 2002), and 20.07 h (Aznar Macias et al, 2016). Our lightcurve is bimodal, and our period estimate is twice that of Polakis' monomodal solution. The period estimates of 9.4 h and 9.36 hours are aliases of our estimate by one half-period per 24 hours. A G value of 0.18 improved the Fourier fit over G of 0.15. RMS error is 9 millimagnitudes.

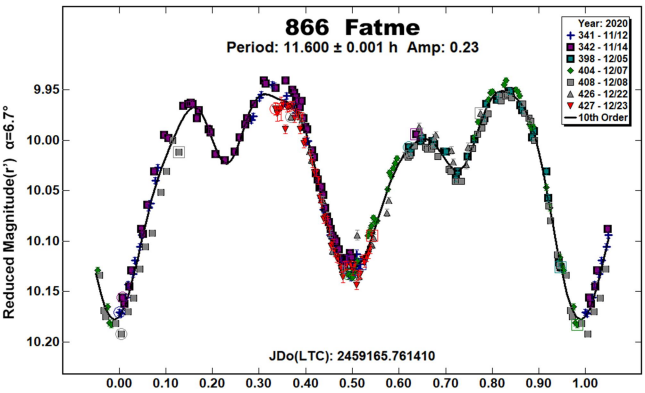

1114 Lorraine. Our synodic rotation period of 20.680(5) h confirms a previous report of 20.7 h (Ditteon et al, 2018) but differs from an earlier report of 32 h (Behrend, 2005web); the latter is entirely absent from our period spectrum. Given the relatively low amplitude and monomodal shape of the lightcurve, our observations emphasized the rapid brightening near phase 0.8-0.95, in an effort to rule out aliases and to sharpen the period estimate. RMS error is 8 millimagnitudes.

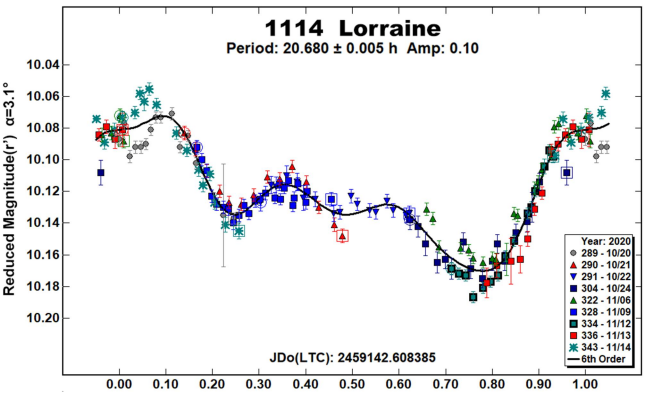

1241 Dysona. The 2020 apparition of this large outer main-belt asteroid offered a new phase angle bisector for shape studies, as well as a declination unusually advantageous for the author's observing site. The period was determined as 8.606(2) h, confirming all known previous reports of 8.61 h (Behrend, 2002web), 8.6080 h (Oey et al, 2007), 8.60738 h (Hanuš et al, 2013), and 8.6092 h (Behrend, 2019web). A *G* value of 0.05 slightly improved the Fourier fit over the default value of 0.15. RMS error is 12 millimagnitudes.

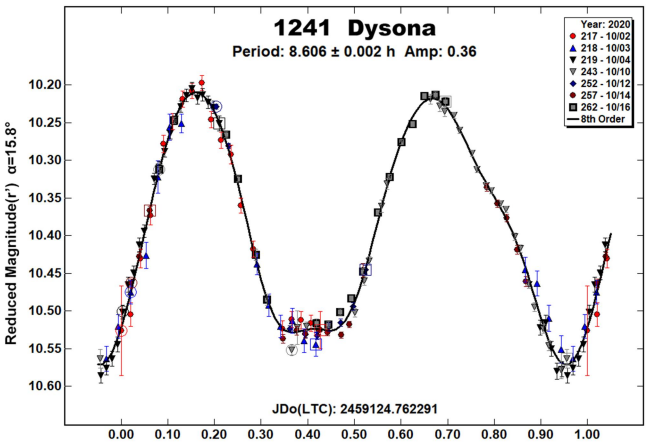

1721 Wells. No previous lightcurve or period reports are known for this outer main-belt asteroid. The 2020 apparition was at advantageous declinations for our observing site, which afforded long observing sessions to help overcome the period's proximity to one-half day. The synodic period determined here is 11.845(1) h. RMS error was 9 millimagnitudes.

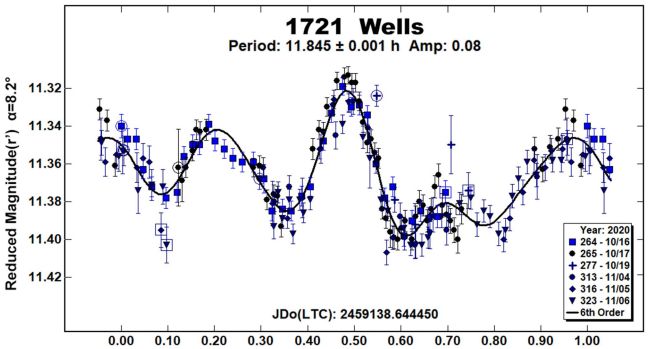

The unusual lightcurve shape, low amplitude, and the period's proximity to one-half day all complicated the *de novo* period search, but the best Fourier fit had low RMS error, and the phase angles ranged less than one degree, effectively removing the need to estimate *G*. The resulting period spectrum appears unambiguous.

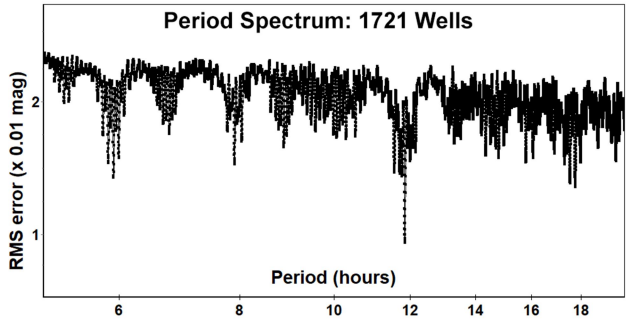

2689 Bruxelles. The previously reported (Hess and Ditteon, 2016) synodic period of 8.71 h and amplitude of perhaps 0.08 magnitude for this Flora-family asteroid were simply not confirmed by data from our first observing sessions. In our surprise, we launched a *de novo* period determination, which converged on 101.80(3) h and amplitude of 0.80 magnitude. RMS error was 19 millimagnitudes.

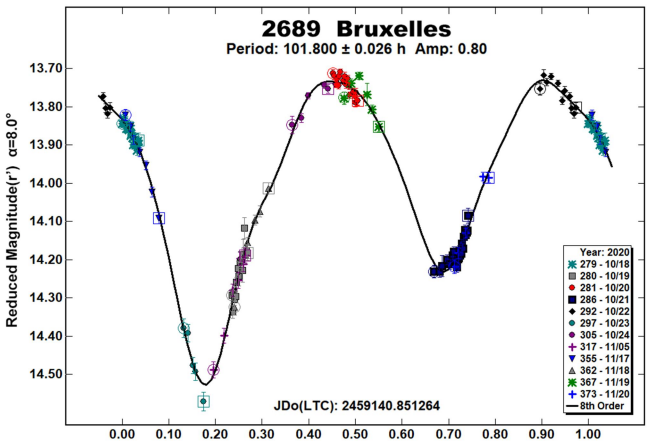

We are confident in our widely differing period estimate — yet both our large amplitude and the small amplitude previously reported could be correct for their observation dates. Our observations' viewing angle (phase angle bisector PAB of 41°, –3°) is very nearly perpendicular to that of the previous observations (PAB 133°, –3°), so it is plausible that in 2020 we observed 2689 Bruxelles near its rotational equator and that in 2015 it was observed near a pole. The favorable 2022 apparition (PAB 201°, 4°) affords a superb opportunity to test this idea, as well as to take data at new viewing angles for shape modeling.

3001 Michelangelo. The synodic rotation period for this inner main-belt asteroid is found to be 8.345(2) h, in agreement with previous reports of 8.338 h (Ditteon et al, 2011), 8.343 h (Waszczak et al, 2015), and 8.35088 h (Pál et al, 2020). A *G* of 0.50 optimized the Fourier fits. RMS error is 11 millimagnitudes.

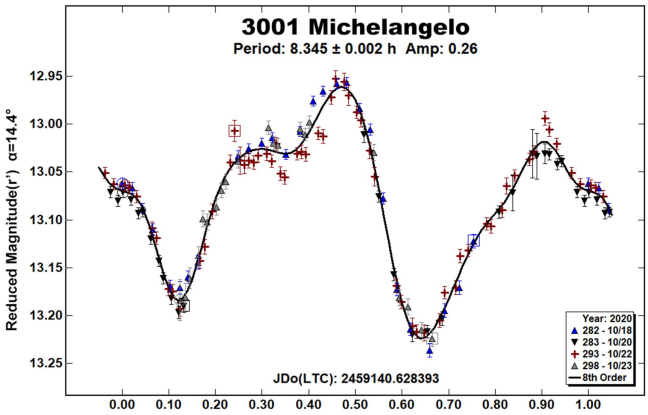

3600 Archimedes. We measure a synodic period for this inner main-belt asteroid as 5.4360(5) h, confirming one previous report of 5.439(1) h (Benishek, 2018). The lightcurve given in that previous report remarkably resembles a time-reversal of the lightcurve given here. A *G* value of 0.45 gave far superior Fourier fits to those with customary *G* of 0.15; RMS error is 16 millimagnitudes.

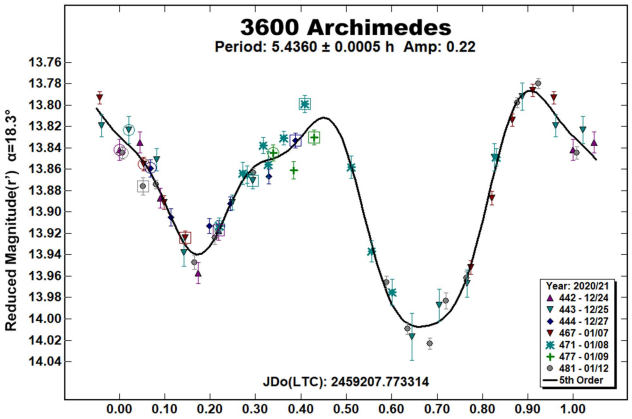

4717 Kaneko. For this Eos-family asteroid, our synodic rotation period of 12.811(1) h confirms two recent reports of 12.7998 h (Pál, 2020) and 12.7082 h (Singh et al, 2020). We estimate a much smaller amplitude (0.23 mag) than does the second report (0.61 mag), and our phase plot is more obviously bimodal. A *G* value of 0.22 improved the Fourier fits over that with $G = 0.15$; RMS error was 13 millimagnitudes.

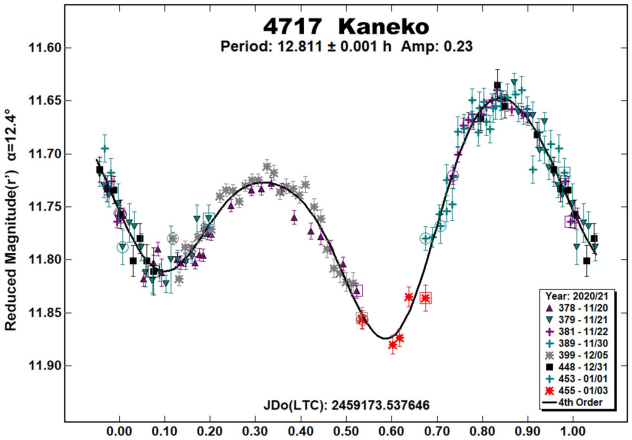

4995 Griffin. This small, high-albedo Mars-crosser was observed near +60° declination for 14 nights during its very favorable 2020 opposition. The period was found to be 26.370(2), in agreement with previous reports of 26.37 h (Warner, 2003, as 1984 QR, partial lightcurve) and 26.3920 h (Ďurech et al, 2016). A *G* value of 0.25 improved Fourier fits over those with $G = 0.15$; RMS error was 14 millimagnitudes.

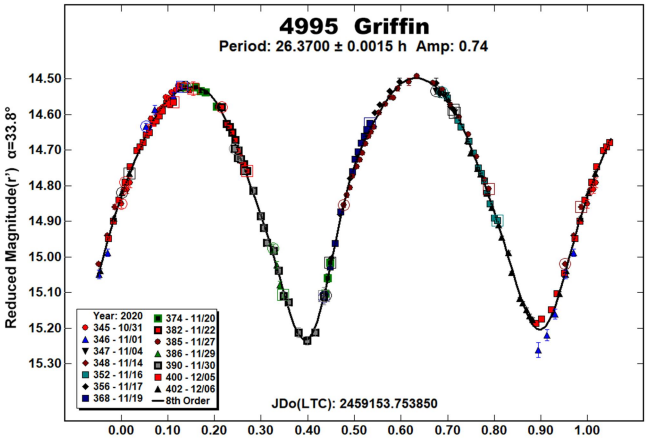

5802 Casteldelpiano. This Flora-family asteroid was detected in images targeting 10221 Kubrick and then was followed in its own right. Our synodic period estimate of 2.9706(2) h confirms previous reports of 2.971 h (Waszczak et al, 2015) and 2.9705 h (Pravec, 2018web). A *G* value of 0.30 markedly improved the Fourier fit over *G* = 0.15; RMS error was 20 millimagnitudes.

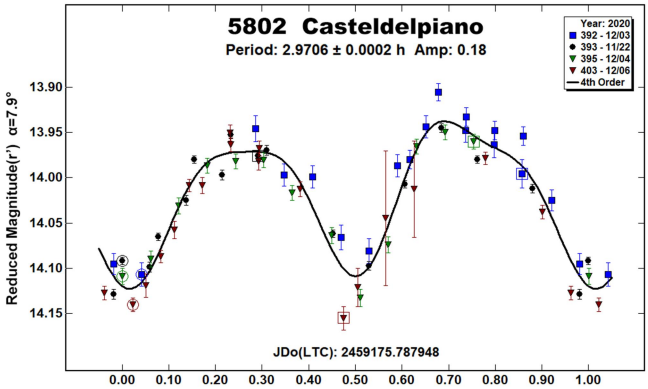

8078 Carolejordan. This small, high-albedo inner main-belt asteroid, observed in three long sessions, was found to have synodic rotation period of 3.0540(4) h, differing from the sole known report: a tentative estimate of 3.5 h (Oey and Groom, 2019). A *G* value of 0.30 slightly improved the Fourier fit over the default value of 0.15; RMS error was 15 millimagnitudes.

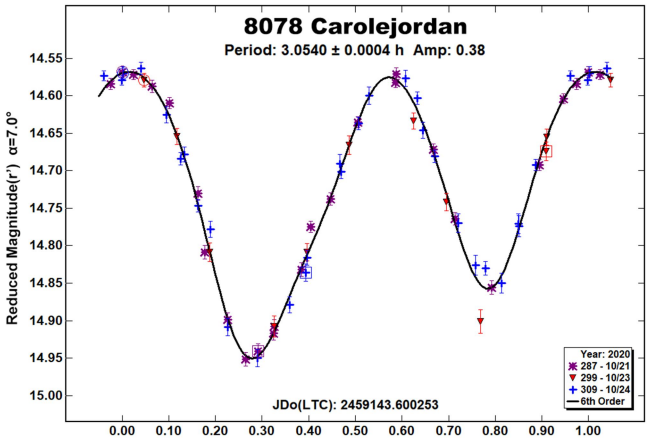

The 2019 period report was offered as only a tentative solution since the asteroid was a target of opportunity and its lightcurve was partial; that 3.5 h estimate does not appear in our period spectrum.

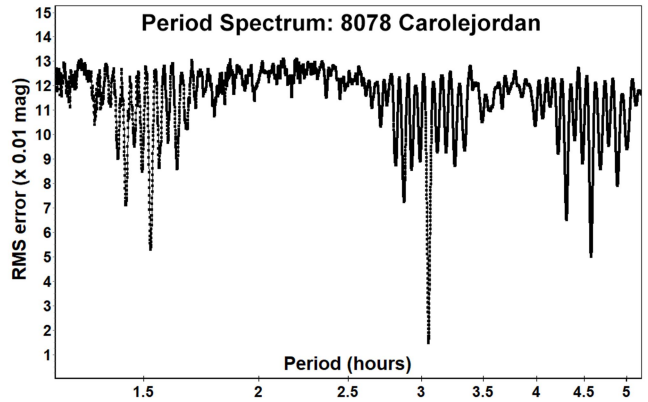

10221 Kubrick. We found the synodic rotation period of this faint Vestoid asteroid to be 11.070(2) h and its amplitude to be 0.20 magnitude, in agreement with the sole known survey estimate of 11.0(2) h and 0.19 magnitude (Chang et al, 2019). A *G* value of 0.38 gave markedly better Fourier fits than did *G* = 0.15; RMS error was 30 millimagnitudes.

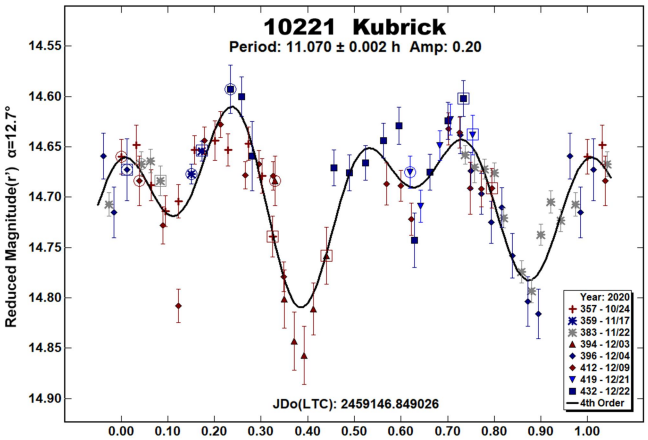

Though the amplitude is modest and the lightcurve is complex in shape, the period spectrum does support the bimodal period proposed, though observational noise allows for an alternative monomodal period of 5.54 h, especially given the relatively small amplitude (Harris et al, 2014).

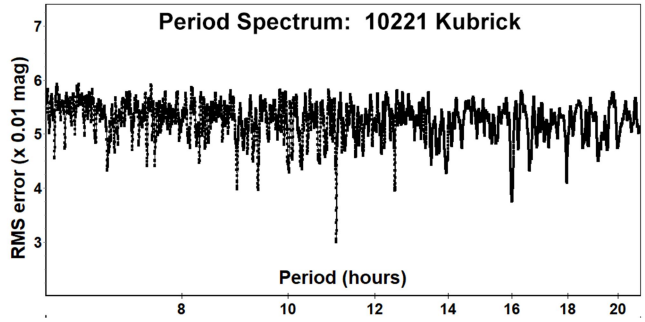

(21787) 1999 SG4. This Eunomia-family asteroid was detected in images targeting 722 Frieda and then was followed in its own right. No previous period or lightcurves are known; we measured a synodic period of 2.9388 (4) h. A *G* value of 0.35 gave far superior Fourier fits to those using *G* = 0.15; RMS error is 26 millimagnitudes.

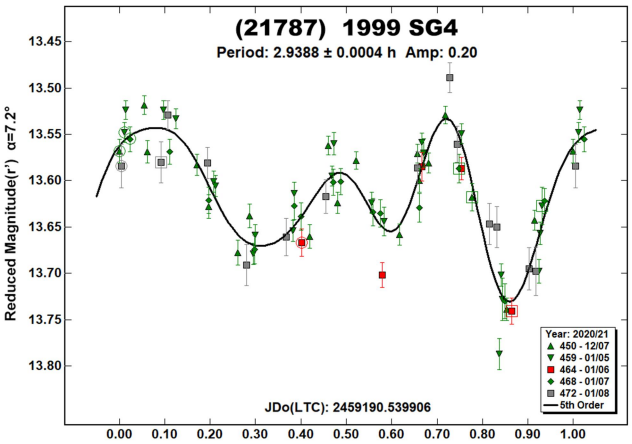

The short period and advantageous declination allowed rapid elimination of alias periods despite Sloan r' magnitudes near 17.

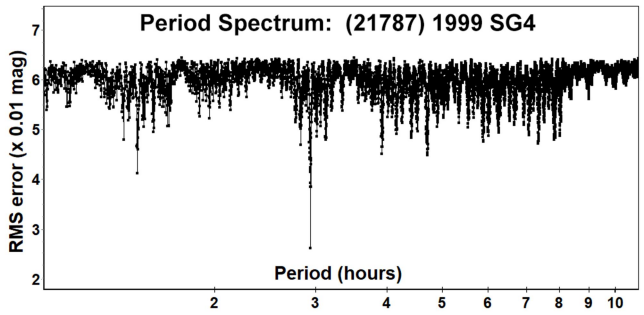

26858 Misterrogers. This Mars-crosser has only a single previous lightcurve and synodic period report of 8.065 h (Skiff, 2019). Our 2020 observations during seven nights over five weeks simply could not discriminate between periods near 6 and 8 hours, which are aliases by one period per 24 hours. RMS error was 12 millimagnitudes.

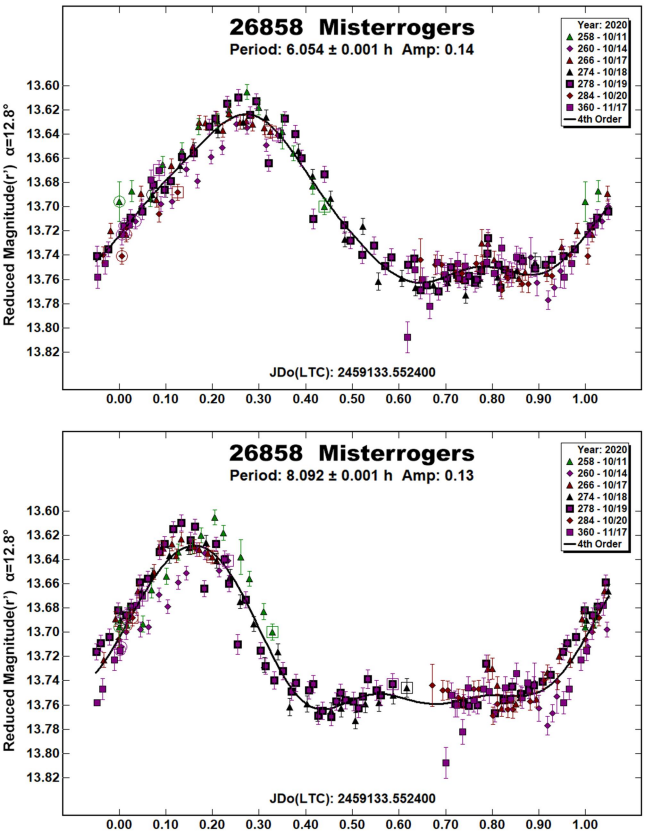

The period spectrum slightly favors the 6.054(1) h over the 8.092(1) h solution, but either solution might well have been accepted if considered in isolation, which serves as a reminder to continue observing until the aliasing symmetry is broken or until one concludes that no additional sessions could do so. This observing campaign falls in the latter case due to several unfortunate conditions: the closeness of both candidate periods to an integral fraction of 24 hours, which guarantees that aliases will emerge; the lightcurve's having only a single feature; and session lengths being limited by the target's declination.

This asteroid's orbit keeps it near the plane of the earth's equator, so it is unclear that an unambiguous rotational period for 26858 Misterrogers could ever be decided by any number of observations from a single terrestrial site. A multi-longitudinal cooperative study is encouraged.

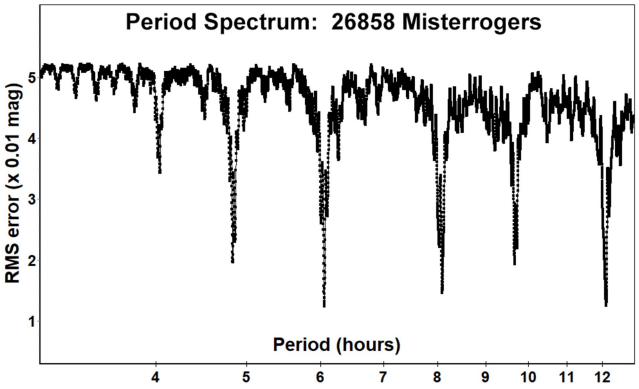

(49125) 1998 SB22. This Vestoid-family asteroid was detected in images targeting asteroid 3061 Cook and then was followed in its own right. No previous lightcurves or synodic period reports are known to the author. The present observations yield a period of 5.9676(8) h despite the RMS error of 77 millimagnitudes. A *G* of 0.40 markedly improved the Fourier fit vs the default *G* of 0.15.

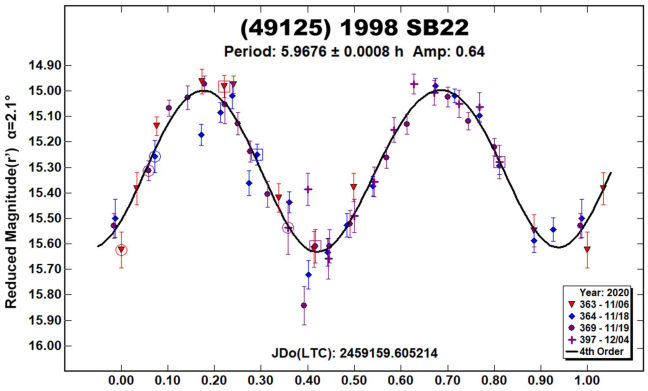

As with 26858 Misterrogers described above, the period is close to an integer fraction of 24 hours, and sessions lengths were limited by an unfavorable declination. However, for (49125) 1998 SB22 the bimodal lightcurve shape and higher amplitude allow for a confident preference for the solution near 6 hours relative to those of 8 and 9 hours, despite their similar RMS errors: the 8- and 9-hour solutions are trimodal and not of reasonable lightcurve shape.

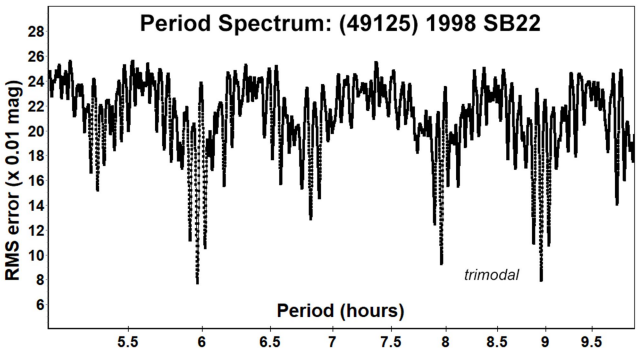

Acknowledgements

The author thanks the authors of the ATLAS paper (Tonry et al, 2018) and the catalog's numerous contributors for providing without cost the ATLAS refcat2 release catalog and its detailed technical descriptions.

This project's computations make extensive use of the python language interpreter and of several supporting packages (notably: pandas, ephem, matplotlib, requests, astropy, and statsmodels), all provided without cost, and without which this work would have been infeasible.

References

Aznar Macias, A.; Carreño Garcerán, A.; Arce Mansego, E.; Brines Rodriguez, P.; Lozano de Haro, J.; Fornas Silva, A.; Fornas Silva, G.; Mas Martinez, V.; Rodrigo Chiner, O.; Herrero Porta, D. (2016). "Twenty-one Asteroid Lightcurves at Group Observadores de Asteroides (OBAS): Late 2015 to Early 2016." *Minor Planet Bull.* **43**, 257-263.

Behrend, R. (2002web, 2004web, 2005web, 2012web, 2013web, 2019web). Observatoire de Geneve web site. *http://obswww.unige.ch/~behrend/page_cou.html*

Benishek, V. (2018). "Lightcurve and Rotation Period Determinations for 29 Asteroids." *Minor Planet Bull.* **45**, 82-91.

Chang, C.-K.; Lin, H.-W.; Ip, W.-H.; Chen, W.-P.; Yeh, T.-S.; Chambers, K.C.; Magnier, E.A.; Huber, M.E.; Flewelling, H.A.; Waters, C.Z.; Wainscoat, R.J.; Schultz, A.S.B. (2019). "Searching for Super-fast Rotators Using the Pan-STARRS 1." *Astrophys. J. Suppl. Series* **241**, 6.

Ditteon, R.; West, J.; McDonald, B. (2011). "Asteroid Lightcurve Analysis at the Oakley Southern Sky Observatory: 2011 January thru April." *Minor Planet Bull.* **38**, 214-217.

Ditteon, R.; Adam, A.; Doyel, M.; Gibson, J.; Lee, S.; Linville, D.; Michalik, D.; Turner, R.; Washburn, K. (2018). "Lightcurve Analysis of Minor Planets Observed at the Oakley Southern Sky Observatory: 2016 October - 2017 March." *Minor Planet Bull.* **45**, 13-16.

Dose, E. (2020a). "A New Photometric Workflow and Lightcurves of Fifteen Asteroids." *Minor Planet Bull.* **47**, 324-330.

Dose, E. (2020b). "Lightcurves of Nineteen Asteroids." *Minor Planet Bull.* **48**, 69-76.

Ďurech, J.; Hanuš, J.; Oszkiewicz, D.; Vančo, R. (2016). "Asteroid models from the Lowell photometric database." *Astron. Astrophys.*, **587**, A48.

Hanuš, J.; Ďurech, J.; Brož, M.; Marciniak, A.; Warner, B.D.; Pilcher, F.; Stephens, R.; Behrend, R.; Carry, B.; and 111 coauthors. (2013). "Asteroids' physical models from combined dense and sparse photometry and scaling of the YORP effect by the observed obliquity distribution." *Astron. Astrophys.* **551**, A67.

Harris, A.W.; Young, J.W.; Scaltriti, F.; Zappala, V. (1984). "Lightcurves and phase relations of the asteroids 82 Alkmene and 444 Gyptis." *Icarus* **57**, 251-258.

Harris, A.W.; Pravec, P.; Galád, A.; Skiff, B.A.; Warner, B.D.; Világi, J.; Gajdoš, Š.; Carbognani, A.; Hornoch, K.; Kušnirák, P.; Cooney, W.R.; Gross, J.; Terrell, D.; Higgins, D.; Bowell, E.; Koehn, B.W. (2014). "On the maximum amplitude of harmonics on an asteroid lightcurve." *Icarus* **235**, 55-59.

Hess, K.; Ditteon, R. (2016). "Asteroid Lightcurve Analysis at the Oakley Southern Sky Observatory: 2015 February." *Minor Planet Bull.* **43**, 87.

Mas, V.; Fornas, G.; Lozano, J.; Rodrigo, O.; Fornas, A.; Carreño, A.; Arce, E.; Brines, P.; Herrero, D. (2018). "Twenty-one Asteroid Lightcurves at Asteroids Observers (OBAS) - MPPD: Nov 2016 - May 2017." *Minor Planet Bull.* **45**, 76-82.

Oey, J.; Világi, J.; Gajdoš, Š.; Kornoš, L.; Galád, A. (2007). "Light Curve Analysis of 8 Asteroids from Leura and Other Collaborating Observatories." *Minor Planet Bull.* **34**, 81-83.

Oey, J.; Groom, R. (2019). "Lightcurve Analysis of Asteroids from BMO and DRO in 2016. II." *Minor Planet Bull.* **46**, 119-125.

Olguín, L.; Saucedo, J.C.; Loera-González, P.; Contreras, M.E.; Valdés, J.R.; Guichard, J.; López-González, R.; Michimani-García, J.; Cerdán-Hernández, G.; Schuster, W.J.; Valdés-Sada, P.; Núñez-López, R.; Ayala-Gómez, S.A. (2020). "The Mexican Asteroid Photometry Campaign." *Minor Planet Bull.* **47**, 340-342.

Pál, A.; Szakáts, R.; Kiss, C.; Bódi, A.; Bognár, Z.; Kalup, C.; Kiss, L.L.; Marton, G.; Molnár, L.; Plachy, E.; Sárneczky, K.; Szabó, G.M.; Szabó, R. (2020). "Solar System Objects Observed with TESS - First Data Release: Bright Main-belt and Trojan Asteroids from the Southern Survey." *Astrophys. J. Suppl. Series* **247**, 1.

Pilcher, F.; Benishek, V. (2009). "Period Determinations for 634 Ute and 805 Hormuthia." *Minor Planet Bull.* **36**, 29-30.

Polakis, T. (2018). "Lightcurve Analysis for Fourteen Main-Belt Minor Planets." *Minor Planet Bull.* **45**, 347-352.

Polakis, T. (2019). "Photometric Observations of Seventeen Minor Planets." *Minor Planet Bull.* **46**, 400-406.

Polakis, T. (2020). "Photometric Observations of Seven Minor Planets." *Minor Planet Bull.* **48**, 23-25.

Pravec, P. (2018web). Ondrejov Asteroid Photometry Project web site. *http://www.asu.cas.cz/~ppravec/neo.htm*

Singh, A.; Sackalosky, C.; Sefik, Y.; Yates, E.; Moore, C.; Pagan, A.; Malwitz, A. (2020). "Lightcurve for Asteroid 4717 Kaneko." *Minor Planet Bull.* **47**, 74.

Skiff, B.A.; McLelland, K.P.; Sanborn, J.J.; Pravec, P.; Koehn, B.W.; Bowell, E. (2019). "Lowell Observatory Near-earth Asteroid Photometric Survey (NEAPS): Paper 3." *Minor Planet Bull.* **46**, 238-265.

Stephens, R.D. (2002). "Photometry of 866 Fatme, 894 Erda, 1008 Demeter, and 3443 Letsungdao." *Minor Planet Bull.* **29**, 2-3.

Tonry, J.L.; Denneau, L.; Flewelling, H.; Heinze, A.N.; Onken, C.A.; Smartt, S.J.; Stalder, B.; Weiland, H.J.; Wolf, C. (2018). "The ATLAS All-Sky Stellar Reference Catalog." *Astrophys. J.* **867,** A105, 1-16.

Warner, B.D. (2003). "Lightcurve analysis for asteroids 607 Jenny, 1177 Gonnessia 4440 Tchantches, 4896 Tomoegozen, and (4995) 1984 QR." *Minor Planet Bull.* **30**, 33-35.

Warner, B.D. (2008). "Asteroid Lightcurve Analysis at the Palmer Divide Observatory: June - October 2007." *Minor Planet Bull.* **35**, 56-60.

Warner, B.D.; Harris, A.W.; Pravec, P. (2009). "The asteroid lightcurve database." *Icarus*, **202**, 134-146. Updated 2020 August. *http://www.minorplanet.info/lightcurvedatabase.html*

Warner, B.D. (2018). *MPO Canopus* Software, version 10.7.12.9. BDW Publishing. *http://www.bdwpublishing.com*

Waszczak, A.; Chang, C.-K.; Ofek, E.O.; Laher, R.; Masci, F.; Levitan, D.; Surace, J.; Cheng, Y.-C.; Ip, W.-H.; Kinoshita, D.; Helou, G.; Prince, T.A.; Kulkarni, S. (2015). "Asteroid Light Curves from the Palomar Transient Factory Survey: Rotation Periods and Phase Functions from Sparse Photometry." *Astron. J.* **150**, 3.

LIGHTCURVES AND ROTATION PERIODS OF 67 ASIA, 74 GALATEA, 356 LIGURIA, 570 KYTHERA, 581 TAUNTONIA, 589 CROATIA, AND 605 JUVISIA

Frederick Pilcher
Organ Mesa Observatory (G50)
4438 Organ Mesa Loop
Las Cruces, NM 88011 USA
fpilcher35@gmail.com

(Received: 2021 Jan 14)

Synodic rotation periods and amplitudes are found for 67 Asia: 15.855 ± 0.002 h, 0.32 ± 0.02 mag; 74 Galatea: 17.266 ± 0.001 h, 0.06 ± 0.01 mag; 356 Liguria: 31.690 ± 0.002 h, 0.14 ± 0.01 mag; 570 Kythera: 8.117 ± 0.001 h, 0.09 ± 0.01 mag; 581 Tauntonia: 24.994 ± 0.002 h, 0.10 ± 0.01 mag; 589 Croatia: 24.932 ± 0.001 h, 0.25 ± 0.01 mag; 605 Juvisia: 15.844 ± 0.001 h, 0.18 ± 0.01 mag.

Observations to obtain the data used in this paper were made at the Organ Mesa Observatory with a 0.35-m Meade LX200 GPS Schmidt-Cassegrain (SCT) and SBIG STL-1001E CCD. Exposures were 60 seconds, unguided, with a clear filter except where otherwise noted. Photometric measurement and lightcurve construction are with *MPO Canopus* software. To reduce the number of points on the lightcurves and make them easier to read, data points have been binned in sets of 3 with a maximum time difference of 5 minutes. For each target a split halves plot of the double period has been plotted that shows the two halves of the double period are very nearly the same. Therefore, the double period may be ruled out for each target. Although not shown in this paper, these plots are available from the author on request.

67 Asia. The Asteroid Lightcurve Database (Warner et al, 2009) states a secure period of 15.853 hours based on six independent period determinations all within 0.05 hours of the preferred value. A lightcurve based on new observations on four nights 2020 Nov. 6-17 at phase angles from 6.7º to 11.8º provide an excellent fit to a period 15.852 ± 0.001 h, amplitude 0.32 ± 0.02 mag. These four sessions were timed to obtain full phase coverage of the double period, whose split halves plot, not presented, shows a near perfect overlap of the two halves. The double period may be safely ruled out.

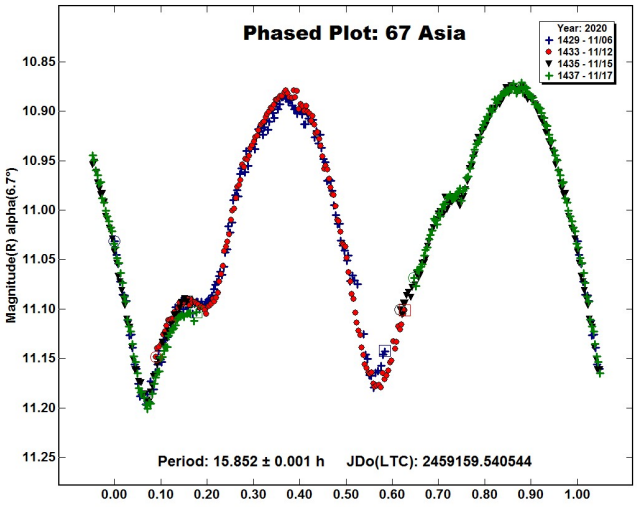

Two additional sessions were obtained 2020 Nov. 30 and Dec. 1 near phase angle 17º as a full moon target. In the phased lightcurve representing all six sessions, the small hump near phase 0.75 had increased slightly on Nov. 30, and the small depression near phase 0.2 was much deeper on Dec. 1 than on Nov. 6-17. Such changes of lightcurve shape with increasing phase angle are commonly found for many asteroids. The lightcurve based on six sessions 2020 Nov. 6 - Dec. 1 has period 15.855 ± 0.002 h, amplitude 0.32 ± 0.02 mag. This result is consistent with all previously published results.

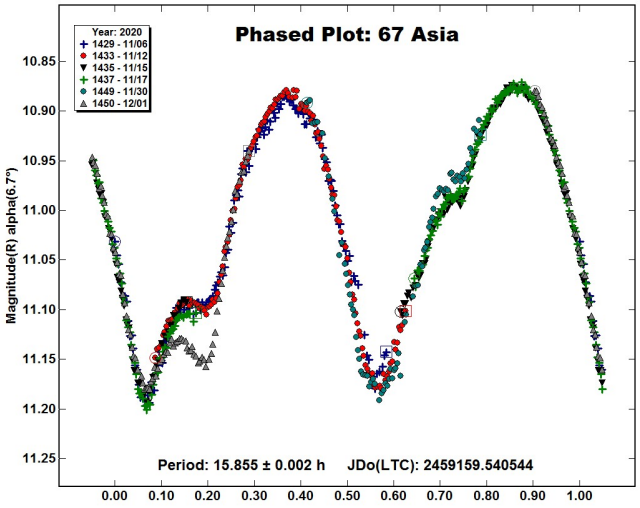

74 Galatea. There are five previously published rotation periods, with periods, amplitudes, and celestial longitudes as stated. Harris and Young (1980), 9.0 h, 0.14 mag, 24º; Behrend (2001), 8.629 h, 0.09 mag, 346º; and Behrend (2013), 8.643 h, 0.13 mag, 179º all published lightcurves with the usual two maxima and minima per rotational cycle. Pilcher (2008), 17.270 h, 0.08 mag, 157º; Pilcher (2009), 17.268 h, 0.16 mag, 216º on both occasions found four unsymmetric maxima and minima per rotation cycle that ruled out a period near 8.6 hours. New observations on six nights 2020 Nov. 18 - Dec. 19 provide a good fit to an unsymmetric lightcurve with period 17.266 ± 0.001h, amplitude 0.06 ± 0.01 mag at celestial longitude 73º. The new result is in excellent agreement with Pilcher (2008) and (2009). Even a cursory examination of the new lightcurve shows again that a period near 8.6 hours is definitively ruled out.

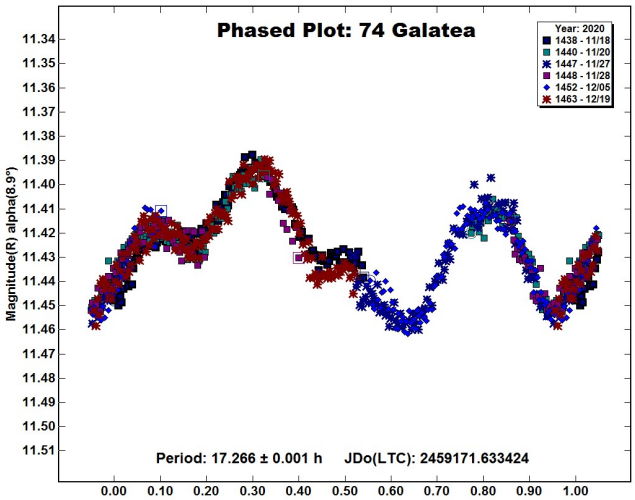

356 Liguria. There have been only two previously published rotation periods for this bright asteroid. Harris and Young (1980), 31.82 hours; and a much more comprehensive campaign 2017 Feb. 22 - May 3 by this author (Pilcher, 2017) that found an ambiguous result. Depending upon the interpretation of the lightcurves, the period might be either 31.701 hours with the usual two maxima and minima per rotational cycle, or twice that amount (63.395 hours) with four maxima and minima per cycle. The two halves of a split halves plot for the longer period did not have a perfect overlap. The observations were not uniformly distributed in time or among the large range of phase angles encountered in the interval. Observations at different phase angles were represented by the two halves of the split halves plot. The period might be 31.701 hours with two maxima and minima per cycle and the lightcurve shape changing with phase angle as is commonly found for many asteroids. Or the period might be 63.395 hours with four unsymmetric maxima and minima per cycle.

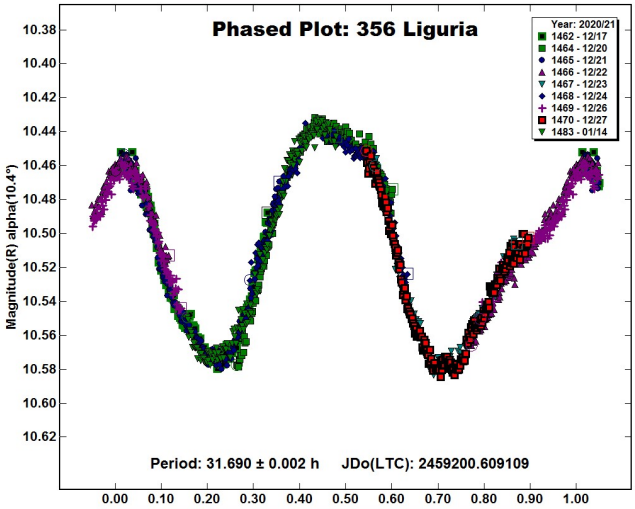

In 2020 December 356 Liguria came to opposition at declination +37º and with the longest nights of the year near winter solstice. Eight single night sessions, each of 10 to 11 hours, 2020 Dec. 17-27 provided complete phase coverage of the longer period with generous 2 to 3 hour overlap between adjacent segments. The R filter was used for this bright target. An excellent fit of all eight sessions was obtained for a lightcurve phased to 31.682 ± 0.004 h, amplitude 0.14 ± 0.01 mag. The split halves lightcurve phased to 63.367 hours shows near perfect overlap between the two halves. The longer period can now be ruled out, and the shorter period supported by data 2020 Dec. 17-27 is secure. Covering fewer than eight rotational cycles of the target, it is, however, not highly accurate.

To improve the accuracy of the period, another session was obtained 2021 Jan. 14, with 21 rotational cycles between the first and last sessions. The accompanying lightcurve aligns the minima of 2020 Dec. 17 and 2021 Jan. 14 with excellent fit to a period 31.690 ± 0.002 h, amplitude 0.14 ± 0.01 mag. This period agrees within 0.03% of the period found in 2017 (Pilcher, 2017).

570 Kythera. Many different rotation periods have been published: Blanco et al., (2000), 6.919 h; Lagerkvist et al. (2001), 5.682 h; Gil-Hutton and Cañada (2003), 6.903 h; Behrend (2004), 8.120 h; Chavez (2014), 10.5h; Aznar Macias et al. (2016), 8.074 h. New observations on six nights 2020 Sept. 30 - Nov. 2 provide a good fit to an irregular lightcurve with period 8.117 ± 0.001 h, amplitude 0.09 ± 0.01 mag. A split halves plot of the double period shows that the two halves are almost identical, and rules out the double period. This result is consistent with Behrend (2004) and Aznar Macias et al. (2016), and rules out all other reported periods.

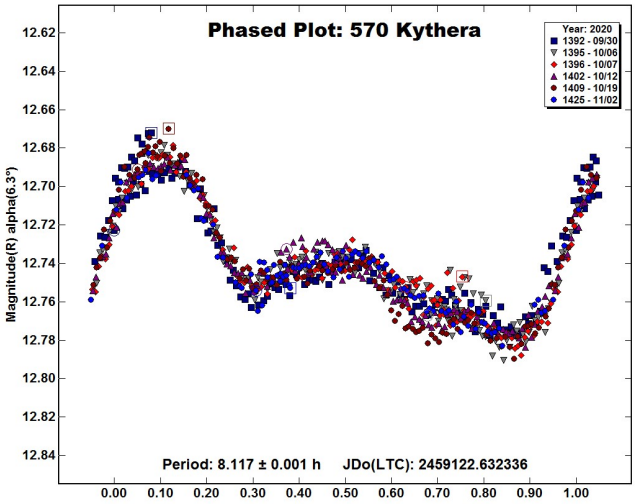

581 Tauntonia. Previously reported rotation periods are by Behrend (2005), 16.54 h; Behrend (2006), 16.19 h; Stephens (2010), 24.90 h; Marciniak et al. (2018), 24.987 h. New observations on 9 nights 2020 Nov 10 - Dec. 4 provide a good fit to an irregular lightcurve with period 24.994 ± 0.002 h, amplitude 0.10 ± 0.01 mag. The nights of observation were selected so that the entire double period was also covered. The split halves plot of the double period, not presented, shows a near perfect overlap of the two halves. A period of 24.994 hours may now be considered secure. This value is very close to Stephens (2010) and Marciniak et al. (2018). The two periods reported by Behrend are now ruled out.

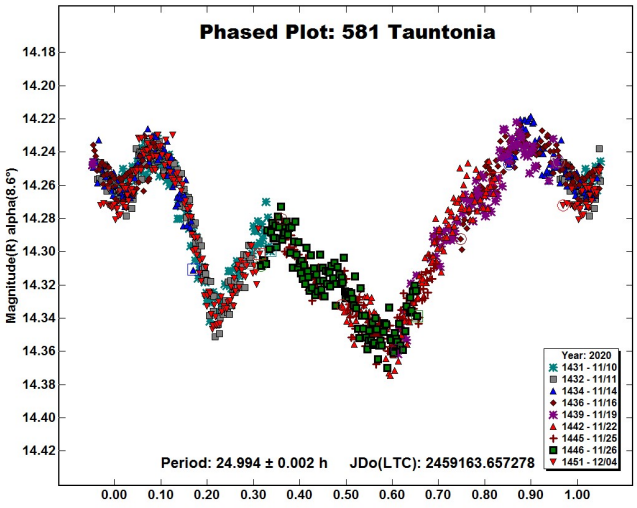

589 Croatia. Several different rotation periods have been published previously: Warner (2008), 11.7 h; Behrend (2013), 24.831 h; Waszczak et al. (2015), 16.385 h; Mas et al. (2018), 24.734 h. New observations on 8 nights 2020 Oct. 2 - 30 provide an excellent fit to a lightcurve with period 24.932 ± 0.001 h, amplitude 0.25 ± 0.01 mag. By selecting an odd number of days between sessions the entire double period was also covered. The split halves plot of the double period, not presented, shows a near perfect overlap of the two halves. A period of 24.932 hours may now be considered secure. This value is close to Behrend (2013) and to Mas et al. (2018) and rules out all other reported periods.

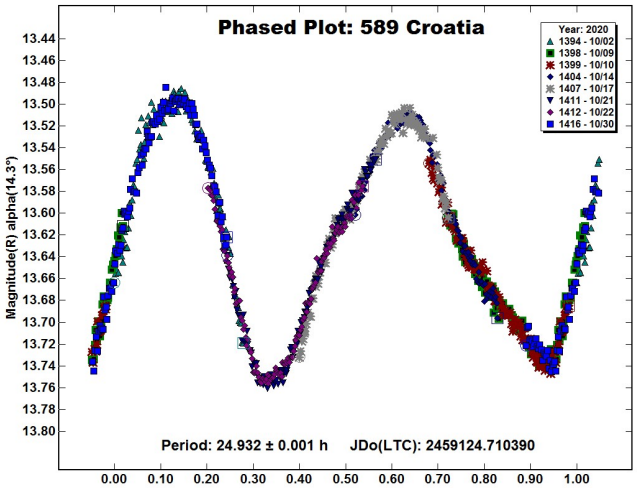

Number	Name	yyyy/mm/dd	Phase	LPAB	BPAB	Period(h)	P.E	Amp	A.E.
67	Asia	2020/11/06-2020/12/01	6.7, 17.0	32	-2	15.855	0.002	0.32	0.02
74	Galatea	2020/11/18-2020/12/19	*8.9, 7.5	73	-4	17.266	0.001	0.06	0.01
356	Liguria	2020/12/17-2021/01/14	*10.4, 9.7	100	11	31.690	0.002	0.14	0.01
570	Kythera	2020/09/30-2020/11/02	*6.3, 6.3	23	1	8.117	0.001	0.09	0.01
581	Tauntonia	2020/11/10-2020/12/04	*8.6, 6.1	65	-17	24.994	0.002	0.10	0.01
589	Croatia	2020/10/02-2020/10/30	14.3 6.4	50	-10	24.932	0.001	0.25	0.01
605	Juvisia	2020/10/13-2020/11/04	*9.3 10.0	30	19	15.844	0.001	0.18	0.01

Table I. Observing circumstances and results. Pts is the number of data points. The phase angle is given for the first and last date, with an asterisk if a minimum was reached between the first and last dates. LPAB and BPAB are the approximate phase angle bisector longitude and latitude at mid-date range (see Harris *et al.*, 1984).

605 Juvisia. Warner (2000) based on data obtained in year 1999, published a period of 15.855 h. Later Warner (2011) reexamined the year 1999 data and obtained a period of 15.93 h. Menke (2005) in a separate investigation published a period of 15.85 h. New observations on six nights 2020 Oct. 13 - Nov. 4 provide a good fit to a period 15.844 ± 0.001 h, amplitude 0.18 ± 0.01 mag. This period is in good agreement with previously reported periods, and the near perfect overlap of the two halves of the split halves plot also rules out the double period.

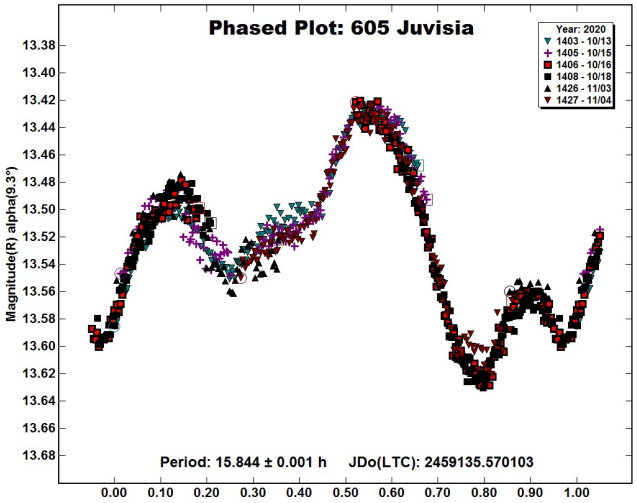

References

Aznar Macias, A.; Garceran, A.C.; Arce Mansego, E.; Brines Rodriguez, P.; Lozano de Haro, J.; Fornas Silva, A.; Fornas Silva, G.; Mas Martinez, V.; Rodrigo Chiner, O.; Herrero Porta, D. (2016). "Twenty-one asteroids lightcurves at Group Observadores de Asteroides (OBAS), late 2015 to early 2016." *Minor Planet Bull.* **43**, 257-263.

Behrend, R. (2001, 2004, 2005, 2006, 2013). Observatoire de Geneve web site. *http://*obswww.unige.ch/*~behrend/page_cou.html*

Blanco, C.; Di Martino, M.; Riccioli, D. (2000). "New rotational periods of 18 asteroids." *Planet. Space Sci.* **48**, 271-284.

Chavez, C.F. (2014). "Photometric observations of asteroid 570 Kythera using the virtual telescope project." *Minor Planet Bull.* **41**, 60.

Gil-Hutton, R.; Cañada, M. (2003). "Photometry of fourteen main belt asteroids." *Revista Mexicana de Astronomica y Astrofisica* **39**, 69-76.

Harris, A.W.; Young, J.W. (1980). "Asteroid rotation III. 1978 observations." *Icarus* **43**, 20-32.

Harris, A.W.; Young, J.W.; Scaltriti, F.; Zappala, V. (1984). "Lightcurves and phase relations of the asteroids 82 Alkmene and 444 Gyptis." *Icarus* **57**, 251-258.

Lagerkvist, C.-I.; Erikson, A.; Lahulla, F.; Di Martino, M.; Nathues, A.; Dahlgren, M. (2001). "A study of Cybele asteroids. I. Spin properties of ten asteroids." *Icarus* **149**, 190-197.

Marciniak, A.; and 42 co-authors (2018). "Photometric survey, modeling, and scaling of long-period and low-amplitude asteroids." *Astron. Astrophys.* **610**, A7.

Mas, V; Fornas, G; Lozano, J.; Rodrigo, O.; Fornas, A.; Cerreño, A.; Arce, E.; Brines, P.; Herrero, D. (2018). "Twenty-one asteroids lightcurves at Asteroids Observers (OBAS)-MPPD: Nov. 2016 - May 2017." *Minor Planet Bull.* **45**, 76-82.

Menke, J. (2005). "Asteroid lightcurve results from Menke Observatory." *Minor Planet Bull.* **32**, 85-88.

Pilcher, F. (2008). "Period determinations for 26 Proserpina, 34 Circe, 74 Galatea, 143 Adria, 272 Antonia, 419 Aurelia, and 557 Violetta." *Minor Planet Bull.* **35**, 135-138.

Pilcher, F. (2009). "New lightcurves of 8 Flora, 13 Egeria, 14 Irene, 25 Phocaea, 40 Harmonia, 74 Galatea, and 122 Gerda." *Minor Planet Bull.* **36**, 133-136.

Pilcher, F. (2017). "Rotation period determinations for 46 Hestia, 118 Peitho, 333 Badenia, 356 Liguria, and 431 Nephele." *Minor Planet Bull.* **44**, 294-297.

Stephens, R.D. (2010). "Lightcurve analysis of 581 Tauntonia, 776 Berbericia, and 968 Petunia." *Minor Planet Bull.* **37**, 122-123.

Warner, B.D. (2000). "Asteroid photometry at the Palmer Divide Observatory." *Minor Planet Bull.* **27**, 4-6.

Warner, B.D. (2008). "Asteroid lightcurve analysis at the Palmer Divide Observatory: June - October 2007. *Minor Planet Bull.* **35**, 56-60.

Warner, B.D.; Harris, A.W.; Pravec, P. (2009) "The Asteroid Lightcurve Database" *Icarus* **202**, 134-146. Updated 2020 Sept. *http://www.minorplanet.info/lightcurvedatabase.html.*

Warner, B.D. (2011). "Upon further review: IV. An examination of previous lightcurve analysis from the Palmer Divide Observatory." *Minor Planet Bull.* **38**, 52-54.

Waszczak, A.; Chang, C.-K.; Ofeck, E.O.; Laher, F.; Masci, F.; Levitan, D.; Surace, J.; Cheng, Y.; Iap, W.; Kinoshita, D.; Helou, G.; Prince, T.A.; Kulkarni, S. (2015). "Asteroid Light Curves from the Palomar Transient Factory Survey: Rotation Periods and Phase Functions from Sparse Photometry." *Astron. J.* **150**, A75.

ASTEROIDS 4092 TYR (FOLLOW UP, ANALYSIS, PRELIMINARY RESULTS) AND 699 HELA (SPIN-SHAPE MODEL)

E. Díez Alonso
Instituto Universitario de Ciencias y Tecnologías Espaciales de Asturias
C/ Independencia, 13, 33004, Oviedo, SPAIN
diezenrique@uniovi.es

F. García
Observatorio La Vara (MPC J38)
Valdés, Asturias, SPAIN

R.G. Farfán
Uraniborg Observatory (MPC Z55)
Écija, Sevilla, SPAIN

P. Pravec
Ondrejov Observatory
Ondrejov, CZECH REPUBLIC

P.J. Gutiérrez
Observatorio de Sierra Nevada, CSIC
Parque Natural de Sierra Nevada, Granada, SPAIN

J. Ruíz
Observatorio de Cantabria (MPC J96)
Cantabria, Spain

F. Limón
Observatorio Mazariegos (MPC Z50)
Palencia, SPAIN

J. Delgado
Observatorio Nuevos Horizontes (MPC Z73)
Camas, Sevilla, SPAIN

R. Naves
Observatorio Montcabrer (MPC 213)
Cabrils, SPAIN

J.M. Bosch
Observatorio de Santa María de Montmagastrell (MPC B74)
Bellpuig, SPAIN

E. Reina
Observatorio Masquefa (MPC 232)
Can Parellada, SPAIN

J. Temprano
Observatorio Linceo (MPC J59)
Santander, SPAIN

Sergio Luis Suárez Gómez, C. González Gutiérrez, F. García Riesgo, S. Fernández, J. de Cos Juez
Instituto Universitario de Ciencias y Tecnologías Espaciales de Asturias
C/ Independencia, 13, 33004, Oviedo, SPAIN

(Received: 2020 Dec 19)

In this work we present the results of the photometric follow up of the asteroid 4092 Tyr carried out by the Grupo de Observadores de Asteroides throughout the months of 2020 August and September. The rotation period derived from the observations is P = 16.091 ± 0.003 h. Furthermore, 4092 Tyr has been revealed to be a synchronous binary asteroid with two main bodies of similar size. We also present a confirmation of the rotation period of the asteroid 699 Hela (0.1415100 ± 0.0000024 d), and a study of its shape and spin. We analyze dense lightcurves acquired in 2020 by the Grupo de Observadores de Asteroides, as well as those available in public databases. We have also used sparse lightcurves from USNO (Flagstaff) and the TESS mission. We find two possible solutions for the spin axis (λ1, β1) = (37°, +51°), (λ2, β2) = (189°, +14°), in agreement with previously published models.

4092 Tyr is a main-belt asteroid discovered by Jensen in 1986. The published diameter is 6.8 km and the albedo is 0.2 (LCDB; Warner et al., 2009), but the rotation period is not confirmed. A search in public databases did not find dense lightcurves prior to 2020. In the Database of Asteroid Models from Inversion Techniques (DAMIT, 2020) are published two models of the asteroid (Ďurech, 2019) made with photometry from the Gaia mission (Gaia collaboration et al., 2018) and sparse photometry from the Asteroids Dynamics Syte (AstDys-2, 2020). These models don't show the binary nature of Tyr but the inferred rotation period (16.0937 h) is in good agreement with the period presented in this work.

An analysis of the sparse photometry (Lowel, Catalina, Gaia) made by researchers from the Instituto Universitario de Ciencias y Tecnologías Espaciales de Asturias (ICTEA) using the Generalyzed Lomb Scargle (GLS) periogram (Zechmeister and Kürster, 2018), also shows a value for the rotation period of Tyr in agreement with that obtained from the Grupo de Observadores de Asteroides (GOAS, 2020) lightcurves.

Since GOAS observes poorly studied asteroids, or those that require revision, 4092 Tyr was included in the photometric monitoring program. Fifty-eight lightcurves were obtained in 25 nights between 2020 August 20 and September 29, with 4092 Tyr in the range of ecliptic longitudes and latitudes λ = 329.6658°, β = 3.9038°, and λ = 344.9986°, β = 4.0247°, elongation in the range 171.4° and 137.7°, and phase angle in the range 4.3° and 19.8°. V Johnson, I cousin, R cousin, Sloan g′ and Sloan i′ were used in the photometric follow up to derive and study the color indices (in preparation).

The images were calibrated in the standard way (bias, darks and flats), rejecting those with SNR < 25 for Tyr. We also reduced to geocentric date and absolute magnitude.

In order to carry out the photometric analysis, we used the *FotoDiF* (2020) and *Periodos* (2020) packages. We derive a period *P* = 16.091 ± 0.003 h, with a confidence interval (probability of 0.95) from 16.082244 to 16.0987385 h and an RMS of 0.028704. The amplitude is 0.53 ± 0.04 mag. In Figure 1, we show the rotation curve of 4092 Tyr, phased with the derived period. In the figure, the magnitudes are in absolute values, and light-time and phase angle corrections have been applied.

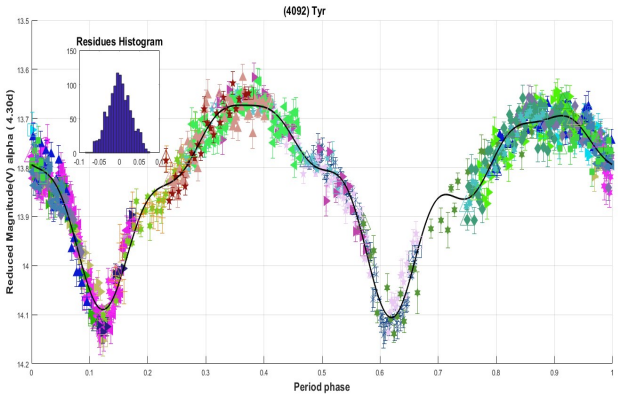

Figure 1. Rotation curve of 4092 Tyr.

In 2020 August and September, an independent photometric follow up of 4092 Tyr was made by D. Romeuf, D. Augustin, E. Barbotin and R. Behrend. None of the teams was aware of the fact that the other were doing the same follow up. A measure of the rotation period (P = 0.670313 ± 0.000022 d) and an announcement of the binary nature of Tyr based on the observations from R. Behrend's team have been published independently (Behrend, 2020web). Simultaneously, the GOAS data were analyzed by P. Pravec (Ondrejov Observatory) and P.J. Gutierrez (CSIC, Observatorio de Sierra Nevada) and reported the asteroid as being binary (Garcia et al., 2020).

A detailed inspection of the temporal evolution of the minimum at phase ~0.63 and the slope in certain regions of the lightcurve, reveals the binary nature of 4092 Tyr (Kwiatkowski et al., 2009).

Figure 2 shows the evolution of the eclipse corresponding to the minimum at phase ~0.63 (typical behavior of a binary asteroid in opposition); as the days go by, a step appears in the ascending size of the lightcurve (centered in the minimum at phase ~0.63), disappearing and reappearing later in the descending size. Simultaneously, the minimum goes deeper and sharpens.

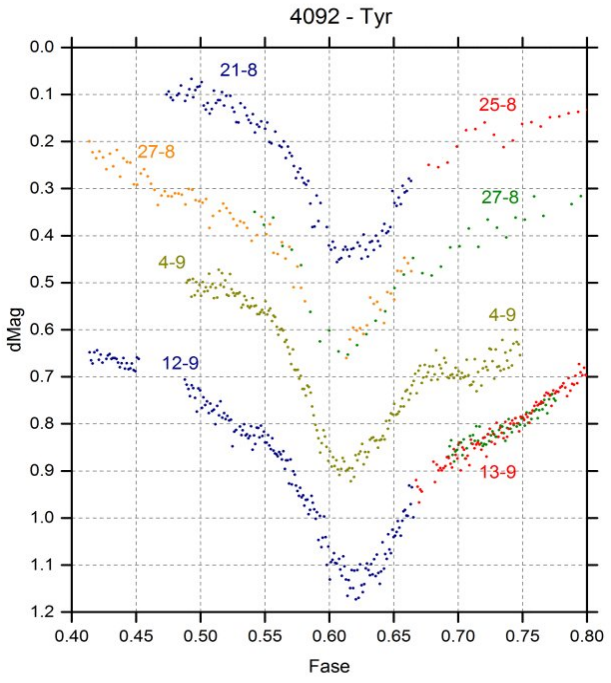

Figure 2. From top to bottom: 1) August 21t^{h} – August 25th. 2) August 27th. 3) September 4th. 4) September 12th – September 13th.

As stated in the CBET 4850, mutual eclipses are 0.17-0.23 mag deep, which implies a lower limit for the ratio of the primary to secondary diameters of 0.45. The rotations of the components are synchronous with the orbital motion, and the combined rotational amplitude of the pair is 0.3 magnitudes at a phase angle between 4° and 12°.

699 Hela has been widely observed in multiple apparitions and its rotation period is well known (Behrend, 2020web), but a unique spin-shape model has not been established yet.

Automatic surveys as ASAS-SN (Kochanek et al., 2017) or ATLAS (Tonry et al., 2018) and space missions as TESS (Ricker et al., 2014) or Gaia (Gaia collaboration et al., 2018), provide a large number of lightcurves with a wide temporal coverage to derive the main parameters of asteroids. However, since many asteroids are too faint for these automatic surveys and space missions, and also their photometry is sparse, the work of amateur astronomers is necessary. Therefore, a balance between both data sources (amateur astronomers and automatic searches) is essential.

In this work we present the first collaboration between the Grupo de Observadores de Asteroides (GOAS, 2020) and the Instituto Universitario de Ciencias y Tecnologías Espaciales de Asturias (ICTEA), confirming the rotation period of asteroid 699 Hela and studying its shape and spin axis. For this matter we analyze observations acquired by GOAS, photometry from the TESS mission, and archival photometry.

699 Hela was observed by GOAS from 2020 July 7-24. The follow up finished with nine dense lightcurves of the asteroid. In the analysis, we used the dense lightcurves of 699 Hela available at the Asteroid Photometry Database (ALCDEF, 2020). Eleven lightcurves are available at ALCDEF, and five of them have already been obtained by GOAS in the 2020 follow up. Therefore, six dense lightcurves covering the 1999, 2016, and 2020 apparitions were used from ALCDEF. We also used the sparse lightcurves from USNO (Flagstaff), available at the Asteroids Dynamics Site (AstDys-2, 2020), as well as the sparse lightcurves reduced by Pál et al. (2020) from the TESS space mission (Ricker et al., 2014).

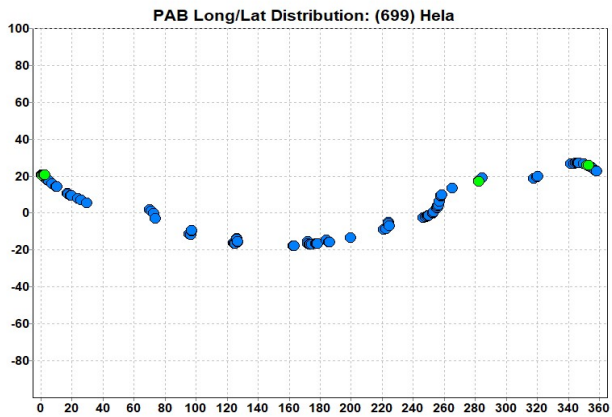

Figure 3. Ecliptic longitude and latitude of phase angle bisector for the observations used. Blue: sparse data. Green: dense data.

The analysis of the light curves obtained by GOAS in the 2020 apparition using the ANOVA method (Schwarzenberg-Czerny, 1996), results in a rotation period of 3.3959 ± 0.0022 h (Figure 4), in agreement with the value of 3.39624 ± 0.00006 h that was published by R. Behrend (2020web) with the same data. We will adopt this second value for the rotation period of 699 Hela.

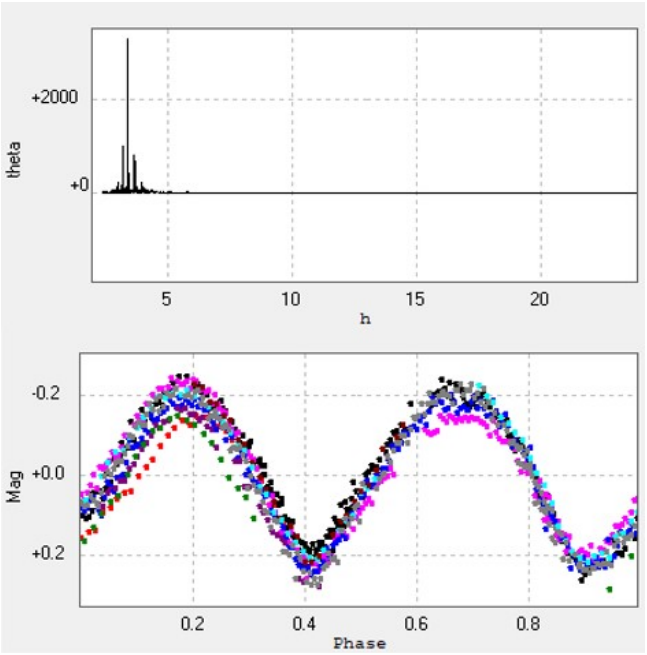

Figure 4. Top panel: ANOVA periodogram obtained with GOAS data of 699 Hela. The highest peak is at 3.3959 ± 0.0022 h. Bottom panel: photometry data phased with the period of 3.3959 ± 0.0022 h.

The lightcurve inversion was made with the *MPO LCInvert* package (BDW Publishing, 2016), which implements the procedures described in Kaasalainen and Torppa (2001) and Kaasalainen et al. (2001). We adopted a weight of 0.3 for the sparse curves (USNO and TESS) and 1.0 for the dense curves (ALCDEF & GOAS). We carried out a medium search adopting P = 3.39624 h, a value of 0.1 for the dark facet factor and 50 iterations. In this way we analyzed 312 different positions of the pole in steps of 15° in latitude and longitude. The analysis finds two regions (Figure 5) that minimize χ2, centered at (λ, β) = (30°, +45°) and (195°, +15°).

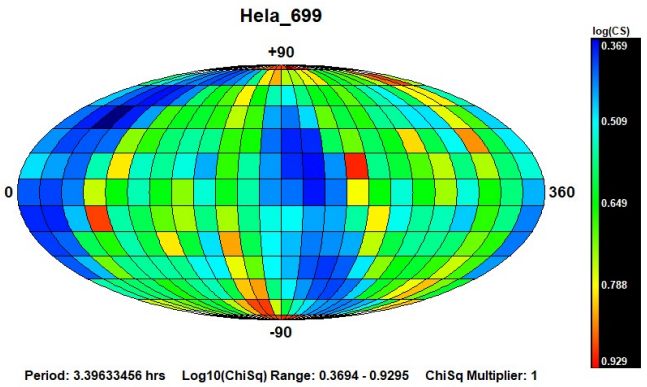

Figure 5: Initial pole search distribution. The darkest blue regions are those that minimize χ2.

After that, we made fine searches centered in these two initial values found. The fine searches find (λ_1, β_1) = (37°, +51°) and (λ_2, β_2) = (189°, +14°), with values $\chi 2$ = 2.34 and $\chi 2$ = 2.30, respectively. These solutions, with a typical uncertainty of ±20°, seem to mirror one another. They are also in moderate agreement with the solutions published in the DAMIT database (Ďurech et al., 2010), (λ, β) = (45°, +44°) or (197°, +31°). However, more observing campaigns are necessary to adopt one of the two solutions.

In Figure 6 we present the shape model obtained corresponding to the solution (λ_2, β_2) = (189°, +14°), while in Figure 7 we present two examples of the fit between the light curves from GOAS and TESS and the theoretical lightcurves based on the derived model.

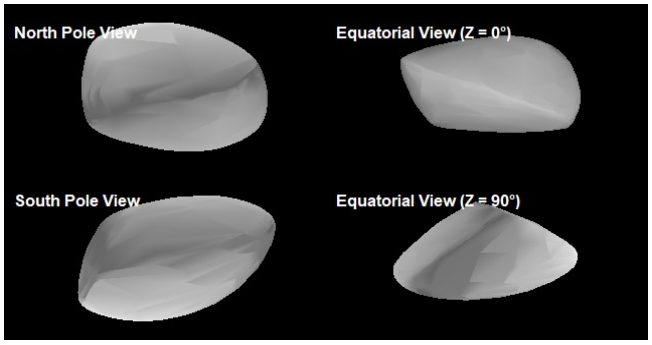

Figure 6. Shape model of (699) Hela corresponding to the solution (λ_2, β_2) = (189°, +14°).

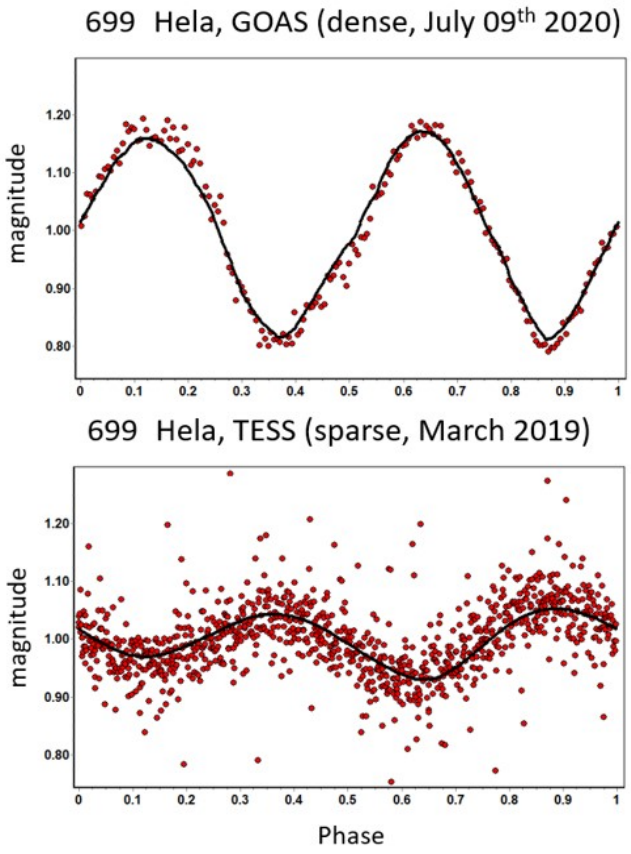

Figure 7. The fit between the experimental (red dots) and theoretical (black lines) lightcurves derived from the model for the solution (λ_2, β_2) = (189°, +14°). Top panel: red dots correspond to dense data obtained by GOAS on 2020 July 9. Bottom panel: red dots correspond to the sparse data from the TESS mission.

Acknowledgements

4092 Tyr co-authors: F.G., R.G.F., P.P., P.J.G., J.R., F.L., J.D., R.N., J.M.B., E.R., E.D.A., J.C.J. 699 Hela co-authors: F.G., J.R., J.D., J.T., S.L.S.G., C.G.G., F.G.R., S.F., E.D.A., J.C.J.

References

ALCDEF (2020). Asteroid Lightcurve Data Exchange Format database. *http://www.alcdef.org/*

AstDys-2 (2020). Asteroids - Dynamic Site web location. *https://newton.spacedys.com/astdys2/*

BDW Publishing (2016). *http://www.minorplanetobserver.com/MPOSoftware/MPOLCInvert.htm*

Behrend, R. (2020web). Observatoire de Geneve web site. *http://obswww.unige.ch/~behrend/page_cou.html*

DAMIT (2020). Database of Asteroid Models from Inversion Techniques (DAMIT). *https://astro.troja.mff.cuni.cz/projects/damit/*

Ďurech, J.; Sidorin, V.; Kaasalainen, M. (2010). "DAMIT: A Database of Asteroid Models." *Astronomy & Astrophysics* ***513***, A46.

Ďurech, J.; Hanuš, J.; Vančo, R. (2019). "Inversion of Asteroid Photometry from Gaia DR2 and the Lowell Observatory Photometric Database." *Astronomy & Astrophysics* **631**, A2.

Fotodif (2020). *http://astrosurf.com/orodeno/fotodif/index.htm*

Gaia Collaboration; Brown, A.G.A.; Vallenari, A.; Prusti, T.; de Bruijne, J.H.J.; Babusiaux, C.; and 448 colleagues. (2018). "Gaia Data Release 2 Summary of the Contents and Survey Properties." *Astronomy & Astrophysics* **616**, A1.

Garcia, F.; Farfan, R.G.; Pravec, P.; Ruiz, J.; et al. (2020). *CBET* **4850**.

GOAS (2020). Grupo de Observación de Asteroides. *https://sites.google.com/view/goas2*

Kaasalainen, M.; Torppa, J. (2001). "Optimization Methods for Asteroid Lightcurve Inversion: I. Shape Determination." *Icarus*, **153**, 24-36.

Kaasalainen, M.; Torppa, J.; Muinonen, K. (2001). "Optimization Methods for Asteroid Lightcurve Inversion: II. The Complete Inverse Problem." *Icarus* **153**, 37-51.

Kochanek, C.S.; Shappee, B.J.; Stanek, K.Z.; Holoien, T.S.; Thompson, T.A.; Prieto, J.L.; Dong, S.; Sheilds, J.V.; Will, D.; Britt, C.; Perzanowski, D.; Pojmanski, G. (2017). "The All-sky Automated Survey for Supernovae (ASAS-SN) Light Curve Server. v1.0." *Publications of the Astronomical Society of the Pacific* **129**, 104502.

Kwiatkowski, T.; Kryszczyńska, A.; Polińska, M.; Buckley, D.A.H.; O'Donoghue, D.; Charles, P.A.; Crause, L.; Crawford, S.; Hashimoto, Y.; Kniazev, A.; Loaring, N.; Romero Colmenero, E.; Sefako, R.; Still, M.; Vaisanen, P. (2009). "Photometry of 2006 RH120: An Asteroid Temporary Captured into a Geocentric Orbit." *Astron. Astrophys.* ***495***, 967-974.

Pál, A.; Szakáts, R.; Kiss, C.; Bódi, A.; Bognár, Z.; Kalup, C.; Kiss, L.L.; Marton, G.; Molnár, L.; Plachy, E.; Sárneczky, K.; Szabó, G.M.; Szabó, R. (2020). "Solar System Objects Observed with TESS - First Data Release: Bright Main-belt and Trojan Asteroids from the Southern Survey." *Ap. J. Suppl. Ser.* **247**, id.26.

Períodos (2020). *http://www.astrosurf.com/salvador/Programas.html*

Ricker, G.R.; Winn, J.N.; Vanderspek, R.; Latham, D.W.; Bakos, G.A. and 53 colleagues (2014). "Transiting Exoplanet Survey Satellite." *Journal Astron. Telescopes, Instruments, and Systems* **1**, p. 014003.

Schwarzenberg-Czerny, A. (1996). "Fast and statistically optimal period search in uneven sampled observations." *Ap. J. Letters* **460**, L107.

Tonry, J.L.; Denneau, L.; Heinze, A.N.; Stalder, B.; Smith, K.W.; Smartt, S.J.; Stubbs, C.W.; Weiland, H.J.; Rest, A. (2018). "ATLAS: A High-cadence All-sky Survey System." *Publications of the Astronomical Society of the Pacific* **130**, 064505.

Warner, B.D.; Harris, A.W.; Pravec, P. (2009). "The Asteroid Lightcurve Database." *Icarus* **202**, 134-146. Updated 2020 June. *http://www.minorplanet.info/lightcurvedatabase.html*

Zechmeister, M.; Kürster, M. (2009). "The generalised Lomb-Scargle periodogram-a new formalism for the floating-mean and Keplerian periodograms." *Astron. Astrophys.* ***496***, 577-584.

ASTEROID PHOTOMETRY AND LIGHTCURVE ANALYSIS AT GORA'S OBSERVATORIES, PART IV.

Milagros Colazo
Instituto de Astronomía Teórica y Experimental
(IATE-CONICET), Argentina
Facultad de Matemática, Astronomía y Física,
Universidad Nacional de Córdoba, Argentina
Grupo de Observadores de Rotaciones de Asteroides (GORA),
Argentina, *https://aoacm.com.ar/gora/index.php*
milirita.colazovinovo@gmail.com

Ariel Stechina, César Fornari, Néstor Suárez, Raúl Melia, Mario Morales, Ezequiel Bellocchio, Eduardo Pulver, Tiago Speranza, Damián Scotta, Aldo Wilberger, Aldo Mottino, Erick Meza, Fabricio Romero, Patricio Tourne Passarino, Matías Suligoy, Ricardo Llanos, Andrés Chapman, Matías Martini, Carlos Colazo

Grupo de Observadores de Rotaciones de Asteroides (GORA), Argentina

Comisión Nacional de Investigación y Desarrollo Aeroespacial del Perú - CONIDA

Observatorio Cruz del Sur (MPC I39) - San Justo (Buenos Aires-Argentina)

Observatorio de Sencelles (MPC K14) - Sencelles (Mallorca-Islas Baleares-España)

Observatorio Los Cabezones (MPC X12) - Santa Rosa (La Pampa-Argentina)

Observatorio Galileo Galilei (MPC X31) - Oro Verde (Entre Ríos-Argentina)

Observatorio Antares (MPC X39) - Pilar (Buenos Aires-Argentina)

Observatorio Astronómico de Moquegua 1 (MPC W73) - Cambrune (Moquegua-Perú)

Observatorio AstroPilar (GORA APB) - Pilar (Buenos Aires-Argentina)

Observatorio Astronómico Calchaquí (GORA OAC) - El Bañado (Tucumán-Argentina)

Observatorio de Aldo Mottino (GORA OAM) - Rosario (Santa Fe-Argentina)

Observatorio Astro Pulver (GORA OAP) - Rosario (Santa Fe-Argentina)

Observatorio de Ariel Stechina 1 (GORA OAS) - Reconquista (Santa Fe-Argentina)

Observatorio de Damián Scotta 2 (GORA OD2) - San Carlos Centro (Santa Fe-Argentina)

Observatorio Astronómico Municipal Reconquista (GORA OMR) - Reconquista (Santa Fe-Argentina)

Observatorio de Raúl Melia (GORA RMG) - Gálvez (Santa Fe-Argentina)

Observatorio Astronómico Aficionado Omega (GORA OAO) - Córdoba (Córdoba-Argentina)

(Received: 2020 Dec 30)

Synodic rotation periods and amplitudes are reported for: 424 Gratia, 579 Sidonia, 589 Croatia, 693 Zerbinetta, 791 Ani, 824 Anastasia, 858 El Djezair, 1024 Hale, 1271 Isergina, 1663 van den Bos.

The periods and amplitudes of asteroid light curves currently presented are the product of a collaborative work by GORA (Grupo de Observadores de Rotaciones de Asteroides) group. In all the studies we have applied relative photometry assigning V magnitudes to the calibration stars.

The image acquisition was performed without filters and with exposure times of a few minutes. All images used were corrected using dark frames and in some cases bias and flat-field were also used. Photometry measurements were performed using *FotoDif* software and for the analysis we employed *Periodos* software (Mazzone, 2012).

Below, we present the results for each asteroid under study. The lightcurve figures contain the following information: the estimated period and period error and the estimated amplitude and amplitude error. In the reference boxes the columns represent, respectively, the marker, observatory MPC code or - failing that - the GORA internal code, session date, session off-set, and number of data points.

Targets were selected based on the following criteria: 1) those asteroids with magnitudes accessible to the equipment of all participants, 2) those with favorable observation conditions from Argentina i.e. with negative declinations δ and 3) objects with few periods reported in the literature and/or with Lightcurve Database (LCDB) (Warner et al., 2009) quality codes (U) of less than 3.

424 Gratia. This asteroid belongs to the main belt and was discovered in 1896 by Auguste Charlois. We found only one period in the literature, published by Florczak et al. (1997): P = 19.47 ± 0.01 h with Δm = 0.32 ± 0.02 mag. Our result of P = 40.106 ± 0.010 h clearly indicates a longer period, whereas our measured amplitude is significantly lower: Δm = 0.18 ± 0.01 mag. We consider this latter difference to be consequence of a change in the aspect angle.

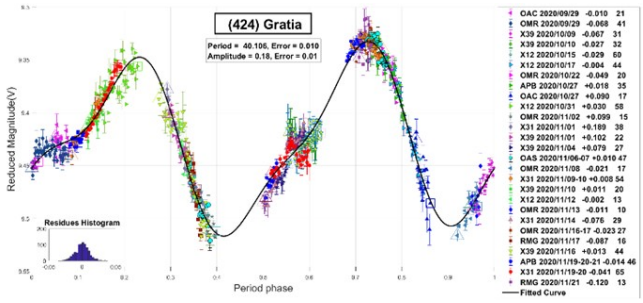

579 Sidonia. Sidonia is a bright S-type asteroid discovered in 1905 by August Kopff. The periods published for this asteroid are: P = 13.00 h (Tedesco, 1979), P = 18.72 h (Behrend, 2005web) and P = 16.286 ± 0.001 h (Stephens, 2010a). We have determined a period of P = 16.279 ± 0.007 h with an amplitude of Δm = 0.10 ± 0.01 mag. Our result on the period agrees with that published by Stephens, which is the most recent we found in the literature.

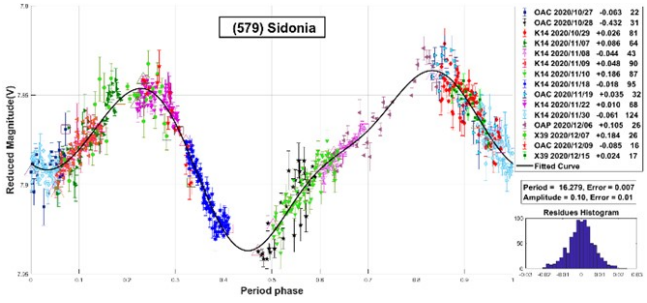

589 Croatia. This asteroid was discovered in 1906 by August Kopff. Three different periods were found in the literature: P = 11.7 ± 0.1 h with Δm = 0.16 ± 0.02 mag (Warner, 2008), P = 24.821 ± 0.002 h with Δm = 0.25 ± 0.03 mag (Behrend, 2013web) and P = 16.3854 ± 0.0931 h with Δm = 0.32 mag (Waszczak et al., 2015). We have calculated a period of P = 24.972 ± 0.013 h with an amplitude of Δm = 0.26 ± 0.02, well in agreement with the period published by Behrend (2013web).

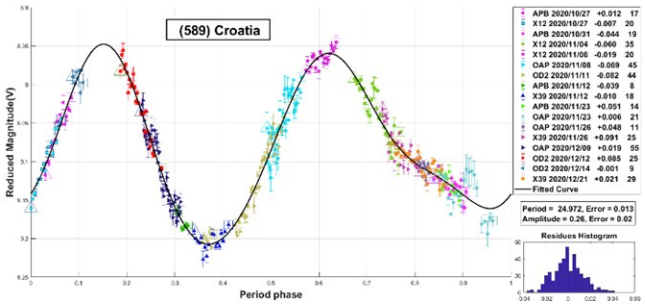

693 Zerbinetta was discovered on September 21, 1909, by August Kopff. Several measurements of the period were reported in the literature for this particular object, such as: P = 11.32 ± 0.05 h with Δm = 0.18 ± 0.01 mag (Behrend, 2005web), P = 11.475 ± 0.001 h with Δm = 0.29 ± 0.2 mag (Chiorny et al., 2007), P = 11.32 ± 0.01 h with Δm = 0.14 ± 0.01 mag (Behrend, 2010web), and P = 11.3 ± 0.5 h with Δm = 0.16 ± 0.01 mag (Behrend, 2011web). We found a period of P = 11.474 ± 0.009 h, in accordance with that obtained by Chiorny et al. (2007), with an amplitude of Δm = 0.15 ± 0.01 mag.

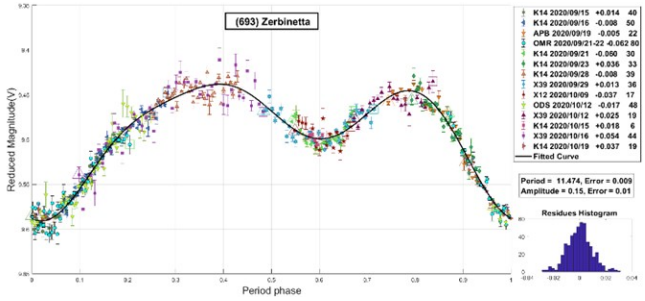

791 Ani is a dark carbonaceous C-type asteroid discovered in 1914 by Grigory Neujmin. In the literature, three different measurements have been published for the period of this object. On the one hand, the Behrend measurement (2011web) suggests a period of P = 12.0 ± 0.5 h with Δm = 0.38 ± 0.02 mag. A slightly longer period was published by Sauppe et al. (2007), P = 16.72 ± 0.03 h with Δm = 0.32 ± 0.05 mag and by Warner (2011web), P = 16.8 ± 0.1 h with Δm = 0.35 ± 0.05. Finally, the longest period estimations correspond to: P = 22.850 ± 0.003 h with Δm = 0.17 ± 0.01 mag and P = 22.85 ± 0.05 h with Δm = 0.38 ± 0.02 mag (Behrend, 2005web, 2007web). Our analysis yields a period of P = 11.159 ± 0.009 h with Δm = 0.13 ± 0.01 mag, consistent with the shortest period reported previously.

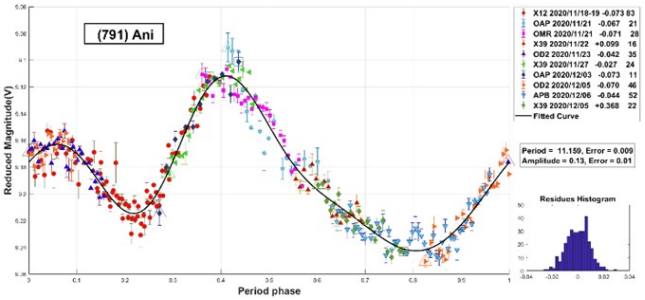

824 Anastasia. Anastasia was discovered on March 25, 1916, by Grigory Neujmin. Our preliminary analysis indicated that we were dealing with a very long-period object and that the study would be harder than expected. Our final results are: P = 250.845 ± 0.015 h with Δm = 1.20 ± 0.02 mag. Previous results in the literature support these data, as is the case of Stephens (2010b), who measured a period of 250 ± 1 h with an amplitude of Δm = 1.20 ± 0.05 mag.

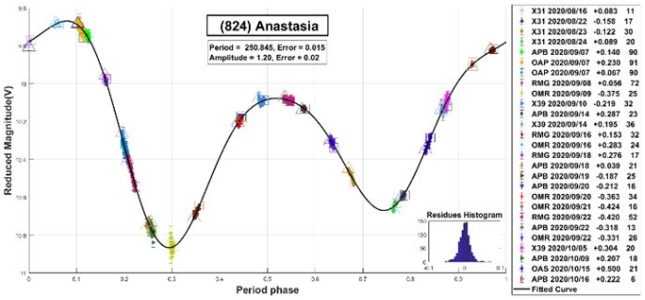

858 El Djezair is a bright S-type asteroid discovered in 1916 by Frédéric Sy. We found in the literature two different periods calculated for this object: P = 22.31 ± 0.02 h with Δm = 0.10 ± 0.02 mag (Warner, 2005) and P = 19 ± 1 h with Δm = 0.06 ± 0.02 mag (Behrend, 2007web). In this work we proposed a different period for this asteroid, which is P = 33.525 ± 0.013 h, with Δm = 0.21 ± 0.02 mag.

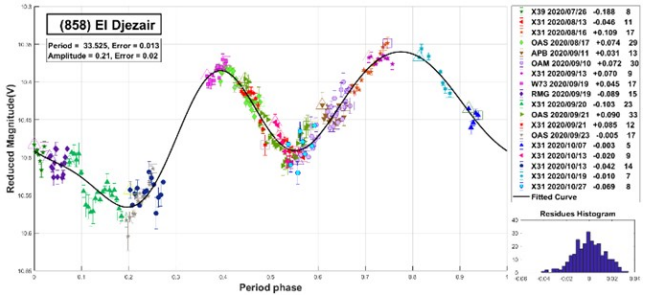

1024 Hale is a carbonaceous C-type asteroid discovered in 1923 by George Van Biesbroeck. We found only one period published in the literature for this asteroid: P = 16.0 ± 0.1 h, with Δm = 0.10 ± 0.02 mag (Alkema, 2013). According to our analysis, this object constitutes another case of long-period asteroid. The results we obtained are P = 106.047 ± 0.012 h and Δm = 0.47 ± 0.02 mag.

Number	Name	yyyy mm/dd	Phase	L_{PAB}	B_{PAB}	Period(h)	P.E.	Amp	A.E.	Grp
424	Gratia	2020 09/29-11/21	*07.7,16.7	19	-10.4	40.106	0.010	0.18	0.01	MB-O
579	Sidonia	2020 10/27-12/15	*09.4,09.2	58	-5.7	16.279	0.007	0.10	0.01	MB-O
589	Croatia	2020 10/27-12/21	*07.4,13.7	50	-10.9	24.972	0.013	0.26	0.02	MB-O
693	Zerbinetta	2020 09/15-10/19	*03.5,10.0	0	3.2	11.474	0.009	0.15	0.01	MB-O
791	Ani	2020 11/18-12/06	*07.6,09.3	57	-19.2	11.159	0.009	0.13	0.01	MB-O
824	Anastasia	2020 08/16-10/16	*05.5,18.3	335	-3.4	250.845	0.015	1.20	0.02	MB-O
858	El Djezair	2020 07/26-10/27	04.6,21.4	304	-9.7	33.525	0.013	0.21	0.02	MB-O
1024	Hale	2020 09/29-11/06	*10.0,17.1	10	-15.5	106.047	0.012	0.47	0.02	MB-O
1271	Isergina	2020 10/27-11/17	*05.4,06.1	43	-8.5	7.599	0.015	0.19	0.02	MB-O
1663	van den Bos	2020 09/19-11/20	*06.8,27.5	3	-7.7	767.148	0.020	0.94	0.03	MB-O

Table I. Observing circumstances and results. The phase angle is given for the first and last date. If preceded by an asterisk, the phase angle reached an extremum during the period. L_{PAB} and B_{PAB} are the approximate phase angle bisector longitude/latitude at mid-date range (see Harris et al., 1984). Grp is the asteroid family/group (Warner et al., 2009). MB-O: main-belt outer.

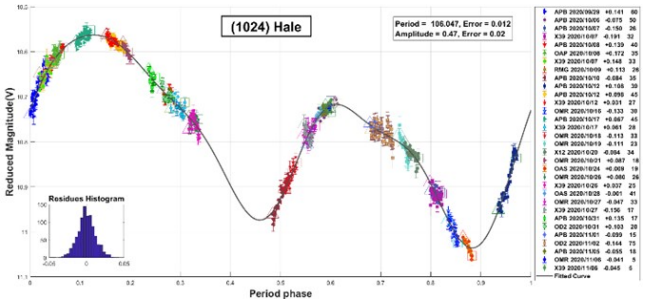

1271 Isergina is a carbonaceous asteroid discovered on October 10, 1931, by Grigory Neujmin. The periods published for this asteroid are: P = 7.59932 ± 0.00009 h with maximum amplitude of 0.24 mag (Benishek, 2016), P = 7.829 ± 0.002 h with maximum amplitude of 0.27 mag (Aznar Macias et al., 2016) and P = 9.864 ± 0.004 h (Behrend, 2017web). Our results show a better concordance with those of Benishek (2016) since we found a period P = 7.599 ± 0.015 h, with Δm = 0.19 ± 0.02 mag. The difference in amplitude may be due to the change in aspect angle.

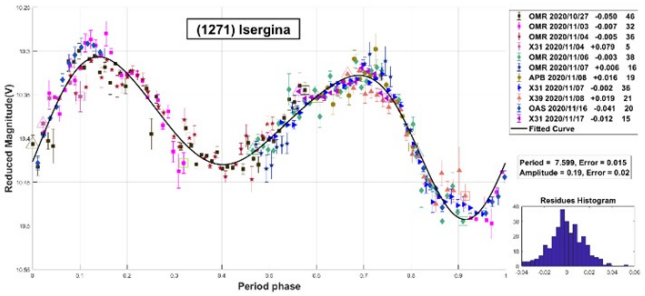

1663 van den Bos is an S-type asteroid discovered in 1926, by Harry Edwin Wood. The periods reported in the literature suggest that it is a case of a slow rotator: P = 155 ± 5 h with Δm = 0.5 ± 0.1 mag (Ruthroff, 2011) and P = 740 ± 10 h with Δm = 0.80 ± 0.05 mag (Stephens and Higgins, 2011). The results we obtained, P = 767.148 ± 0.020 h with Δm = 0.94 ± 0.03 mag, are similar to those obtained by Stephens and Higgins (2011), thus supporting the hypothesis that it is indeed a slow rotator.

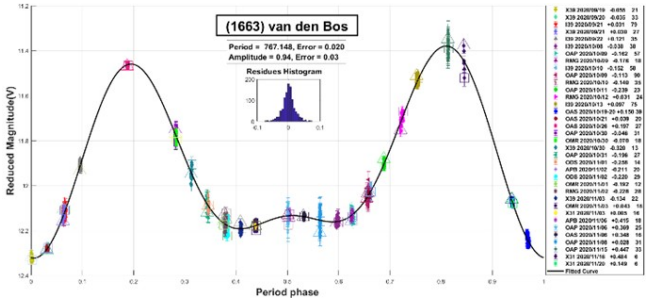

Acknowledgements

We want to thank Julio Castellano as we use his *FotoDif* program for preliminary analyses, and to Fernando Mazzone for his *Periods* program, used in final analyses. This research has made use of the Small Bodies Data Ferret (*http://sbn.psi.edu/ferret/*), supported by the NASA Planetary System. This research has made use of data and/or services provided by the International Astronomical Union's Minor Planet Center.

Observatory	Telescope	Camera
I39 Obs.Astr.Cruz del Sur	Telesc. Newtoniano (D=200mm; f=4.0)	CMOS QHY174
K14 Obs.Astr.de Sencelles	Telesc. SCT (D=254mm; f=4.3)	CCD SBIG ST-7XME
X12 Obs.Astr.Los Cabezones	Telesc. Newtoniano (D=200mm; f=5.0)	CMOS QHY174MGPS
X31 Obs.Astr.Galileo Galilei	Telesc. RCT ap (D=405mm; f=8.0)	CCD SBIG STF8300M
X39 Obs.Astr.Antares	Telesc. Newtoniano (D=250mm; f=5.0)	CCD QHY9 Mono
W73 Obs.Astr.de Moquegua	Telesc. RCT APM (D=1000mm; f=8.0)	CCD FLI ProLine 16803
APB Obs.Astr.AstroPilar	Telesc. ODK (D=250mm; f=6.8)	CCD FLI8300M
OAC Obs.Astr.Calchaquí	Telesc. Refractor (D=100mm; F=9.0)	CCD QHY9S
OAM Obs.Astr.de Aldo Mottino	Telesc. Newtoniano (D=250mm; f=4.7)	CCD SBIG STF8300M
OAP Obs.Astr.Astro Pulver	Telesc. SCT (D=203mm; f=7.0)	CMOS QHY5 LII M
OAS Obs.Astr.de Ariel Stechina 1	Telesc. Newtoniano (D=254mm; f=4.7)	CCD SBIG STF402
OD2 Obs.Astr.de Damián Scotta 2	Telesc. Newtoniano (D=200mm; f=5.0)	CCD Atik 314L+
OMR Obs.Astr.Municipal Reconquista	Telesc. Newtoniano (D=254mm; f=4.0)	CMOS QHY 174M
RMG Obs.Astr.de Raúl Melia	Telesc. SCT (D=200mm; f=10.0)	CCD Meade DSI Pro II

Table II. List of observatories and equipment.

References

Alkema, M.S. (2013). "Asteroid Lightcurve Analysis at Elephant Head Observatory: 2012 November-2013 April." *Minor Planet Bulletin*, **40(3)**, 133-137.

Aznar Macias, A.; Carreno Garcerain, A.; Arce Masego, E.; Brines Rodriguez, P.; Lozano de Haro, J.; Fornas Silva, A.; Fornas Silva, G.; Mas Martinez, V.; Rodrigo Chiner, O.; Herrero Porta, D. (2016). "Twenty-one Asteroid Lightcurves at Group Observadores de Asteroides (OBAS): Late 2015 to Early 2016." MPBu, 43(3), 257-263.

Behrend, R. (2005, 2007, 2010, 2011, 2013, 2017). Observatoire de Geneve web site.
http://obswww.unige.ch/~behrend/page_cou.html

Benishek, V. (2016). "Lightcurves and rotation periods for 14 asteroids." *Minor Planet Bulletin*, **43(4)**, 339-342.

Chiorny, V.G.; Shevchenko, V.G.; Krugly, Y.N.; Velichko, F.P.; Gaftonyuk, N.M. (2007). "Photometry of asteroids: Lightcurves of 24 asteroids obtained in 1993–2005." *Planetary and Space Science*, **55(7-8)**, 986-997.

Florczak, M.; Dotto, E.; Barucci, M.A.; Birlan, M.; Erikson, A.; Fulchignoni, M.; Nathues, A; Perret, L.; Thebault, P. (1997). "Rotational properties of main belt asteroids: photoelectric and CCD observations of 15 objects." *Planetary and Space Science*, **45(11)**, 1423-1435.

Harris, A.W.; Young, J.W.; Scaltriti, F.; Zappala, V. (1984). "Lightcurves and phase relations of the asteroids 82 Alkmene and 444 Gyptis." *Icarus* **57**, 251-258.

Mazzone, F.D. (2012). Periodos software, version 1.0.
http://www.astrosurf.com/salvador/Programas.html

Ruthroff, J.C. (2011). "Lightcurve Analysis of Eight Main-belt Asteroids and a Revised Period for 185 Eunike." *Minor Planet Bulletin*, **38(2)**, 86-88.

Sauppe, J.; Torno, S.; Lemke-Oliver, R.; Ditteon, R. (2007). "Asteroid Lightcurve Analysis at the Oakley Observatory-March/April 2007." *Minor Planet Bulletin*, **34(4)**, 119-122.

Stephens, R.D. (2010a). "Asteroids Observed from GMARS and Santana Observatories: 2009 June-September." *Minor Planet Bulletin*, **37**, 28-29.

Stephens, R.D. (2010b). "Asteroids Observed from GMARS and Santana Observatories: 2010 April-June." *Minor Planet Bulletin*, **37(4)**, 159-161.

Stephens, R.D., Higgins, D. (2011). "The Lightcurve for the Long-period Asteroid 1663 van den Bos." *Minor Planet Bulletin*, **38(2)**, 72.

Tedesco, E.F. (1979). "A photometric investigation of the colors, shapes and spin rates of Hirayama family asteroids." PhD Dissertation. New Mexico State University.

Warner, B.D. (2005). "Asteroid lightcurve analysis at the Palmer Divide Observatory-spring 2005." *Minor Planet Bulletin*, **32**, 90-92.

Warner, B.D. (2008). "Asteroid Lightcurve Analysis at the Palmer Divide Observatory-June-October 2007." *Minor Planet Bulletin*, **35(2)**, 56-60.

Warner, B.D.; Harris, A.W.; Pravec, P. (2009). "The Asteroid Lightcurve Database." *Icarus* **202**, 134-146. Updated 2016 Sep. *http://www.minorplanet.info/lightcurvedatabase.html*

Warner,B.D. (2011).
http://www.minorplanetobserver.com/PDO/PDOLightcurves.htm

Waszczak, A.; Chang, C.-K.; Ofek, E.O.; Laher, R.; Masci, F.; Levitan, D.; Surace, J.; Cheng, Y.-C.; Ip, W.-H.; Kinoshita, D.; Helou, G.; Prince, T.A.; Kulkarni, S. (2015). "Asteroid Light Curves from the Palomar Transient Factory Survey: Rotation Periods and Phase Functions from Sparse Photometry." *Astron. J.* **150**, A75.

PHOTOMETRIC OBSERVATIONS OF EIGHT MINOR PLANETS FOR SHAPE MODELING

Tom Polakis
Command Module Observatory
121 W. Alameda Dr.
Tempe, AZ 85282
tpolakis@cox.net

(Received: 2020 Dec 28)

Phased lightcurves and synodic rotation periods for eight main-belt asteroids are presented, based on CCD observations made in 2020 October. The purpose of obtaining these particular lightcurves is to augment shape modeling efforts. All the data have been submitted to the ALCDEF database.

CCD photometric observations of eight main-belt asteroids were performed at Command Module Observatory (MPC V02) in Tempe, AZ. Images were taken using a 0.32-m f/6.7 Modified Dall-Kirkham telescope, SBIG STXL-6303 CCD camera, and a 'clear' glass filter. Exposure time for all the images was 2 minutes. The image scale after 2×2 binning was 1.76 arcsec/pixel. Table I shows the observing circumstances and results. All of the images for these eight asteroids were obtained in 2020 October.

Images were calibrated using a dozen bias, dark, and flat frames. Flat-field images were made using an electroluminescent panel. Image calibration and alignment was performed using MaxIm DL software.

The data reduction and period analysis were done using MPO Canopus (Warner, 2020). The 45′×30′ field of the CCD typically enables the use of the same field center for three consecutive nights. In these fields, the asteroid and three to five comparison stars were measured. Comparison stars were selected with colors within the range of 0.5 < B-V < 0.95 to correspond with color ranges of asteroids. In order to reduce the internal scatter in the data, the brightest stars of appropriate color that had peak ADU counts below the range where chip response becomes nonlinear were selected. MPO Canopus plots instrumental vs. catalog magnitudes for solar-colored stars, which is useful for selecting comp stars of suitable color and brightness.

Since the sensitivity of the KAF-6303 chip peaks in the red, the clear-filtered images were reduced to Sloan r′ to minimize error with respect to a color term. Comparison star magnitudes were obtained from the ATLAS catalog (Tonry et al., 2018), which is incorporated directly into MPO Canopus. The ATLAS catalog derives Sloan griz magnitudes using a number of available catalogs. The consistency of the ATLAS comp star magnitudes and color-indices allowed the separate nightly runs to be linked often with no zero-point offset required or shifts of only a few hundredths of a magnitude in a series.

A 9-pixel (16 arcsec) diameter measuring aperture was used for asteroids and comp stars. It was typically necessary to employ star subtraction to remove contamination by field stars. For the asteroids described here, I note the RMS scatter on the phased lightcurves, which gives an indication of the overall data quality including errors from the calibration of the frames, measurement of the comp stars, the asteroid itself, and the period-fit. Period determination was done using the MPO Canopus Fourier-type FALC fitting method (cf. Harris et al., 1989). Phased lightcurves show the maximum at phase zero. Magnitudes in these plots are apparent and scaled by MPO Canopus to the first night.

Most issues of the *Minor Planet Bulletin* provide a table of candidates for photometry opportunities to perform or improve shape modeling. These eight asteroids were selected based on criteria that they are rated better than U = 3-, and have at least three entries in the LCDB with U ≥ 2, preferably all with different phase angle bisectors.

Three of the eight asteroids already have shape models at the DAMIT web site (Ďurech et al., 2010). They are 754 Malabar, 911 Agamemnon, and 1590 Tsiolkovskaja.

The Asteroid Lightcurve Database (LCDB; Warner et al., 2009) was consulted to locate previously published results. All the new data for these asteroids can be found in the ALCDEF database.

284 Amalia. Auguste Charlois discovered this asteroid in a highly eccentric orbit from Nice in 1889. Harris and Young (1989) found a period of 8.545 ± 0.015 h. Behrend (2004, 2006) shows periods of 8.56 ± 0.05 h and 8.559 ± 0.001 h, respectively. More recently, Pál et al. (2020) computed 8.5599 ± 0.0005 h. A total of 233 images were taken during three nights, yielding a period solution of 8.565 ± 0.004 h, and an amplitude of 0.18 ± 0.008 mag.

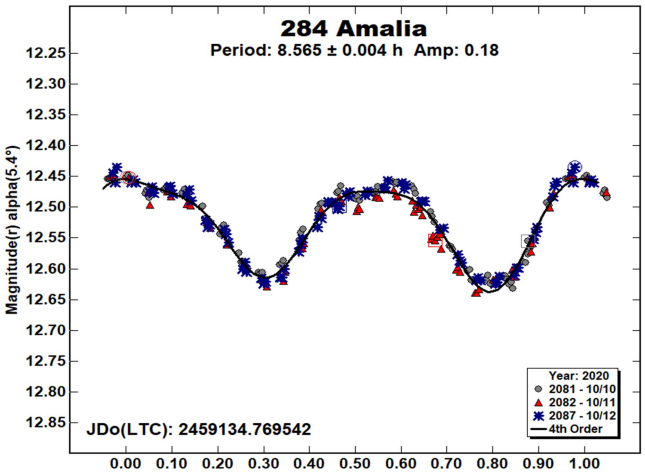

754 Malabar. August Kopff discovered this outer main-belt asteroid at Heidelberg in 1906. Behrend (2004, 2005, 2019) shows synodic period solutions of 11.7267 ± 0.0005 h, 11.732 ± 0.001 h, and 11.7314 ± 0.0006 h. Stephens (2003) computed 11.740 ± 0.005 h. During six nights, 271 data points were obtained to compute a rotational period of 11.735 ± 0.008 h. The amplitude is 0.13 mag., and the RMS error on the fit is 0.011 mag.

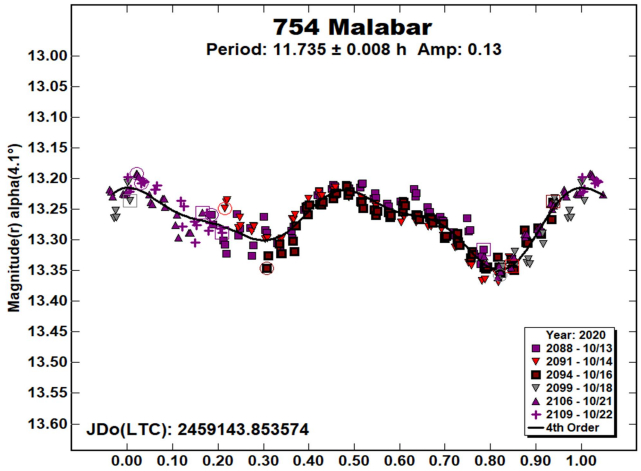

Number	Name	2020/mm/dd	Phase	L_{PAB}	B_{PAB}	Period(h)	P.E.	Amp	A.E.	Grp
284	Amalia	10/10-10/12	5.4,6.0	12	7	8.565	0.004	0.18	0.01	MB-I
754	Malabar	10/13-10/22	4.1,6.8	14	-9	11.735	0.008	0.13	0.01	MB-O
911	Agamemnon	10/10-10/12	4.0,4.3	1	11	6.582	0.007	0.17	0.03	TR-J
1156	Kira	10/19-10/19	2.6,2.6	22	-2	2.791	0.008	0.19	0.03	MB-I
1314	Paula	10/10-10/12	8.3,9.2	7	8	5.948	0.001	0.84	0.01	FLOR
1590	Tsiolkovskaja	10/13-10/17	3.8,5.8	14	3	6.728	0.001	0.36	0.02	FLOR
2346	Lilio	10/18-10/20	3.6,3.8	24	6	3.029	0.001	0.19	0.01	ERI
8256	Shenzhou	10/13-10/17	8.9,11.2	10	-5	3.396	0.001	0.34	0.03	MC

Table I. Observing circumstances and results. The phase angle is given for the first and last date. If preceded by an asterisk, the phase angle reached an extrema during the period. L_{PAB} and B_{PAB} are the approximate phase angle bisector longitude/latitude at mid-date range (see Harris et al., 1984). Grp is the asteroid family/group (Warner et al., 2009).

911 Agamemnon. This Trojan was discovered in 1918 by Karl Reinmuth at Heidelberg. Stephens (2009) first determined a period of 6.592 ± 0.004 h, and Mottola et al. (2011) published 6.5819 ± 0.0007 h. Stephens et al. (2014a) again observed the asteroid, determining a period of 6.59 ± 0.001 h. During three nights at V02, 196 images were gathered. The rotational period is 6.582 ± 0.007 h, with an amplitude of 0.17 ± 0.027 mag.

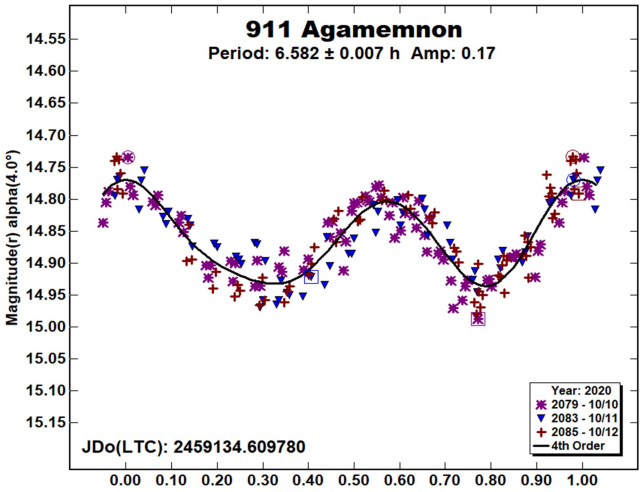

1314 Paula. This Flora-family asteroid was discovered by Sylvain Arend in 1933 at Uccle. Rotational periods with U = 3 are listed: Pravec et al. (2006), 5.9498 ± 0.0003 h; Stephens (2014b), 5.949 ± 0.001 h; and Behrend (2018), 5.95 ± 0.05 h. A total of 222 images taken over the course of three nights were used to determine a synodic period of 5.948 ± 0.001 h, with an amplitude of 0.84 ± 0.003 mag.

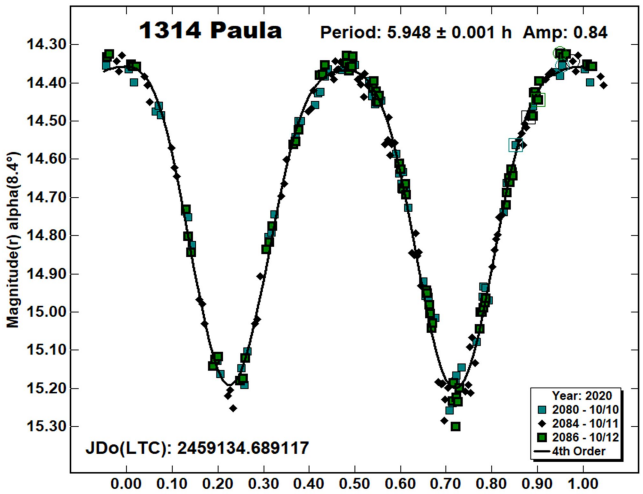

1156 Kira. Karl Reinmuth discovered this minor planet at Heidelberg in 1928. Synodic periods are as follows. Pravec et al. (2012), 2.9710 ± 0.0005 h; Dykhuis et al. (2016), 2.79103 ± 0.00004 h and 2.79113 ± 0.00008 h. During a single night, 233 images were taken, producing a period of 2.791 ± 0.008 h. The amplitude of the lightcurve is 0.19 mag, with an RMS error on the fit of 0.028 mag.

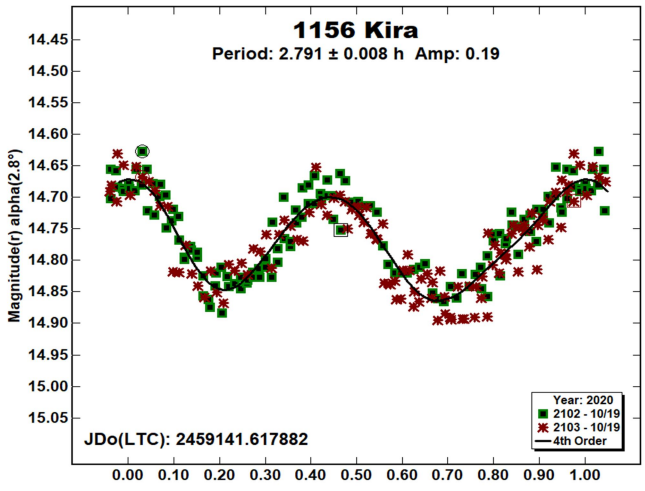

1590 Tsiolkovskaja was discovered by Grigory Neujmin at Siemis in 1933. Photometric results with unique position angle bisectors include: Warner (2008), 6.737 ± 0.004 h; Carbo et al. (2009), 6.731 ± 0.002 h; and Klinglesmith III and Hendrickx (2018), 6.729 ± 0.001 h. During four nights, 376 images were taken. The computed synodic period is 6.728 ± 0.001h, and the amplitude is 0.36 ± 0.022 mag.

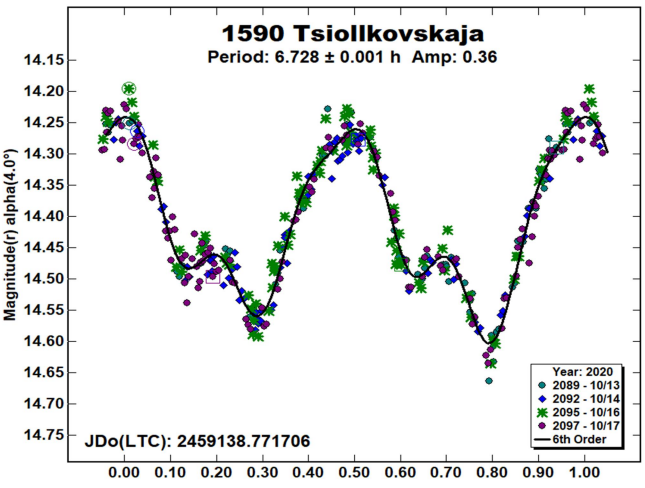

2346 Lilio. Karl Reinmuth discovered this Erigone-family minor planet in 1934 at Heidelberg. Unfortunately for shape modeling, the published U = 3 periods share roughly the same position angle bisector: Behrend (2005), 3.02883 ± 0.0003 h; Warner (2006), 3.029 ± 0.002 h; and Behrend (2016), 3.0285 ± 0.0002 h. During three nights, 280 images were obtained, and the derived period is 3.029 ± 0.001 h. The amplitude of the lightcurve is 0.19 mag., with an RMS error on the fit of 0.001 mag.

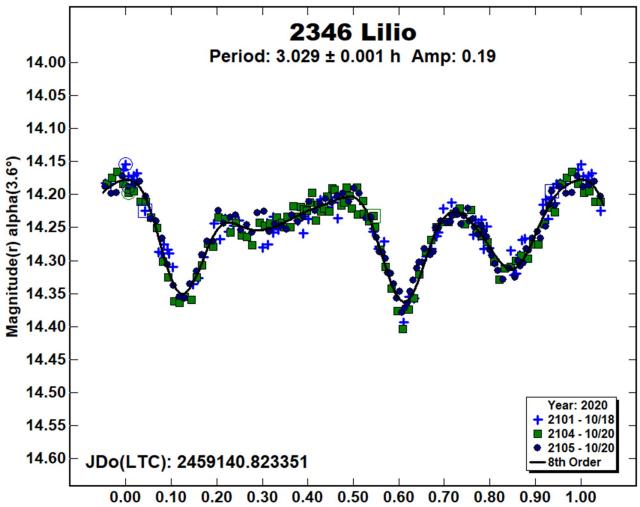

8526 Shenzhou is a Mars crosser, discovered at Purple Mountain Observatory in 1981. Crawford (2008) published a period of 3.395 ± 0.001 h, Pravec et al. (2015) shows 3.3960 ± 0.0003 h, Benishek (2018) computed 3.394 ± 0.001 h, and Stephens (2018) published 3.397 ± 0.001 h. Using 299 images taken during four nights, the calculated synodic period is 3.396 ± 0.001 h, with an amplitude of 0.34 ± 0.033 mag.

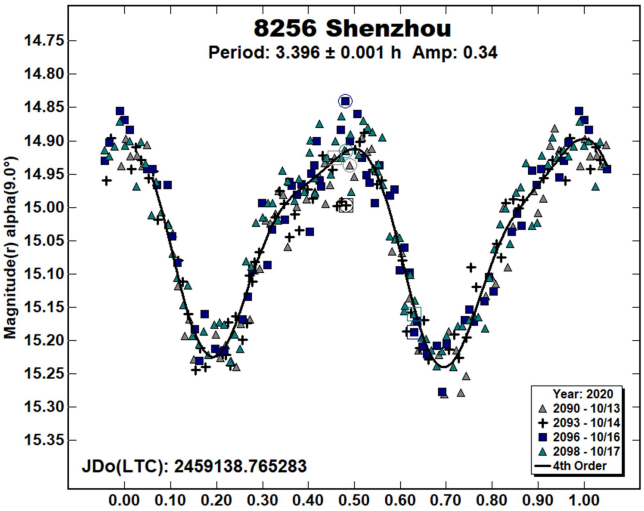

Acknowledgements

The author would like to express his gratitude to Brian Skiff for his indispensable mentoring in data acquisition and reduction. Thanks also go out to Brian Warner for support of his MPO Canopus software package.

References

Behrend, R. (2004, 2005, 2006, 2016, 2018, 2019). Observatoire de Geneve web site. *http://obswww.unige.ch/~behrend/page_cou.html*

Benishek, V. (2018) "Lightcurve and Rotation Period Determinations for 8 Asteroids." *Minor Planet Bull.* **45**, 187, 189.

Carbo, L.; Green, D.; Kragh, K.; Krotz, J.; Meiers, A.; Patino, B.; Pligge, Z.; Shaffer, N.; Ditteon, R. (2009). "Asteroid Lightcurve Analysis at the Oakley Southern Sky Observatory: 2008 October thru 2009 March." *Minor Planet Bull.* **36**, 152-157.

Crawford, G. (2008). "Lightcurve Analysis of 8256 Shenzhou." *Minor Planet Bull.* **35**, 15.

Ďurech, J.; Sidorin, V.; Kaasalainen, M. (2010). "DAMIT: a database of asteroid models." *Astron. Astrophys.* **513**, A46.

Dykhuis, M.J.; Molnar, L.A.; Gates, C.J.; Gonzales, J.A.; Huffman, J.J.; Maat, A.R.; Maat, S.L.; Marks, M.I.; Massey-Plantinga, A.R.; McReynolds, N.D.; Schut, J.A.; Stoep, J.P.; Stutzman, A.J.; Thomas, B.C.; Vander Tuig, G.W.; Vriesema, J.W.; Greenberg, R. (2016). "Efficient spin sense determination of Flora-region asteroids via the epoch method." *Icarus* **267**, 174-203.

Harris, A.W.; Young, J.W.; Scaltriti, F.; Zappala, V. (1984). "Lightcurves and phase relations of the asteroids 82 Alkmene and 444 Gyptis." *Icarus* **57**, 251-258.

Harris, A.W.; Young, J.W. (1989). "Asteroid lightcurve observations from 1979-1981." *Icarus* **81**, 314-364.

Harris, A.W.; Young, J.W.; Bowell, E.; Martin, L.J.; Millis, R.L.; Poutanen, M.; Scaltriti, F.; Zappala, V.; Schober, H.J.; Debehogne, H.; Zeigler, K.W. (1989). "Photoelectric Observations of Asteroids 3, 24, 60, 261, and 863." *Icarus* **77**, 171-186.

Klinglesmith III, D.A.; Hendrickx, S. (2018). "Asteroid Lightcurve Observations at Etscorn Observatory." *Minor Planet Bull.* **45**, 162-165.

Mottola, S.; Di Martino, M.; Erikson, A.; Gonano-Beurer, M.; Carbognani, A.; Carsenty, U.; Hahn, G.; Schober, H.-J.; Lahulla, F.; Delbò, M.; Lagerkvist, C.-I. (2011). "Rotational Properties of Jupiter Trojans. I. Light Curves of 80 Objects." *Astron. J.* **141**, A170.

Pál, A.; Szakáts, R.; Kiss, C.; Bódi, A.; Bognár, Z.; Kalup, C.; Kiss, L.; Marton, G.; Molnár, L.; Plachy, E.; Sárneczky, K.; Szabó, G.; Szabó, R. (2020). "Solar System Objects Observed with TESS - First Data Release: Bright Main-belt and Trojan Asteroids from the Southern Survey." *Ap. J. Supl. Ser.* **247**, 26-34.

Pravec, P.; Wolf, M.; Sarounova, L. (2006, 2012, 2015). Ondrejov Asteroid Photometry Project. *http://www.asu.cas.cz/~ppravec/neo.htm*

Stephens, R.D. (2003). "Photometry of 628 Christine, 754 Malabar, 815 Coppelia, and 1025 Riema." *Minor Planet Bull.* **30**, 69-70.

Stephens, R.D. (2009). "Asteroids Observed from GMARS and Santana Observatories." *Minor Planet Bull.* **36**, 59-62.

Stephens, R.D.; Coley, D.R.; French, L.M. (2014a). "Trojan Asteroids Observed from CS3: 2014 January-May." *Minor Planet Bull.* **41**, 210-212.

Stephens, R.D. (2014b). "Asteroids Observed from CS3: 2013 July-September." *Minor Planet Bull.* **41**, 13-15.

Stephens, R.D. (2018). "Asteroids Observed from CS3: 2018 January - March." *Minor Planet Bull.* **45**, 299-301.

Tonry, J.L.; Denneau, L.; Flewelling, H.; Heinze, A.N.; Onken, C.A.; Smartt, S.J.; Stalder, B.; Weiland, H.J.; Wolf, C. (2018). "The ATLAS All-Sky Stellar Reference Catalog." *Astrophys. J.* **867**, A105.

Warner, B.D. (2006). "Asteroid lightcurve analysis at the Palmer Divide Observatory: July-September 2005." *Minor Planet Bull.* **33**, 35-39.

Warner, B.D. (2008). "Asteroid Lightcurve Analysis at the Palmer Divide Observatory: September-December 2007." *Minor Planet Bull.* **35**, 67-71.

Warner, B.D.; Harris, A.W.; Pravec, P. (2009). "The Asteroid Lightcurve Database." *Icarus* **202**, 134-146. Updated 2020 Aug. *http://www.minorplanet.info/lightcurvedatabase.html*

Warner, B.D. (2020). MPO Canopus software. *http://bdwpublishing.com*

ROTATIONAL PERIOD AND LIGHTCURVE DETERMINATION OF 4625 SHCHEDRIN, (8823) 1987 WS3, (15010) 1998 QL92, (19755) 2000 EH34, AND 21082 ARAIMASARU

Alfonso Noschese
AstroCampania Associazione, Naples, Italy
Osservatorio Salvatore Di Giacomo (L07)
Via Salvatore Di Giacomo 7b
Agerola (Na) Italy
and
Osservatorio Elianto (K68)
via V. Emanuele III, 95, 84098
Pontecagnano (SA) Italy
a.noschese@astrocampania.it

Nello Ruocco
AstroCampania Associazione, Naples, Italy
and
Osservatorio Astronomico Nastro Verde (C82),
Sorrento (Na) Italy

Antonio Catapano, Maurizio Mollica, Antonio Vecchione
AstroCampania ETS, Naples, Italy
Osservatorio Salvatore Di Giacomo (L07)
Via Salvatore Di Giacomo 7b, 80051
Agerola (Na) Italy

(Received: 2021 Jan 13)

Photometric observations of five asteroids were performed in order to acquire lightcurves and to determine the rotational periods. The synodic period and lightcurve amplitude were found for 4625 Shchedrin, (8823) 1987 WS3, (15010) 1998 QL92, (19755) 2000 EH34, and 21082 Araimasaru.

This asteroid photometry campaign was done from Amateur Astronomers belonging to AstroCampania Association. The targets were selected mainly in order to acquire lightcurves to determine rotational periods not reported before. All the images reported here were unbinned with no filter and had master flats and darks applied. The exposure time depended upon various experimental conditions such as magnitude of the target, sky motion, and Moon illumination. Image processing, measurement, and period analysis were done using *MPO Canopus* (Warner, 2019), which incorporates the Fourier analysis algorithm (FALC) developed by Harris (Harris et al., 1989). The Comp Star Selector feature in *MPO Canopus* was used to limit the comparison stars to near solar color. Night-to-night calibration was done using field stars from the ATLAS catalog (Tonry et al., 2018). Observations of 4625 Shchedrin was carried out at 'Nastro Verde' observatory (C82) located at Sorrento (Naples), Italy by means of a 0.35-m Schmidt-Cassegrain telescope operating at f/6.3 using a SBIG ST-10 XME CCD camera with 2148×1472 array of 6.8-micron pixels with a clear filter.

Observations of (15010) 1998 QL92 and (19755) 2000 EH34 were carried out by means of Elianto observatory (K68) located in the south of Italy (Pontecagnano) using a 0.3-m Newton telescope operating at f/4 equipped with a Moravian KAF1603 ME CCD camera (1536×1024 array of 9-micron pixels) with a clear filter.

Observations of (8823) 1987 WS3 and 21082 Araimasaru were conducted using the main telescope of the "Salvatore Di Giacomo" Observatory (L07) in Agerola (NA), a 0.50-m Ritchey Chrétien telescope operating at f/8, with a FLI PL 4240 back-illuminated camera, 13.5-micron pixels and 2048×2048 array, Rc filtered.

4625 Shchedrin was discovered on October 20, 1982 by L. G. Karachkina, Crimean Astrophysical Observatory at Nauchnyj. It is a main-belt asteroid with a semi-major axis of 2.60 AU, orbital period of 4.2 years, eccentricity of 0.237 and inclination of 1.595°. This asteroid has an estimated diameter ranging from 4.837 to 10.815 kilometers and an absolute magnitude of 13.7 (JPL, 2020). There were no previous lightcurve entries in the LCDB for this this asteroid. CCD photometric observations were performed between 2020 December 13 and 2020 December 17. Four observation sessions were produced for lightcurve analysis to collect 363 data points and adopting an exposure time of 150 s. Our observations led to a well-defined period of 6.1188 ± 0.0006 h with an amplitude of 0.98 magnitudes.

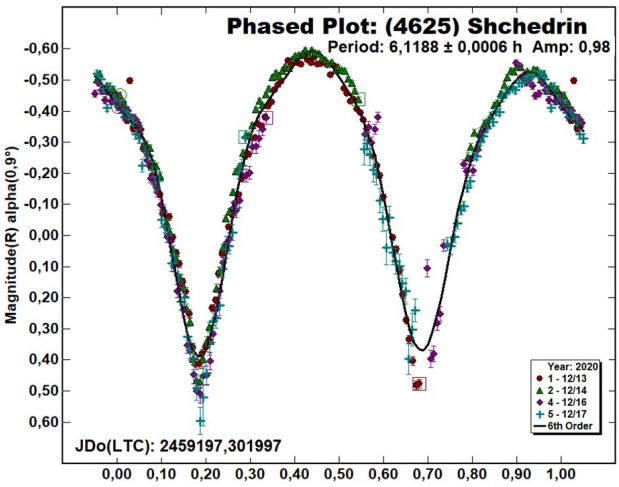

(8823) 1987 WS3 is a main-belt asteroid, discovered by S. McDonald at Anderson Mesa, in 1987. It has a semi-major axis of 2.570 AU, orbital period of 4.12 years, eccentricity of 0.240 and inclination of 13.557°. This ten-kilometer body has an absolute magnitude of 12.80 and a geometric albedo of 0.142 (Neowise_diameters_albedo 2.0). No rotational period and lightcurve were reported for this object at the best of our knowledge (JPL, 2020). A total of 1167 lightcurve data points were collected in seven observing sessions between 2020 November 26th and 2020 December 21th, with 90 s exposure time. All but three sessions (152,155 and 162), were divided into pre- and post-meridian flip, so that the total number shown is eleven. We found a period of 80.811 ± 0.029 h with a lightcurve amplitude change of 0.17 magnitudes. Sessions 153 and 154 were corrected for 0.22-0.26 mag in order to align respect to the others. Data shown are not enough to guarantee an unambiguous result and a greater coverage of the curve would be desirable. Unfortunately, due to weather related issues, we were unable to extend the observation campaign. However, based on the measurements we have, the rotational period found is the most plausible one (thus with lowest RMS in the period spectrum).

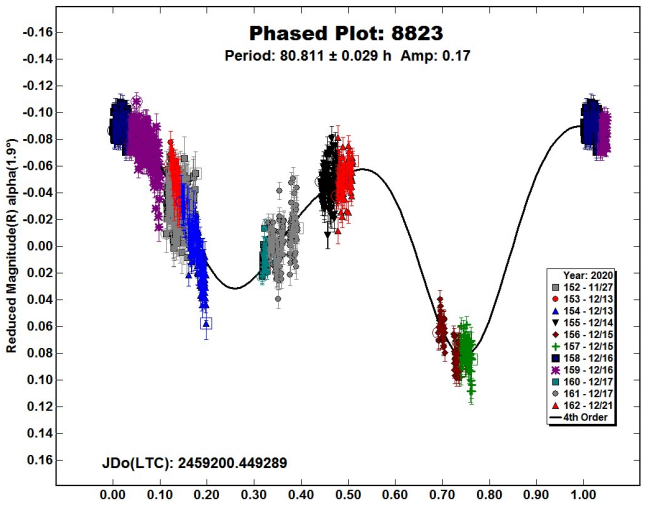

(15010) 1998 QL92 was discovered on August 28, 1998 by LINEAR at Socorro. It is a main-belt asteroid with a semi-major axis of 2.375 AU, orbital period of 3.66 years, eccentricity of 0.211, inclination of 2.021°. It has a diameter of 4.590 kilometers and an absolute magnitude of 14.0 and geometrical albedo of 0.275 (JPL, 2020). There were no previous lightcurve entries in the LCDB for this asteroid. CCD photometric observations were performed between 2020 November 18 and 2020 November 30. Five observation sessions were produced for lightcurve analysis to collect 149 data points and adopting an exposure time of 360 s. (15010) 2000 EH34 is a very difficult low amplitude asteroid. We were unable to resolve a rotational period unambiguously. The period spectrum showed several possible solutions and we adopted the one (8.11 ± 0.02 h) with the lowest RMS.

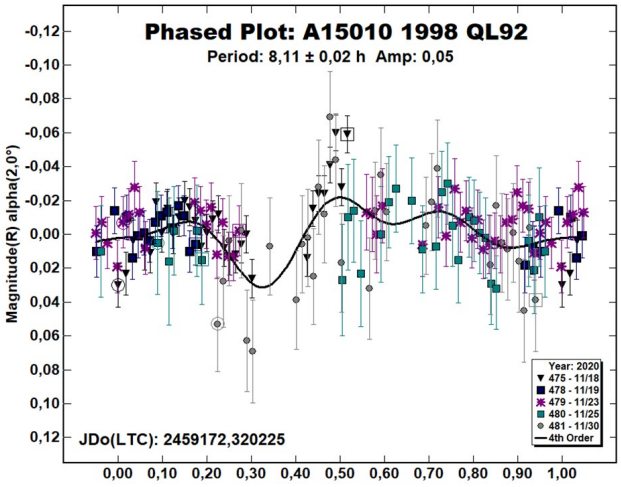

(19755) 2000 EH34 was discovered on March 05, 2000 by LINEAR at Socorro. It is a main-belt asteroid with a semi-major axis of 2.669 AU, orbital period of 4.36 years, eccentricity of 0.189, inclination of 15.483°. It has a diameter of 6.718 kilometers and an absolute magnitude of 13.0 and geometrical albedo of 0.471 (JPL, 2020). There were no previous lightcurve entries in the LCDB for this asteroid. CCD photometric observations were performed between 2020 November 7 and 2020 November 10. Four observation sessions were produced for lightcurve analysis to collect 179 data points and adopting an exposure time of 360 s. Our observations led to period of 3.564 ± 0.001 h with an amplitude of 0.35 magnitudes.

Number	Name	20yy mm/dd	Pts	Phase	L_{PAB}	B_{PAB}	Period(h)	P.E.	Amp	A.E.	Grp
4625	Shchedrin	20/12/13-20/12/17	363	0.87-2.99	196.5	1.0	6.1188	0.0006	0.98	0.02	MB
8823	1987 WS3	20/11/26-20/12/21	1167	1.86,13.17	68.4	-2.8	80.811	0.029	0.17	0.01	MB
15010	1998 QL92	20/11/18-20/11/30	149	1.99-8.33	56.5	-2.7	8.11	0.02	0.05	0.02	MB
19755	2000 EH34	20/11/07-20/11/10	179	3.60-2.09	51.5	-2.4	3.564	0.001	0.35	0.02	MB
21082	Araimasaru	20/11/18-20/11/25	834	1.94-6.19	55.3	1.9	7.900	0.003	0.11	0.01	MB

Table I. Observing circumstances and results. The phase angle is given for the first and last date. L_{PAB} and B_{PAB} are the approximate phase angle bisector longitude and latitude at mid-date range (Harris *et al.*, 1984). Grp is the asteroid family/group (Warner et al., 2009).

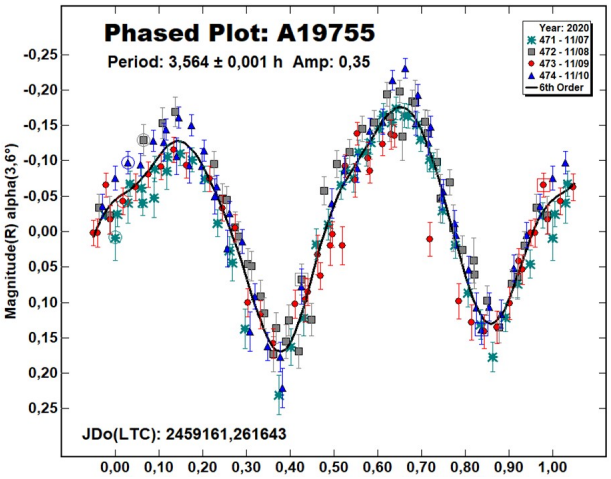

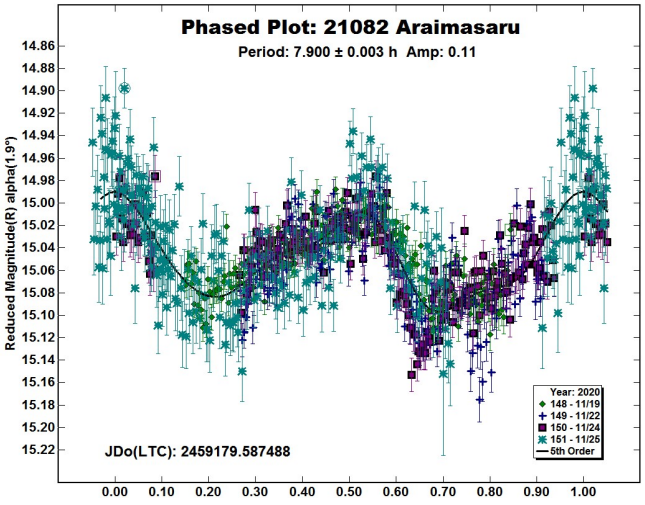

21082 Araimasaru is a main-belt asteroid, discovered by T. Hioki and S. Hayakawa at Okutama, in 1991, named after the famous Japanese amateur astronomer, a devoted observer of small bodies. It has a semi-major axis of 2.573 AU, orbital period of 4.13 years, eccentricity of 0.305 and inclination of 5.980°, absolute magnitude of 14.9 (JPL, 2020). We have not found any data regarding geometric albedo and physical dimension for this body. No rotational period and lightcurve are previously reported for this object to the best of our knowledge. A total of 834 lightcurve data points were collected in four observing sessions between November 18, 2020 and November 25, with 90 s exposure time. We found a period of 7.900 ± 0.003 h. The data indicate a lightcurve amplitude change of 0.11 magnitudes. We believe that the data are barely sufficient to guarantee, without great ambiguity, that the period found is the most plausible one. From the data shown, it is clear that the phased curve has a nearly multiple coverage. The whole process has been quite straightforward, providing a result without any particular ambiguity.

References

Harris, A.W.; Young, J.W.; Scaltriti, F.; Zappala, V. (1984). "Lightcurves and phase relations of the asteroids 82 Alkmene and 444 Gyptis." *Icarus* **57**, 251-258.

Harris, A.W.; Young, J.W.; Bowell, E.; Martin, L.J.; Millis, R.L.; Poutanen, M.; Scaltriti, F.; Zappala, V.; Schober, H.J.; Debehogne, H.; Zeigler, K.W. (1989). "Photoelectric Observations of Asteroids 3, 24, 60, 261, and 863." *Icarus* **77**, 171-186.

JPL (2020). Small-Body Database Browser. *https://ssd.jpl.nasa.gov/sbdb.cgi*

Tonry, J.L.; Denneau, L.; Flewelling, H.; Heinze, A.N.; Onken, C.A.; Smartt, S.J.; Stalder, B.; Weiland, H.J.; Wolf, C. (2018). "The ATLAS All-Sky Stellar Reference Catalog." *Astrophys. J.* **867**, A105.

Warner, B.D.; Harris, A.W.; Pravec, P. (2009). "The Asteroid Lightcurve Database." *Icarus* **202**, 134-146. Updated 2020 Nov. *http://www.minorplanet.info/lightcurvedatabase.html*

Warner, B.D. (2019). MPO Software, MPO Canopus version 10.8.1.1. Bdw Publishing. *http://minorplanetobserver.com*

MAIN-BELT ASTEROIDS OBSERVED FROM CS3: 2020 OCTOBER TO DECEMBER

Robert D. Stephens
Center for Solar System Studies (CS3) / MoreData!
11355 Mount Johnson Ct., Rancho Cucamonga, CA 91737 USA
rstephens@foxandstephens.com

Brian D. Warner
Center for Solar System Studies (CS3) / MoreData!
Eaton, CO

(Received: 2021 Jan 6)

CCD photometric observations of 12 main-belt asteroids were obtained at the Center for Solar System Studies (CS3) from 2020 October to December.

The Center for Solar System Studies (CS3) has seven telescopes which are normally used in program asteroid family studies. The focus is on near-Earth asteroids, but when suitable targets are not available, Jovian Trojans and Hildas are observed. When a nearly full moon is too close to the family targets being studied, targets of opportunity amongst the main-belt families were selected.

Table I lists the telescopes and CCD cameras that were used to make the observations. Images were unbinned with no filter and had master flats and darks applied. The exposures depended upon various factors including magnitude of the target, sky motion, and Moon illumination.

Telescope	Camera
0.30-m f/6.3 Schmidt-Cass	FLI Microline 1001E
0.35-m f/9.1 Schmidt-Cass	FLI Microline 1001E
0.35-m f/9.1 Schmidt-Cass	FLI Microline 1001E
0.35-m f/9.1 Schmidt-Cass	FLI Microline 1001E
0.35-m f/11 Schmidt-Cass	FLI Microline 1001E
0.40-m f/10 Schmidt-Cass	FLI Proline 1001E
0.50-m F8.1 R-C	FLI Proline 1001E

Table I: List of CS3 telescope/CCD camera combinations.

Image processing, measurement, and period analysis were done using *MPO Canopus* (Bdw Publishing), which incorporates the Fourier analysis algorithm (FALC) developed by Harris (Harris et al., 1989). The Comp Star Selector feature in *MPO Canopus* was used to limit the comparison stars to near solar color. Night-to-night calibration was done using field stars from the ATLAS catalog (Tonry et al., 2018), which has Sloan *griz* magnitudes that were derived from the GAIA and Pan-STARR catalogs and are "native" magnitudes of the catalog.

We used the ATLAS r′ (SR) magnitudes. Zero-point adjustments are mostly ≤ 0.03 mag. The occasions where larger corrections were required may have been related in part to using unfiltered observations, poor centroiding of the reference stars, and not correcting for second-order extinction terms.

The Y-axis values are ATLAS SR "sky" (catalog) magnitudes. The two values in the parentheses are the phase angle (a) and the value of *G* used to normalize the data to the comparison stars used in the earliest session. This, in effect, made all the observations seem to be made at a single fixed date/time and phase angle, leaving any variations due only to the asteroid's rotation and/or albedo changes. The X-axis shows rotational phase from –0.05 to 1.05. If the plot includes the amplitude, e.g., "Amp: 0.65", this is the amplitude of the Fourier model curve and *not necessarily the adopted amplitude for the lightcurve*.

For brevity, only some of the previously reported rotational periods may be referenced. A complete list is available at the asteroid lightcurve database (LCDB; Warner et al., 2009).

1063 Aquilegia. We observed this member of the Flora family/group once before (Stephens, 2018) finding a rotational period of 5.794 h. The result from this apparition is similar.

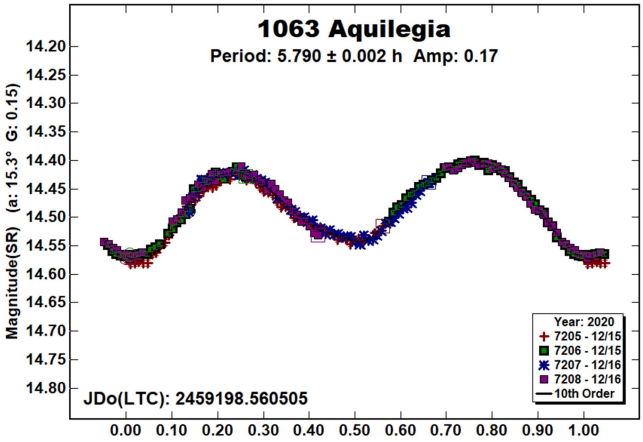

In addition to our dense data from the two apparitions, we used sparse data from the AstDyS-2 site and dense data from Waszczak et al. (2015) in the Asteroid Lightcurve Data Exchange Format database (ALCDEF, 2020), to solve for the sidereal period and pole position and create a shape model. These data were combined using *MPO LCInvert* (Bdw Publishing). This Windows-based program incorporates the algorithms developed by Kaasalainen and Torppa (2001) and Kaasalainen et al (2001) and converted by Josef Durech from the original FORTRAN to C. A period search was made over a sufficiently wide range to assure finding a global minimum in χ^2 values.

Our pole model showed two possible solutions 180° apart; (λ, β, *P*) = (46°, 26°, 5.791760 h) and (λ, β, *P*) = (231°, 33°, 5.791761 h). Our preferred solution is (46°, 26°). The full set of inversion graphics are given at the end of this paper.

1570 Brunonia. Using data from the Kepler Space Telescope, Molnár et al. (2018) previously reported a period > 45 h for this member of the Koronis family/group.

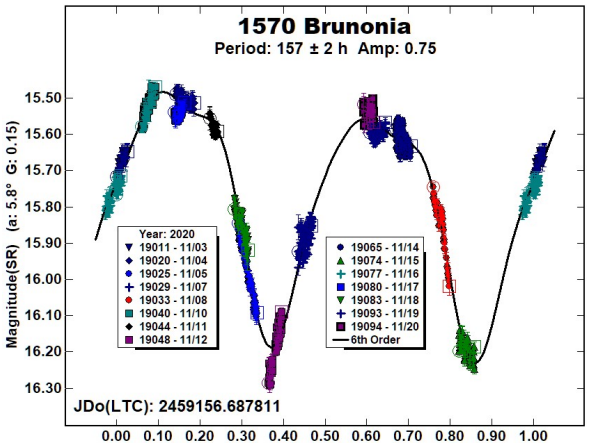

With observations spanning nearly three weeks, we were able to determine a period of 157 h. There is a hint of tumbling, which is probable given that the damping time period is about 137 h (Pravec et al., 2014; short damping times on F-D plot).

2254 Requiem. We have observed this member of the Flora family/group twice in the past (Stephens, 2018, 4.432 h; Warner, 2013, 4.430 h).

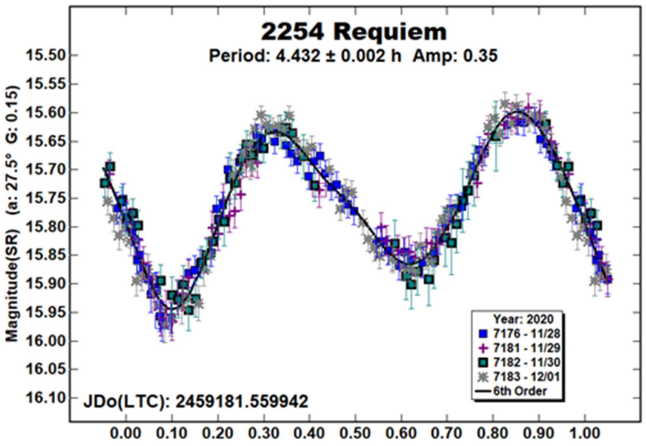

In addition to our dense data from four apparitions, we used sparse data from the AstDyS-2 site and dense data from Waszczak et al. (2015) in the ACLDEF database (ALCDEF, 2020), to solve for the sidereal period and pole position and create a shape model.

Our pole model showed two possible solutions 180° apart; (λ, β, *P*) = (38°, 48°, 4.430326 h) and (λ, β, *P*) = (223°, 38°, 4.430327 h). Our preferred solution is (223°, 38°). The full set of inversion graphics are given at the end of this paper.

2346 Lilio. This member of the Erigone family/group has four rotational periods reported by Behrend (2003web; 2005web; 2007web; 2016web). We observed it twice in the past (Warner, 2006; Stephens, 2016a). Each time the period was near 3.03 h.

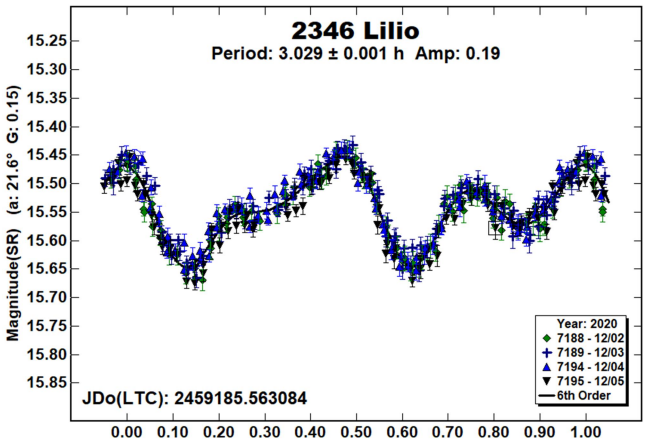

In addition to our dense data from four apparitions, we used sparse data from the AstDyS-2 site to solve for the sidereal period and pole position and create a shape model. We found two possible pole solutions 180° apart: (λ, β, *P*) = (164°, 5°, 3.029079 h) and (λ, β, *P*) = (349°, 19°, 3.029079 h). Our preferred solution is (164°, 5°). The full set of inversion graphics are given at the end of this paper.

2510 Shandong. This member of the Flora family/group observed twice in the past (Higgins and Goncalves, 2006, 5.9463 h; Stephens and Warner, 2019, 5.949 h). Hanuš et al. (2013) reported a spin axis model with (λ, β, *P*) = (256°, 27°) or (71°, 17°) and a sidereal period of 5.94639 h.

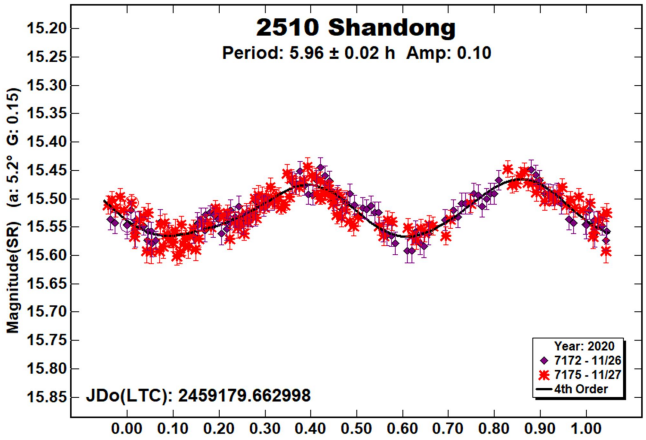

Because of the availability of the dense data from Higgins et al. in the ALCDEF database (ALCDEF, 2020), sparse data at the Asteroids - Dynamic web site (AstDyS-2, 2020), and our dense data from two apparitions, we attempted to solve for the sidereal period and pole position and create a shape model. A period search was made over a sufficiently wide range to assure finding a global minimum in χ^2 values.

Our pole model showed two possible solutions 180° apart and reversed the preference of the Hanuš et al. solution; (λ, β, *P*) = (80°, –45°, 5.947032 h) and (λ, β, *P*) = (250°, –35°, 5.947033 h). Our preferred solution is (80°, –45°). The addition of future dense and sparse datasets will eventually break the tie. The full set of inversion graphics are given at the end of this paper.

2912 Lapalma. This member of the Flora family was observed in 2008 by Brinsfield (2008, 5.71 h) and Pravec et al. (2008web, 5.71076 h). Our work this year is in good agreement.

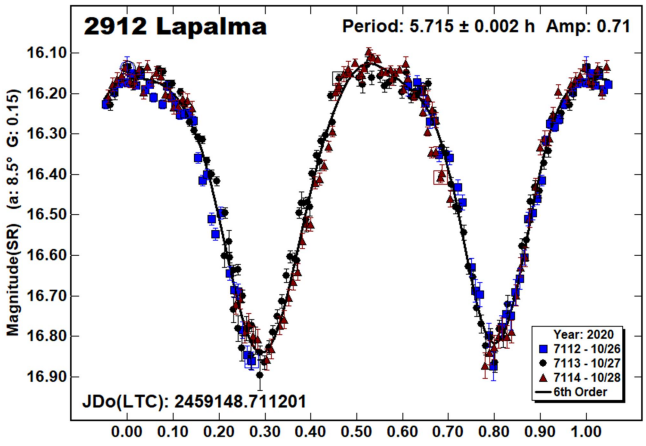

3781 Dufek. We could not find any entries in the LCDB for this member of the Koronis family/group. There are presently only five asteroids in the LCDB with a longer rotational period and U ≥ 2–. A general rule of thumb (Pravec et al., 2014) would have Dufek tumbling. There are no obvious signs of that.

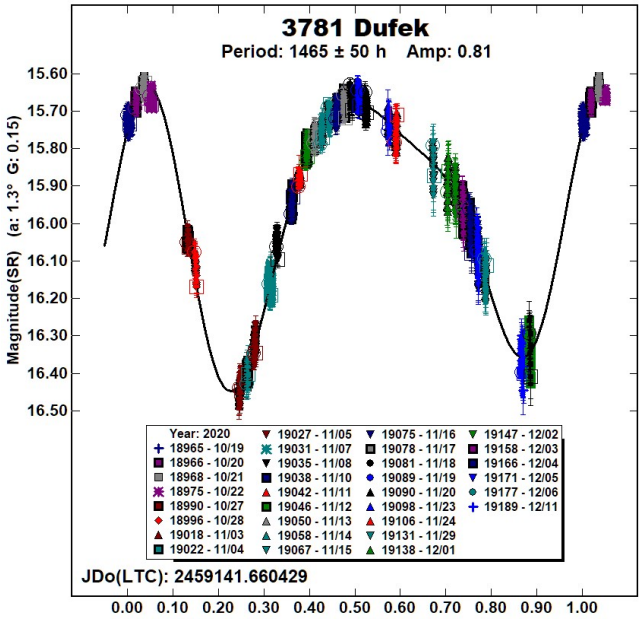

(20498) 1999 RT1. This member of the Eunomia family/group was a target of opportunity, being in the field of the Jovian Trojan, 3063 Makhaon for three nights. It was observed in 2019 May by Pál et al. (2020), using data from TESS. They reported a period of 14.4512 h, in good agreement with the results from this year.

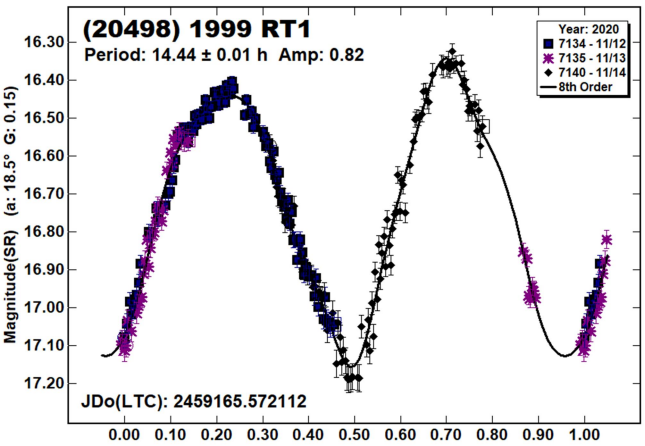

(21182) 1994 EC2. There are no previous rotational periods listed in the LCDB for this member of the Phocaea family/group.

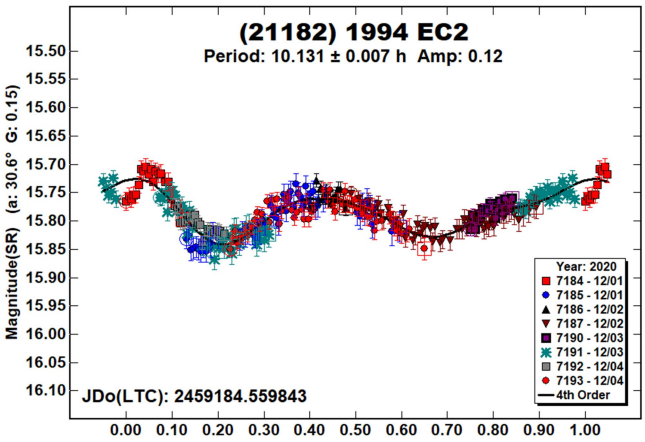

(32772) 1986 JL. We have observed this 4-km sized member of the Hungaria group/family three times in the past (Warner, 2013, 6.047 h; Stephens, 2016b, 6.049 h; Stephens and Warner, 2019, 6.046 h). The results this year are in good agreement, while having the lowest amplitude of all the apparitions.

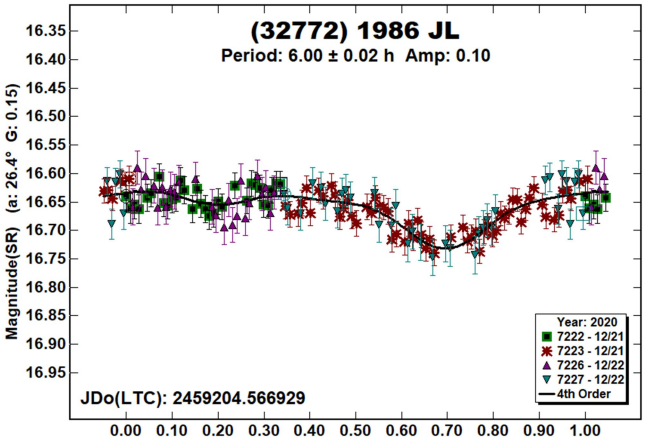

(69274) 1989 UZ1. There are no previous references in the LCDB for this 2.5-km Mars-crosser.

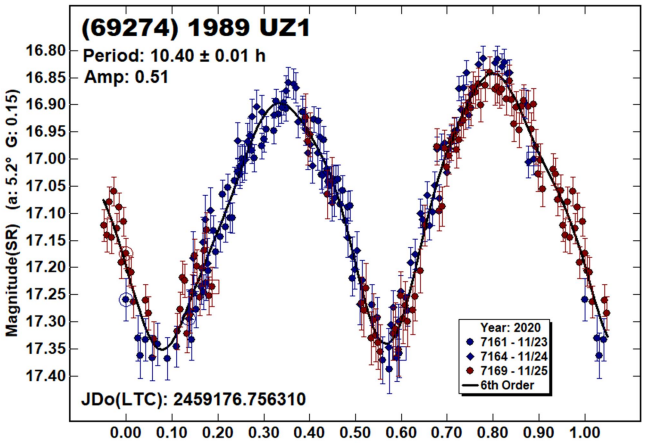

SPIN/SHAPE MODEL FOR 1063 Aquilegia

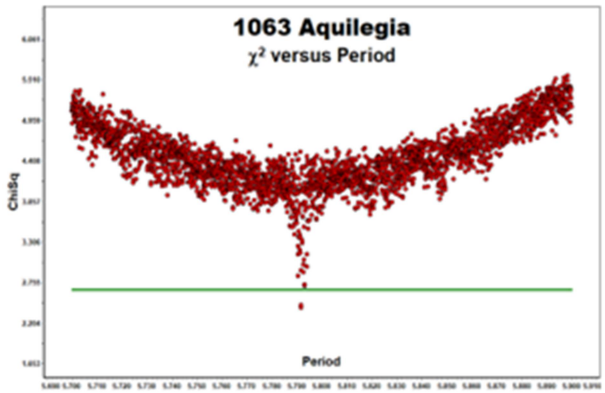

Figure 1. The initial period search results.

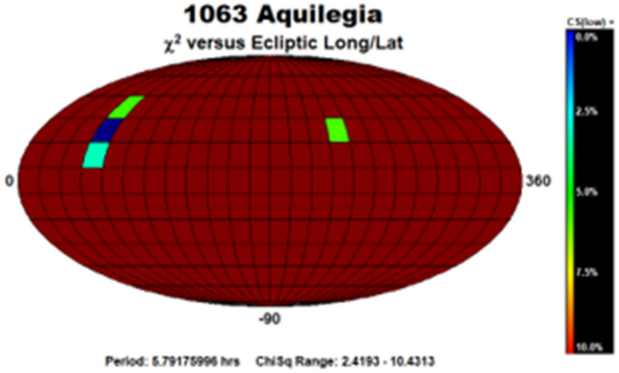

Figure 2. The pole search found two probable solutions.

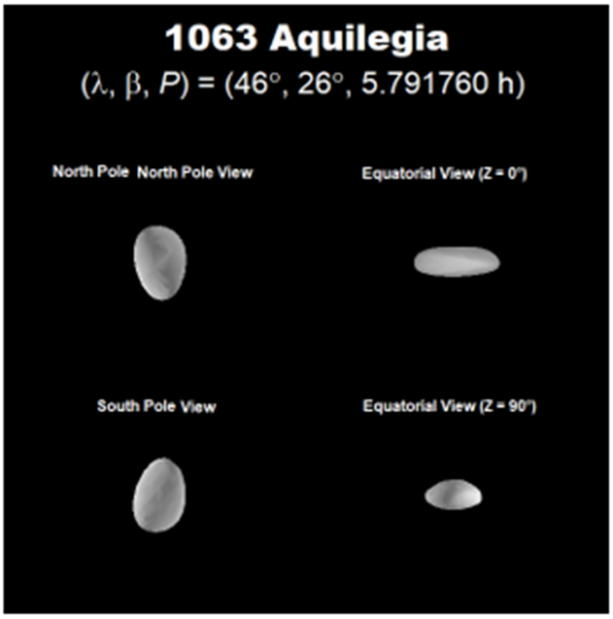

Figure 3. The shape of the asteroid based on the preferred solution.

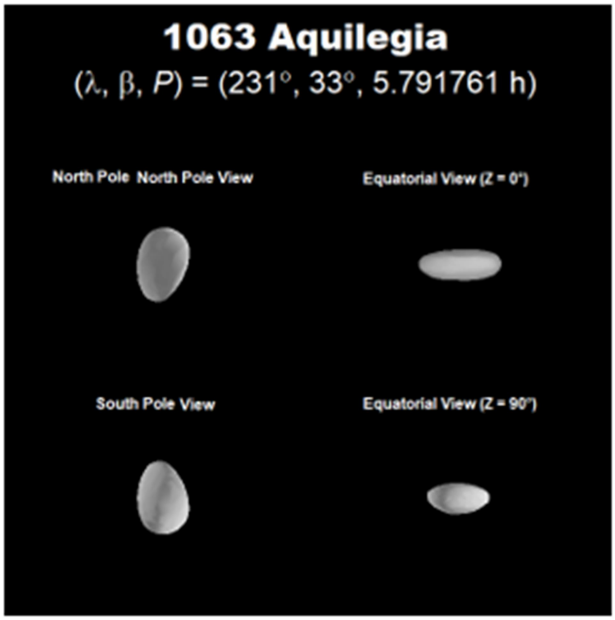

Figure 4. The shape of the asteroid based upon the secondary solution.

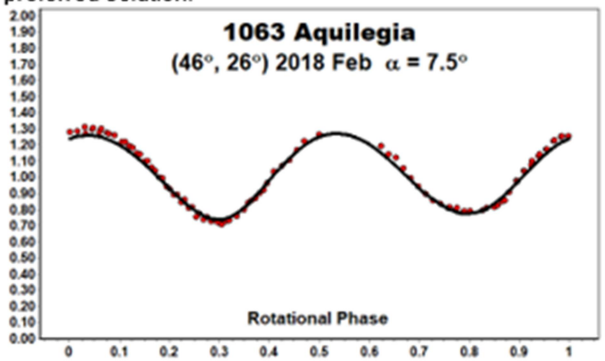

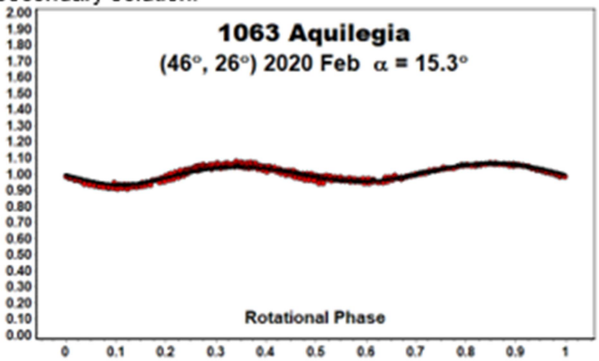

Figure 5/6. The comparison plots are against the preferred pole solution. The red dots indicate the data used for modeling while the black line is the smoothed lightcurve for generated by the shape at the time of the observations. The match is very close on both occasions, which gives confidence in the shape/spin axis model.

SPIN/SHAPE MODEL FOR 2254 Requiem

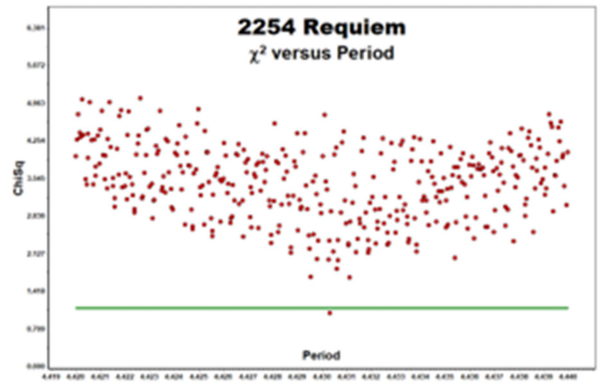

Figure 1. The initial period search results.

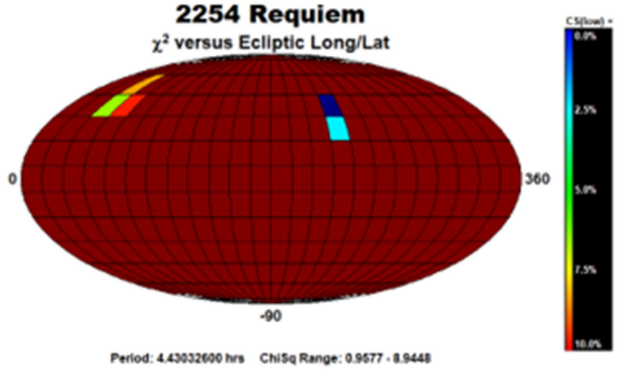

Figure 2. The pole search found two probable solutions.

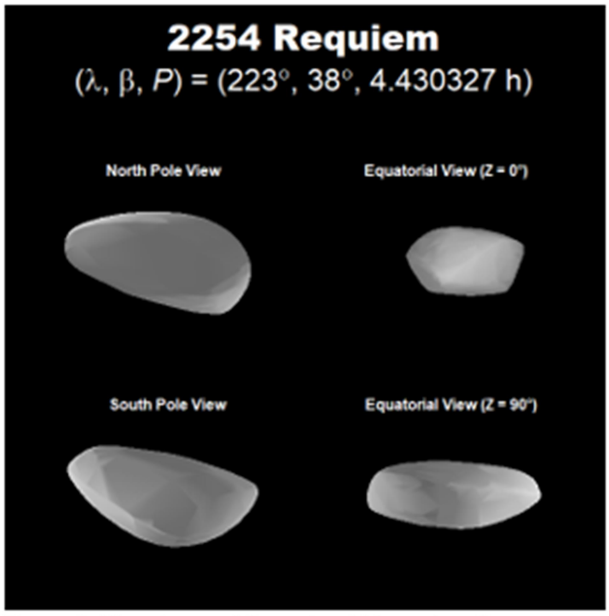

Figure 3. The shape of the asteroid based on the preferred solution.

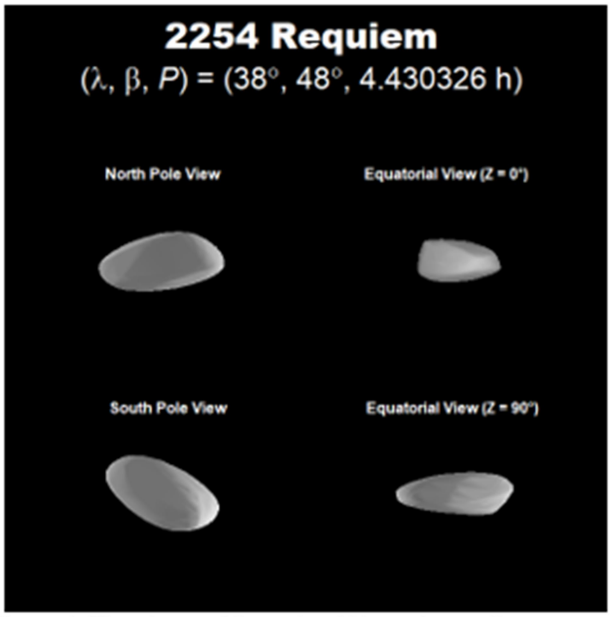

Figure 4. The shape of the asteroid based upon the secondary solution.

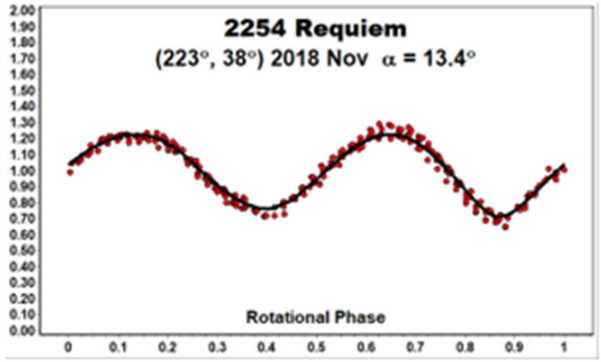

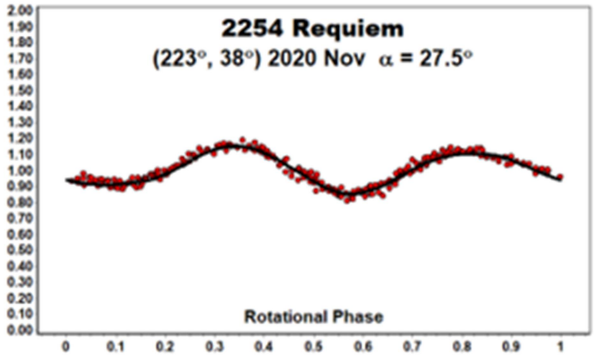

Figure 5/6. The comparison plots are against the preferred pole solution. The red dots indicate the data used for modeling while the black line is the smoothed lightcurve for generated by the shape at the time of the observations. The match is very close on both occasions, which gives confidence in the shape/spin axis model.

SPIN/SHAPE MODEL FOR 2346 LILIO

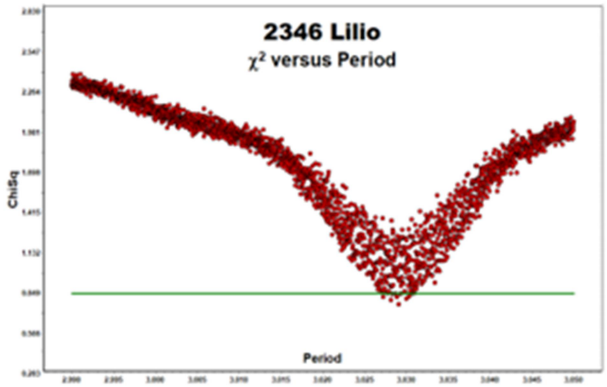

Figure 1. The initial period search results.

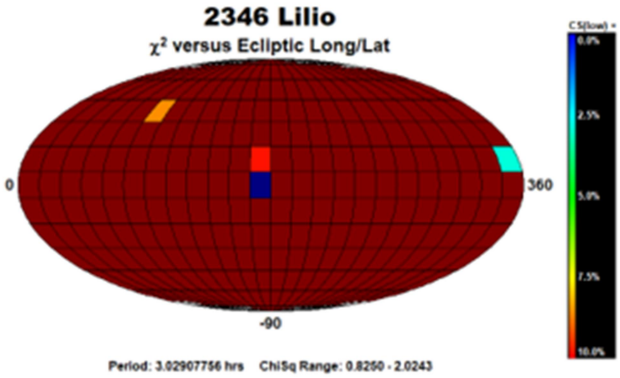

Figure 2. The pole search found two probable solutions.

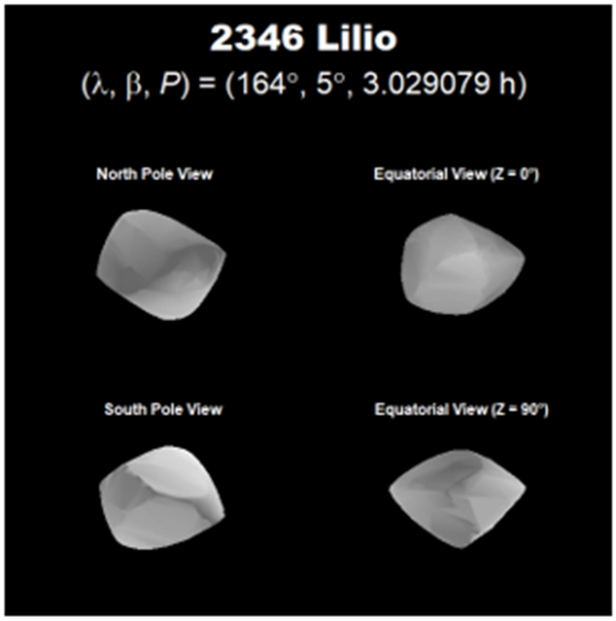

Figure 3. The shape of the asteroid based on the preferred solution.

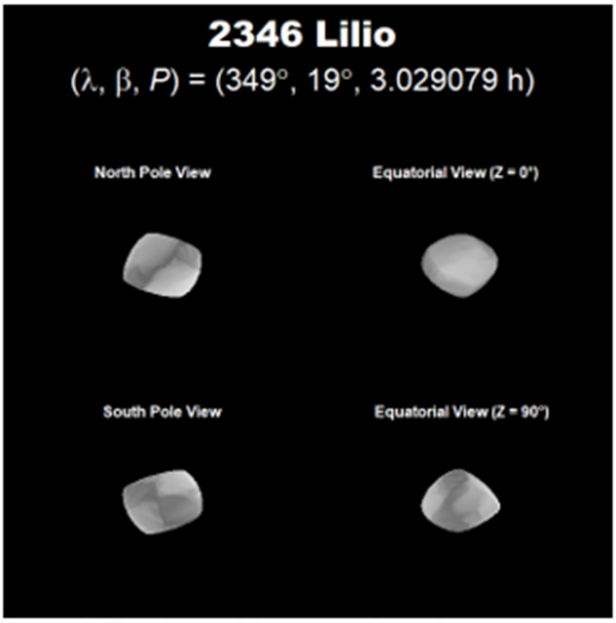

Figure 4. The shape of the asteroid based upon the secondary solution.

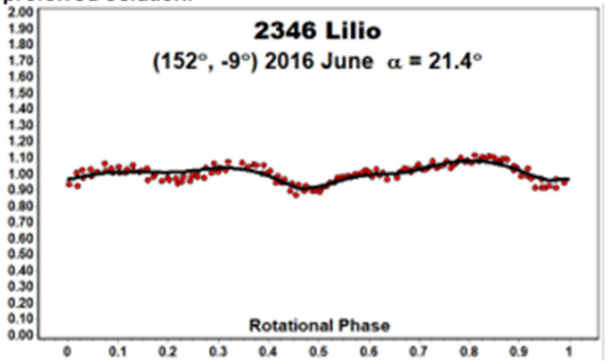

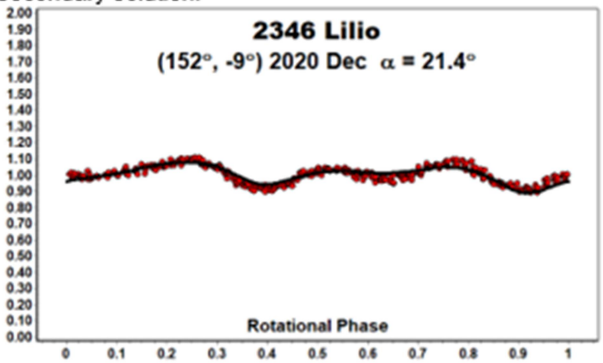

Figure 5/6. The comparison plots are against the preferred pole solution. The red dots indicate the data used for modeling while the black line is the smoothed lightcurve for generated by the shape at the time of the observations. The match is very close on both occasions, which gives confidence in the shape/spin axis model.

SPIN/SHAPE MODEL FOR 2510 Shandong

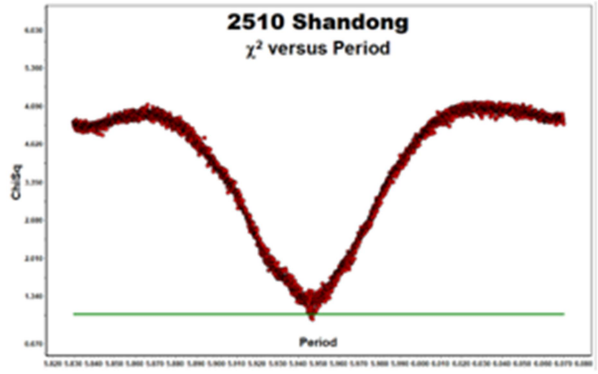

Figure 1. The initial period search results.

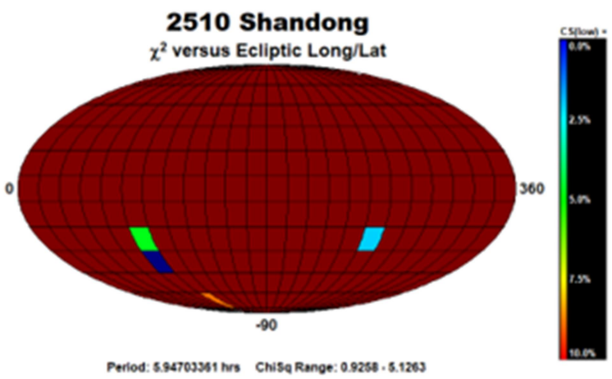

Figure 2. The pole search found two probable solutions.

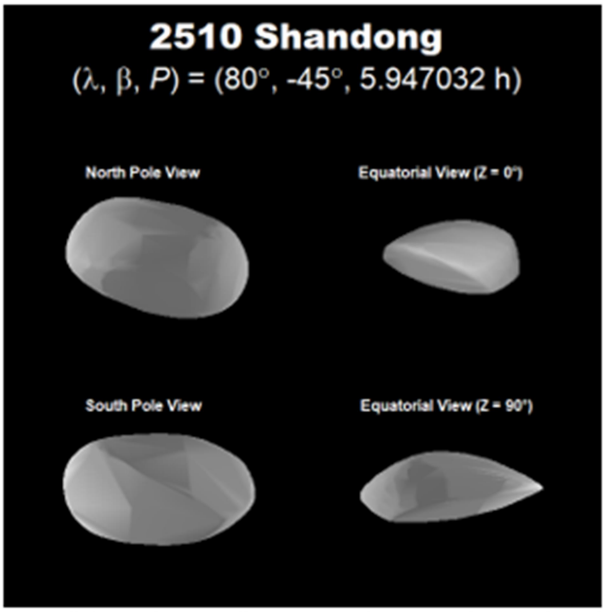

Figure 3. The shape of the asteroid based on the preferred solution.

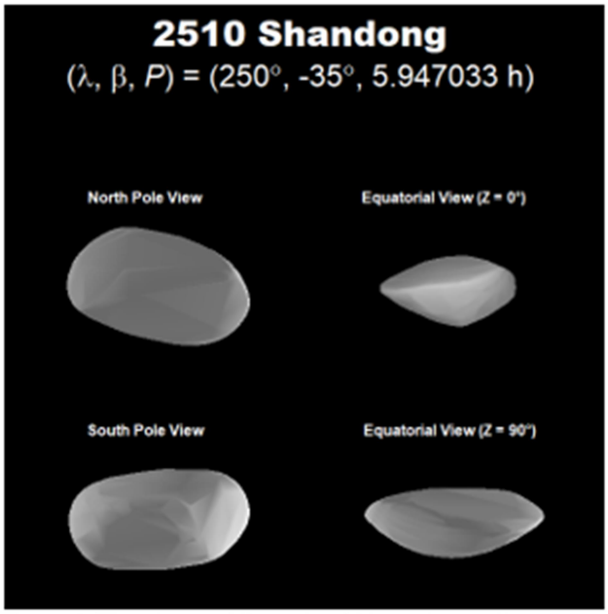

Figure 4. The shape of the asteroid based upon the secondary solution.

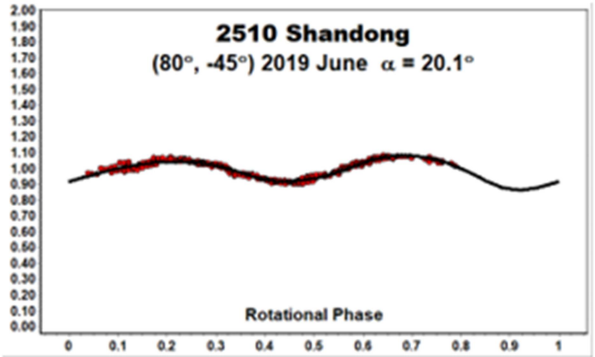

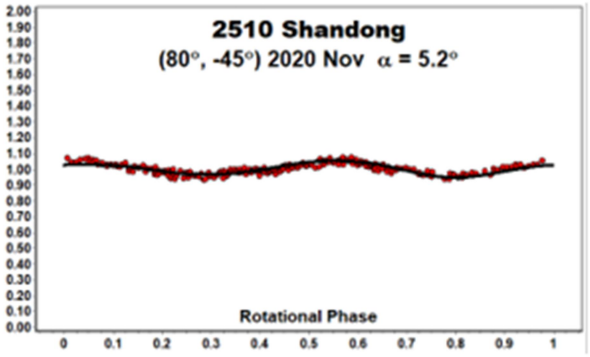

Figure 5/6. The comparison plots are against the preferred pole solution. The red dots indicate the data used for modeling while the black line is the smoothed lightcurve for generated by the shape at the time of the observations. The match is very close on both occasions, which gives confidence in the shape/spin axis model.

Number	Name	2020 mm/dd	Phase	L_{PAB}	B_{PAB}	Period(h)	P.E.	Amp	A.E.	Grp
1063	Aquilegia	12/15-12/16	15.4,15.7	51	-5	5.790	0.002	0.17	0.01	FLOR
	Pole (λ, β, P)	**(46°, 26°, 5.791760 h)**	(231°, 33°, 5.791761 h)			**a/b: 1.84**	**a/c: 2.49**			
1570	Brunonia	11/03-11/20	5.9,12.4	28	-1	157	2	0.8	0.05	KOR
2254	Requiem	11/28-12/01	27.6,27.9	10	4	4.432	0.002	0.35	0.02	FLOR
	Pole (λ, β, P)	**(223°, 38°, 4.430327 h)**	(38°, 48°, 4.430326 h)			**a/b: 1.67**	**a/c: 2.27**			
2346	Lilio	12/02-12/05	21.6,22.4	30	3	3.029	0.001	0.19	0.02	ERI
	Pole (λ, β, P)	**(164°, 5°, 3.029079 h)**	(349°, 19°, 3.029079 h)			**a/b: 1.26**	**a/c: 1.30**			
2510	Shandong	11/26-11/27	16.6,4.7	86	-2	5.96	0.02	0.1	0.01	FLOR
	Pole (λ, β, P)	**(80°, -45°, 5.947032 h)**	(250°, -35°, 5.947033 h)			**a/b: 1.32**	**a/c: 2.27**			
2912	Lapalma	10/26-10/28	8.5,7.7	47	-9	5.715	0.002	0.71	0.02	FLOR
3781	Dufek	10/19-12/12	*1.3,17.8	30	-1	1465	50	0.82	0.03	KOR
20498	1999 RT1	11/12-11/14	18.5,19.2	17	12	14.44	0.01	0.82	0.03	EUN
21182	1994 EC2	12/01-12/04	30.7,31.4	25	17	10.131	0.007	0.12	0.02	PHO
32772	1986 JL	12/21-12/22	26.5,26.8	47	-6	6.00	0.02	0.10	0.02	H
69274	1989 UZ1	11/23-11/25	5.2,4.0	68	-2	10.40	0.01	0.51	0.02	MC
306517	1999 WY	09/30-10/10	34.5,35.9	353	41	14.807	0.004	0.32	0.03	MC

Table II. Observing circumstances and results. The phase angle is given for the first and last date. If preceded by an asterisk, the phase angle reached an extrema during the period. L_{PAB} and B_{PAB} are the approximate phase angle bisector longitude/latitude at mid-date range (see Harris et al., 1984). Grp is the asteroid family/group (Warner et al., 2009): ERI, Erigone; EUN, Eunomia; FLOR, Flora; H, Hungaria; KOR, Koronis; MC, Mars-crosser; PHO, Phocaea. For 1063, 2254, 2346, and 2510, the second line gives the spin axis/shape modeling results. The preferred solution is in bold text.

(306517) 1999 WY. We could not find any entries in the LCDB for this Mars-crosser.

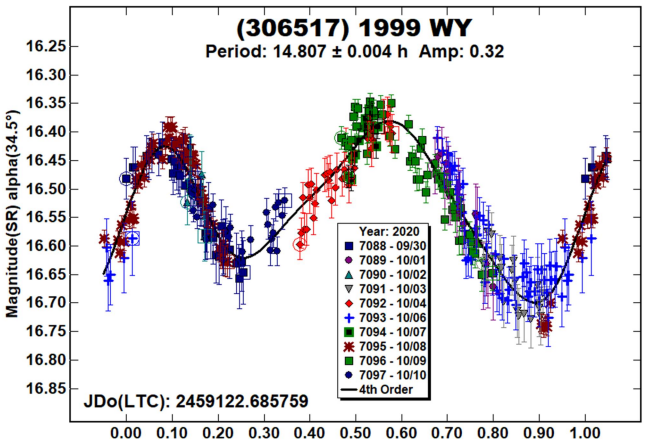

Acknowledgements

Observations at CS3 and continued support of the asteroid lightcurve database (LCDB; Warner et al., 2009) are supported by NASA grant 80NSSC18K0851.

This work includes data from the Asteroid Terrestrial-impact Last Alert System (ATLAS) project. ATLAS is primarily funded to search for near earth asteroids through NASA grants NN12AR55G, 80NSSC18K0284, and 80NSSC18K1575; byproducts of the NEO search include images and catalogs from the survey area. The ATLAS science products have been made possible through the contributions of the University of Hawaii Institute for Astronomy, the Queen's University Belfast, the Space Telescope Science Institute, and the South African Astronomical Observatory.

The authors gratefully acknowledge Shoemaker NEO Grants from the Planetary Society (2007, 2013). These were used to purchase some of the telescopes and CCD cameras used in this research.

References

AstDys-2 (2020). Asteroids - Dynamic site. *https://newton.spacedys.com/astdys/*

Asteroid Lightcurve Data Exchange Format database (ALCDEF). *http://www.alcdef.org/*

Behrend, R., (2003web, 2005web, 2007web, 2016web). Observatoire de Geneve web site. *http://obswww.unige.ch/~behrend/page_cou.html*

Brinsfield, J.W. (2008). "Asteroid Lightcurve Analysis at the Via Capote Observatory: First Quarter 2008." *Minor Planet Bul.* **35**, 119-122.

Hanuš, J.; Ďurech, J.; Brož, M.; Marciniak, A.; Warner, B.D.; Pilcher, F.; Stephens, R.; Behrend, R.; Carry, B.; and 111 coauthors. (2013). "Asteroids' physical models from combined dense and sparse photometry and scaling of the YORP effect by the observed obliquity distribution." *Astron. Astrophys.* **551**, A67.

Harris, A.W.; Young, J.W.; Scaltriti, F.; Zappala, V. (1984). "Lightcurves and phase relations of the asteroids 82 Alkmene and 444 Gyptis." *Icarus* **57**, 251-258.

Harris, A.W.; Young, J.W.; Bowell, E.; Martin, L.J.; Millis, R.L.; Poutanen, M.; Scaltriti, F.; Zappala, V.; Schober, H.J.; Debehogne, H.; Zeigler, K.W. (1989). "Photoelectric Observations of Asteroids 3, 24, 60, 261, and 863." *Icarus* **77**, 171-186.

Higgins, D.; Goncalves, R. (2006). "Asteroid Lightcurve Analysis at Hunters Hill Observatory and Collaborating Stations - June-September 2006." *Minor Planet Bull*. **34**, 16-18.

Kaasalainen, M.; Torppa J. (2001). "Optimization Methods for Asteroid Lightcurve Inversion. I. Shape Determination." *Icarus* **153**, 24-36.

Kaasalainen, M.; Torppa J.; Muinonen, K. (2001). "Optimization Methods for Asteroid Lightcurve Inversion. II. The Complete Inverse Problem." *Icarus* **153**, 37-51

Molnár, L.; Pál, A.; Sáneczky, K.; Szabó, R.; Vinkó, J.; Szabó, Gy.M.; Kiss, Cs.; Hanyecz, O.; Marton, G.; Kiss, L.L. (2018) "Main-belt Asteroids in the K2 Uranus Field." *Ap. J. Supp. Ser.* **234,** A37

Pál, A.; Szakáts, R.; Kiss, C.; Bódi, A.; Bognár, Z.; Kalup, C.; Kiss, L.L.; Marton, G.; Molnár, L.; Plachy, E.; Sárneczky, K.; Szabó, G.M.; Szabó, R. (2020). "Solar System Objects Observed with TESS - First Data Release: Bright Main-belt and Trojan Asteroids from the Southern Survey." *Ap. J.* **247**, A26.

Pravec, P.; Wolf, M.; Sarounova, L. (2008web). *http://www.asu.cas.cz/~ppravec/neo.htm*

Pravec, P.; Scheirich, P.; Durech, J.; Pollock, J.; Kusnirak, P.; Hornoch, K.; Galad, A.; Vokrouhlicky, D.; Harris, A.W.; Jehin, E.; Manfroid, J.; Opitom, C.; Gillon, M.; Colas, F.; Oey, J.; Vrastil, J.; Reichart, D.; Ivarsen, K.; Haislip, J.; LaCluyze, A. (2014). "The tumbling state of (99942) Apophis." *Icarus* **233**, 48-60.

Stephens, R.D. (2016a). "Asteroids Observed from CS3: 2016 January-March." *Minor Planet Bull*. **43**, 252-255.

Stephens, R.D. (2016b). "Asteroids Observed from CS3: 2016 April - June." *Minor Planet Bull*. **43**, 336-339.

Stephens, R.D. (2018). "Asteroids Observed from CS3: 2018 January - March." *Minor Planet Bull*. **45**, 299-301.

Stephens, R.D.; Warner, B.D. (2019). "Main-belt Asteroids Observed from CS3: 2019 April to June." *Minor Planet Bull*. **46**, 449-456.

Tonry, J.L.; Denneau, L.; Flewelling, H.; Heinze, A.N.; Onken, C.A.; Smartt, S.J.; Stalder, B.; Weiland, H.J.; Wolf, C. (2018). "The ATLAS All-Sky Stellar Reference Catalog." *Astrophys. J.* **867**, A105.

Warner, B.D. (2006). "Asteroid lightcurve analysis at the Palmer Divide Observatory: July-September 2005." *Minor Planet Bull*. **33**, 35-39.

Warner, B.D.; Harris, A.W.; Pravec, P. (2009). "The Asteroid Lightcurve Database." *Icarus* **202**, 134-146. Updated 2020 Oct. *http://www.minorplanet.info/lightcurvedatabase.html*

Warner, B.D. (2013). "Asteroid Lightcurve Analysis at the Palmer Divide Observatory: 2013 January - March." *Minor Planet Bull*. **40**, 137-145.

Waszczak, A.; Chang, C.-K.; Ofek, E.O.; Laher, R.; Masci, F.; Levitan, D.; Surace, J.; Cheng, Y.-C.; Ip, W.-H.; Kinoshita, D.; Helou, G.; Prince, T.A.; Kulkarni, S. (2015). "Asteroid Light Curves from the Palomar Transient Factory Survey: Rotation Periods and Phase Functions from Sparse Photometry." *Astron. J.* **150**, A75.

PERIOD DETERMINATIONS FOR SEVENTEEN MINOR PLANETS

Tom Polakis
Command Module Observatory
121 W. Alameda Dr.
Tempe, AZ 85282
tpolakis@cox.net

(Received: 2020 Dec 28)

Phased lightcurves and synodic rotation periods for 17 main-belt asteroids are presented, based on CCD observations made from 2020 October through 2020 December. All the data have been submitted to the ALCDEF database.

CCD photometric observations of 17 main-belt asteroids were performed at Command Module Observatory (MPC V02) in Tempe, AZ. Images were taken using a 0.32-m f/6.7 Modified Dall-Kirkham telescope, SBIG STXL-6303 CCD camera, and a 'clear' glass filter. Exposure time for all the images was 2 minutes. The image scale after 2×2 binning was 1.76 arcsec/pixel. Table I shows the observing circumstances and results. All of the images for these asteroids were obtained between 2020 October and 2020 December.

Images were calibrated using a dozen bias, dark, and flat frames. Flat-field images were made using an electroluminescent panel. Image calibration and alignment was performed using MaxIm DL software.

The data reduction and period analysis were done using MPO Canopus (Warner, 2020). The 45′×30′ field of the CCD typically enables the use of the same field center for three consecutive nights. In these fields, the asteroid and three to five comparison stars were measured. Comparison stars were selected with colors within the range of $0.5 < B\text{-}V < 0.95$ to correspond with color ranges of asteroids. In order to reduce the internal scatter in the data, the brightest stars of appropriate color that had peak ADU counts below the range where chip response becomes nonlinear were selected. MPO Canopus plots instrumental vs. catalog magnitudes for solar-colored stars, which is useful for selecting comp stars of suitable color and brightness.

Since the sensitivity of the KAF-6303 chip peaks in the red, the clear-filtered images were reduced to Sloan r′ to minimize error with respect to a color term. Comparison star magnitudes were obtained from the ATLAS catalog (Tonry et al., 2018), which is incorporated directly into MPO Canopus. The ATLAS catalog derives Sloan griz magnitudes using a number of available catalogs. The consistency of the ATLAS comp star magnitudes and color-indices allowed the separate nightly runs to be linked often with no zero-point offset required or shifts of only a few hundredths of a magnitude in a series.

A 9-pixel (16 arcsec) diameter measuring aperture was used for asteroids and comp stars. It was typically necessary to employ star subtraction to remove contamination by field stars. For the asteroids described here, I note the RMS scatter on the phased lightcurves, which gives an indication of the overall data quality including errors from the calibration of the frames, measurement of the comp stars, the asteroid itself, and the period-fit. Period determination was done using the MPO Canopus Fourier-type FALC fitting method (cf. Harris et al., 1989). Phased lightcurves show the maximum at phase zero. Magnitudes in these plots are apparent and scaled by MPO Canopus to the first night.

Most asteroids were selected from the CALL website (Warner, 2011a) using the criteria of magnitude greater than 15.5 and quality of results, U, less than 2+. In this set of observations, 6 of the 17 asteroids had no previous period analysis, 1 had U = 1, and 9 had U = 2. The Asteroid Lightcurve Database (LCDB; Warner et al., 2009) was consulted to locate previously published results. All the new data for these asteroids can be found in the ALCDEF database.

897 Lysistrata is a Eunomia-family asteroid, discovered by Max Wolf at Heidelberg in 1918. Kim (2014) published a rotational period of 11.26 ± 0.05 h, and Mas (2018) shows 11.275 ± 0.009 h. During eight nights, 458 images were gathered, producing a period of 11.303 ± 0.004 h, in agreement with previous values. The lightcurve has an amplitude of 0.12 mag. with an RMS error of 0.001 mag.

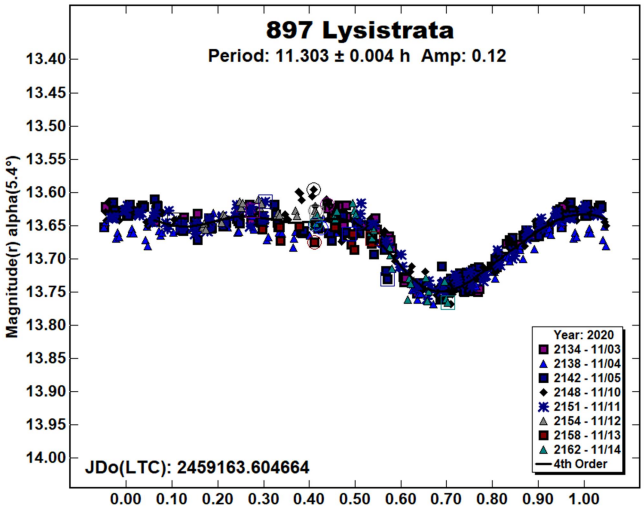

982 Franklina. This outer main-belt asteroid in an eccentric orbit was discovered at Heidelberg in 1922 by H.E. Wood. Behrend (2020) computed a period of 41.5 ± 0.1 h, and Pál (2020) obtained 186.48 ± 0.05 h. In ten nights, 477 data points were used to calculate a period of 263.5 ± 0.9 h, with an amplitude of 0.58 ± 0.021 mag. The period spectrum did not show matches at the previously published periods.

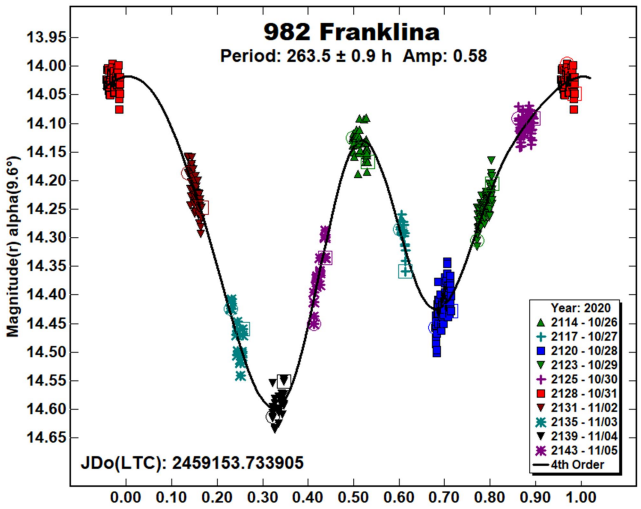

1032 Pafuri is also an H.E. Wood discovery, made in 1924 at Heidelberg. Ditteon (2019) shows a good fit to a period of 33.39 ± 0.03 h. A total of 581 data images obtained during nine nights were used to calculate a period solution of 113.0 ± 0.2 h, disagreeing with Ditteon's assessment. The amplitude of the lightcurve is 0.51 ± 0.026 mag, which is much larger than the previously published amplitude.

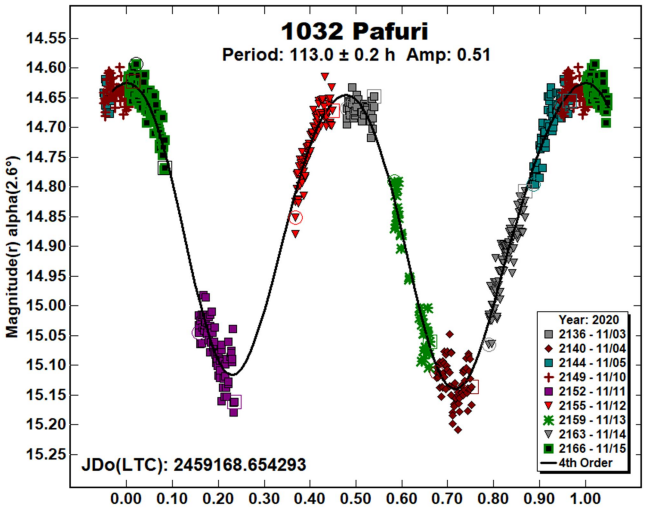

1541 Estonia was discovered at Turku in 1939 by Yrjö Väisälä. The LCDB shows only one period of 10.1 ± 1.0 h derived by Behrend (2015). After three nights, 211 images were collected. The period spectrum shows a weak signal at the bimodal solution of 12.86 ± 0.05 h, disagreeing with Behrend's result. The RMS error of 0.032 mag. is significant relative to the amplitude of 0.10 mag.

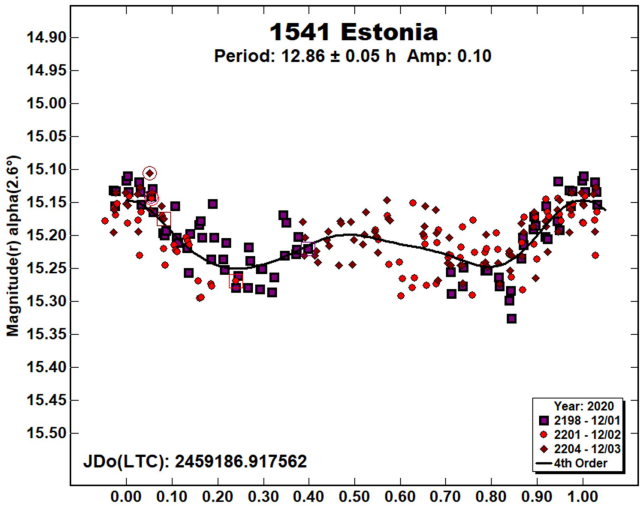

1615 Bardwell is a Themis-family asteroid that came to a favorable opposition in 2020. It was discovered at Goethe Link Observatory in 1950. The single period in the LCDB dates back to 1979, when Tedesco (1979) calculated >18 h. A total of 339 images taken during four nights produced a period solution of 17.00 ± 0.04 h, with an amplitude of 0.12 ± 0.023 mag.

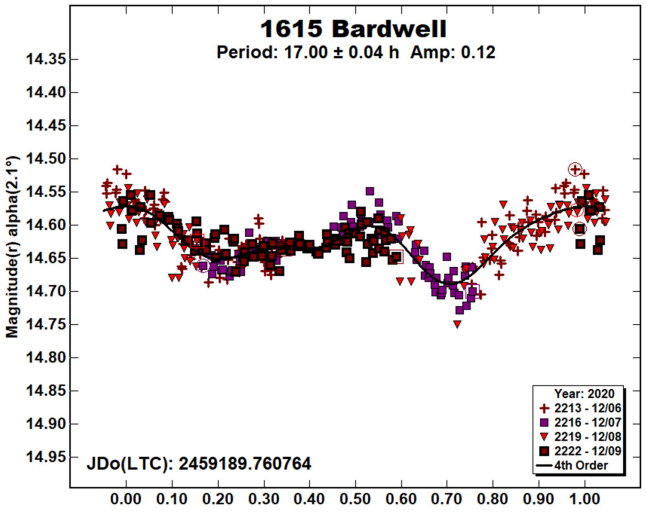

2191 Uppsala. This Eos-family asteroid was discovered by C.I. Lagerqvist at Mt. Stromlo in 1977. No period solutions appear in the LCDB. Over a four-night interval, 302 images were obtained, yielding a synodic period of 31.39 ± 0.04 h. The amplitude is 0.52 mag., with an RMS error on the fit of 0.026 mag.

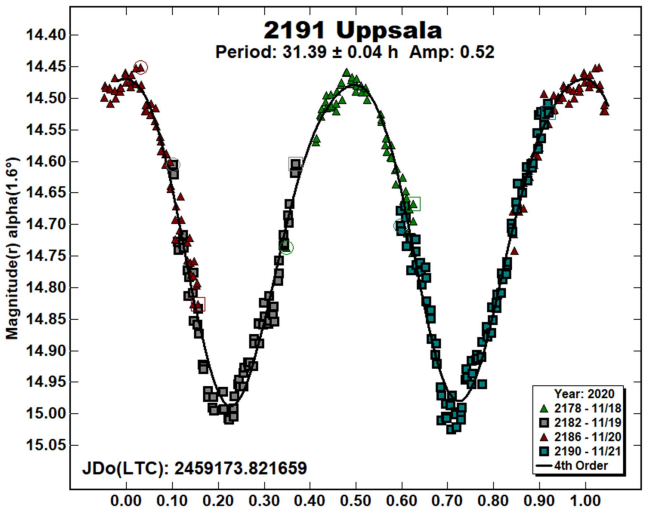

2262 Mitidika lies in a very eccentric orbit which brought it to a favorable opposition in 2020. It was discovered Paul Wild at Zimmerwald in 1978. Pál (2020) shows a period of 28.0933 ± 0.0005 h. During five nights, 440 images were used to compute a period of 28.53 ± 0.07 h, in agreement with Pál's value. The amplitude is 0.24 mag., with an RMS error on the fit of 0.032 mag.

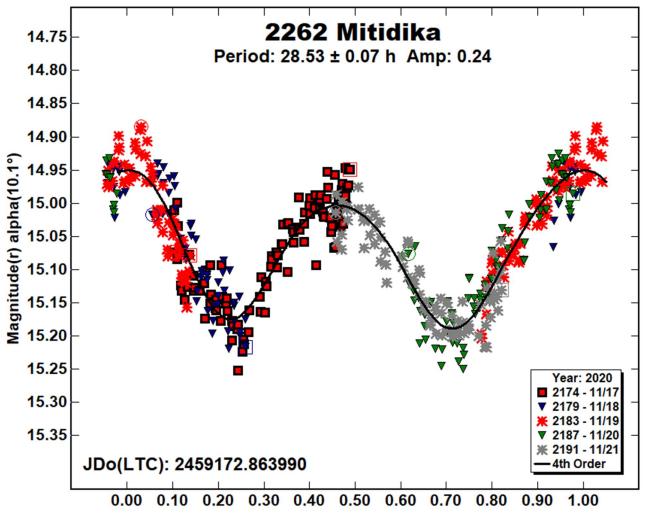

2263 Shaanxi was discovered in 1978 at Purple Mountain Observatory. Warner (2011b) published a period of 41.7 ± 0.1 h. A total of 988 data points were obtained in 13 nights. The period solution is 277.2 ± 0.3 h. The lightcurve features an extremely deep primary minimum, producing an amplitude of 1.45 ± 0.063 mag.

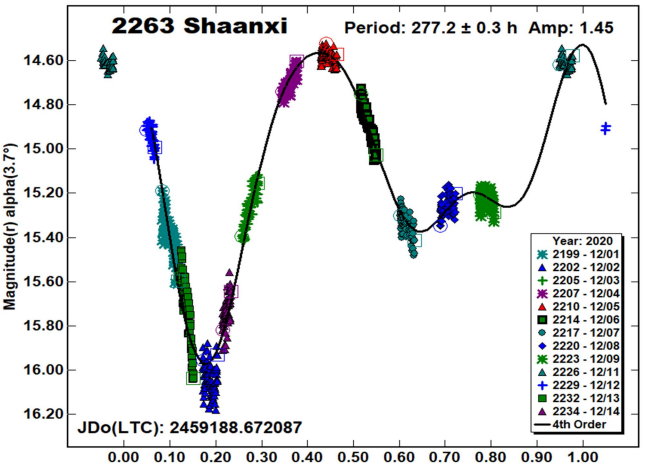

2322 Kitt Peak is a member of the Flora family, discovered at Goethe Link Observatory in 1954. No period solutions appear in the LCDB. Due to its short period and high amplitude, it was observed for only three nights, with 175 data points. The rotational period is 8.460 ± 0.006 h, with an amplitude of 0.47 ± 0.043 mag.

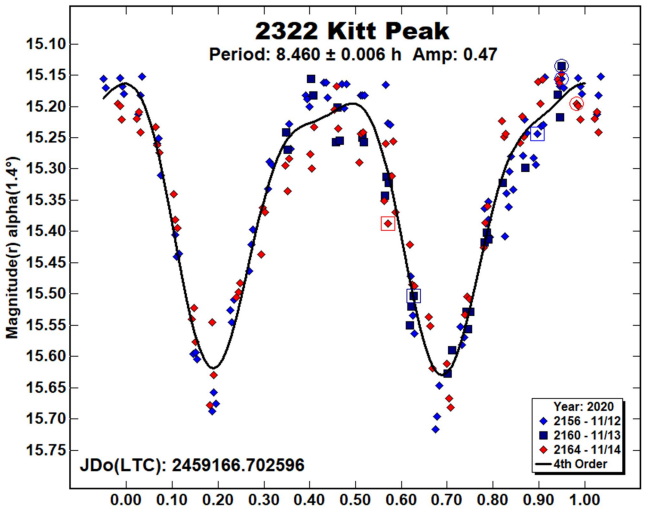

2403 Sumava. This minor planet was discovered in 1979 at Klet Observatory by Antonín Mrkos. No known period solutions exist. In a span of 12 observing nights, 911 images were taken. This produced a period solution of 152.5 ± 0.2 h, with a large amplitude of 1.12 ± 0.050 mag.

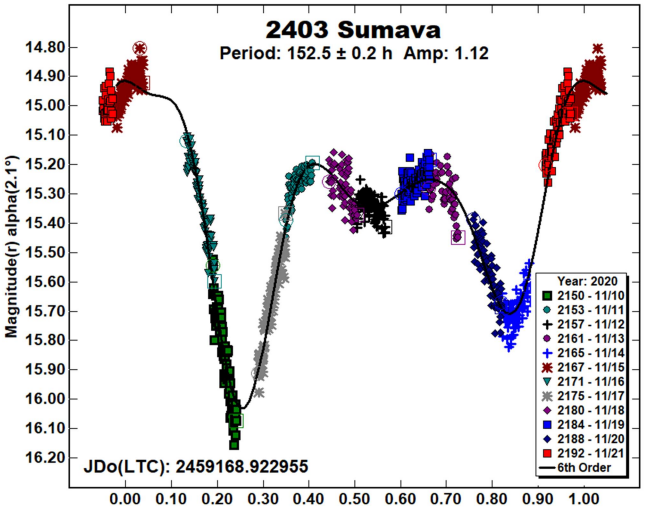

2819 Ensor lies in the outer main belt. It was discovered by Eugène Joseph Delporte at Uccle in 1933. The LCDB shows no period solutions. It was observed during a favorable opposition on 11 nights, and 541 images were obtained. The rotational period is 159.7 ± 0.2 h, with an amplitude of 0.72 ± 0.031 mag.

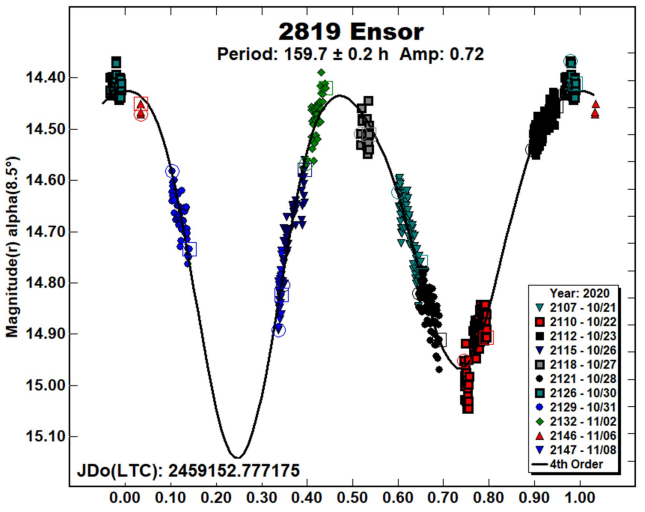

3578 Carestia occupies the outer main belt, in a highly inclined and eccentric orbit. Its discovery was made at Félix Aguilar Observatory in 1977 in El Leoncito. Holliday (1997) computed a period of 7.08 h, and Behrend (2008) calculated 9.93 ± 0.01 h. Three nights and 239 images were sufficient to calculate a period of 9.93 ± 0.02 h, in accordance with Behrend's value. The lightcurve has an amplitude of 0.16 ± 0.032 h.

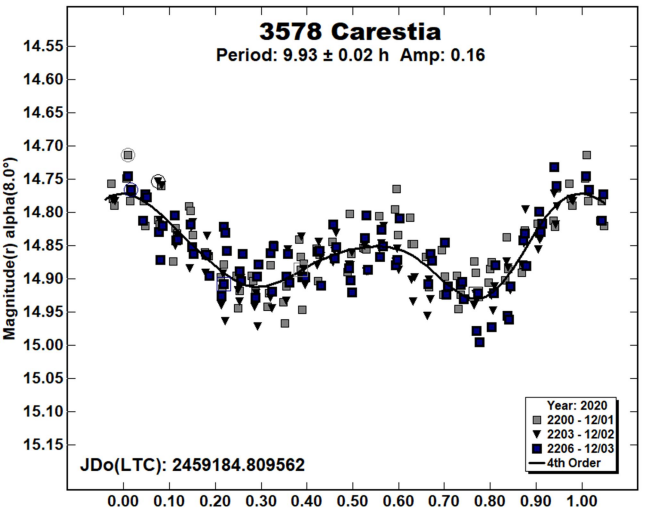

4103 Chahine. Eleanor Helin discovered this Phocaea-region asteroid in a highly inclined orbit in 1989 at Palomar Observatory. Behrend (2020) shows a period of 92.8 ± 0.3 h, and Pál (2020) published 105.161 ± 0.005 h. During seven nights, 642 images were secured. The rotation period is 103.2 ± 0.1 h, roughly agreeing with Pál. The amplitude is 0.53 mag., with an RMS error on the fit of 0.017 mag.

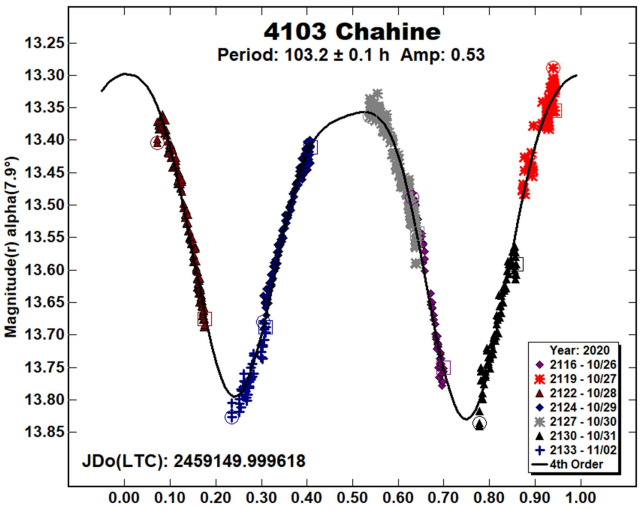

4729 Mikhailmil' is a member of the Flora family, discovered at Nauchnyj in 1980 by Lyudmila Vasilyevna. Ruthroff (2012) published a period of 17.74 ± 0.01 h. Over the course of seven nights, 485 images were obtained, yielding a synodic period of 38.31 ± 0.03 h, disagreeing with Ruthroff's value. The lightcurve has an amplitude of 0.37 ± 0.028 mag.

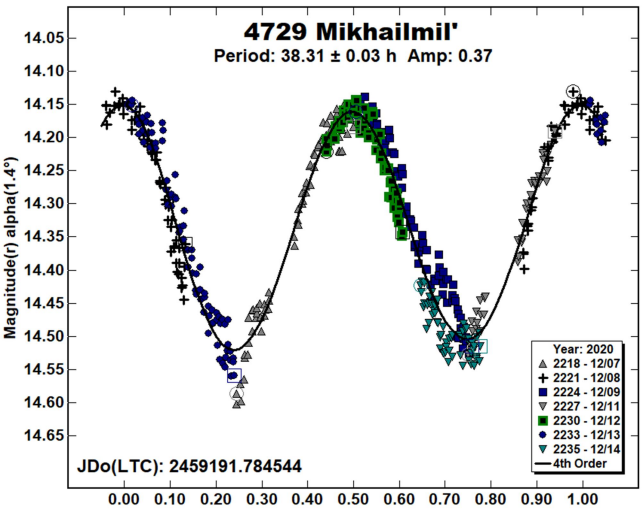

8190 Bouguer. Eric Walter Elst discovered this Flora-family minor planet in 1993. It was named after the mathematician Pierre Bouguer, sometimes called the father of photometry. Waszczak et al. (2015) published a period of 6.842 ± 0.0015 h. This asteroid serendipitously appeared in three frames with 2403 Sumava, so photometry was performed, despite it being a full magnitude fainter than the practical limit for this equipment and site. The 242 images were employed to calculate a rotational period of 6.854 ± 0.009 h, in good agreement with Waszczak. The amplitude is 0.34 mag., with a significant RMS error on the fit of 0.075 mag.

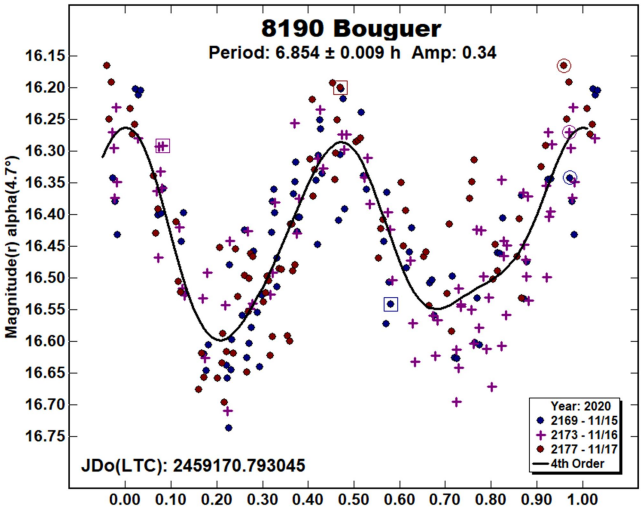

9144 Hollisjohnson was discovered at Goethe Link Observatory in 1955. Its highly eccentric orbit brought it to a favorable 2020 opposition. No period solutions have been published. Three nights and 171 data points were sufficient to produce a clean period solution of 10.464 ± 0.016 h. The amplitude is 0.20 ± 0.029 mag.

Number	Name	2020/mm/dd	Phase	L_{PAB}	B_{PAB}	Period(h)	P.E.	Amp	A.E.	Grp
897	Lysistrata	11/03-11/14	5.4,7.5	39	11	11.303	0.004	0.12	0.01	EUN
982	Franklina	10/26-11/05	9.5,11.0	15	17	263.5	0.9	0.58	0.02	MB-O
1032	Pafuri	11/03-11/15	*2.6,3.1	46	-6	113.0	0.02	0.51	0.03	MB-O
1541	Estonia	12/01-12/03	2.5,2.9	67	6	12.86	0.05	0.10	0.03	MB-O
1615	Bardwell	12/06-12/09	2.3.1.2	78	-2	17.00	0.04	0.12	0.02	THM
2191	Uppsala	11/18-11/21	1.7,0.7	59	2	31.39	0.04	0.52	0.03	EOS
2262	Mitidika	11/17-11/21	10.1,9.5	62	16	28.53	0.07	0.24	0.03	MB-I
2263	Shaanxi	12/01-12/14	3.6,8.8	61	2	277.2	0.3	1.45	0.06	EOS
2322	Kitt Peak	11/12-11/14	1.2,2.1	49	-2	8.460	0.006	0.47	0.04	FLOR
2403	Sumava	11/10-11/21	2.1,6.3	47	4	152.5	0.2	1.12	0.05	MB-I
2819	Ensor	10/21-11/08	8.4,16.2	14	0	159.7	0.2	0.72	0.03	MB-O
3578	Carestia	12/01-12/03	5.4,4.2	77	0	9.93	0.02	0.16	0.03	MB-O
4103	Chahine	10/26-11/02	*7.9,7.6	39	11	103.2	0.1	0.53	0.02	PHO
4729	Mikhailmil'	12/07-12/14	*1.6,3.0	78	0	38.31	0.03	0.37	0.03	FLOR
8190	Bouguer	11/15-11/17	4.5,5.6	47	4	6.854	0.009	0.34	0.08	FLOR
9144	Hollisjohnson	11/03-11/05	7.5,6.7	49	7	10.464	0.016	0.20	0.03	MB-I
21182	1994 EC2	10/21-10/23	9.5,11.1	17	6	10.130	0.018	0.11	0.02	PHO

Table I. Observing circumstances and results. The phase angle is given for the first and last date. If preceded by an asterisk, the phase angle reached an extrema during the period. L_{PAB} and B_{PAB} are the approximate phase angle bisector longitude/latitude at mid-date range (see Harris et al., 1984). Grp is the asteroid family/group (Warner et al., 2009).

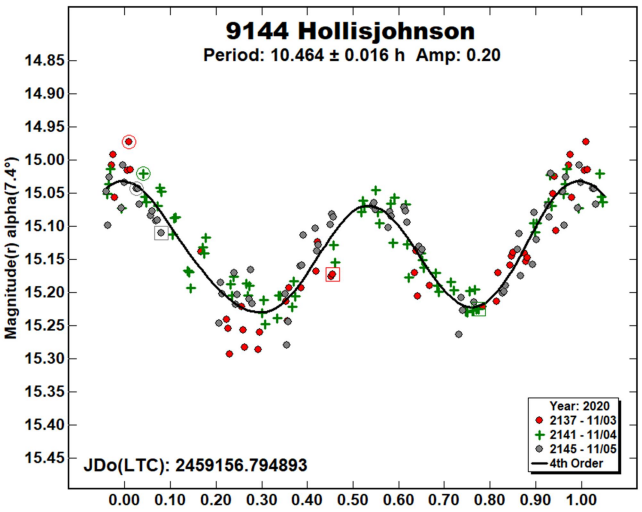

21182 1994 EC2 was discovered at Kitame in 1994 by Kin Endate. The LCDB shows no period solutions for it. A total of 285 images were taken during three nights. The computed synodic period is 10.130 ± 0.018 h, with an amplitude of 0.11 ± 0.022 mag.

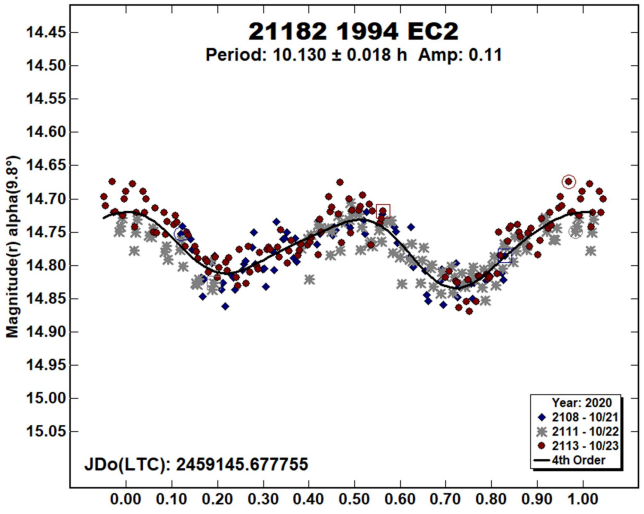

Acknowledgements

The author would like to express his gratitude to Brian Skiff for his indispensable mentoring in data acquisition and reduction. Thanks also go out to Brian Warner for support of his MPO Canopus software package.

References

Behrend, R. (-2008, -2015, -2020). Observatoire de Geneve web site. *http://obswww.unige.ch/~behrend/page_cou.html*

Ditteon, R.; Weichang, L.; Sheerin, M. (2019). "Lightcurve Analysis of Minor Planets Observed at the Oakley Southern Sky Observatory: 2018 May-June." *Minor Planet Bull.* **46**, 276-276.

Harris, A.W.; Young, J.W.; Scaltriti, F.; Zappala, V. (1984). "Lightcurves and phase relations of the asteroids 82 Alkmene and 444 Gyptis." *Icarus* **57**, 251-258.

Harris, A.W.; Young, J.W.; Bowell, E.; Martin, L.J.; Millis, R.L.; Poutanen, M.; Scaltriti, F.; Zappala, V.; Schober, H.J.; Debehogne, H.; Zeigler, K.W. (1989). "Photoelectric Observations of Asteroids 3, 24, 60, 261, and 863." *Icarus* **77**, 171-186.

Holliday, B. (1997). "Photometric Observations of Minor Planet 3578 Caresia." *Minor Planet Bull.* **24**, 1.

Kim, M.-J. et al. (2014). "Rotational Properties of the Maria Asteroid Family." *Astron. J.* **147**, 56-138.

Mas, V. et al. (2018). "Twenty-one Asteroid Lightcurves at Asteroids Observers (OBAS) - MPPD: Nov 2016 - May 2017." *Minor Planet Bull.* **45**, 76-82.

Pál, A.; Szakáts, R.; Kiss, C.; Bódi, A.; Bognár, Z.; Kalup, C.; Kiss, L.; Marton, G.; Molnár, L.; Plachy, E.; Sárneczky, K.; Szabó, G.; Szabó, R. (2020). "Solar System Objects Observed with TESS - First Data Release: Bright Main-belt and Trojan Asteroids from the Southern Survey." *Ap. J. Supl. Ser.* **247**, 26-34.

Ruthroff, J. (2012). "Lightcurve Analysis of 1786 Raahe and 4729 Mikhailmil'". *Minor Planet Bull.* **39**, 39.

Tedesco, E.F. (1979). "A photometric investigation of the colors, shapes and spin rates of Hirayama family asteroids." PhD Dissertation. New Mexico State University.

Tonry, J.L.; Denneau, L.; Flewelling, H.; Heinze, A.N.; Onken, C.A.; Smartt, S.J.; Stalder, B.; Weiland, H.J.; Wolf, C. (2018). "The ATLAS All-Sky Stellar Reference Catalog." *Astrophys. J.* **867**, A105.

Warner, B.D.; Harris, A.W.; Pravec, P. (2009). "The Asteroid Lightcurve Database." *Icarus* **202**, 134-146. Updated 2020 Aug. *http://www.minorplanet.info/lightcurvedatabase.html*

Warner, B.D. (2011a). Collaborative Asteroid Lightcurve Link website. *http://www.minorplanet.info/call.html*

Warner, B.D. (2011b). "Asteroid Lightcurve Analysis at the Palmer Divide Observatory: Unpublished Results from 1999 to 2008." *Minor Planet Bull.***38**, 89-92.

Warner, B.D. (2020). MPO Canopus software. *http://bdwpublishing.com*

Waszczak, A.; Chang, C.-K.; Ofek, E.O.; Laher, R.; Masci, F.; Levitan, D.; Surace, J.; Cheng, Y.-C.; Ip, W.-H.; Kinoshita, D.; Helou, G.; Prince, T.A.; Kulkarni, S. (2015). "Asteroid Light Curves from the Palomar Transient Factory Survey: Rotation Periods and Phase Functions from Sparse Photometry." *Astron. J.* **150**, A75.

LIGHTCURVE ANALYSIS OF HILDA ASTEROIDS AT THE CENTER FOR SOLAR SYSTEM STUDIES: 2020 OCTOBER-DECEMBER

Brian D. Warner
Center for Solar System Studies / MoreData!
446 Sycamore Ave.
Eaton, CO 80615 USA
brian@MinorPlanetObserver.com

Robert D. Stephens
Center for Solar System Studies / MoreData!
Rancho Cucamonga, CA

(Received: 2021 Jan 7)

New CCD photometric observations of two Hilda asteroid members were made from 2020 October through December: 748 Simeisa and 1754 Cunningham. The latest data for Simeisa conclusively reject earlier reports of a period near 11.9 h.

CCD photometric observations of Hilda asteroids are made at the Center for Solar System Studies (CS3) as part of an ongoing study of this family/group that is located between the outer main-belt and Jupiter Trojans in a 3:2 orbital resonance with Jupiter. The goal is to determine the spin rate statistics of the Hildas and to find pole and shape models when possible. We also look to examine the degree of influence that the YORP (Yarkovsky–O'Keefe–Radzievskii–Paddack) effect (Rubincam, 2000) has on distant objects and to compare the spin rate distribution against the Jupiter Trojans, which can provide evidence that the Hildas are more "comet-like" than main-belt asteroids.

Telescopes	Cameras
0.30-m *f*/6.3 Schmidt-Cass	FLI Microline 1001E
0.35-m *f*/9.1 Schmidt-Cass	FLI Proline 1001E
0.35-m *f*/11 Schmidt-Cass	SBIG STL-1001E
0.40-m f/10 Schmidt-Cass	
0.50-m *f*/8.1 Ritchey-Chrétien	

Table I. List of available telescopes and CCD cameras at CS3. The exact combination for each telescope/camera pair can vary due to maintenance or specific needs.

Table I lists the telescopes and CCD cameras that are combined to make observations. Up to seven telescopes are commonly used for observations. All the cameras use CCD chips from the KAF blue-enhanced family and so have essentially the same response. The pixel scales ranged from 1.24-1.60 arcsec/pixel. All lightcurve observations were unfiltered since a clear filter can result in a 0.1-0.3 magnitude loss. The exposures varied depending on the asteroid's brightness.

To reduce the number of times and amounts of adjusting nightly zero points, we use the ATLAS catalog r′ (SR) magnitudes (Tonry et al., 2018). Those adjustments are usually ≤ ±0.03 mag. The rare greater corrections may have been related in part to using unfiltered observations, poor centroiding of the reference stars, and not correcting for second-order extinction. Another cause may be selecting what appears to be a single star but is actually an unresolved pair.

The Y-axis values are ATLAS SR "sky" (catalog) magnitudes. The two values in the parentheses are the phase angle (a) and the value of *G* used to normalize the data to the comparison stars used in the earliest session. This, in effect, made all the observations seem to be made at a single fixed date/time and phase angle, leaving any variations due only to the asteroid's rotation and/or albedo changes. The X-axis shows rotational phase from –0.05 to 1.05. If the plot includes the amplitude, e.g., "Amp: 0.65", this is the amplitude of the Fourier model curve and *not necessarily the adopted amplitude for the lightcurve*.

748 Simeisa. The estimated effective diameter of Semeisa is about 105 km. Dahlgren et al. (1998) reported a period of 11.88 h and Behrend (2011web) found 11.919 h. This made the period very close to one-half an Earth day, which can lead to rotational aliasing if the lightcurve shape is highly symmetrical.

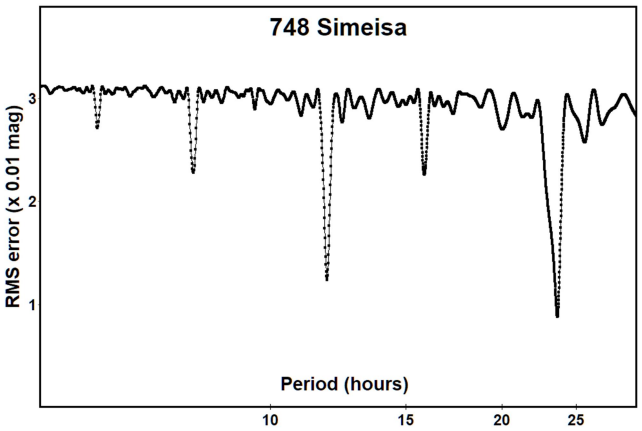

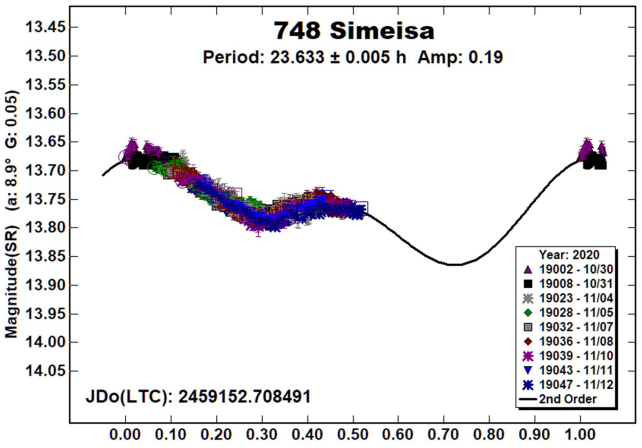

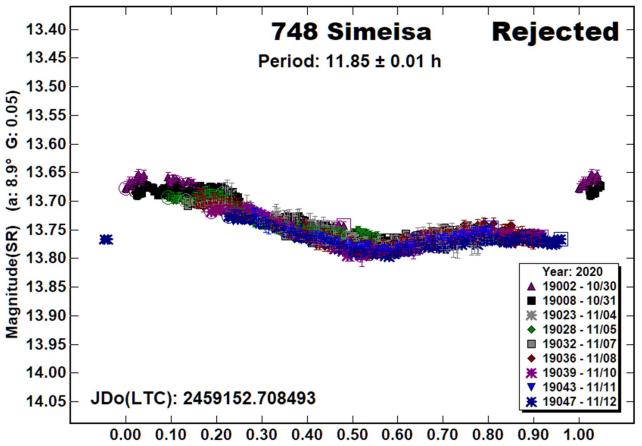

Number	Name	20yy/mm/dd	Phase	L_{PAB}	B_{PAB}	Period(h)	P.E.	Amp	A.E.
748	Simeisa	10/30-11/12	8.9,4.7	63	1	23.633	0.005	0.19	0.01
1754	Cunningham	12/26-12/30	9.6,9.0	138	-7	7.737	0.005	0.17	0.03

Table II. Observing circumstances. The phase angle (α) is given at the start and end of each date range. L_{PAB} and B_{PAB} are the average phase angle bisector longitude and latitude (see Harris *et al.*, 1984).

Ideally, a collaboration among several observers at different longitudes is best suited to reject at least some potential ambiguous solutions. Despite this, analysis of our observations from only CS3 provided a convincing case that the true period is 23.633 h, or very close to double the earlier results. This is supported by forcing the data to a period near 11.9 h as shown in the "Rejected" lightcurve. This shows a sharp discontinuity that has no reasonable physical interpretation.

1754 Cunningham. There were several previous entries in the asteroid lightcurve database (LCDB; Warner et al., 2009). Dahlgren et al. (1998) found a period of 4.285 while Slyusarev et al. (2012) reported 5.16 h. All other results, however, are close to 7.7 h: Behrend (2008web; 7.7398 h), Stephens (2015; 7.7416 h), and Warner and Stephens (2018; 7.709 h). The analysis of our most recent data supports the previous results near 7.7 h.

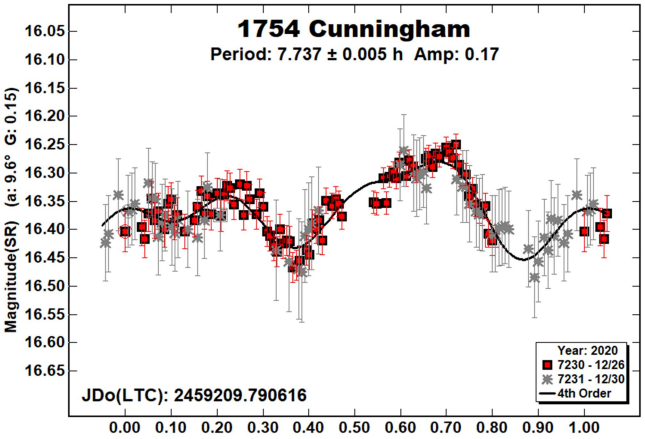

Acknowledgements

Funding for observations at CS3 and work on the asteroid lightcurve database (Warner et al., 2009) and ALCDEF database (*alcdef.org*) are supported by NASA grant 80NSSC18K0851.

This work includes data from the Asteroid Terrestrial-impact Last Alert System (ATLAS) project. ATLAS is primarily funded to search for near earth asteroids through NASA grants NN12AR55G, 80NSSC18K0284, and 80NSSC18K1575; byproducts of the NEO search include images and catalogs from the survey area. The ATLAS science products have been made possible through the contributions of the University of Hawaii Institute for Astronomy, the Queen's University Belfast, the Space Telescope Science Institute, and the South African Astronomical Observatory.

The authors gratefully acknowledge Shoemaker NEO Grants from the Planetary Society (2007, 2013). These were used to purchase some of the telescopes and CCD cameras used in this research.

References

Behrend, R. (-2008web; -2011web). Observatoire de Geneve web site., *http://obswww.unige.ch/~behrend/page_cou.html*

Dahlgren, M.; Lahulla, J.F.; Lagerkvist, C.-I.; Lagerros, J.; Mottola, S.; Erikson, A.; Gonano-Beurer, M.; Di Martino, M. (1998). "A Study of Hilda Asteroids. V. Lightcurves of 47 Hilda Asteroids." *Icarus* **133**, 247-285.

Harris, A.W.; Young, J.W.; Scaltriti, F.; Zappala, V. (1984). "Lightcurves and phase relations of the asteroids 82 Alkmene and 444 Gyptis." *Icarus* **57**, 251-258.

Rubincam, D.P. (2000). "Relative Spin-up and Spin-down of Small Asteroids." *Icarus* **148**, 2-11.

Stephens, R.D. (2015). "Asteroids Observed from CS3: Results for 1754 Cunningham and 7023 Heiankyo." *Minor Planet Bull.* **42**, 279.

Slyusarev, I.G.; Shevchenko, V.G.; Belskaya, I.N.; Krugly, Yu.N.; Chiorny, V.G. (2012). "CCD Photometry of Hilda Asteroids." ACM 2012, #6398.

Tonry, J.L.; Denneau, L.; Flewelling, H.; Heinze, A.N.; Onken, C.A.; Smartt, S.J.; Stalder, B.; Weiland, H.J.; Wolf, C. (2018). "The ATLAS All-Sky Stellar Reference Catalog." *Astrophys. J.* **867**, A105.

Warner, B.D.; Harris, A.W.; Pravec, P. (2009). "The Asteroid Lightcurve Database." *Icarus* **202**, 134-146. Updated 2020 Sep. *http://www.minorplanet.info/lightcurvedatabase.html*

Warner, B.D.; Stephens, R.D. (2018). "Lightcurve Analysis of Hilda Asteroids at the Center for Solar System Studies: 2017 July Through September" *Minor Planet Bull.* **45**, 35-39.

LIGHTCURVE BASED DETERMINATION OF 10 HYGIEA'S ROTATIONAL PERIOD WITH TRAPPIST-NORTH AND -SOUTH

Marin Ferrais[1,2], Emmanuël Jehin[1], Pierre Vernazza[2], Laurent Jorda[2], Youssef Moulane[1], Francisco J. Pozuelos[1], Jean Manfroid[1], Khalid Barkaoui[1,3], Zouhair Benkhaldoun[3]

[1]Space sciences, Technologies & Astrophysics Research (STAR) Institute
University of Liège
Allée du 6 Août 19, 4000 Liège, BELGIUM
marin.ferrais@uliege.be

[2]Aix Marseille Université, CNRS, LAM, Laboratoire d'Astrophysique de Marseille, Marseille, FRANCE

[3]Oukaïmenden Observatory
Cadi Ayyad University, Marrakech, MOROCCO

(Received: 2020 Dec 11)

A densely-sampled lightcurve of the large main-belt asteroid 10 Hygiea was obtained with the TRAPPIST-South (TS) and TRAPPIST-North (TN) telescopes in 2018 September and October. We found its synodic rotation period and amplitude to be 13.8224 ± 0.0005 h and 0.27 mag. The data have been submitted to the ALCDEF database.

Observations of the large main-belt asteroid (MBA) 10 Hygiea were acquired with the robotic telescopes TRAPPIST-North (TN, Z53) and TRAPPIST-South (TS, I40) of the Liège University (Jehin et al., 2011). They are located, respectively, at the Oukaïmeden Observatory in Morocco and the ESO La Silla Observatory in Chile. Both are 0.6-m Ritchey-Chrétien telescopes operating at *f*/8 on German Equatorial mounts. TN camera is an Andor IKONL BEX2 DD (0.60 arcsec/pixel) and the one of TS is a FLI ProLine 3041-BB (0.64 arcsec/pixel).

The raw images were calibrated with corresponding flat fields, bias and dark frames and photometric measurements were obtained using *IRAF* (Tody, 1986) scripts. The differential photometry and lightcurves were made with Python scripts. For the differential photometry, all the stars with a high enough SNR were used and checked to discard the variable stars. Various apertures were tested to maximize the SNR. In the composite lightcurve below, the normalized relative flux is plotted against the rotational phase. The rotation period was determined with the software *Peranso* (Vanmunster, 2018), which implements the FALC algorithm (Harris et al., 1989). The reported amplitude is from the Fourier model curve.

10 Hygiea is the fourth largest MBA with a diameter of 434 ± 14 km (Vernazza et al., 2019). Since 1991, all of Hygiea's reported rotation periods agreed with a value close to 27.6 h (LCBD, Warner et al., 2009) but were each time built from sparsely sampled lightcurves. In support of the ESO Large Programme 199.C-0074 (Vernazza et al., 2018) aiming to determine precise volumes and densities of the 40 largest MBAs, we started extensive photometric observations of Hygiea to refine its rotation period and help in the shape and spin axis determination. Such a long period is challenging to cover, especially when it is close to 24 h (the 27.6 h period translates in a phase shift of only 13% of the rotation each night), explaining the lack of dense lightcurves for this large and bright asteroid. To tackle this challenge, the complementarity of the two TRAPPIST telescopes at two different longitudes was decisive to acquire long and continuous photometric series as illustrated in Ferrais et al. (2020).

We observed Hygiea in 2018 from September 10 to October 17 with TN and TS using the Johnson-Cousins broad band Rc filter, no binning, and an exposure time of 8 seconds. As more data were gathered, the phased lightcurve started to show a classic double-sinusoidal shape with the previously reported period but with the high quality of the data, we noticed it was perfectly symmetric (see Fig. 1 for the final lightcurve phased with P = 27.6 h). Therefore, we produced the split halves plot which showed two identical halves and a very convincing fit (Fig. 2). From the final data set rich of 9490 images split in 13 long photometric series for a total of 73 h, a new synodic period of 13.8224 ± 0.0005 h was derived and confirmed by the converging 3D model built with the VLT/SPHERE adaptive optics images (Vernazza et al., 2019). These images revealed the spherical shape of Hygiea and albedo features at its surface, explaining the single-peak shape of its lightcurve.

Following the publication of the new period in Vernazza et al. (2019), Pilcher (2020) derived a similar synodic period of 13.828 ± 0.001 h from photometric observations obtained in 2019. We stress with this example the importance of high-quality photometric data to derive asteroid rotation periods, especially for those having a period close to a multiple of a day and to be careful with symmetric double-peak lightcurves which might have in reality half the period due to an albedo feature rather than due to their shape.

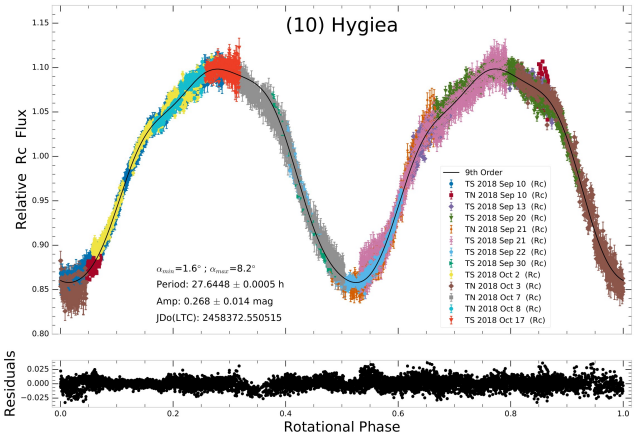

Figure 1. Phased lightcurve using the previously reported rotation period of 27.6 h.

Number	Name	2018 mm/dd	Pts	Phase	L_{PAB}	B_{PAB}	Period(h)	P.E.	Amp	A.E.	Grp
10	Hygiea	09/10-11/17	9490	*4.8,8.2	0.6	4.6	13.8224	0.0005	0.27	0.01	MB-O

Table I. Observing circumstances and results. Pts is the number of data points. The phase angle is given for the first and last date and reached a minimum during the period. L_{PAB} and B_{PAB} are the approximate phase angle bisector longitude and latitude at mid-date range (see Harris et al., 1984). Grp is the asteroid family/group (Warner *et al.*, 2009).

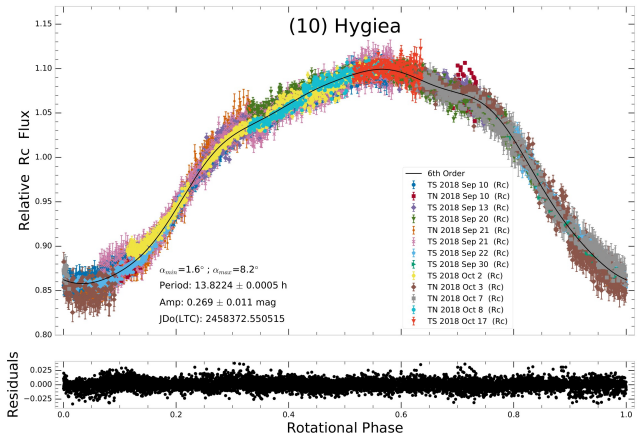

Figure 2. The lightcurve phased using the new period of 13.8224 h.

Acknowledgements

TRAPPIST-South is a project funded by the Belgian Fonds (National) de la Recherche Scientifique (F.R.S.-FNRS) under grant PDR T.0120.21. TRAPPIST-North is a project funded by the University of Liège, in collaboration with the Cadi Ayyad University of Marrakech (Morocco). E. Jehin is FNRS Senior Research Associate. The website of the TRAPPIST project can be visited at *https://www.trappist.uliege.be*.

References

Ferrais, M.; Jehin, E.; Moulane, Y.; Pozuelos, F.J.; Barkaoui, K.; Benkhaldoun, Z. (2020). "Trappist-North and -South Combined Lightcurves of Near-Earth Asteroid 3122 Florence." *Minor Planet Bull.* **47**, 21-22.

Harris, A.W.; Young, J.W.; Scaltriti, F.; Zappala, V. (1984). "Lightcurves and phase relations of the asteroids 82 Alkmene and 444 Gyptis." *Icarus* **57**, 251-258.

Harris, A.W.; Young, J.W.; Bowell, E.; Martin, L.J.; Millis, R.L.; Poutanen, M.; Scaltriti, F.; Zappala, V.; Schober, H.J.; Debehogne, H.; Zeigler, K.W. (1989). "Photoelectric Observations of Asteroids 3, 24, 60, 261, and 863." *Icarus* **77**, 171-186.

Jehin, E.; Gillon, M.; Queloz, D.; Magain, P.; Manfroid, J.; Chantry V.; Lendl, M.; Hutsemékers, D.; Udry, S. (2011). "TRAPPIST: TRAnsiting Planets and PlanetesImals Small Telescope." *The Messenger* **145**, 2-6.

Pilcher, F. (2020). "Lightcurves and rotation periods of 10 Hygiea, 47 Aglaja, 455 Bruchsalia, 463 Lola, and 576 Emanuela." *Minor Planet Bull.* **47**, 133-135.

Tody, D. (1986). "The IRAF Data Reduction and Analysis System." *Proc. SPIE Instrumentation in Astronomy VI* **627**, 733.

Vanmunster, T. (2018). *Peranso* software. *www.cbabelgium.com/peranso/*

Vernazza, P.; Broz, M.; Drouard, A.; and 40 colleagues (2018). "The impact crater at the origin of the Julia family detected with VLT/SPHERE?" *Astronomy & Astrophysics*, **618**, 154.

Vernazza, P.; Jorda, L.; Ševeček, P.; and 44 colleagues (2019). "A basin-free spherical shape as an outcome of a giant impact on asteroid Hygiea." *Nature Astronomy* **4**, 136-141.

Warner, B.D.; Harris, A.W.; Pravec, P. (2009). "The Asteroid Lightcurve Database." *Icarus* **202**, 134-146. Updated 2020 Mar. *http://www.minorplanet.info/lightcurvedatabase.html*

LIGHTCURVE ANALYSIS OF L4 TROJAN ASTERIODS AT THE CENTER FOR SOLAR SYSTEM STUDIES: 2020 OCTOBER TO DECEMBER

Robert D. Stephens
Center for Solar System Studies (CS3) / MoreData!
11355 Mount Johnson Ct., Rancho Cucamonga, CA 91737 USA
rstephens@foxandstephens.com

Brian D. Warner
Center for Solar System Studies (CS3) / MoreData!
Eaton, CO

(Received: 2021 Jan 9)

Lightcurves for six L4 Jovian Trojan asteroids were obtained at the Center for Solar System Studies (CS3) from 2020 October to December.

CCD photometric observations of six Trojan asteroids from the L_4 (Greek) Lagrange point were obtained at the Center for Solar System Studies (CS3, MPC U81). For several years, CS3 has been conducting a study of Jovian Trojan asteroids. This is another in a series of papers reporting data analysis being accumulated for family pole and shape model studies. It is anticipated that for most Jovian Trojans, two to five dense lightcurves per target at oppositions well distributed in ecliptic longitudes will be needed and can be supplemented with reliable sparse data for the brighter Trojan asteroids. For two of these targets we were able to get preliminary pole positions and create shape models from sparse data and the dense lightcurves obtained to date. These preliminary models will be improved as more data are acquired at future oppositions and will be published at a later date.

Table I lists the telescopes and CCD cameras that were used to make the observations. Images were unbinned with no filter and had master flats and darks applied. The exposures depended upon various factors including magnitude of the target, sky motion, and Moon illumination.

Telescope	Camera
0.40-m f/10 Schmidt-Cass	FLI Proline 1001E
0.40-m f/10 Schmidt-Cass	Fli Microline 1001E
0.35-m f/10 Schmidt-Cass	Fli Microline 1001E

Table I. List of telescopes and CCD cameras used at CS3.

Image processing, measurement, and period analysis were done using *MPO Canopus* (Bdw Publishing), which incorporates the Fourier analysis algorithm (FALC) developed by Harris (Harris et al., 1989). The Comp Star Selector feature in *MPO Canopus* was used to limit the comparison stars to near solar color. Night-to-night calibration was done using field stars from the ATLAS catalog (Tonry et al., 2018), which has Sloan *griz* magnitudes that were derived from the GAIA and Pan-STARR catalogs and are the "native" magnitudes of the catalog.

To reduce the resetting nightly zero points, we use the ATLAS r′ (SR) magnitudes. Those adjustments are mostly ≤ 0.03 mag. The occasions where larger corrections were required may have been related in part to using unfiltered observations, poor centroiding of the reference stars, and not correcting for second-order extinction terms.

Unless otherwise indicated, the Y-axis of lightcurves gives ATLAS SR "sky" (catalog) magnitudes. During period analysis, the magnitudes were normalized to the phase angle and value for *G* given in the parentheses. The X-axis rotational phase ranges from –0.05 to 1.05.

The amplitude indicated in the plots (e.g., Amp. 0.23) is the amplitude of the Fourier model curve and not necessarily the adopted amplitude of the lightcurve.

Targets selected for this L_4 observing campaign were mostly based upon the availability of dense lightcurves acquired in previous years. We obtained two to four lightcurves for most of these Trojans at previous oppositions. For brevity, only some of the previously reported rotational periods may be referenced. A complete list is available at the lightcurve database (LCDB; Warner et al., 2009).

To evaluate the quality of the data obtained and to determine how much more data might be needed, preliminary pole and shape models were created for all of these targets. Sparse data observations were obtained from the Catalina Sky Survey and USNO-Flagstaff survey using the AstDyS-2 (2020) site. These sparse data were combined with our dense data as well as any other dense data found in the ALCDEF asteroid photometry database (*http://www.alcdef.org/*) using *MPO LCInvert*, (Bdw Publishing). This Windows-based program incorporates the algorithms developed by Kassalainen and Torppa (2001) and Kassalainen et al. (2001) and converted by Josef Durech from the original FORTRAN to C. A period search was made over a sufficiently wide range to assure finding a global minimum in χ^2 values.

1583 Antilochus. We obtained rotational rates for this Trojan five times in the past (Stephens and Warner, 2020; and references therein), each time finding a period near 15.8 h. The 2020 results are in good agreement. In addition to our six dense lightcurves, we used sparse data from the AstDyS-2 site to find a preliminary shape model with a sidereal rotational period of 15.771329 ± 0.00001 h.

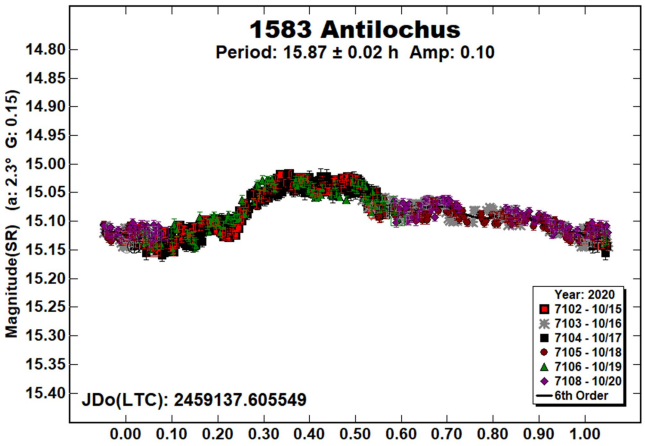

2456 Palamedes. We had only observed this Trojan once in the past (Stephens 2010), finding a rotational period of 7.24 h. Mottola et al. (2011) found a similar period of 7.258 h. Observations were made in 2020 in hope of being able to determine a shape model and pole solution. Our period is in good agreement with previous results.

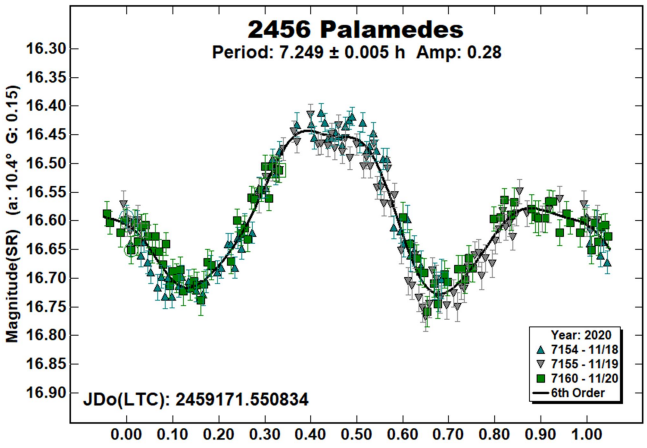

2920 Automedon. We have observed this Trojan three times in the past (Stephens and Warner, 2020; and references therein). In addition to these dense lightcurves, we used sparse data from the AstDyS-2 site to create a preliminary shape model with a sidereal rotational period of 10.212444 ± 0.00001 h.

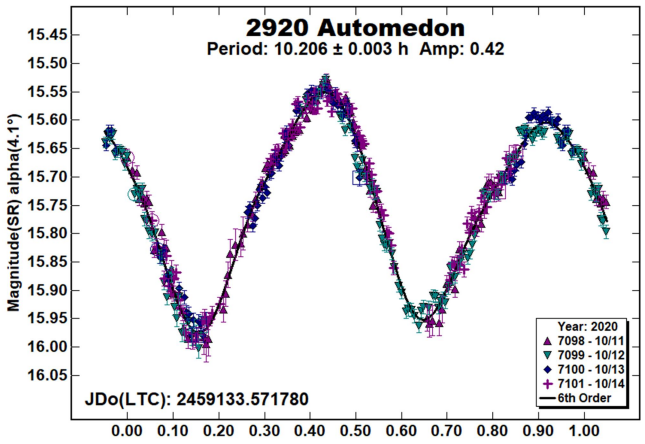

3063 Makhaon. We observed this L_4 Trojan twice in the past (French et al., 2011; Stephens et al., 2016). Mottola et al. (2011) also observed it twice. Our results from 2020 are in good agreement with those findings. Despite having only three dense lightcurves and some sparse data from the AstDyS-2 site, we were able to create a preliminary shape model with a sidereal rotational period of 8.63422 ± 0.0001 h.

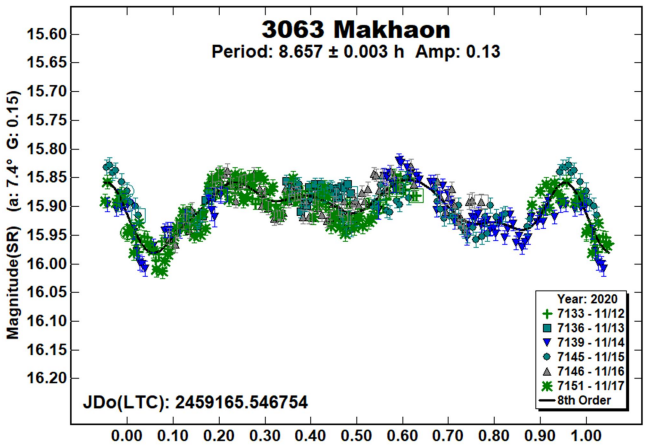

Number	Name	2020 mm/dd	Phase	L_{PAB}	B_{PAB}	Period(h)	P.E.	Amp	A.E.
1583	Antilochus	10/15-10/20	2.3,2.2	25	10	15.87	0.02	0.10	0.01
2456	Palamedes	11/18-11/20	10.4,10.6	358	9	7.249	0.005	0.28	0.02
2920	Automedon	10/11-10/14	4.2,4.5	8	16	10.206	0.003	0.42	0.02
3063	Makhaon	11/12-11/17	7.4,8.0	12	13	8.657	0.003	0.13	0.01
3709	Polypoites	10/29-11/11	9.2,10.3	345	6	9.979	0.004	0.07	0.02
3793	Leonteus	10/21-10/23	4.9,5.2	5	6	5.622	0.004	0.17	0.02

Table II. Observing circumstances and results. The phase angle is given for the first and last date. If preceded by an asterisk, the phase angle reached an extrema during the period. L_{PAB} and B_{PAB} are the approximate phase angle bisector longitude/latitude at mid-date range (see Harris et al., 1984).

3709 Polypoites. We have observed this Trojan six times in the past (Stephens and Warner, 2020; and references within). The result from the 2020 data is a little faster than these previous findings, no doubt noise from the nearly flat, four extrema lightcurve. Even with this slightly different period, we were able to use our seven dense lightcurves to create a preliminary shape model with a sidereal rotational period of 10.037046 ± 0.00001 h.

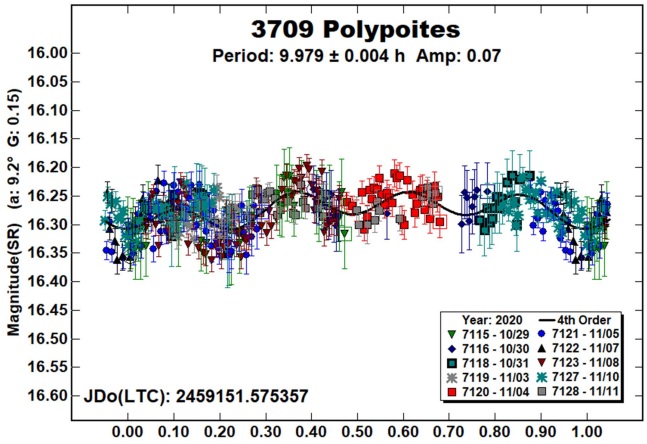

3793 Leonteus. This is another L_4 Trojan that we have observed six times in the past (Stephens and Warner, 2020; and references therein). Adding our seventh dense lightcurve allowed us to create a preliminary shape model with a sidereal rotational period of 5.621931 ± 0.0001 h.

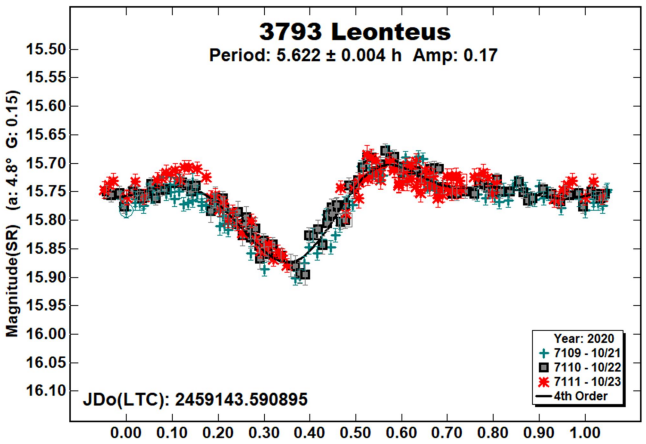

Acknowledgements

Observations at CS3 and continued support of the asteroid lightcurve database (LCDB; Warner et al., 2009) are supported by NASA grant 80NSSC18K0851. This work includes data from the Asteroid Terrestrial-impact Last Alert System (ATLAS) project. ATLAS is primarily funded to search for near earth asteroids through NASA grants NN12AR55G, 80NSSC18K0284, and 80NSSC18K1575; byproducts of the NEO search include images and catalogs from the survey area. The ATLAS science products have been made possible through the contributions of the University of Hawaii Institute for Astronomy, the Queen's University Belfast, the Space Telescope Science Institute, and the South African Astronomical Observatory. The purchase of a FLI-1001E CCD camera was made possible by a 2013 Gene Shoemaker NEO Grants from the Planetary Society.

References

AstDyS-2 (2020) Asteroids – Dynamic Site. *https://newton.spacedys.com/astdys/*

Asteroid Lightcurve Data Exchange Format Database (ALCDEF). *http://www.alcdef.org/*

French, L.M.; Stephens, R.D.; Lederer, S.M.; Coley, D.R.; Rhol, D.A. (2011). "Preliminary Results from a Study of Trojan Asteroids." *Minor Planet Bull.* **38**, 116-120.

Harris, A.W.; Young, J.W.; Scaltriti, F.; Zappala, V. (1984). "Lightcurves and phase relations of the asteroids 82 Alkmene and 444 Gyptis." *Icarus* **57**, 251-258.

Harris, A.W.; Young, J.W.; Bowell, E.; Martin, L.J.; Millis, R.L.; Poutanen, M.; Scaltriti, F.; Zappala, V.; Schober, H.J.; Debehogne, H.; Zeigler, K.W. (1989). "Photoelectric Observations of Asteroids 3, 24, 60, 261, and 863." *Icarus* **77**, 171-186.

Kassalainen, M.; Torppa J. (2001). "Optimization Methods for Asteroid Lightcurve Inversion. I. Shape Determination." *Icarus* **153**, 24-36.

Kassalainen, M.; Torppa J.; Muinonen, K. (2001). "Optimization Methods for Asteroid Lightcurve Inversion. II. The Complete Inverse Problem." *Icarus* **153**, 37-51.

Mottola, S.; Di Martino, M.; Erikson, A.; Gonano-Beurer, M.; Carbognani, A.; Carsenty, U.; Hahn, G.; Schober, H.; Lahulla, F.; Delbò, M.; Lagerkvist, C. (2011). "Rotational Properties of Jupiter Trojans. I. Light Curves of 80 Objects." *Astron. J.* **141**, A170.

Stephens, R.D. (2010). "Trojan Asteroids Observed from GMARS and Santana Observatories: 2009 October - December." *Minor Planet Bull.* **37**, 47-48.

Stephens, R.D.; Coley, D.R.; Warner, B.D.; French, L.M. (2016). "Lightcurves of Jovian Trojan Asteroids from the Center for Solar System Studies: L4 Greek Camp and Spies." *Minor Planet Bull*. **43**, 323-331.

Stephens, R.D.; Warner, B.D. (2020). "Lightcurve Analysis of L4 Trojan Asteroids at the Center for Solar System Studies: 2019 July To September." *Minor Planet Bull*. **47**, 43-47.

Tonry, J.L.; Denneau, L.; Flewelling, H.; Heinze, A.N.; Onken, C.A.; Smartt, S.J.; Stalder, B.; Weiland, H.J.; Wolf, C. (2018). "The ATLAS All-Sky Stellar Reference Catalog." *Astrophys. J.* **867**, A105.

Warner, B.D.; Harris, A.W.; Pravec, P. (2009). "The Asteroid Lightcurve Database." *Icarus* **202**, 134-146. Updated 2020 Oct. *http://www.minorplanet.info/lightcurvedatabase.html*

CALL FOR OBSERVATIONS

Frederick Pilcher
4438 Organ Mesa Loop
Las Cruces, NM 88011 USA
fpilcher35@gmail.com

Observers who have made visual, photographic, or CCD measurements of positions of minor planets in calendar year 2020 are encouraged to report them to this author on or before 2021 April 1. This will be the deadline for receipt of reports, for which results can be included in the "General Report of Position Observations for 2020," to be published in *MPB* Vol. 48, No. 3.

NEAR-EARTH ASTEROID LIGHTCURVE ANALYSIS AT THE CENTER FOR SOLAR SYSTEM STUDIES: 2020 SEPTEMBER TO 2021 JANUARY

Brian D. Warner
Center for Solar System Studies / MoreData!
446 Sycamore Ave.
Eaton, CO 80615 USA
brian@MinorPlanetObserver.com

Robert D. Stephens
Center for Solar System Studies / MoreData!
Rancho Cucamonga, CA

(Received: 2021 Jan 10)

Lightcurves of 22 Near-Earth asteroids (NEAs) obtained at the Center for Solar System Studies (CS3) from 2020 October to early 2021 January were analyzed for rotation period, peak-to-peak amplitude, and signs of satellites or tumbling.

CCD photometric observations of 22 near-Earth asteroids (NEAs) were made at the Center for Solar System Studies (CS3) from 2020 September to early 2021 January. Table I lists the telescopes and CCD cameras that were combined to make observations.

Up to nine telescopes can be used for the campaign, although seven is more common. All the cameras use CCD chips from the KAF blue-enhanced family and so have essentially the same response. The pixel scales ranged from 1.24-1.60 arcsec/pixel.

Telescopes	Cameras
0.30-m *f*/6.3 Schmidt-Cass	FLI Microline 1001E
0.35-m *f*/9.1 Schmidt-Cass	FLI Proline 1001E
0.40-m *f*/10 Schmidt-Cass	SBIG STL-1001E
0.40-m *f*/10 Schmidt-Cass	
0.50-m *f*/8.1 Ritchey-Chrétien	

Table I. List of available telescopes and CCD cameras at CS3. The exact combination for each telescope/camera pair can vary due to maintenance or specific needs.

All lightcurve observations were unfiltered since a clear filter can cause a 0.1-0.3 mag loss. The exposure duration varied depending on the asteroid's brightness and sky motion. Guiding on a field star sometimes resulted in a trailed image for the asteroid.

Measurements were made using *MPO Canopus*. The Comp Star Selector utility in *MPO Canopus* found up to five comparison stars of near solar-color for differential photometry. To reduce the number of times and amounts of adjusting nightly zero points, we use the ATLAS catalog r′ (SR) magnitudes (Tonry et al., 2018). Those adjustments are usually ≤ ±0.03 mag. The rare greater corrections may have been related in part to using unfiltered observations, poor centroiding of the reference stars, and not correcting for second-order extinction. Another cause may be selecting what appears to be a single star but is actually an unresolved pair.

The Y-axis values are ATLAS SR "sky" (catalog) magnitudes. The two values in the parentheses are the phase angle (a) and the value of *G* used to normalize the data to the comparison stars used in the earliest session. This, in effect, had all the observations made at a single fixed date/time and phase angle, leaving any variations due only to the asteroid's rotation and/or albedo

changes. The X-axis shows rotational phase from –0.05 to 1.05. If the plot includes the amplitude, e.g., "Amp: 0.65", this is the amplitude of the Fourier model curve and *not necessarily the adopted amplitude for the lightcurve*.

2212 Hephaistos. The estimated diameter for this NEA is 5.54 km (Mainzer et al., 2016). Pravec et al. (1997) reported a period of >20 h but the result was considered unreliable. Our data led to two probable results near 16 h and 48 h when using a second-order fit. We adopted a period of 48 h with a bimodal lightcurve based on the presumed amplitude of about 0.35 mag, which makes a bimodal lightcurve more likely than not (Harris et al., 2014) and because the slopes of the data agreed with the slopes of the Fourier model curve.

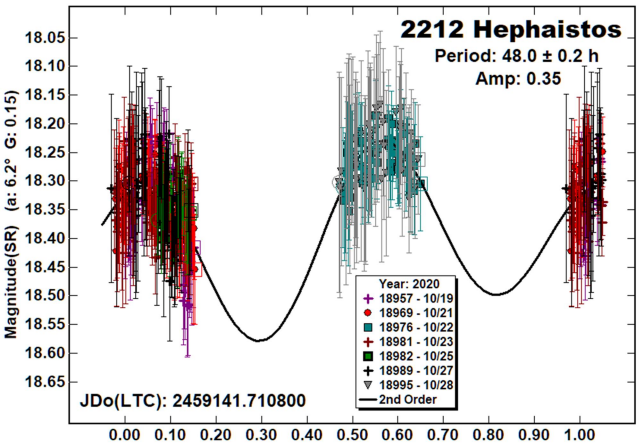

2368 Beltrovata. Pál et al. (2020) used TESS data to find a period of 5.793 h. Our result confirms their finding.

The 6th-order Fourier curve gave a good approximate peak-to-peak amplitude of 0.91 mag, but fell short of the bottom of the second minimum at 0.65 rotation phase by about 0.1 mag, giving a false impression of asymmetry in the lightcurve. In reality, the two minimums are actually close to the same depth. Lightcurves using higher order fits had too many artificial deviations from a smooth curve as the Fourier analysis locked onto noise.

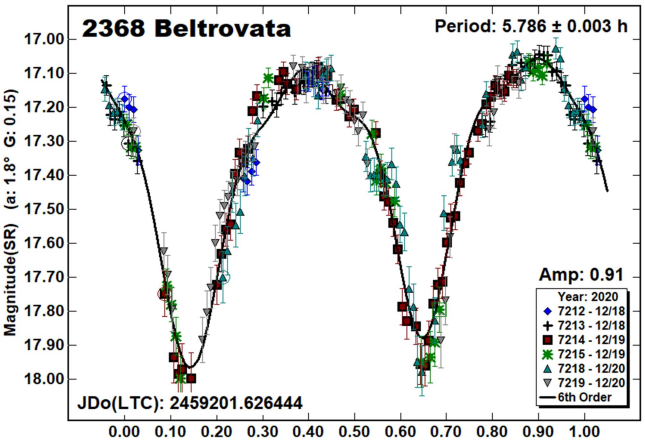

(7753) 1988 XB. There were no previously reported periods in the LCDB for this 560-m NEA. The high phase angle helped produce a somewhat unusual shape. Despite that and the incomplete coverage, we have high confidence in the result.

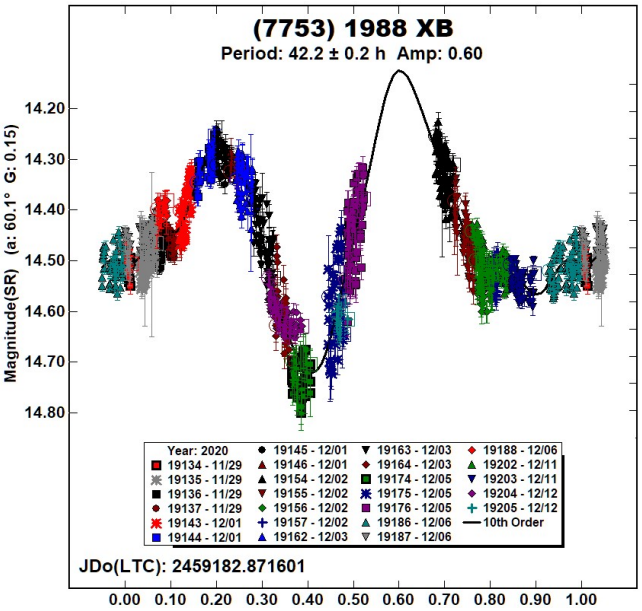

(10115) 1992 SK. This 1-km NEA has been worked numerous times before, e.g., Pravec et al. (1999web, 7.328 h) and Polishook (2012, 7.31 h). The first time we observed 1992 SK was in 2013 November (Warner, 2014), which led to a period of 7.323 h. Our most recent result is in good agreement with the previous works.

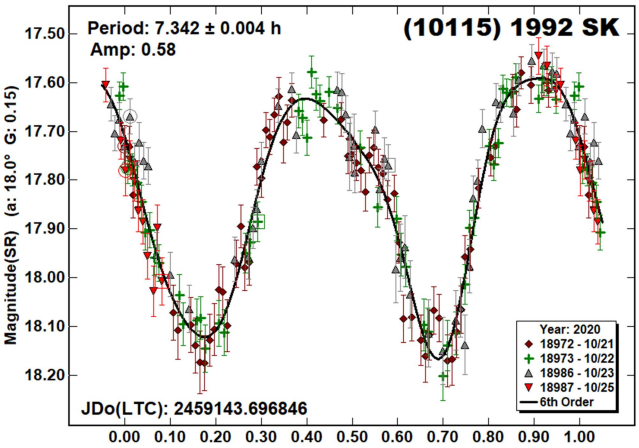

(16834) 1997 WU22. Pravec et al. (2000web) found a period of 9.345 h using data from 2000 August. Vaduvescu et al. (2017) reported 9.36 h. This is the fourth time the asteroid has been observed at CS3. The three previous results were Stephens (2013web, 9.374 h), Warner (2017a, 9.343 h), and Warner and Stephens (2019, 9.348 h).

Source	α°	L_{PAB}	Amp	$Amp_{0°}$
Pravec et al. (2000web)	59	300	0.38	0.14
Stephens (2013web)	5	66	0.29	0.25
Vaduvescu et al. (2017)	58	300	0.48	0.18
Warner (2017a)	77	274	0.60	0.26
Warner and Stephens (2019)	27	21	0.63	0.35
This work	6	53	0.31	0.26

Table II. A comparison of amplitudes versus phase angle at different phase angle bisector longitudes for (16834). Amp is the measured amplitude of the lightcurve. $Amp_{0°}$ is the derived magnitude at 0° phase angle (Zappala et al., 1990).

An accurate comparison of amplitudes versus phase angle bisector longitude (L_{PAB}) requires reducing the amplitudes to a fixed phase angle, usually 0° by using the formula from Zappala et al. (1990):

$$A_{0^\circ} = A_a/(1 + ma)$$

Where α is the phase angle of the observations and *m* is a value based on taxonomic type. Assuming type S, the case for most NEAs, *m* = 0.030.

From Table II, a few suppositions can be made. The observations near L_{PAB} = 300° show the lowest adjusted amplitudes. From this, it can be assumed that the pole of the asteroid has an ecliptic longitude near 300° (or 120°). Since the adjusted amplitudes show a significant, though not extreme, range, the pole of the spin axis is moderately inclined from the ecliptic plane. Assuming the observations by Warner and Stephens (2019) were at a nearly equatorial view of the asteroid, then the *a/b* ratio of a smoothed triaxial ellipsoid is *a/b* ~ 1.38. Proper lightcurve inversion analysis is required to confirm the veracity of these results.

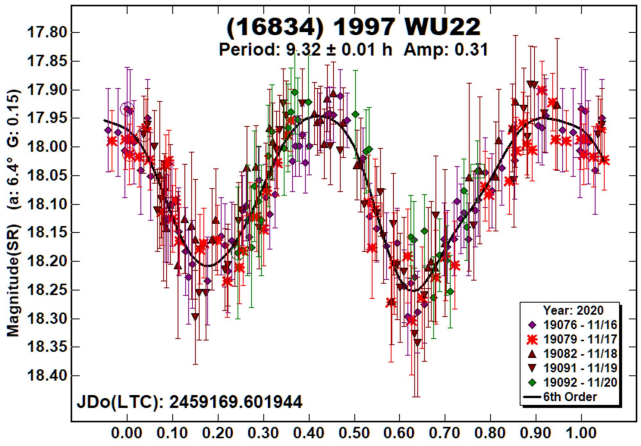

21088 Chelyabinsk. Pravec et al. (2002web) found a period of 22.49 h and *A* > 0.13 mag. They followed up in 2014 (Pravec et al., 2014), finding a period of 22.426 but could not put a firm cap on the amplitude.

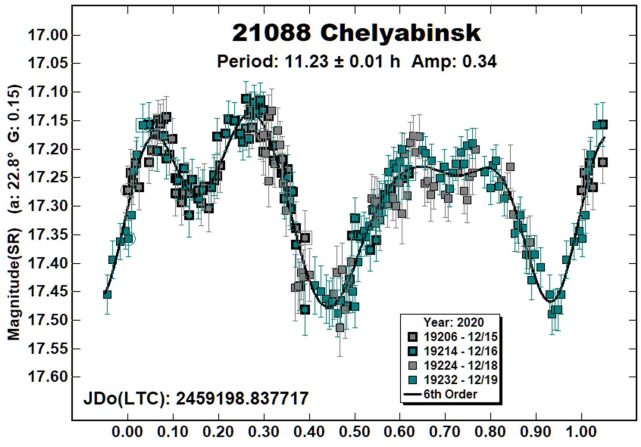

Our data from long nights in 2020 December allowed following the lightcurve for a large portion of its lightcurve, if adopting our period of 11.23 h. Given the amplitude and modest phase angle, the bimodal solution seems secure (Harris et al., 2014). More so, the asymmetry of the two halves of the lightcurve led us to reject the nearly double-period found by Pravec et al (2014).

(66272) 1999 JW6. There were no previous rotation periods listed in the LCDB. Mainzer et al. (2016) estimated the effective diameter to be 750 ± 350 m. Using *H* = 17.1, they found an albedo of p_V = 0.453. This is unusually high for an NEA (Warner et al., 2009) but several other NEAs in the LCDB have similar values.

Initial analysis of the observations offered the possibility that the asteroid might be a member of the very wide binary asteroids (see Warner, 2016; and Jacobson et al., 2014). As more data became available, the more probable interpretation was that the asteroid was tumbling.

MPO Canopus is not able to handle tumbling asteroids correctly since it cannot perform a simultaneous dual-period search. The best it could do in this case was find the most dominant period in the data set and then, using an iterative dual-period search, find the dominant period after subtracting the first period. This led to finding periods of P_1 = 502 h and P_2 = 401 h.

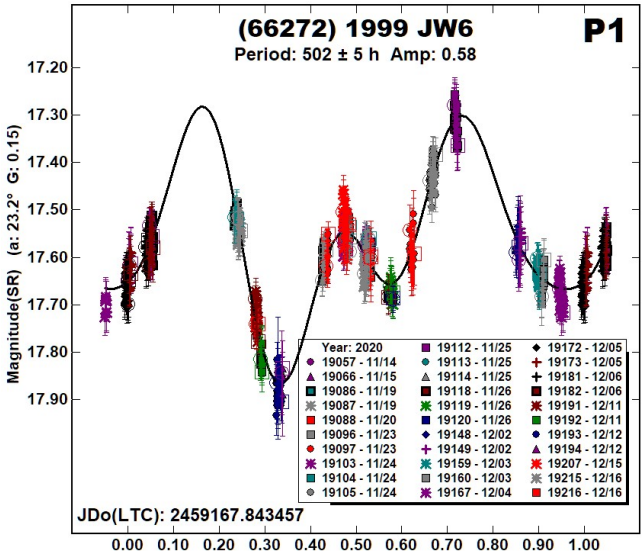

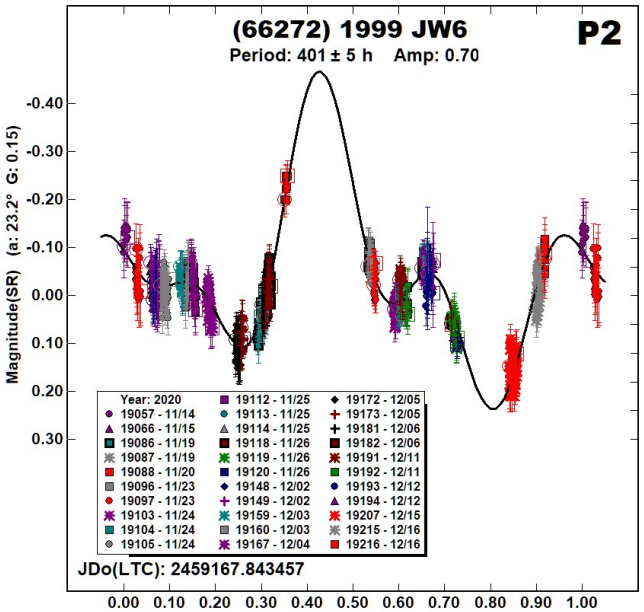

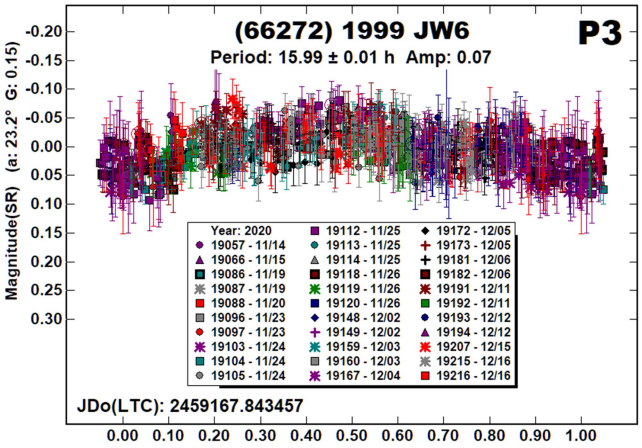

While not obvious from the lightcurves, the slope of the data in various sessions closely matches the slope of the Fourier curve; this lends at least some support for the derived periods. However, as with many tumbling asteroids, the two periods may not be the true periods of rotation and precession but are related to them by integral multiples of frequency, i.e., 1/*P*.

After find the two periods, there were still some residuals that led to a third period of 15.99 h. This is almost exactly 2/3 of an Earth day and could easily be the result of systematic errors and the sampling of the lightcurve at fixed intervals of about 24 hours.

Using the rules of thumb for tumbling damping time (Pravec et al., 2014; 2005), the diameter and periods make this a good candidate for tumbling, which lends further support to the results.

(68359) 2001 OZ13. Pál et al. (2020) found a period of 2.9103 h. Our data were extremely noisy. Even so, we could not find a period near 2.9, as shown in the period spectrum. We do not have high confidence in the result. The next favorable apparition is in 2023 January when the asteroid will be V ~ 16.7 at +37° declination.

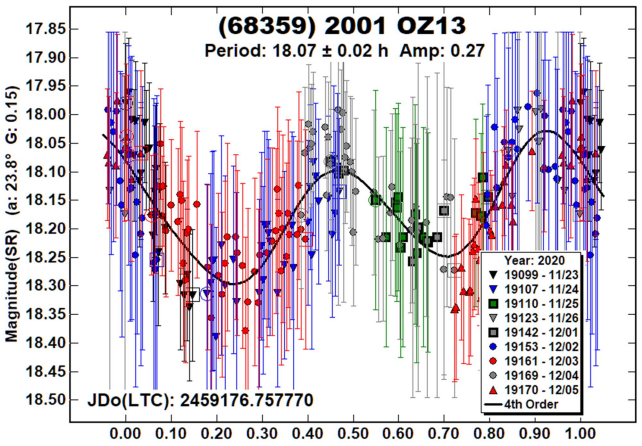

69230 Hermes. Pravec et al. (2003web) and Margot et al. (2003) reported this to be a binary asteroid. The radar observations by Margot et al. (2003) showed the asteroid to be "strongly bifurcated," being comprised to two bodies and "consistent with a rotating binary pair." They estimated the two bodies to have effective diameters of 300-450 m but they could not fully constrain the period (13-21 h). Pravec et al. (2003web) were able to find a period of 13.894 h. Those 2003 observations and results were the last to be reported in the LCDB for a rotation period.

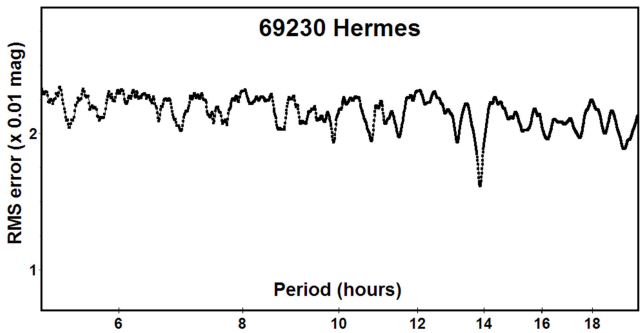

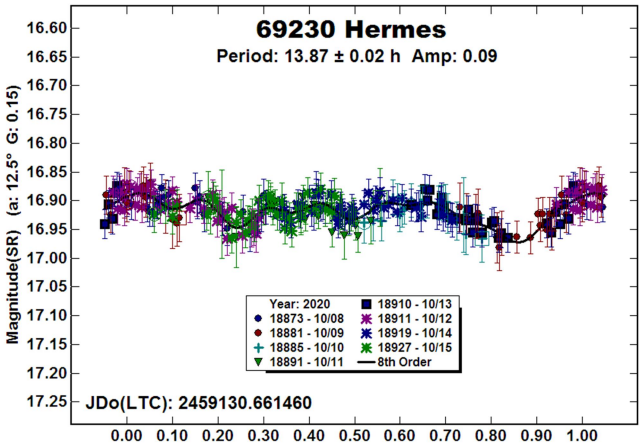

Our observations some 17 years later confirm the original period and, as in 2003, a very low amplitude. This is not surprising since the 2003 and 2020 observations were at nearly the same viewing aspect (L_{PAB} = 10° ± 10°).

(144411) 2004 EW9. Pravec et al. (2004web) found a period of 49.94 h based on data from 2004 October. Behrend (2020web) found 51.150 h. Our result of 50.0 h, based on incomplete coverage, is in good agreement. We assumed a bimodal lightcurve because of the large amplitude and relatively low phase angle (Harris et al., 2014).

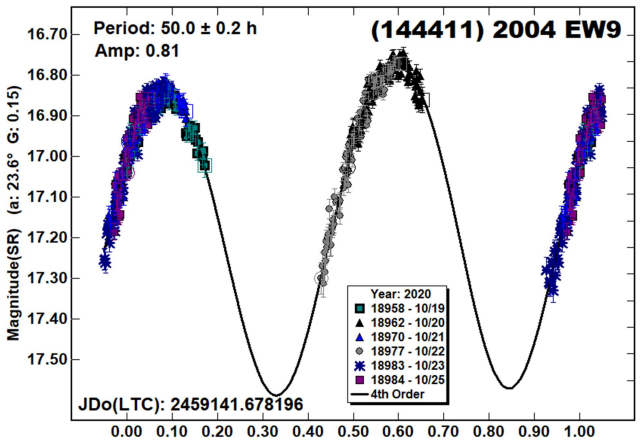

(153201) 2000 WO107. The lightcurve for this 400-m NEA changed significantly over the short time it was observed (2020 Dec 6-12). Analysis was best done by subdividing the data set.

The combined lightcurve shows the derived period assuming a fixed synodic period. However, the individual lightcurves for Dec 6, 11, and 12 distinctly show how the shape and depth of the shallower minimum evolved and that the synodic period was not fixed. This is expected when the viewing aspect and and/or viewing aspect (L_{PAB}) change significantly over the range of the data set.

The high-order fits were required to get to the bottom of the deep minimum.

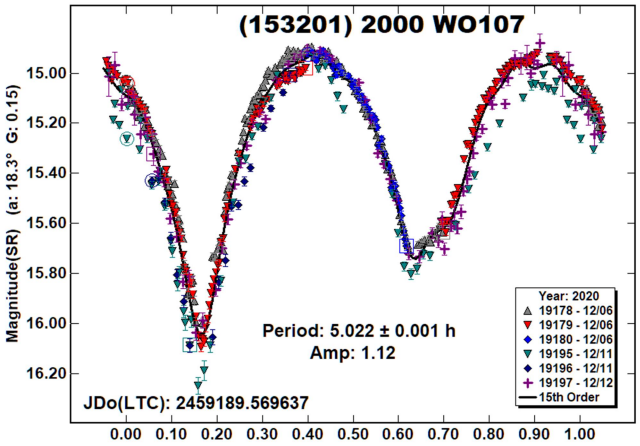

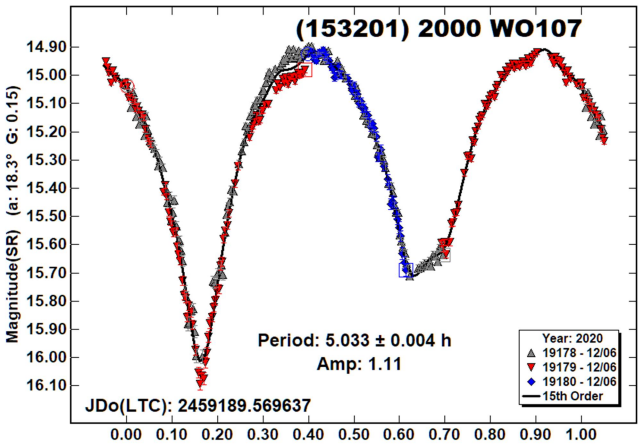

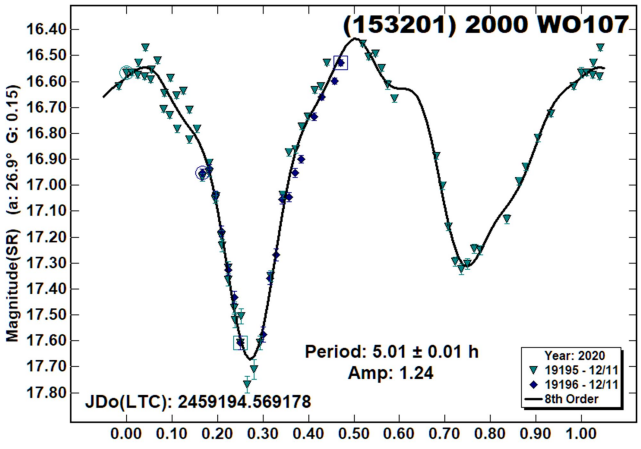

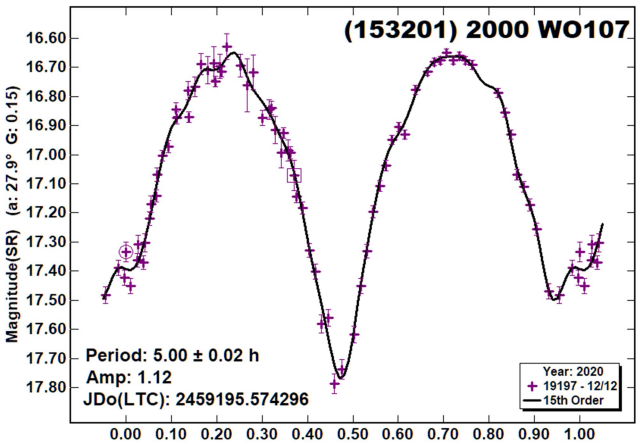

(154302) 2002 UQ3. Other than Binzel et al. (2019) reporting this 900-m NEA to be taxonomic class Sq, there were no previous entries in the LCDB. Assuming our adopted period of 4.328 h is correct, we were able to capture most of the lightcurve during each observing run. The amplitude and phase angle do not automatically preclude solutions other than a bimodal lightcurve (Harris et al., 2014). However, the very slight asymmetry in our result would seem to exclude a monomodal solution.

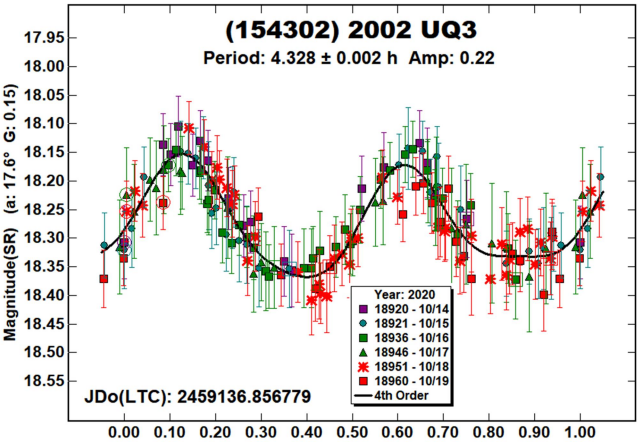

(159402) 1999 AP10. We (Warner and Stephens, 2021) previously reported the possibility that this asteroid is either binary or, at the least, has some physical trait that produces a second period beyond the dominant one near 7.9 h. The previous results are in Table III but their plots are not included here.

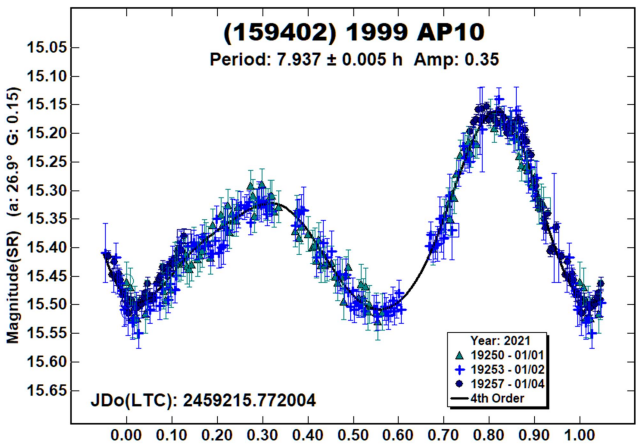

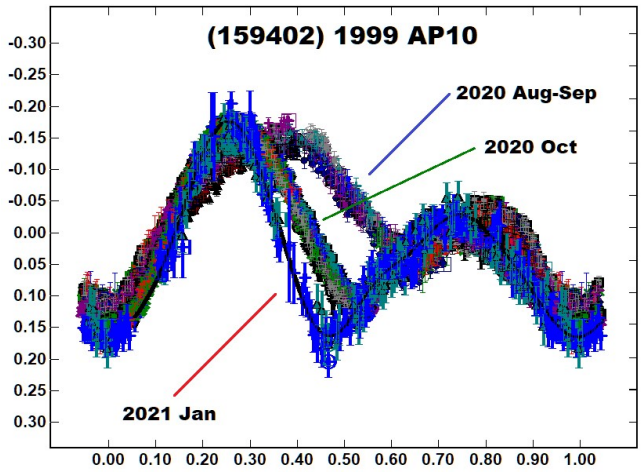

The main point of interest is that the amplitude of the secondary lightcurve diminished as the phase angle rose from 11° to 30° and, more important, the L_{PAB} changed by more than 30 degrees. The shape also changed, being much better defined in late August to early September than in early October.

Given this, when we reobserved the asteroid in early 2021 January, it was not surprising that any indications of a secondary period were not found, or were hidden within the noise. Our period (7.937 h) from the most recent observations closely agrees with the earlier results when accounting for changes in the synodic-sidereal difference over the span of the observations.

A composite of the three primary period solutions that forced the lowest minimum to 0° rotation phase provides a dramatic picture of the lightcurve evolution.

(163902) 2003 SW222. There were no previous reports of a period in the LCDB for this NEA with an estimated diameter of 1 km.

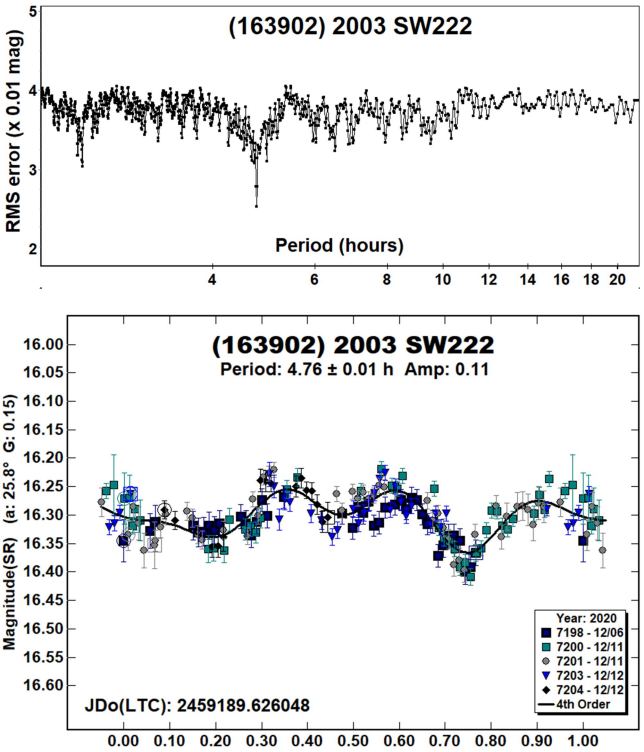

The Fourier analysis locked onto a seemingly clear solution of 4.76 h. However, the somewhat noisy data, especially compared to the low amplitude, makes this solution useable but hardly secure.

(275714) 2000 YH4. There were no previous entries in the LCDB of any kind for 2000 YH4, which has an effective diameter of 500-600 m. We consider the solution to be secure, but additional observations are encouraged. The 2022 June apparition (V ~ 18.5) is the only one with V < 19 until 2031.

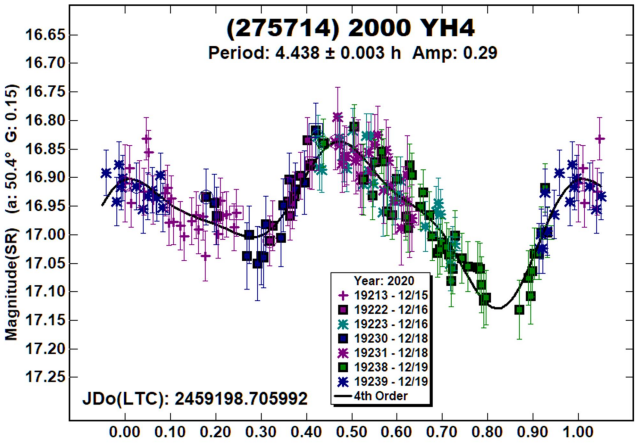

(465749) 2009 WO6. Mainzer et al. (2016) found this to be an usually low albedo object among the NEA population, p_V 0.034. Using H = 17.3, they found a diameter of 2.49 km. Our data set was obtained over 10 days in 2020 November but was not able to fully cover the presumed bimodal lightcurve with a period of 86.2 h. Based on Harris et al. (2014), a bimodal lightcurve is virtually assured.

Using the rule of thumb for the damping time for a tumbling asteroid (Pravec et al., 2005; 2014), i.e., to go from tumbling to single axis rotation, the period leads to a time considerably greater than the age of the Solar System. The shape of the lightcurve, where the slope of some sessions doesn't match the slope of the Fourier model curve, would suggest that the asteroid is in a low-level tumbling state.

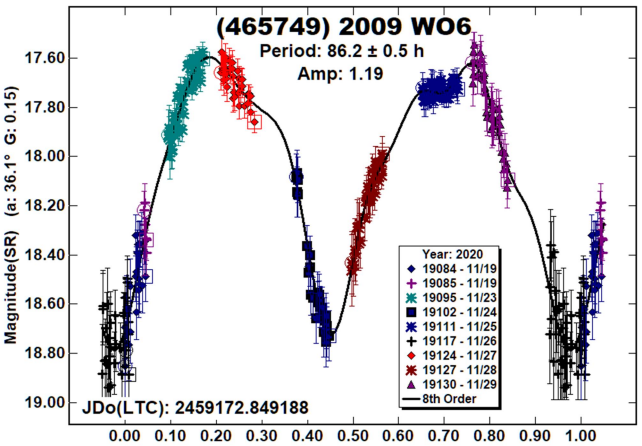

(474179) 1999 VS6. Warner (2017b) found a period of 16.91 h using data from 2017. Our 2020 data set led to a shorter period of 15.88 h, which we consider to be significantly more likely than the one from 2017 since that solution had large gaps in the lightcurve and the data had much higher noise.

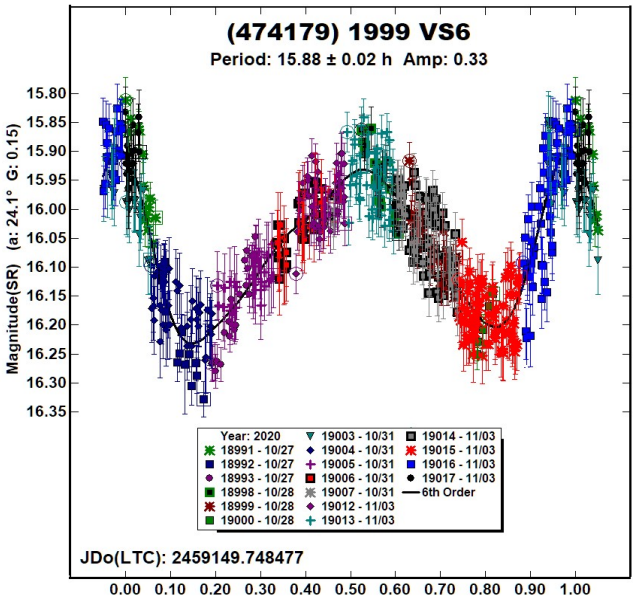

2000 TU28. There were no previous entries in the LCDB for 2000 TU28, which has an estimated diameter of 200 m. This is close to the approximate point of about 170 m when the rotation period can easily be < 2 h. This NEA is completely contrary in that regard. The large amplitude and phase angle assure a bimodal solution (Harris et al., 2014). The main issues were tying the sessions together over the period of ten days and the fact that each one covered only a short segment of the lightcurve. This is where the ATLAS catalog (Tonry et al., 2018) proved to be essential since the systematic errors are on the order of ±0.03 mag and less. This meant leaving the zero points alone (0.0 mag offset) and waiting until a good portion of the lightcurve was covered. In the end, all zero-point adjustments were ≤ ±0.03 mag.

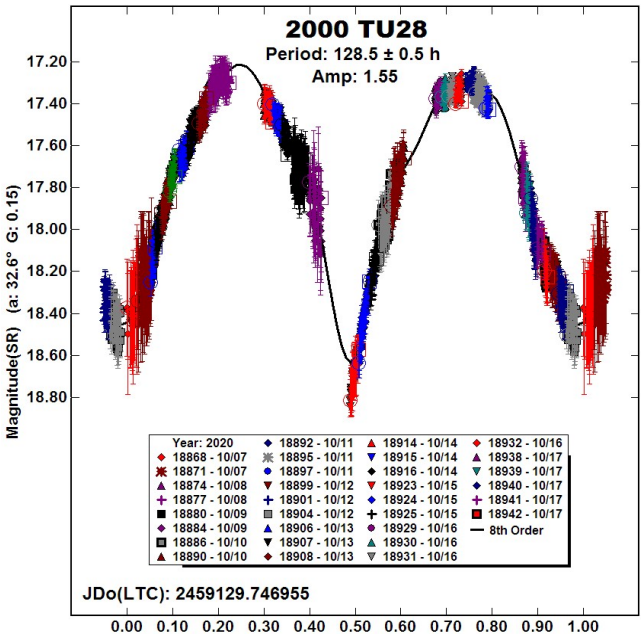

The shorter tumbling damping times in Pravec et al. (2014) would favor this being in a tumbling state. The longer times found in Pravec et al. (2005) allow for a damping time a little less than the age of the Solar System. There don't appear to be clear signs of even low-level tumbling but it cannot be formally excluded.

2002 GZ8. This was the first entry of any kind into the LCDB. The solution is considered secure and there don't appear to be any signs of tumbling, which fits the rule of thumb for longer damping times found in Pravec et al. (2005).

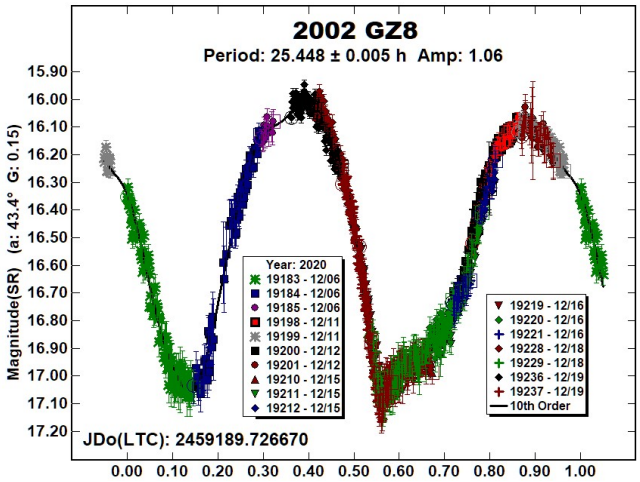

2003 YJ. This is good demonstration of "beating down the noise" to find a good solution in what might otherwise be a marginal data set. We consider the solution to be secure, but verification is warranted. A reasonable chance doesn't come again until 2029 December when the asteroid will be V ~ 16.4 and +28° declination.

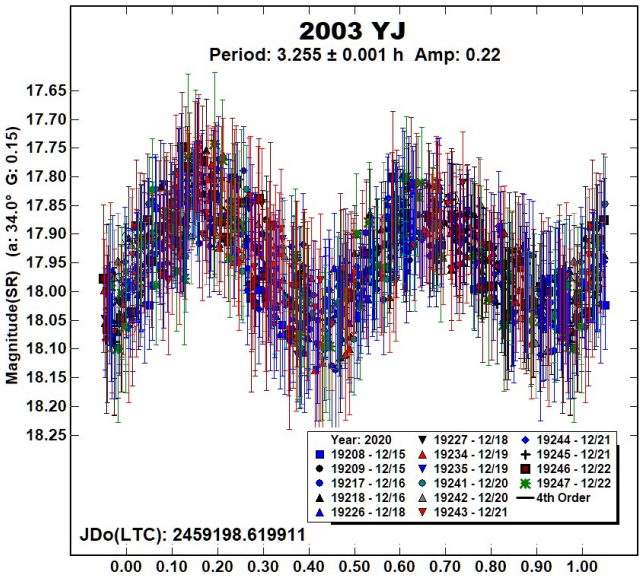

2013 UX14. There were no previous entries in the LCDB. The estimated diameter of this NEA is 650 m. There are gaps in the coverage and some of the data runs have noisy data, but we still consider the solution to be secure since no other period that was examined produced a plausible lightcurve shape.

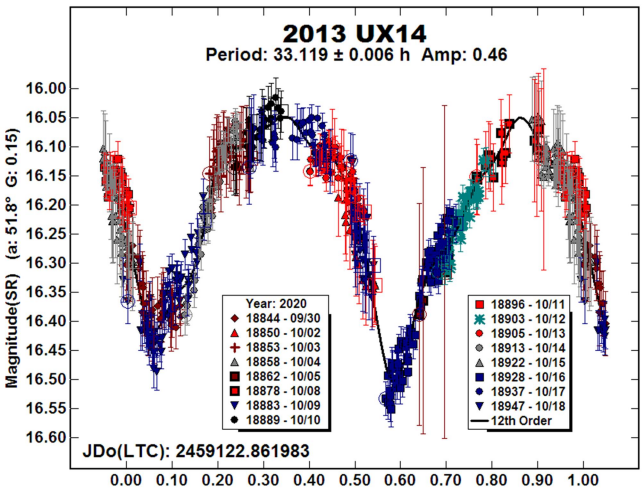

2020 ST1. If ever an asteroid showed clear signs of tumbling from the start of observations, 2020 ST1 was it. Each run covered more than what appeared to be a full cycle but the data could not be fit to a single period with a plausible lightcurve, even when using only one night's observations, as seen with the individual lightcurves for Nov 13-15.

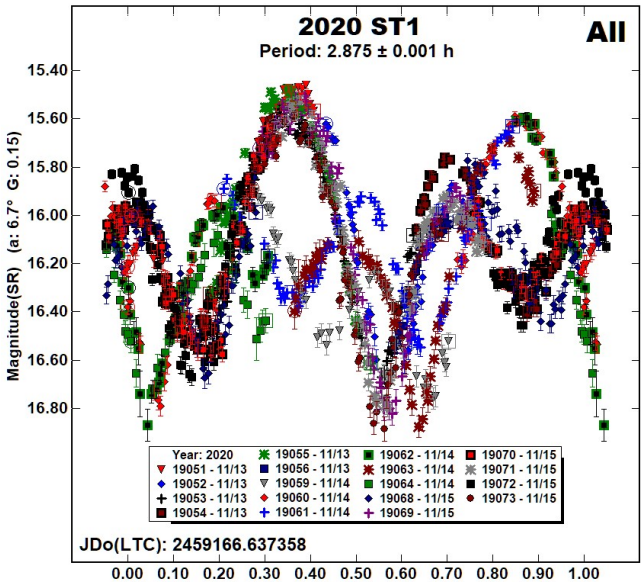

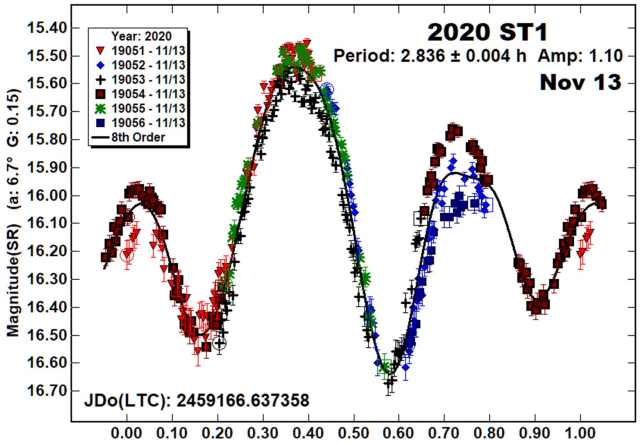

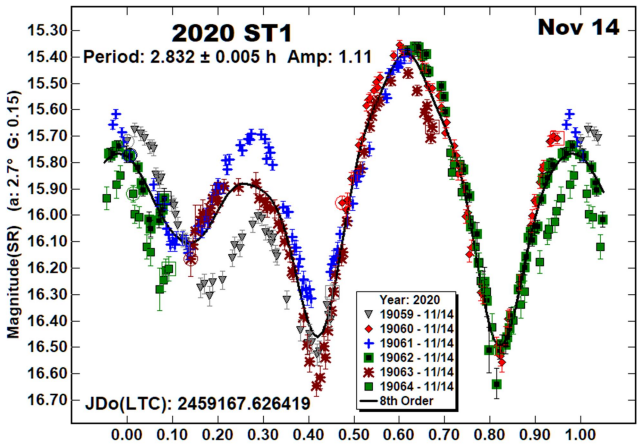

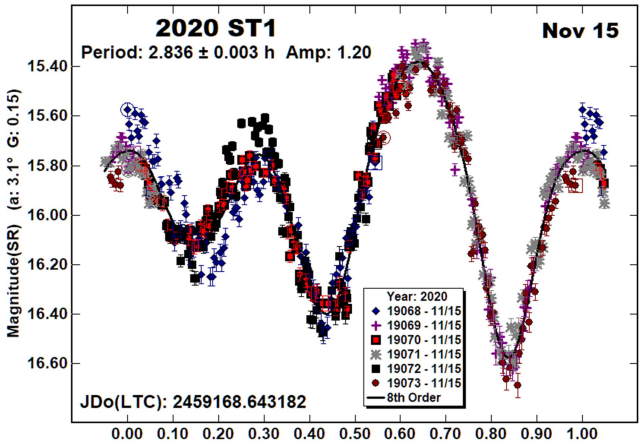

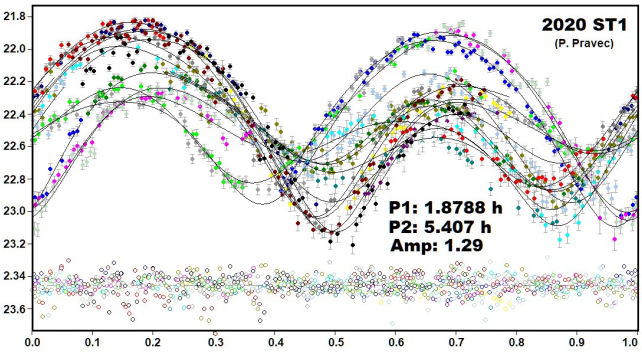

The data from Nov 13 came the closes to fitting a single period but the lightcurve had three extrema pairs. Given the amplitude and low phase angle, this was highly unlikely (Harris et al, 2014). The Nov 14 data set led the worst fit to a single period while the set from Nov 15 almost fit a single, but implausible, period.

MPO Canopus cannot properly handle the data from a tumbling asteroid since it does not do a simultaneous search for two periods. To have any chance of finding the true periods of precession and rotation, the complete data set was sent to Petr Pravec for his analysis. He confirmed the tumbling state (private communications):

> *My full 2-period Fourier series analysis shows [the] following three periods with the highest signal: 1.879, 2.879 and 5.407 h. Two of the three are real periods of the tumbler, while a third one is related to them; note that 1/2.879 = 1/1.879 - 1/5.407. However, we cannot resolve which two of the three are the real ones based just on this analysis. … future physical modeling may reveal it.*

His plot shows the two stronger periods of 1.879 h and 5.407 h and how confused lightcurves can be with a tumbling asteroid since the lightcurve almost never repeats itself. It can come close, as on Nov 13 and 15, but those are unlikely solutions, even though they are each close to the period of 2.879 h found by Pravec.

Acknowledgements

Funding for observations at CS3 and work on the asteroid lightcurve database (Warner et al., 2009) and ALCDEF database (*alcdef.org*) are supported by NASA grant 80NSSC18K0851.

The authors gratefully acknowledge Shoemaker NEO Grants from the Planetary Society (2007, 2013). These were used to purchase some of the telescopes and CCD cameras used in this research.

This work includes data from the Asteroid Terrestrial-impact Last Alert System (ATLAS) project. ATLAS is primarily funded to search for near earth asteroids through NASA grants NN12AR55G, 80NSSC18K0284, and 80NSSC18K1575; byproducts of the NEO search include images and catalogs from the survey area. The ATLAS science products have been made possible through the contributions of the University of Hawaii Institute for Astronomy, the Queen's University Belfast, the Space Telescope Science Institute, and the South African Astronomical Observatory.

References

References from web sites should be considered transitory, unless from an agency with a long lifetime expectancy. Sites run by private individuals, even if on an institutional web site, do not necessarily fall into this category.

Behrend, R. (2020web). Observatoire de Geneve web site. *http://obswww.unige.ch/~behrend/page_cou.html*

Binzel, R.P.; DeMeo, F.E.; Turtelboom, E.V.; Bus, S.J.; Tokunaga, A.; Burbine, T.H.; Lantz, C.; Polishook, D.; Carry, B.; Morbidelli, A.; Birlan, M.; Vernazza, P.; Burt, B.J.; Moskovitz, N.; Slivan, S.M.; Thomas, C.A.; Rivkin, A.S.; Hicks, M.D.; Dunn, T.; Reddy, V. (2019). "Compositional distributions and evolutionary processes for the near-Earth object population: Results from the MIT-Hawaii Near-Earth Object Spectroscopic Survey (MITHNEOS)." *Icarus* **324**, 41-76.

Harris, A.W.; Young, J.W.; Scaltriti, F.; Zappala, V. (1984). "Lightcurves and phase relations of the asteroids 82 Alkmene and 444 Gyptis." *Icarus* **57**, 251-258.

Harris, A.W.; Pravec, P.; Galad, A.; Skiff, B.A.; Warner, B.D.; Vilagi, J.; Gajdos, S.; Carbognani, A.; Hornoch, K.; Kusnirak, P.; Cooney, W.R.; Gross, J.; Terrell, D.; Higgins, D.; Bowell, E.; Koehn, B.W. (2014). "On the maximum amplitude of harmonics on an asteroid lightcurve." *Icarus* **235**, 55-59.

Jacobson, S.A., Scheeres, D.J., McMahon, J. (2014). "Formation of the Wide Asynchronous Binary Asteroid Population." *Ap. J.* **780,** A60.

Mainzer, A.K.; Bauer, J.M.; Cutri, R.M.; Grav, T.; Kramer, E.A.; Masiero, J.R.; Nugent, C.R.; Sonnett, S.M.; Stevenson, R.A.; Wright, E.L. (2016). "NEOWISE Diameters and Albedos V1.0." NASA Planetary Data System.
EAR-A-COMPIL-5-NEOWISEDIAM-V1.0.

Margot, J.L.; Nolan, M.C.; Negron, V.; Hine, A.A.; Campbell, D.B.; Howell, E.S.; Benner, L.A.M.; Ostro, S.J.; Giorgini, J.D.; Marsden, B.G. (2003). "1937 UB (Hermes)." *IAUC* **8227**.

Pál, A.; Szakáts, R.; Kiss, C.; Bódi, A.; Bognár, Z.; Kalup, C.; Kiss, L.L.; Marton, G.; Molnár, L.; Plachy, E.; Sárneczky, K.; Szabó, G.M.; Szabó, R. (2020). "Solar System Objects Observed with TESS - First Data Release: Bright Main-belt and Trojan Asteroids from the Southern Survey." *Ap. J. Supl. Ser.* **247**, id.26.

Polishook, D. (2012). "Lightcurves and Spin Periods of Near-Earth Asteroids, The Wise Observatory, 2005 - 2010." *Minor Planet Bull*. **39**, 187-192.

Pravec, P.; Wolf, M.; Šarounová, L.; Mottola, S.; Erickson, A.; Hahn, G.; Harris, A.W.; Harris, A.W.; Young, J.W. (1997). "The Near-Earth Objects Follow-Up Program." *Icarus* **130**, 275-286.

Pravec, P.; Wolf, M.; Sarounova, L. (1999web; 2000web; 2002web; 2003web; 2004web).
http://www.asu.cas.cz/~ppravec/neo.htm

Pravec, P.; Harris, A.W.; Scheirich, P.; Kušnirák, P.; Šarounová, L.; Hergenrother, C.W.; Mottola, S.; Hicks, M.D.; Masi, G.; Krugly, Yu.N.; Shevchenko, V.G.; Nolan, M.C.; Howell, E.S.; Kaasalainen, M.; Galád, A.; Brown, P.; Degraff, D.R.; Lambert, J.V.; Cooney, W.R.; Foglia, S. (2005). "Tumbling asteroids." *Icarus* **173**, 108-131.

Pravec, P.; Scheirich, P.; Durech, J.; Pollock, J.; Kusnirak, P.; Hornoch, K.; Galad, A.; Vokrouhlicky, D.; Harris, A.W.; Jehin, E.; Manfroid, J.; Opitom, C.; Gillon, M.; Colas, F.; Oey, J.; Vrastil, J.; Reichart, D.; Ivarsen, K.; Haislip, J.; LaCluyze, A. (2014). "The tumbling state of (99942) Apophis." *Icarus* **233**, 48-60.

Stephens, R.D. (2013web). Center for Solar System Studies web site. *http://www.planetarysciences.org/PHP/CS3_Lightcurves.php*

Tonry, J.L.; Denneau, L.; Flewelling, H.; Heinze, A.N.; Onken, C.A.; Smartt, S.J.; Stalder, B.; Weiland, H.J.; Wolf, C. (2018). "The ATLAS All-Sky Stellar Reference Catalog." *Ap. J.* **867**, A105.

Vaduvescu, O.; Macias, A.A; Tudor, V.; Predatu, M.; Galád, A.; Gajdoš, Š.; Világi, J.; Stevance, H.F.; Errmann, R.; Unda-Sanzana, E.; Char, F.; Peixinho, N.; Popescu, M.; Sonka, A.; Cornea, R.; Suciu, O.; Toma, R.; Santos-Sanz, P.; Sota, A.; Licandro, J. Serra-Ricart, M.; Morate, D.; Mocnik, T.; Diaz Alfaro, M.; Lopez-Martinez, F.; McCormac, J.; Humphries, N. (2017). "The EURONEAR Lightcurve Survey of Near-Earth Asteroids." *Earth, Moon, and Planets* **120**, 41-100.

Number	Name	2020 mm/dd	Phase	L_{PAB}	B_{PAB}	Period(h)	P.E.	Amp	A.E.
2212	Hephaistos	10/19-10/28	6.2,2.9	43	3	48	0.2	0.35	0.04
2368	Beltrovata	12/18-12/20	1.8,2.5	85	3	5.786	0.003	0.91	0.03
7753	1988 XB	11/29-12/12	60.5,18.2	96	1	42.2	0.2	0.65	0.05
10115	1992 SK	10/21-10/25	*18.0,15.8	36	9	7.342	0.004	0.58	0.04
16834	1997 WU22	11/16-11/20	6.4,6.9	53	10	9.32	0.01	0.31	0.03
21088	Chelyabinsk	12/15-12/19	22.8,21.1	124	5	11.23	0.01	0.34	0.03
66272	1999 JW6	11/14-12/20	*23.3,34.8	68	8	^{T1}502	5	0.58	0.05
						^{T2}401	5	0.4	0.1
						^{3}15.99	0.01	0.07	0.02
68359	2001 OZ13	11/23-12/05	23.9,30.7	44	-13	18.07	0.02	0.27	0.04
69230	Hermes	10/08-10/15	12.5,22.1	4	-5	13.82	0.02	0.08	0.01
144411	2004 EW9	10/19-10/25	23.6,18.7	47	15	50	0.2	0.81	0.05
153201	2000 WO107	12/06-12/12	18.8,28.1	62	3	5.022	0.001	1.22	0.05
154302	2002 UQ3	10/14-10/19	17.7,14.5	36	13	4.328	0.002	0.22	0.03
159402	*1999 AP10*	*08/24-09/17*	**11.3,12.4*	*341*	*-5*	*^{P}7.9219*	*0.0003*	*0.27*	*0.02*
						28.461	*0.006*	*0.06*	*0.01*
159402	*1999 AP10*	*10/02-10/07*	*26.3,32.9*	*356*	*9*	*^{P}7.9186*	*0.0004*	*0.33*	*0.02*
						29.30	*0.01*	*0.04*	*0.01*
159402	1999 AP10	01/04-01/04	24.4	112	18	7.937	0.005	0.35	0.02
163902	2003 SW222	12/06-12/12	25.7,22.7	78	19	4.76	0.01	0.11	0.02
275714	2000 YH4	12/15-12/19	50.2,45.0	55	-10	4.438	0.003	0.29	0.03
465749	2009 WO6	11/19-11/29	36.1,34.4	97	4	86.2	0.5	1.19	0.06
474179	1999 VS6	10/27-11/03	24.0,32.9	49	10	15.88	0.02	0.33	0.04
	2000 TU28	10/07-10/18	*32.6,25.2	35	1	128.5	0.5	1.55	0.10
	2002 GZ8	12/06-12/19	43.4,61.3	110	19	25.448	0.005	1.06	0.03
	2003 YJ	12/15-12/22	34.1,39.0	66	-11	3.255	0.001	0.22	0.04
	2013 UX14	10/02-10/18	51.6,45.4	48	-8	33.119	0.006	0.46	0.03
	2020 ST1	11/13-11/15	*5.9,3.8	52	1	2.875	0.003	1.2	0.06

Table III. Observing circumstances. ^{P}Period of the primary in a binary system. ^{T1,2}Period associated with tumbling. ^{3}Third period in a solution. The phase angle (α) is given at the start and end of each date range. If there is an asterisk before the first phase value, the phase angle reached a maximum or minimum during the period. L_{PAB} and B_{PAB} are, respectively the average phase angle bisector longitude and latitude (see Harris et al.,1984). The results for 159402 in 2020 (in italics) are shown here for comparison (see Warner and Stephens, 2021).

Warner, B.D. (2014). "Near-Earth Asteroid Lightcurve Analysis at CS3-Palmer Divide Station: 2013 September - December." *Minor Planet Bull.* **41**, 113-124.

Warner, B.D. (2016). "Three Additional Candidates for the Group of Very Wide Binaries." *Minor Planet Bul.* **43**, 306-309.

Warner, B.D. (2017a). "Near-Earth Asteroid Lightcurve Analysis at CS3-Palmer Divide Station: 2016 July - September." *Minor Planet Bull*. **44**, 22-36.

Warner, B.D. (2017b). "Near-Earth Asteroid Lightcurve at CS3-Palmer Divide Station: 2017 April thru June." *Minor Planet Bull*. **44**, 335-344.

Warner, B.D.; Stephens, R.D. (2019). "Near-Earth Asteroid Lightcurve Analysis at the Center for Solar System Studies: 2018 July - September." *Minor Planet Bull*. **46**, 27-40.

Warner, B.D.; Stephens, R.D. (2021). "On Confirmed and Suspected Binary Asteroids Observed at the Center for Solar System Studies." *Minor Planet Bull.* **48**, 40-49.

Warner, B.D., Harris, A.W., Pravec, P. (2009). "The Asteroid Lightcurve Database." *Icarus* **202**, 134-146. Updated 2020 Sep. *http://www.minorplanet.info/lightcurvedatabase.html*

Zappala, V.; Cellini, A.; Barucci, A.M.; Fulchignoni, M.; Lupishko, D.E. (1990). "An anlaysis of the amplitude-phase relationship among asteroids." *Astron. Astrophys*. **231**, 548-560.

LIGHTCURVE ANALYSIS FOR TEN NEAR-EARTH ASTEROIDS

Peter Birtwhistle
Great Shefford Observatory
Phlox Cottage, Wantage Road
Great Shefford, Berkshire, RG17 7DA
United Kingdom
peter@birtwhistle.org.uk

(Received: 2021 Jan 3)

Lightcurves and amplitudes for ten near-Earth asteroids observed from Great Shefford Observatory during close approaches in 2018 and 2020 are reported: 2018 KF1, 2020 GF2, 2020 OH3, 2020 RA6, 2020 RZ6, 2020 TP1, 2020 TD8, 2020 UQ6, 2020 VZ6 and 2020 XX3. 2020 UQ6 is the largest, with H = 22.6, all others are small objects, H > 24.5. Seven have superfast rotation periods, P < 10 min, including 2020 RZ6 and 2020 TD8 with P < 1 min.

Photometric observations of near-Earth asteroids during close approaches to Earth in 2018 and 2020 were made at Great Shefford Observatory using a 0.40-m Schmidt-Cassegrain and Apogee Alta U47+ CCD camera. All observations were made unfiltered and with the telescope operating with a focal reducer at *f*/6. The 1K×1K, 13-micron CCD was binned 2×2 resulting in an image scale of 2.16 arcsec/pixel. All the images were calibrated with dark and flat frames. *Astrometrica* (Raab, 2018) was used to measure photometry using APASS Johnson V band data from the UCAC4 catalogue. *MPO Canopus* (Warner, 2020), incorporating the Fourier algorithm developed by Harris (Harris et al., 1989), was used for lightcurve analysis.

2018 KF1. An Amor object with estimated diameter of 21 m and a perihelion distance of 1.01 AU was discovered by the Catalina Sky Survey on 2018 May 19 (Bacci et al., 2018) and had a close approach of 2 Lunar Distances (LD) on 2018 May 21.36 UT. A search of the Astrophysics Data System (ADS, 2020), the Asteroid Lightcurve Database (LCDB, Warner et al., 2009), and wider searches did not find any previously reported results for 2018 KF1. It was observed for 3.25 hours on the night of 2018 May 20/21, moving at ~110 arcsec/min.

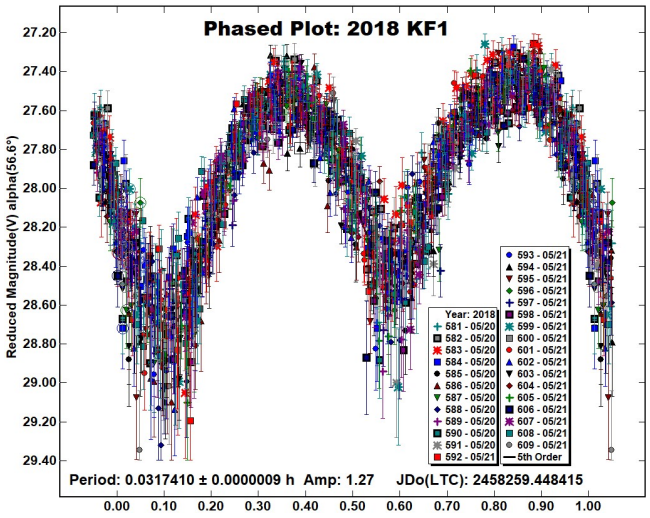

Large variations in brightness were evident between consecutive short exposures taken early in the evening for astrometry and so for photometry, exposures were kept to less than 4 seconds to keep the object from trailing and to ensure potential lightcurve smearing was reduced (Pravec et al., 2000). The asteroid reached apparent magnitude +16 and was visible in all images, but only weakly recorded at some of the deepest minima. Using 1,498 data points, an asymmetrical bimodal lightcurve is evident with a superfast rotation period of 1.9 minutes. 2018 KF1 completed 102 rotations during the 3h 45 m it was under observation.

2020 GF2. This Apollo object was well observed by a number of observatories in the three days following the discovery by the ATLAS team on 2020 Apr 10 (Melnikov et al., 2020a).

No previously reported results have been found in the ADS, LCDB, or from wider searches. 2020 GF2 passed Earth by 2.4 LD on 2020 Apr 12.5 UT and was a mag 16-17 object throughout. It was followed at Great Shefford on the night of 2020 Apr 11/12 and 1,417 images were measured from exposures ranging from 2 - 4.6 seconds. The sky motion reached 122 arcsec/min and the short exposures kept the trailing within the 3-pixel radius measurement annulus used in *Astrometrica*.

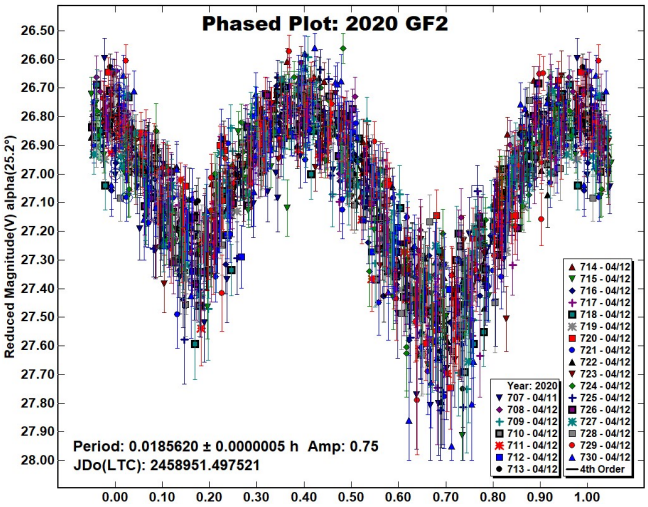

2020 GF2 is another small (estimated 19 m diameter) superfast rotator with a period of 1.1 minutes. 174 rotations occurred during the 3h 14 m it was under observation.

2020 OH3. An ATLAS discovery from Mauna Loa on 2020 July 22.56 UT (Melnikov et al., 2020b) with an estimated diameter of 36 m was a 16th magnitude target of opportunity on the night of 2020 July 22/23 from Great Shefford. It was under observation for 2.5 hours, moving at ~100 arcsec/min at a range of 5.4 LD and would pass Earth at 5.1 LD on 2020 July 23.46 UT, but moving swiftly south, would be below the horizon by the next night.

Exposures were limited to 4 seconds to allow the asteroid trail to be enclosed within the measurement annulus in *Astrometrica* and the apparent speed dictated that the telescope needed to be repositioned 12 times. 1,076 images were used in the analysis, indicating an only slightly asymmetric bimodal lightcurve with P = 23.5 min. There are no previous entries for 2020 OH3 in ADS or the LCDB.

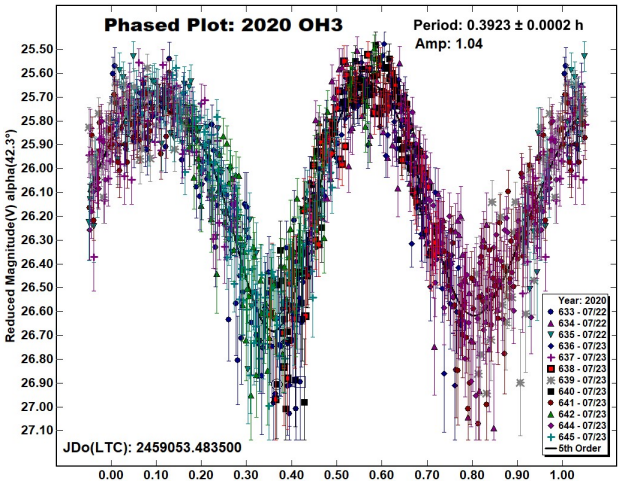

2020 RA6. An Apollo object with estimated diameter 19 m was discovered by the ZTF team at Palomar on 2020 Sep 14 with pre-discovery astrometry reported by Pan-STARRS 1 & 2 and Mt. Lemmon back to 2020 Sep 6 (Buzzi et al., 2020). It made an approach to within 1.4 LD of Earth on 2020 Sep 18.04 UT; it was observed from Great Shefford from 2020 Sep 17.84 UT for 27 minutes and then 3 hours later for a further 22 minutes (Table I).

No previous results for 2020 RA6 were found in the ADS, in the LCDB, or from wider searches. Apparent speed increased from 310 to 410 arcsec/min during the period and exposures were limited to 1 second throughout so that trailing of the target would always be enclosed within a 13 arcsec diameter measurement annulus used in *Astrometrica*. It is noted that 2020 RA6 passed 67 arcmin from the N. Celestial Pole on 2020 Sep 17.986 UT, which increased the length of time required to reposition the telescope. Peak-to-peak variations in magnitude were evident every ~10 minutes and at minimum brightness the individual measurements had low SNR. Three sets of images taken at minimum light were stacked in *Astrometrica* to increase signal strength, with 11-12 individual exposures being selected for each stack, resulting in each stack spanning a maximum of 44 seconds of time. These allowed four higher SNR measurements to be made for each of these three sets of images. Because the length of the two observing runs were similar to the apparent rotation period, the period spectrum shows multiple potential solutions.

Bimodal curves occur at ~0.33 h, with trimodal solutions appearing around 0.5 h and quadrimodal above 0.55 h.

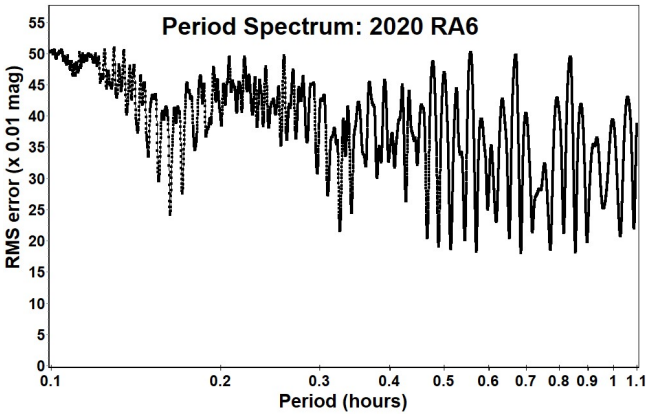

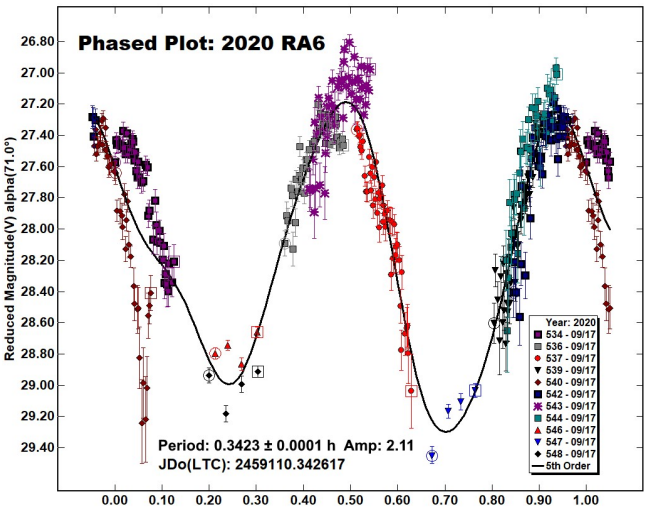

With the short coverage unable to discount longer periods, a bimodal solution is assumed here. The two strongest bimodal solutions were investigated (0.3265 h and 0.3423 h), representing a difference of 0.5 of the period over the observed arc. The longer period is preferred since, although the RMS was slightly greater, the direction of slope of the derived curve fitted the observations better.

The phase angle increased by 20° to $\alpha > 90°$ during the time under observation and the amplitude is likely to have increased and caused some extra scatter in the solution. It is noted that an anomalous fade of ~1 magnitude is apparent in a single set of measures centred at phase 0.06, from images spanning ~60-90 seconds.

2020 RZ6. The ATLAS system on Haleakala discovered this small Apollo (estimated diameter 14 m) on 2020 Sep 15 (Tichy et al., 2020), two days before passing just inside the orbit of the Moon, reaching 0.9 LD on 2020 Sep 17.77 UT. No previous results were found in the LCDB or from wider searches. Three separate sets of images were obtained in the hours after closest approach (Table I). Exposures were initially limited to 1 second due to the fast 315 arcsec/min apparent speed, but were increased to 1.5 seconds by the last run as the speed reduced to 195 arcsec/min.

Large variations in brightness were immediately evident between consecutive exposures and some of the deepest minima were either below the limiting magnitude or too faint to be measured reliably; however, the majority of the exposures were usable. As a fast rotation period was suspected, a period spectrum was produced in *MPO Canopus* searching for short periods in the range 18 seconds up to 6.3 minutes.

This initial search indicated that a quadrimodal solution with period 0.01771 h was preferred. However, the step size in this coarse period spectrum was 1×10^{-5} h and examining the bimodal and quadrimodal times with a finer step size of 1×10^{-7} h showed that the initial search was too coarse and the bimodal solution was actually a significantly better fit. The period spectrum figure shows the rejected solutions marked with crosses and the accepted bimodal solution with a tick.

There was a 3.9 h gap between runs 1 and 2 and then a further gap of 2.1 h between runs 2 and 3. Independent reductions from the three runs all produced similar periods and lightcurves. However, trying to fit all three runs together was not satisfactory, introducing significantly more noise to the lightcurve. During the time 2020 RZ6 was under observation it was receding from Earth and the phase angle was also increasing by 2.4°/h from 86° to 103°. The ephemeris, calculated with G = 0.15 in the H-G system predicted the brightness would be fading by 0.17 mag/h but at the high phase angles encountered, this can only be taken as a very rough guide. The photometry indicated a much slower fall of ~0.085 mag/h. *MPO Canopus* was used to vary the adopted value of G to find a minimum in the RMS of the fitted curve. The RMS was reduced from 0.32 to a minimum of 0.23 using a value of G = -0.25 and this value has been used to produce the lightcurve, including all 550 data points. Derived at such high phase angles, this value of G does not represent the lightcurve well at smaller phase angles, e.g., the discovery astrometry at phase angle 53° lists magnitudes that are ~1.4 mag fainter than this value of G would predict.

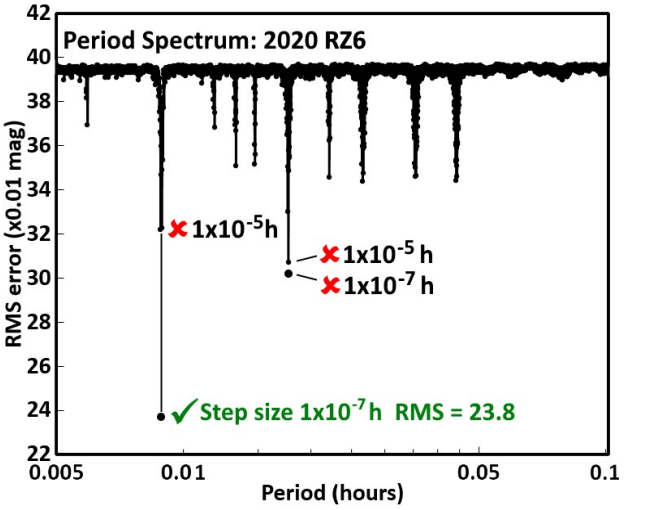

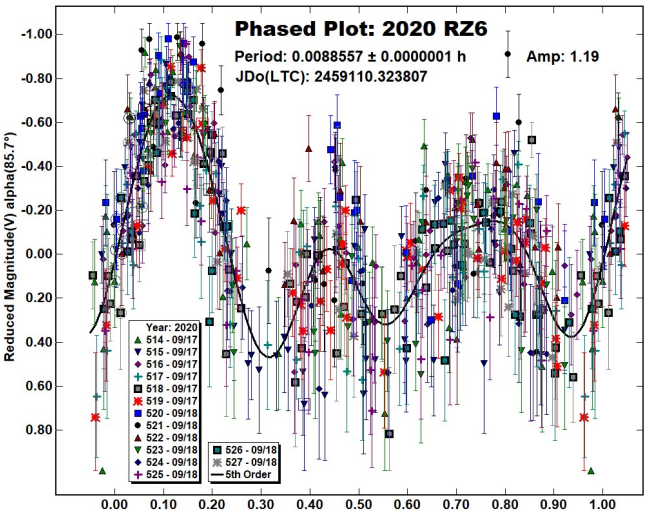

2020 RZ6 is a superfast rotator with a period of 31.9 seconds and completed 46 revolutions in run 1, 22 in run 2 and 35 in run 3. Independent of the lightcurve solution in *MPO Canopus*, a check was made to see whether the three runs could be unambiguously linked by estimating the likely error in the number of rotations ΔN when propagating a calculated period with its associated error to another time, derived from Eq (3) in Kwiatkowski et al. (2010) by:

$$\Delta N \approx \Delta t \, \Delta P / P^2. \quad (1)$$

where Δt is the time interval separating two individual lightcurves, P is the period from one of the individual solutions, and ΔP is the maximum period uncertainty, in practice taken here to be 3× the formal uncertainty from *MPO Canopus*, and Δt, ΔP and P in the same units. For a bimodal curve ΔN < 0.25 implies a maximum (or minimum) can be matched unambiguously, less than ¼ cycle from reality. The error propagated from run 3 to run 2 (a shorter interval than run 1 to 2) is ΔN = 0.21, allowing runs 2 and 3 to be linked unambiguously. The revised period and error from a solution combining runs 2 and 3 then allowed linking run 2 to run 1 with ΔN = 0.04. The lightcurve using all three runs indicates that 2020 RZ6 completed a total of 775 revolutions during the observing period. Since the minima of the lightcurve were incompletely covered, it is likely that the actual amplitude is somewhat larger than the calculated value of 1.19 mag.

2020 TP1. This ~13 m diameter Apollo was discovered by the ATLAS-HKO, Haleakala team on 2020 Oct 9 at a distance of 3 LD, already receding from Earth after passing just inside 1 LD 20 hours earlier (Pettarin et al., 2020). A search of the ADS, the LCDB, and wider searches did not find any previously reported results for 2020 TP1. It was observed for 93 minutes starting at 2020 Oct 9 19:34 UT and then again for 104 minutes starting the same night at 22:17 UT (Table I). No obvious superfast rotation had been evident during earlier image acquisition for astrometry and with sky motion at 26 arcsec/min, 16 second exposures were taken for photometry.

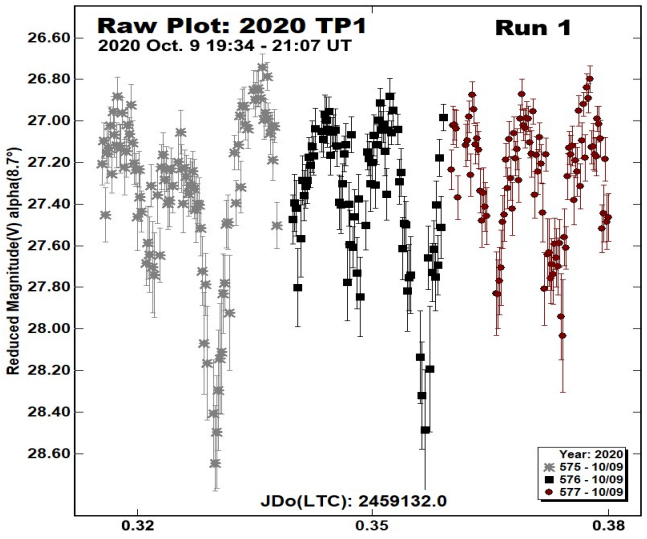

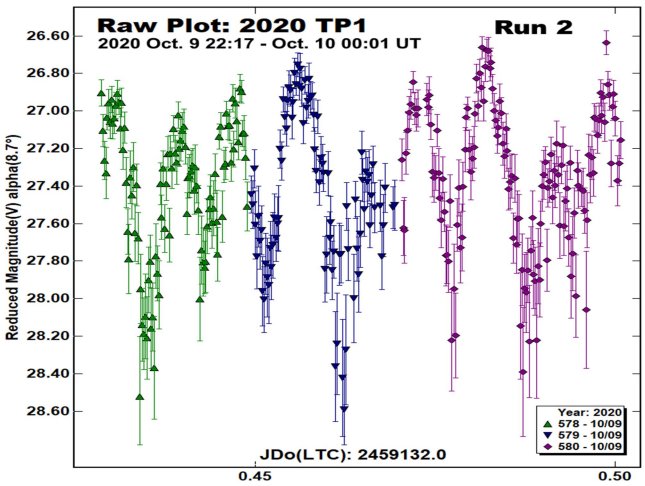

A period spectrum shows a bimodal solution at 0.42 h, but with the best fit being a trimodal one at 0.63 h and solutions at 0.83 h and 1.04 h, all having slightly better RMS fits than the bimodal one. The raw plots of the two periods of observation, run 1 and run 2, show regular variations of about 0.7 magnitudes amplitude every ~12 minutes, but with every third minima being very deep.

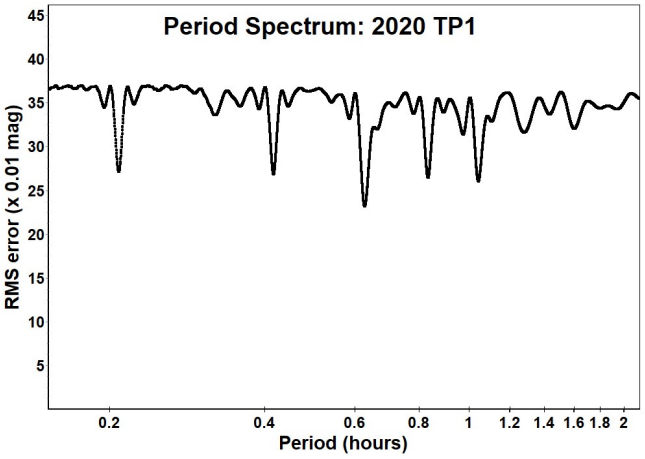

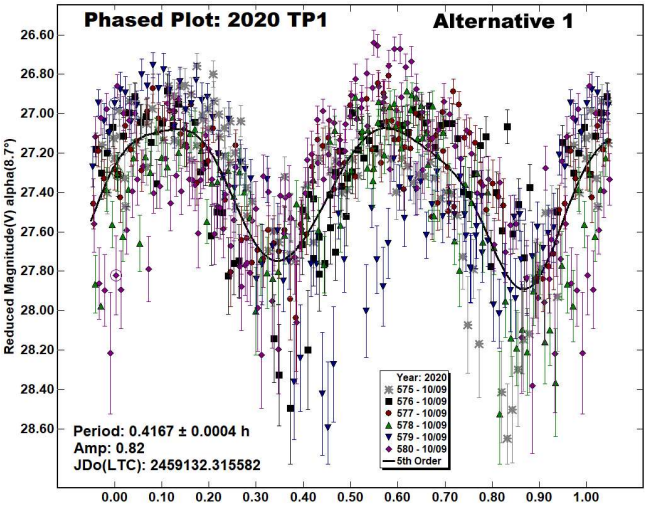

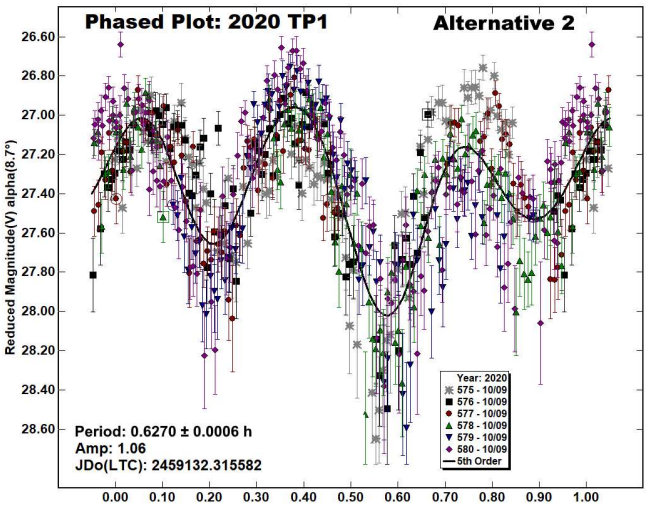

Additionally, the three maxima between these minima appear relatively equal during run 1 but are progressively unequal during run 2. Lightcurves are given for bimodal (alternative 1) and trimodal (alternative 2) solutions, but significant trends in both may indicate that 2020 TP1 is tumbling This is not resolved conclusively, so it is expected to be rated as PAR = -1 (Non-Principal Axis rotation possible, but not conclusively) on the scale of Pravec et. al. (2005).

2020 TD8. Pan-STARRS 2 discovered this small Apollo object 12 days before it made a close approach to 1.6 LD on 2020 Oct. 27.36 UT (Jahn et al., 2020). No previously reported results for 2020 TD8 were found in the ADS, the LCDB, or from wider searches. It was followed over a period of 3.7 h starting 11.5 hours before closest approach, when it reached apparent magnitude +16. With the fast apparent motion of ~125 arcsec/min, exposures were limited to 2 and 3 seconds to keep trailing short enough to allow measurement in a 3-pixel radius annulus in *Astrometrica*. Large variations in brightness were obvious between consecutive exposures and it was only recorded weakly in some of the images at minima and occasionally not visible at all but 582 images were able to be measured.

A period spectrum shows the bimodal solution at 0.008 h to be marginally the strongest and, with the level of noise present, none of the other periods can be justified.

2020 TD8 is another superfast rotator with a period of 29.6 seconds. It is noted that it is included in the JPL Sentry Impact Risk Data table (JPL, 2020b) as a 14 m diameter virtual impactor, with a series of low probability potential impacts listed from 2045 onwards.

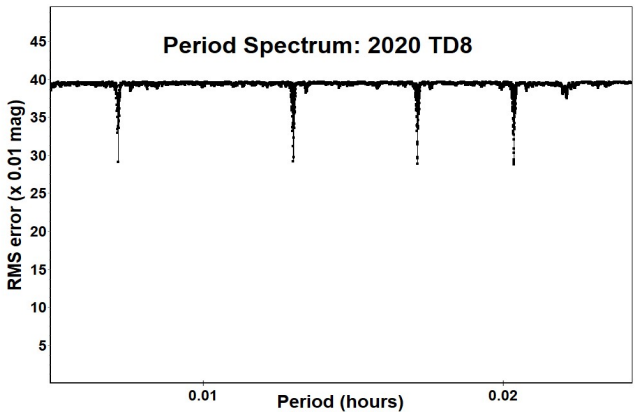

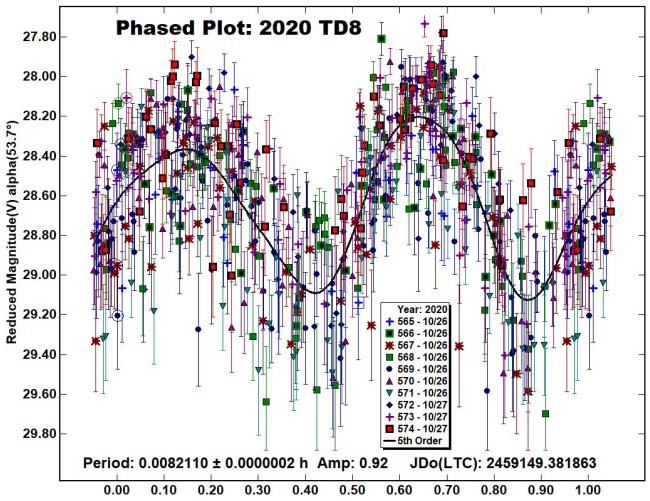

2020 UQ6. This Apollo with an estimated diameter of 90 m was discovered at magnitude 14 with the 1.05-m Schmidt at the Tokyo-Kiso station on 2020 Oct 27 and had passed Earth at 0.010 AU the day before. (Beniyama et al., 2020). When observed on 2020 Oct 28.0 UT it was 15th mag and 10 s exposures were taken over a period of 2 h 39 m resulting in 440 points being measured for the analysis.

A search of the ADS and the LCDB did not find any previously reported results for 2020 UQ6 but wider searches located a preliminary result published on Twitter (Wells and Bamberger, 2020) of P = 0.04519 ± 0.00005 h, amp = 0.74 mag, agreeing well with this analysis.

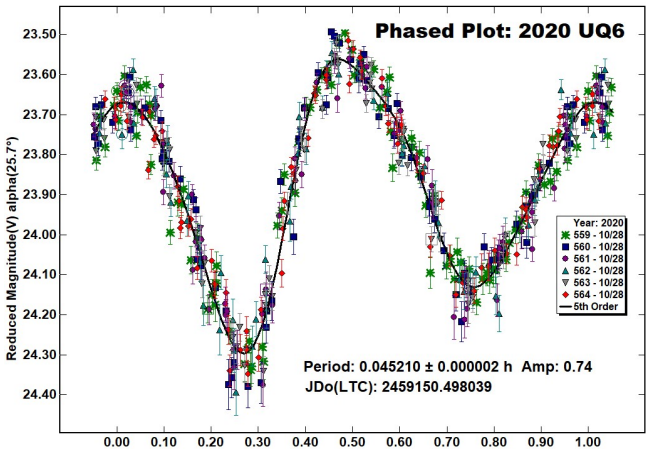

2020 VZ6. This Apollo with an estimated diameter of 27 m was submitted to the NEO Confirmation Page (MPC, 2020) as a magnitude 17 object by the ATLAS team on the night of the full Moon, 2020 Nov 30, but was subsequently matched with a magnitude 21 object observed from Mt. Lemmon and PanSTARRS two weeks earlier (Panterotto et al., 2020). It passed the Earth at 0.9 LD on 2020 Dec 3 and was followed from Great Shefford for 73 minutes on 2020 Dec 1. It was then at a distance of 3.5 LD, moving at 20 arcsec/min at low altitude, < +34°, in poor conditions with occasional high cloud interruptions and with the Moon 1 day past full, 48° distant. Exposures were 8 and 12 s and 333 points used to produce the rather noisy curve indicating a bimodal solution with a period of 5.9 minutes. No entries for 2020 VZ6 were found in the LCDB or in wider searches.

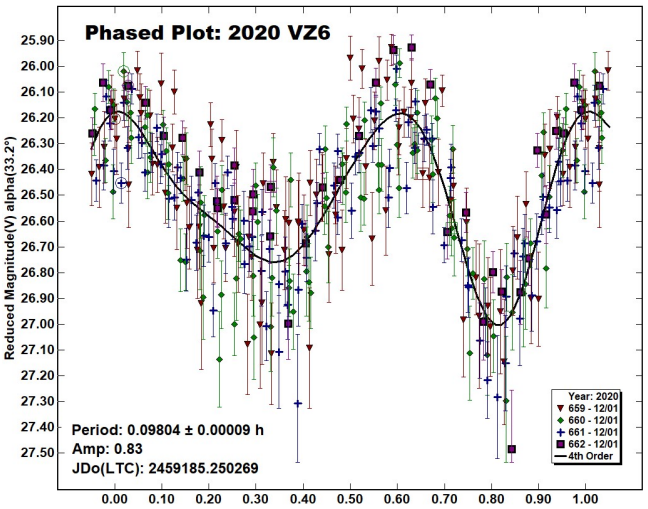

2020 XX3. A very small, 6 m diameter Apollo discovered by Pan-STARRS 1 (Read et al., 2020) 8 days before passing Earth on 2020 Dec 18.3 UT at 0.15 LD was followed over a 1 h 40 min period on 2020 Dec 17.0 UT when it was 16/17th mag and moving at 20 arcsec/min. Exposure length was set at 16 s but soon reduced to 10 s when it became obvious that a large drop in magnitude between consecutive exposures was occurring every ~2.3 minutes, in case finer resolution of the lightcurve would be useful. 17 of the longer exposures and 381 of the shorter were used in the lightcurve analysis. The period spectrum shows that a bimodal lightcurve of period 0.038 h (2.28 min) gives a slightly better fit than the quadrimodal solution at 0.076 h.

A split halves plot shows that the two halves of the quadrimodal solution are almost identical, so the bimodal solution is adopted.

No previously results have been found in the LCDB or from wider searches. It is noted that 2020 XX3 is included in the JPL Sentry Impact Risk Data table (JPL, 2020b) as a virtual impactor, with four very low probability potential impacts listed, starting in 2086.

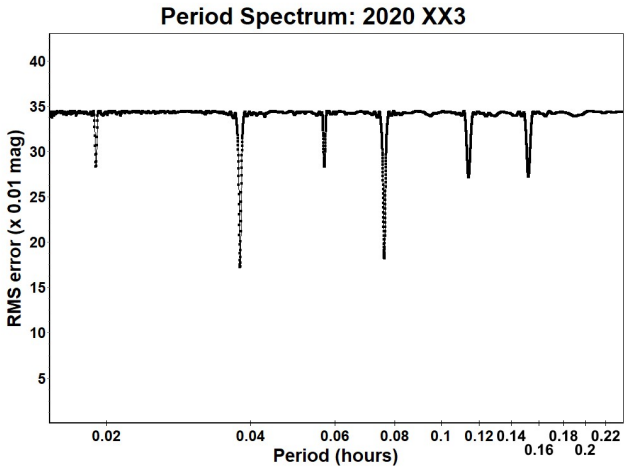

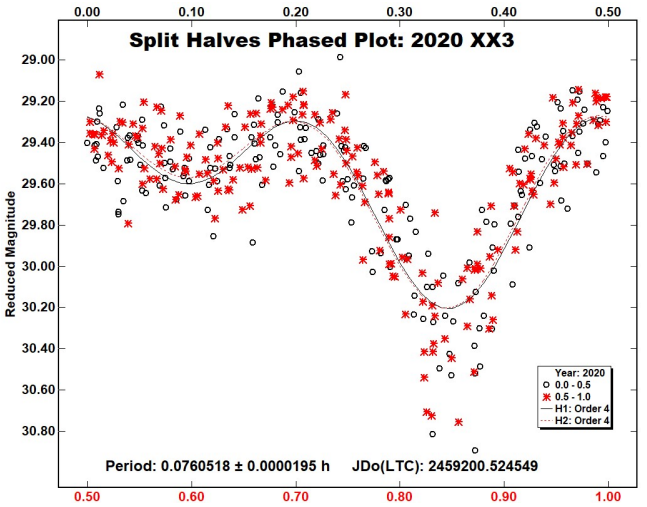

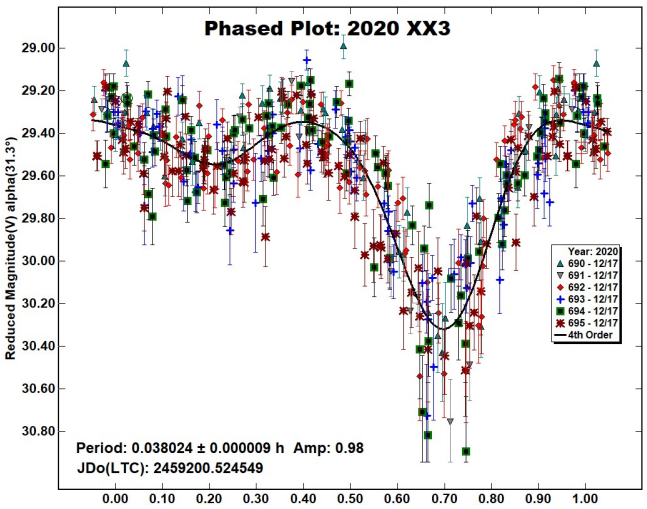

References

ADS (2020). Astrophysics Data System. *https://ui.adsabs.harvard.edu/*

Bacci, P.; Maestripieri, M.; Tesi, L.; Fagioli, G.; Jaeger, M.; Prosperi, E.; Vollmann, W.; Africano, B.M.; Christensen, E.J.; Fuls, D.C.; Gibbs, A.R.; Grauer, A.D.; Groeller, H.; Johnson, J.A.; Kowalski, R.A. and 22 colleagues (2018). "2018 KF1" *MPEC* 2018-K47. *https://minorplanetcenter.net/mpec/K20/K20RG6.html*

Beniyama, J.; Baransky, A.; Khorolsky, A.; Solomakha, M.; Pettarin, E.; Panterotto, G.; Wiggins, P.; James, N.; Bolin, B.T.; Bhalerao, V.; Copperwheat, C.M.; Deshmukh, K.P.; Hsu, C.-Y.; Lin, Z.-Y.; Purdum, J. and 33 colleagues (2020). "2020 UQ6" *MPEC* 2020-U259. *https://minorplanetcenter.net/mpec/K20/K20UP9.html*

Buzzi, L.; Pettarin, E.; Hug, G.; Cromer, D.; Valentine, R.; James, N.; Bulger, J.; Chambers, K.; Lowe, T.; Schultz, A.; Willman, M.; Chastel, S.; Huber, M.; Ramanjooloo, Y.; Wainscoat, R. and 16 colleagues (2020). "2020 RA6" *MPEC* 2020-R166. *https://minorplanetcenter.net/mpec/K20/K20RG6.html*

Harris, A.W.; Young, J.W.; Scaltriti, F.; Zappala, V. (1984). "Lightcurves and phase relations of the asteroids 82 Alkmene and 444 Gyptis." *Icarus* **57**, 251-258.

Harris, A.W.; Young, J.W.; Bowell, E.; Martin, L.J.; Millis, R.L.; Poutanen, M.; Scaltriti, F.; Zappala, V.; Schober, H.J.; Debehogne, H.; Zeigler, K. (1989). "Photoelectric Observations of Asteroids 3, 24, 60, 261, and 863." *Icarus* **77**, 171-186.

Jahn, J.; Bulger, J.; Lowe, T.; Schultz, A.; Willman, M.; Chambers, K.; Chastel, S.; de Boer, T.; Denneau, L.; Fairlamb, J.; Flewelling, H.; Huber, M.; Lin, C.-C.; Magnier, E.; Ramanjooloo, Y. and 7 colleagues (2020). "2020 TD8" *MPEC* 2020-U97. *https://minorplanetcenter.net/mpec/K20/K20U97.html*

Number	Name	Integration times	Max intg. / Period	Min a/b	Points	Fields	Acquiring images for	Total Span	Run#	Run times (2020) mm/dd From-To
	2018 KF1	3.4-3.6	0.03	1.5	1498	29	2 h 47 m	3 h 15 m		
	2020 GF2	2,4.2-4.6	0.07	1.5	1417	24	2 h 31 m	3 h 14 m		
	2020 OH3	1,4	0.003	1.5	1076	13	2 h 00 m	2 h 33 m		
	2020 RA6	1,44$^{\Sigma}$	0.04	1.7	491	11	0 h 29 m	3 h 45 m		
					365	8			1	09/17 20:13-20:35
					126	3			2	09/17 23:35-23:58
	2020 RZ6	1,1.5	0.05	1.3	550	14	0 h 40 m	6 h 44 m		
					294	6			1	09/17 19:46-20:10
					93	3			2	09/18 00:03-00:15
					163	5			3	09/18 02:19-02:38
	2020 TP1	16	0.01	1.8	596	6	3 h 15 m	4 h 30 m		
					266	3			1	10/09 19:31-21:07
					330	3			2	10/09 22:17-10/10 00:01
	2020 TD8	2,3	0.10	1.4	582	10	1 h 02 m	3 h 44 m		
	2020 UQ6	10	0.06	1.5	440	6	1 h 55 m	2 h 40 m		
	2020 VZ6	8,12	0.03	1.5	333	4	1 h 12 m	1 h 15 m		
	2020 XX3	10,16	0.12	1.6	394	6	1 h 35 m	1 h 40 m		

Table I. Ancillary information, listing the integration times used (seconds), the fraction of the period represented by the longest integration time (see Pravec et al., 2000), the calculated minimum elongation of the asteroid (Kwiatkowski et al., 2010), the number of data points used in the analysis, the number of times the telescope was repositioned to different fields, the total elapsed time actively acquiring images, the time span of first to last image used in the analysis and run details where gaps in coverage are significant, including Run number and start-end date/times. Note: Σ = Longest elapsed integration time for stacked images (start of first to end of last exposure used).

Number	Name	yyyy mm/ dd	Phase	L_{PAB}	B_{PAB}	Period(h)	P.E.	Amp	A.E	Grp	H
	2018 KF1	2018 05/20-05/21	56.6,57.4	250	27	0.0317410	0.0000009	1.3	0.2	NEA	25.8
	2020 GF2	2020 04 11-04/12	25.0,30.1	205	14	0.0185620	0.0000005	0.75	0.15	NEA	26.0
	2020 OH3	2020 07/22-07/23	42.2,43.1	322	2	0.3923	0.0002	1.0	0.2	NEA	24.6
	2020 RA6	2020 09/17-09/17	71.1,93.9	12	38	0.3423	0.0001	2.1	0.2	NEA	26.0
	2020 RZ6	2020 09/17-09/18	86.2,103.0	41	20	0.0088557	0.0000001	1.2	0.3	NEA	26.6
	2020 TP1	2020 10/09-10/10	8.5,8.6	18	4	$0.4167^{NPA?}$	0.0004	0.8	0.2	NEA	26.8
	2020 TD8	2020 10/26-10/27	53.9,59.9	58	15	0.0082110	0.0000002	0.9	0.2	NEA	26.9
	2020 UQ6	2020 10/27-10/28	23.8,25.8	47	-4	0.045210	0.000002	0.74	0.09	NEA	22.6
	2020 VZ6	2020 12/01-12/01	33.2,33.1	54	-5	0.09804	0.00009	0.8	0.3	NEA	25.2
	2020 XX3	2020 12/17-12/17	31.7,32.3	69	1	0.038024	0.000009	1.0	0.2	NEA	28.5

Table II. Observing circumstances and results. The phase angle is given for the first and last date. If preceded by an asterisk, the phase angle reached an extrema during the period. L_{PAB} and B_{PAB} are the approximate phase angle bisector longitude/latitude at mid-date range (see Harris et al., 1984). Grp is the asteroid family/group (Warner et al., 2009), and H is the absolute magnitude at 1 au from Sun and Earth taken from the Small-Body Database Browser (JPL, 2020a). Note: NPA? = Possible Non-Principal Axis rotation.

JPL (2020a). Small-Body Database Browser *https://ssd.jpl.nasa.gov/sbdb.cgi*

JPL (2020b). Sentry: Earth Impact Monitoring Impact Risk Data *https://cneos.jpl.nasa.gov/sentry/*

Kwiatkowski, T.; Buckley, D.A.H.; O'Donoghue, D.; Crause, L.; Crawford, S.; Hashimoto, Y.; Kniazev, A.; Loaring, N.; Romero Colmenero, E.; Sefako, R.; Still, M.; Vaisanen, P. (2010). "Photometric survey of the very small near-Earth asteroids with the SALT telescope - I. Lightcurves and periods for 14 objects." *Astron. Astrophys.* **509**, A94.

Melnikov, S.; Hoegner, C.; Stecklum, B.; Mikuz, B.; Jaeger, M.; Prosperi, E.; Prosperi, S.; Foglia, S.; Galli, G.; Buzzi, L.; Donati, S.; Biagini, F.; Simon, A.; Baransky, A.; Zoltowski, F.B. and 47 colleagues (2020a). "2020 GF2" *MPEC* 2020-G86. *https://minorplanetcenter.net/mpec/K20/K20G86.html*

Melnikov, S.; Stecklum, B.; Buzzi, L.; Gilmore, A.C.; Kilmartin, P.M.; Bulger, J.; Chambers, K.; Lowe, T.; Schultz, A.; Willman, M.; Chastel, S.; Huber, M.; Ramanjooloo, Y.; Wainscoat, R.; Weryk, R. and 21 colleagues (2020b). "2020 OH3" *MPEC* 2020-O92. *https://minorplanetcenter.net/mpec/K20/K20O92.html*

MPC (2020) Minor Planet Center NEO Confirmation Page *https://www.minorplanetcenter.net/iau/NEO/toconfirm_tabular.html*

Panterotto, G.; Pettarin, E.; Bulger, J.; Lowe, T.; Schultz, A.; Willman, M.; Chambers, K.; Chastel, S.; de Boer, T.; Denneau, L.; Fairlamb, J.; Flewelling, H.; Huber, M.; Lin, C.-C.; Magnier, E. and 23 colleagues (2020). "2020 VZ6" *MPEC* 2020-W192. *https://minorplanetcenter.net/mpec/K20/K20WJ2.html*

Pettarin, E.; James, N.; Bolin, B.T.; Bhalerao, V.; Copperwheat, C.M.; Deshmukh, K.P.; Hsu, C.-Y.; Lin, Z.-Y.; Purdum, J.; Sharma, K.; Zhai, C.; Z.T.F. Collaboration; Duev, D.A.; Lin, H.-W.; Masci F.J. and 16 colleagues (2020). "2020 TP1" *MPEC* 2020-T55. *https://minorplanetcenter.net/mpec/K20/K20T55.html*

Pravec, P.; Hergenrother, C.; Whiteley, R.; Sarounova, L.; Kusnirak, P.; Wolf, M. (2000). "Fast Rotating Asteroids 1999 TY2, 1999 SF10, and 1998 WB2" *Icarus* **147**, 477-486.

Pravec, P.; Harris, A.W.; Scheirich, P.; Kušnirák, P.; Šarounová, L.; Hergenrother, C.W.; Mottola, S.; Hicks, M.D.; Masi, G.; Krugly, Yu.N.; Shevchenko, V.G.; Nolan, M.C.; Howell, E.S.; Kaasalainen, M.; Galád, A. and 5 colleagues (2005). "Tumbling Asteroids." *Icarus* **173**, 108-131.

Raab, H. (2018). Astrometrica software, version 4.12.0.448. *http://www.astrometrica.at/*

Read, M.T.; Bulger, J.; Lowe, T.; Schultz, A.; Willman, M.; Chambers, K.; Chastel, S.; de Boer, T.; Denneau, L.; Fairlamb, J.; Flewelling, H.; Huber, M.; Lin, C.-C.; Magnier, E.; Ramanjooloo, Y. and 31 colleagues (2020). "2020 XX3" MPEC 2020-X132. *https://minorplanetcenter.net/mpec/K20/K20XD2.html*

Tichy, M.; Ticha, J.; Dupouy, P.; Holmes, R.; Foglia, S.; Buzzi, L.; Linder, T.; Hug, G.; Losse, F.; Birtwhistle, P.; Adamovsky, M.; Korlevic, K.; Lyon, I.; Denneau, L.; Tonry, J. and 13 colleagues (2020). "2020 RZ6" MPEC 2020-S16. *https://minorplanetcenter.net/mpec/K20/K20S16.html*

Warner, B.D.; Harris, A.W.; Pravec, P. (2009). "The Asteroid Lightcurve Database." *Icarus* **202**, 134-146. Updated 2020 Oct. *http://www.MinorPlanet.info/lightcurvedatabase.html*

Warner, B.D. (2020). MPO Software, *MPO Canopus* v10.8.2.8. Bdw Publishing, Eaton, CO. *http://minorplanetobserver.com*

Wells, G.; Bamberger, D. (2020). "2020 UQ6". *https://twitter.com/NBObservatories/status/1322554380923666434*

ON CONFIRMED AND SUSPECTED BINARY ASTEROIDS OBSERVED AT THE CENTER FOR SOLAR SYSTEM STUDIES

Brian D. Warner
Center for Solar System Studies / MoreData!
446 Sycamore Ave.
Eaton, CO 80615 USA
brian@MinorPlanetObserver.com

Robert D. Stephens
Center for Solar System Studies / MoreData!
Rancho Cucamonga, CA 91730

(Received: 2021 Jan 8)

The analysis of observations made at the Center for Solar System Studies from 2020 September to 2021 January led to the discovery that the Vestoid asteroid 3865 Lindbloom is a fully synchronous binary. The orbital period is 26.016 h and the ratio of the effective diameters is 0.65 ≤ Ds/Dp ≤ 1.0. Assuming a bulk density of 2 g/cm, *Dp* ≤ 7.2 km, *Ds* ≥ 4.6 km, and the center-to-center separation is 20 km. Other objects presented here were found to have secondary periods: 4503 Cleobulus, (22056) 2000 AU31, 25465 Rajagopalan, (46818) 1998 MZ24, (48205) 2012 TQ78, 2013 PY6, and 2020 PD1. Of those, only 1998 MZ24 and 2013 PY6 might be said to show mutual events due to a satellite.

CCD photometric observations at the Center for Solar System Studies in 2020 September to early 2021 January led to discovery at least one confirmed binary asteroid, 3865 Lindbloom. Several other asteroids that were observed could not be adequately defined with a single period solution. Two of those additional objects, (46818) 1998 MZ24 and 2013 PY6, came closest to showing the requisite mutual events (occultations/eclipses) due to a satellite.

Table I lists the telescopes and CCD cameras that were combined to make the observations. All the cameras use CCD chips from the KAF blue-enhanced family and so have essentially the same response. The pixel scales ranged from 1.24-1.60 arcsec/pixel.

Telescopes	Cameras
0.30-m *f*/6.3 Schmidt-Cass	FLI Microline 1001E
0.35-m *f*/9.1 Schmidt-Cass	FLI Proline 1001E
0.40-m *f*/10 Schmidt-Cass	SBIG STL-1001E
0.40-m *f*/10 Schmidt-Cass	
0.50-m *f*/8.1 Ritchey-Chrétien	

Table I. List of available telescopes and CCD cameras at CS3. The exact combination for each telescope/camera pair can vary due to maintenance or specific needs.

All lightcurve observations were unfiltered since a clear filter can cause a 0.1-0.3 mag loss. The exposure duration varied depending on the asteroid's brightness and sky motion. Guiding on a field star sometimes resulted in a trailed image for the asteroid.

Measurements were made using *MPO Canopus*. The Comp Star Selector utility in *MPO Canopus* found up to five comparison stars of near solar-color for differential photometry. To reduce the number of adjusted nightly zero points and their amounts, we use the ATLAS catalog r′ (SR) magnitudes (Tonry et al., 2018). This makes most zero-point adjustments ≤ ±0.03 mag. The rare greater corrections may have been related in part to using unfiltered observations, poor centroiding of the reference stars, and not correcting for second-order extinction. Another cause may be selecting what appears to be a single star but is actually an unresolved pair.

The Y-axis values are ATLAS SR "sky" (catalog) magnitudes. The two values in the parentheses are the phase angle (a) and the value of *G* used to normalize the data to the comparison stars used in the earliest session. This, in effect, had all the observations made at a single fixed date/time and phase angle, leaving any variations due only to the asteroid's rotation and/or albedo changes. The X-axis shows rotational phase from –0.05 to 1.05. If the plot includes the amplitude, e.g., "Amp: 0.65", this is the amplitude of the Fourier model curve and *not necessarily the adopted amplitude for the lightcurve*.

3865 Lindbloom. There was only one previously reported rotation period found in the LCDB for this 8-km Vestoid: Pravec et al. (2018web), who found *P* = 5.42 h, *A* = 0.03 mag. Our extensive data set, obtained 2020 Nov 8-20, led to a much different solution.

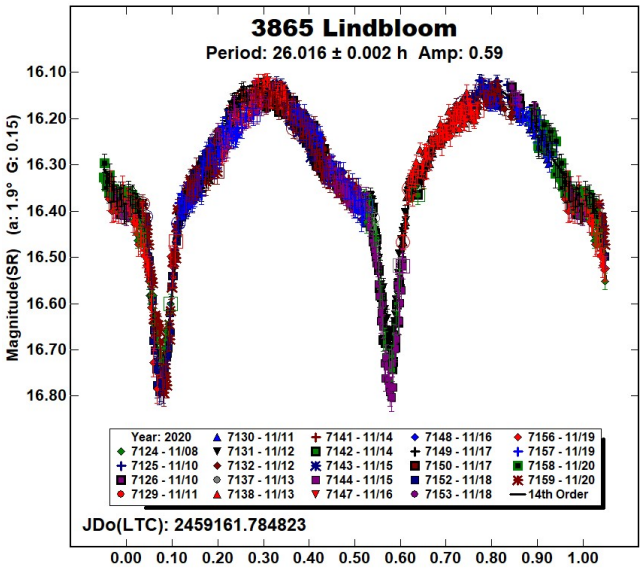

The final lightcurve has a period of 26.016 h and clearly shows the *shoulders* (sudden changes in slope in the descending/ascending sections) associated with a fully synchronous binary with the two bodies separated by a small distance.

The depth of the lightcurve outside the mutual events is 0.27 mag. If both bodies have the same elongation, and assuming a smoothed ellipsoid, this would imply an *a/b* ratio of 1.27:1. The mutual events themselves are 0.38 mag and, since they present sharp minimums, the events are not total. From this, the estimated effective diameter ratio is 0.65 ≤ Ds/Dp ≤ 1.0.

Mainzer et al. (2016) give an effective diameter 8 km for the system. Assuming a bulk density of 2 g/cc for both bodies sets D_1 ≤ 7.2 km, D_2 ≥ 4.6 km, and the center-to-center separation of 20 km. These numbers are consistent with the narrow events that are <0.1 rotation phase wide.

4503 Cleobulus. This NEA has an estimated effective diameter of 1.9 km (LCDB; Warner et al., 2009). The LCDB lists only one previous rotation period, that being 3.13 h from Wisniewski et al. (1997).

The data set appeared to be excessively noisy, even though the errors for individual data points were on the order of 0.2-0.3 mag. We've found that the excessive noise can be due to the presence of a second period and so we tried a dual-period search using *MPO Canopus*. The P_1 period spectrum shows that several solutions stood out, some in addition to our adopted period of about 2.82 h, which we used as the basis in the search for the second period.

The P_2 period spectrum showed potential solutions near 35 h and 65 h. After several iterations of finding one period, subtracting it to find a second period, and subtracting that to find a revised first period, our final result was P_1 = 2.8164 h and P_2 = 66.1 h. The P_2 lightcurve does not show evidence of mutual events (occultations/eclipses), which are required to elevate the asteroid to a confirmed binary. It is also sufficiently asymmetrical to raise at least some doubt about the validity of the solution. However, as seen in the P_1 lightcurve, subtracting P_2 removes a large portion of the noise from a single period lightcurve.

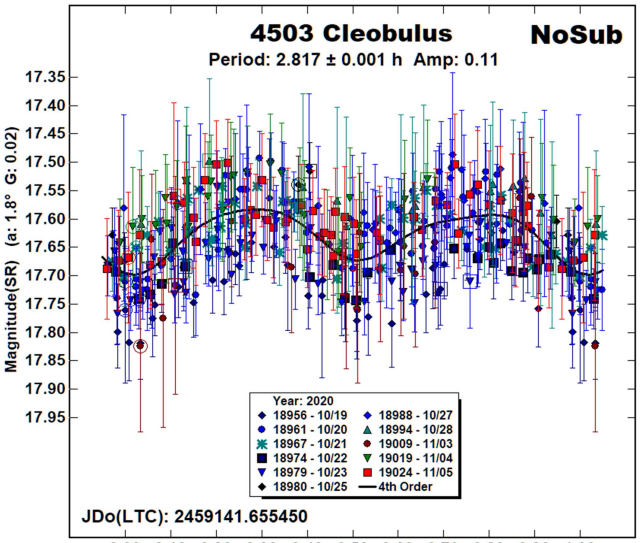

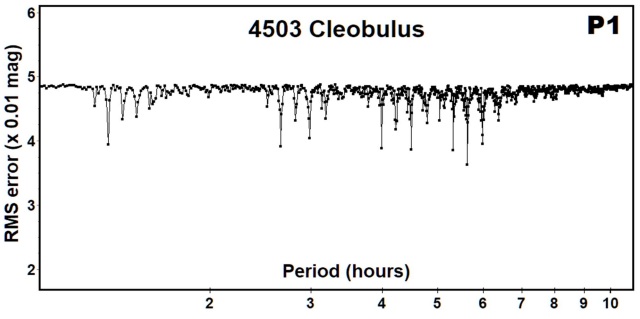

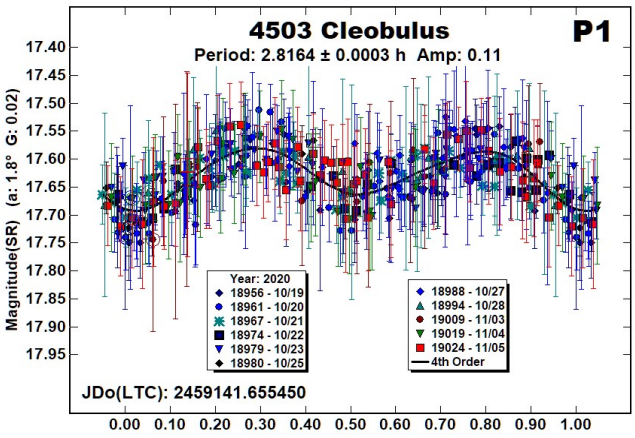

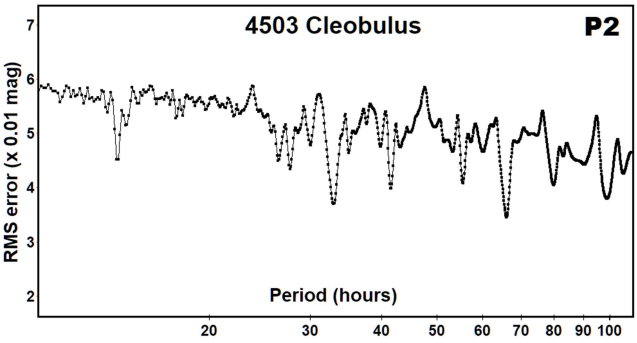

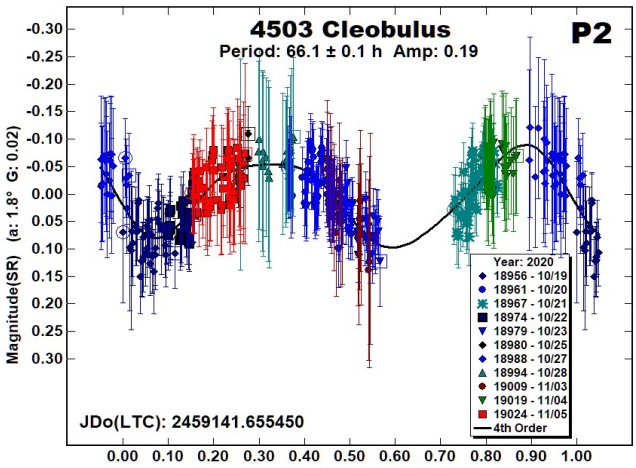

Unfortunately, the NEA remains well below V ~ 18.5 for some time. The next best chance for follow-up observations is not until 2029 November when it will be about 1.5 mag brighter (15.7) at +21° declination.

(22056) 2000 AU31. This is a Jupiter trojan with an estimated diameter of 25 km (Mainzer et al., 2016). Ryan et al. (2017) and Szabó et al. (2017) observed the asteroid in 2015 August, finding periods of 356 h and 358 h, respectively. Our data set, even though sparse in coverage, led to a significantly different result.

The "Raw" plot shows the data set as magnitude versus JD, with the magnitudes being normalized to the Nov 3 observations using $G = 0.15$. Taken at face value, it implies a period on the order of about 12 days, or 288 hours. However, it can happen that the 24-hour sampling interval is actually catching slightly different portions of a lightcurve with a much shorter period. Keeping this mind, a period search beyond 400 h found a more likely solution to be under 100 hours.

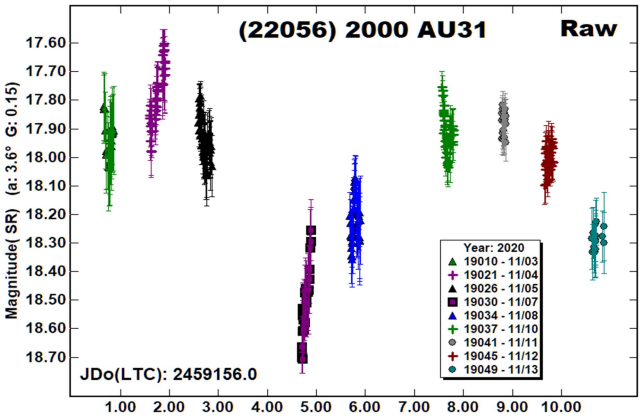

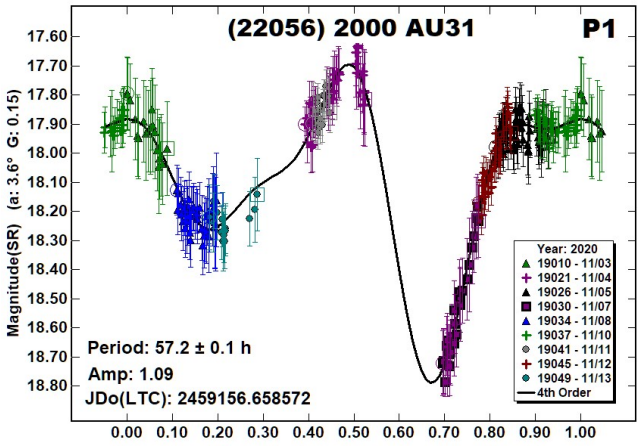

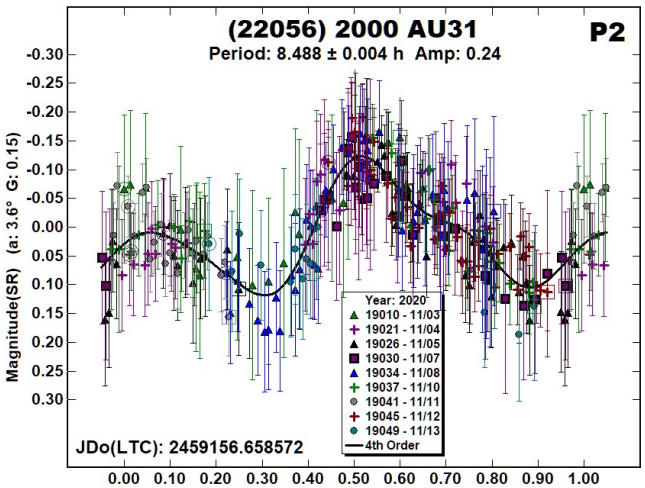

The eventual P_1 lightcurve, found using the dual-period search feature of MPO Canopus, has a highly asymmetrical shape due exclusively to the data from Nov 7. Removing those from the analysis found a similar period and a more symmetrical shape. After reviewing the Nov 7 data, the zero-point adjustment required to bring them "into line" with the rest of the data was deemed too excessive and with no apparent systematic cause. Its physical cause is a matter of speculation.

Removing the P_1 result from the data found two very strong solutions of about 8.5 h and 17 h. We have adopted $P_2 = 8.488$ h, which produces a symmetrical lightcurve along the X-axis. One *suggested* model of the system is a wide binary with an elongated secondary and an orbital inclination that may allow seeing mutual events. This, of course, requires validation with higher quality data.

25465 Rajagopalan, a member of the Flora family/group, had no previous entries of any kind in the LCDB. The estimated diameter is 2.3 km. The data set was noisy but, here again, a single-period solution did not provide an acceptable fit, or at least could be considerably improved by removing a secondary period.

The initial period search found $P \sim 65$ h that was further refined to 63.2 h. The lightcurve has some hints of mutual events near 0.05 and 0.55 rotation phase (P_1 plot). The additional attenuation near 0.35 phase is most likely an artifact of the Fourier analysis since it has no counterpart near 0.85 phase. Subtracting P_1 lead to an ambiguous solution for a weak secondary period of either 4.961 h or 3.303 h, the former being the preferred solution even though it results in a trimodal lightcurve.

The purported events in P_1 are about 0.07 mag deep, leading to Ds/Dp ≥ 0.25 ± 0.04. Given the quality of the limited data set, the results presented here should be considered to be no more than an alert to future observers of the possibility, admittedly a small one, that the asteroid is binary.

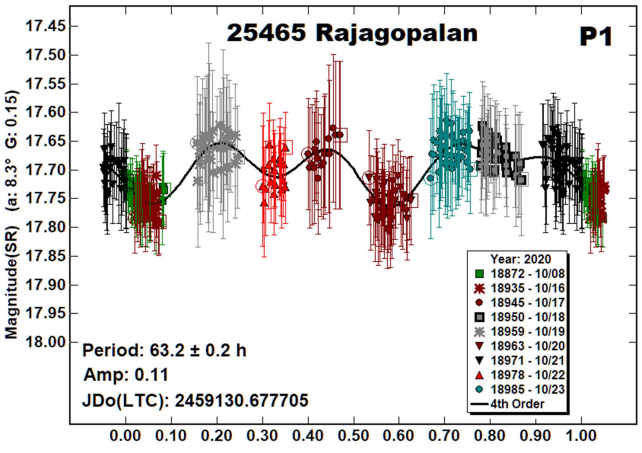

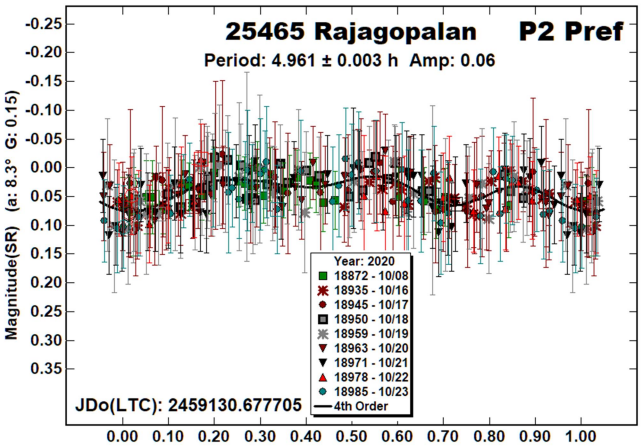

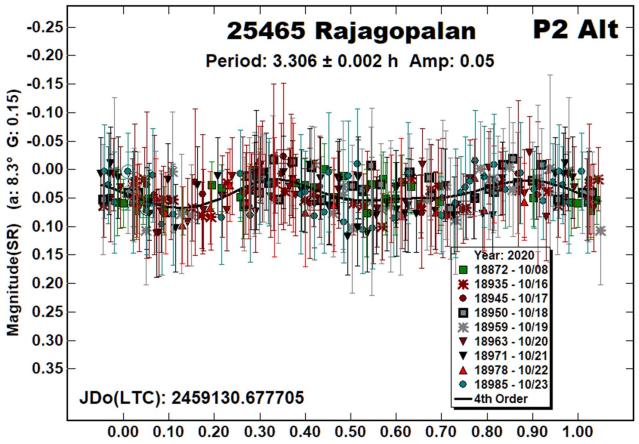

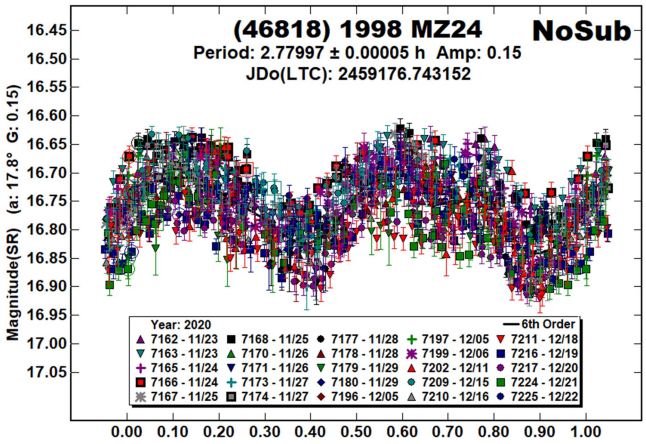

(46818) 1998 MZ24. Warner (2010) observed this 4-km Mars-crosser in 2009 August and fond a period of 2.779 h. There were no indications of a satellite at that time. Stephens (2017) observed it in 2016, finding a rotation period of 2.78 h and, again, no signs of a satellite. Our observations in 2020 were close to being diametrically opposed in ecliptic longitude from the 2016 observations, 90° versus 293°. On the other hand, the ecliptic latitude of the phase angle bisector differed by about 20°. This, along with a longer observing campaign, may be why signs of a satellite were found in 2020.

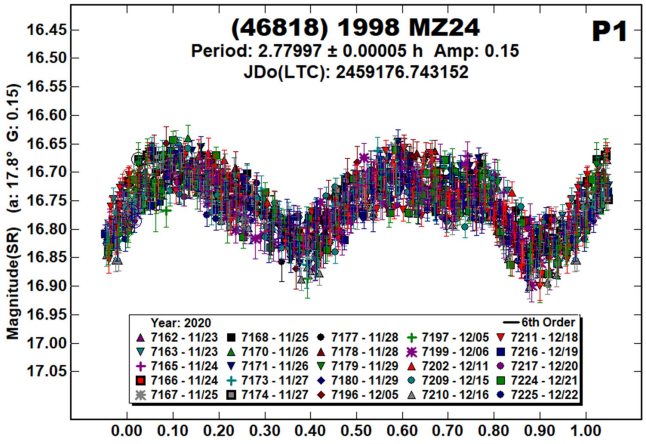

Number	Name	2020 mm/dd	Phase	L_{PAB}	B_{PAB}	Period(h)	P.E.	Amp	A.E.	Grp/Dr
3865	Lindbloom	11/08-11/20	1.9,7.4	42	-1	[FS]26.016	0.002	0.64	0.02	V
										0.65-1.0
4503	Cleobulus	10/19-11/05	*1.8,9.5	29	-1	2.8164	0.0003	0.11	0.03	NEA
						66.1	0.1	0.19	0.03	
22056	2000 AU31	11/03-11/13	3.6,6.0	27	-1	57.2	0.1	1.09	0.06	TR-J
						8.488	0.004	0.24	0.04	
25465	Rajagopalan	10/08-10/22	8.3,15.0	4	-6	63.2	0.1	0.11	0.02	FLOR
						[A1]4.961	0.003	0.06	0.02	
						[A2]3.306	0.002	0.05	0.02	
46818	1998 MZ24	11/23-12/22	*17.8,3.3	90	-3	2.77997	0.00005	0.15	0.01	MC
						53.20	0.02	0.13	0.02	
482505	2012 TQ78	11/23-12/02	*28.2,38.0	105	13	11.418	0.005	0.25	0.03	NEA
						12.35	0.03	0.09	0.03	
	2013 PY6	09/20-10/13	14.0,2.7	15	1	3.9210	0.0004	0.05	0.01	NEA
						19.130	0.004	0.11	0.02	
	2020 PD1	10/08-10/18	*7.1,9.7	20	-5	2.8367	0.0004	0.15	0.02	NEA
						37.8	0.1	0.13	0.02	

Table II. Observing circumstances. [FS]Period is orbital and rotation for each body. [A1,2]Preferred and alternate period of an ambiguous solution. The first line gives the primary period for the system. The second line gives the secondary period. The phase angle (α) is given at the start and end of each date range. An asterisk indicates that the phase angle reached a maximum or minimum during the period. L_{PAB} and B_{PAB} are, respectively the average phase angle bisector longitude and latitude (see Harris et al.,1984). For the Grp/Dr column, the first line gives the group/family based on Warner et al. (2009). FLOR Flora; MC Mars-crosser; NEA: Near-Earth asteroid; TR-J Jupiter trojan; V

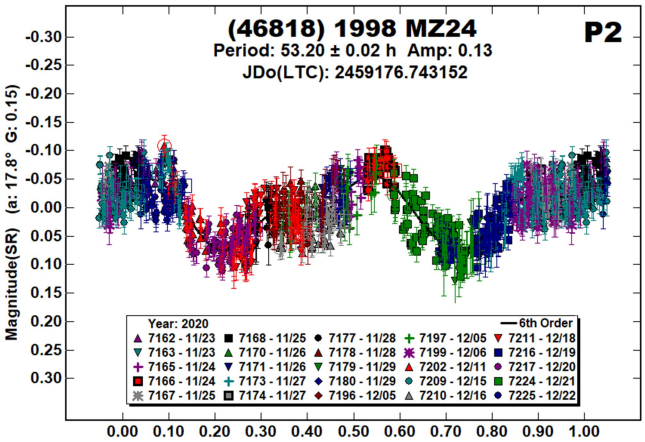

The single-period lightcurve (P1) scatter is considerably in excess of the individual errors of the observations, which prompted a dual period search using *MPO Canopus*. After several iterations, we found P_1 = 2.77997 h and P_2 = 53.2 h.

A "simple" lightcurve showing mutual events is mostly flat save the events themselves. In this case, the continually changing amplitude implies an elongated secondary that is likely tidally-locked to the orbital period, i.e., its rotation and orbital periods are the same.

For southern observers, the next opportunity for confirmation comes in 2023 June with V = 16.3 and –20° declination. Northern observers need to wait until 2027 November when the asteroid reaches V = 15.6 at +37° declination.

(482505) 2012 TQ78. There were no previously reported rotation periods in the LCDB for 2012 TQ78, which has an estimated diameter of 370 m. The signs of a secondary period in the NoSub plot are weak but were sufficient to try searching for a better fit than one to a single-period solution. We eventually adopted P_2 = 12.35 h with a significant amplitude of 0.09 mag. This is somewhat surprising since subtracting the second period produces very little change in the fit of the P_1 lightcurve and its period.

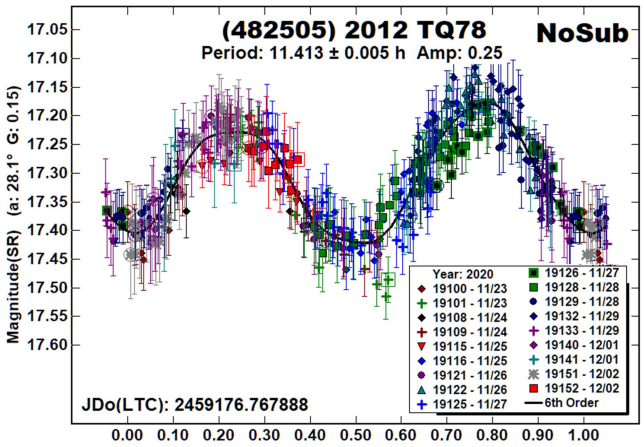

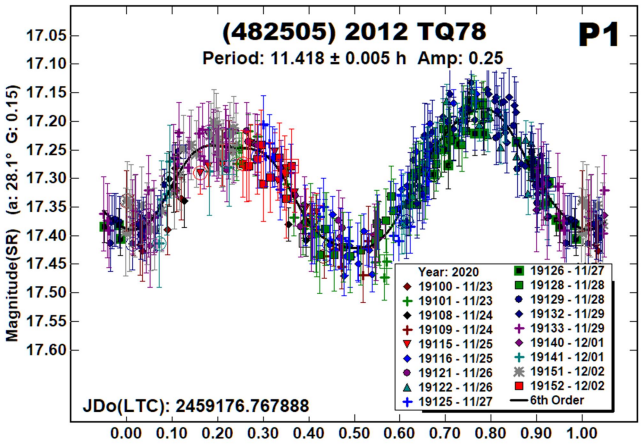

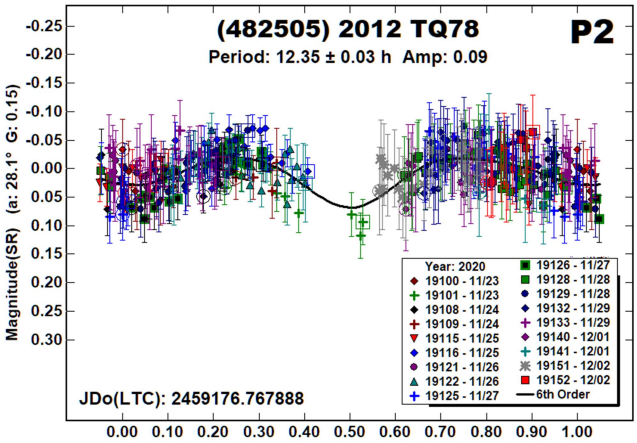

It's possible that P_2 is some sort of systematic artifact of the data set and the 24-hour sampling intervals. Assuming it's not, the two periods don't fit the usual models for a binary asteroid. In that case, the possibility falls to the two being the periods of rotation and precession of a tumbling asteroid, or their frequencies ($1/P$) being integral multiples of the true periods. The rule of thumb for damping time given in Pravec et al. (2014) is about 2.5 Ga, so tumbling is not unexpected.

2013 PY6. There were no previous entries of any kind the LCDB for this 400-m NEA. The initial data showed indications of a second period, became more certain as additional data were obtained. Our final analysis found P_1 = 3.9210 h, A_1 = 0.05 mag for the primary of the assumed binary asteroid. The lightcurve for the secondary period, P_2 = 19.130 h, shows signs of mutual events at about 0.15 and 0.65 rotation phase. Using the shallower event, we derived an effective diameter ratio of Ds/Dp ≥ 0.19 ± 0.02.

The data set covered a sufficient range of phase angles to find preliminary values of H_{SR} = 19.12 ± 0.03 and G = 0.04 ± 0.04. Based on Warner et al. (2009), the value for G implies a low albedo object, which is not entirely uncommon with the NEA population.

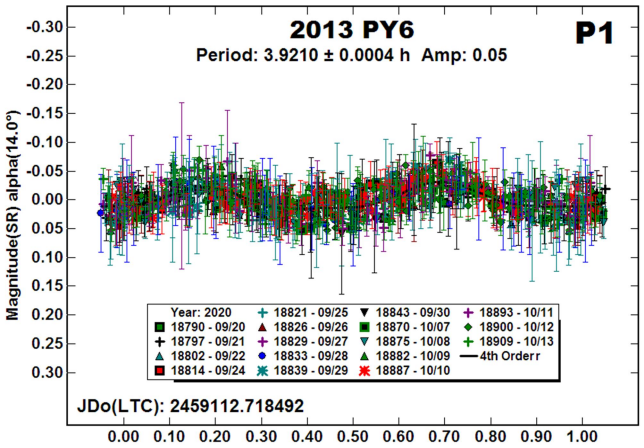

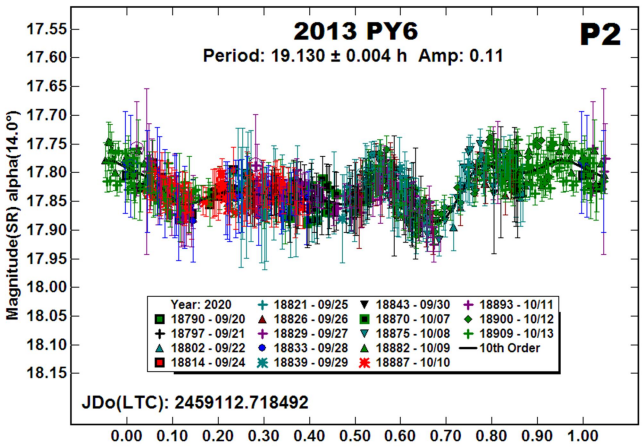

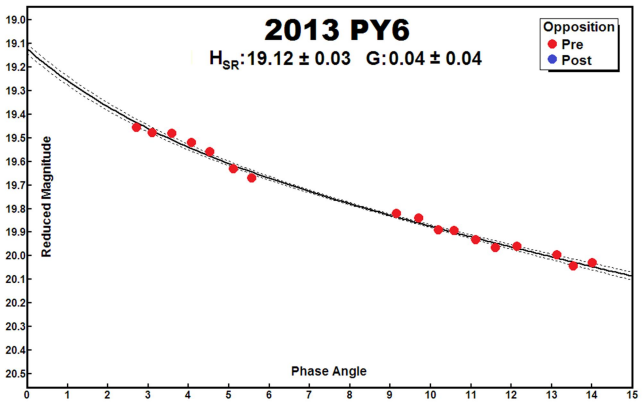

To transform from H_{SR} to H requires using known values of

$$(SG\text{-}SR)_{Sun} = 0.44 \text{ (Rodgers et al., 2006)}$$

$$V = SR + 0.44(SG\text{-}SR) \text{ (Fukugita et al., 1996)}$$

and assuming that $(SG\text{-}SR)_{Asteroid} = (SG\text{-}SR)_{Sun}$ because its presumed low albedo is consistent with type D asteroid (Warner et al., 2009) and a type D asteroid is similar in color to the Sun (Dandy et al., 2003). Substituting values

$$V = 19.12 + 0.44(0.44) = 19.31$$

The MPCOrb file (MPC, 2021) gives H = 19.3. We caution that deriving a result from several "ifs" (assumptions) makes the result less than fully-reliable. Furthermore, it should be not be used as the foundation for another series of assumptions.

2020 PD1. The single-period solution for this 400-m NEA showed the typical signs of a secondary period. Using the dual-period search feature of *MPO Canopus*, we found P_1 = 2.8367 h and P_2 = 37.8 h.

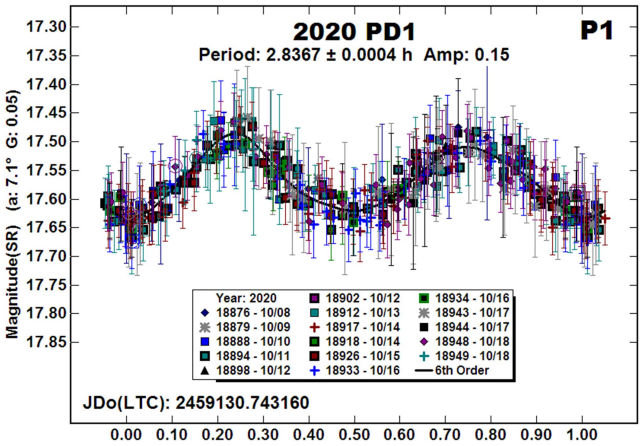

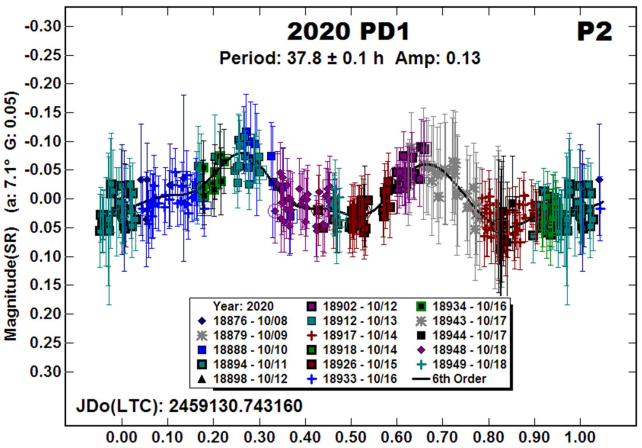

The P_2 lightcurve doesn't show signs of mutual events but it is consistent with a slightly-elongated satellite that is tidally locked to its orbit. Confirmation will be a long-time coming. The brightest the asteroid gets through 2050 is V ~ 20.3 in 2029 Nov. Otherwise, it ranges from about 21.5 to 25.0.

Acknowledgements

Funding for observations at CS3 and work on the asteroid lightcurve database (Warner et al., 2009) and ALCDEF database (*alcdef.org*) are supported by NASA grant 80NSSC18K0851.

The authors gratefully acknowledge Shoemaker NEO Grants from the Planetary Society (2007, 2013). These were used to purchase some of the telescopes and CCD cameras used in this research.

This work includes data from the Asteroid Terrestrial-impact Last Alert System (ATLAS) project. ATLAS is primarily funded to search for near earth asteroids through NASA grants NN12AR55G, 80NSSC18K0284, and 80NSSC18K1575; byproducts of the NEO search include images and catalogs from the survey area. The ATLAS science products have been made possible through the contributions of the University of Hawaii Institute for Astronomy, the Queen's University Belfast, the Space Telescope Science Institute, and the South African Astronomical Observatory.

References

References from web sites should be considered transitory, unless from an agency with a long lifetime expectancy. Sites run by private individuals, even if on an institutional web site, do not necessarily fall into this category.

Dandy, C.L.; Fitzsimmon, A.; Collander-Brown, S.J. (2003). "Optical colors of 56 near-Earth objects: trends with size and orbit." *Icarus* **163**, 363-373.

Fukugita, M.; Ichikawa, T.; Gunn, J.E.; Doi, M.; Shimasaku, K.; Schneider, D.P. (1996). "The Sloan Digital Sky Survey Photometric System." *Aston. J.* **111**, 1748.

Harris, A.W.; Young, J.W.; Scaltriti, F.; Zappala, V. (1984). "Lightcurves and phase relations of the asteroids 82 Alkmene and 444 Gyptis." *Icarus* **57**, 251-258.

Mainzer, A.K.; Bauer, J.M.; Cutri, R.M.; Grav, T.; Kramer, E.A.; Masiero, J.R.; Nugent, C.R.; Sonnett, S.M.; Stevenson, R.A.; Wright, E.L. (2016). "NEOWISE Diameters and Albedos V1.0." NASA Planetary Data System.
EAR-A-COMPIL-5-NEOWISEDIAM-V1.0.

MPC (2021). Minor Planet Center web site, MPCORB page. *https://minorplanetcenter.net/iau/MPCORB.html*

Pravec, P.; Wolf, M.; Sarounova, L. (2018web). *http://www.asu.cas.cz/~ppravec/neo.htm*

Pravec, P.; Scheirich, P.; Durech, J.; Pollock, J.; Kusnirak, P.; Hornoch, K.; Galad, A.; Vokrouhlicky, D.; Harris, A.W.; Jehin, E.; Manfroid, J.; Opitom, C.; Gillon, M.; Colas, F.; Oey, J.; Vrastil, J.; Reichart, D.; Ivarsen, K.; Haislip, J.; LaCluyze, A. (2014). "The tumbling state of (99942) Apophis." *Icarus* **233**, 48-60.

Rodgers, C.T.; Canterna, R.; Smith, J.A.; Pierce, M.J.; Tucker, D.L. (2006). "Improved u′g′r′i′z′ to UBV$R_C I_C$ Transformation Equations for Main-Sequence Stars." *Astron. J.* 132, 989-993.

Ryan, E.L.; Sharkey, B.N.L.; Woodward, C.E. (2017). "Trojan Asteroids in the Kepler Campaign 6 Field." *Astron. J*. **153**, A116.

Stephens, R.D. (2017). "Asteroids Observed from CS3: 2016 July - September." *Minor Planet Bull*. **44**, 49-52.

Szabó, Gy.M.; Pál, A.; Kiss, Cs.; Kiss, L.L.; Molnár, L.; Hanyecz, O.; Plachy, E.; Sárneczky, K.; Szabó, R. (2017). "The heart of the swarm: K2 photometry and rotational characteristics of 56 Jovian Trojan asteroids." *Astron. Astrophys.* **599**, A44.

Tonry, J.L.; Denneau, L.; Flewelling, H.; Heinze, A.N.; Onken, C.A.; Smartt, S.J.; Stalder, B.; Weiland, H.J.; Wolf, C. (2018). "The ATLAS All-Sky Stellar Reference Catalog." *Ap. J.* **867**, A105.

Warner, B.D. (2010). "Asteroid Lightcurve Analysis at the Palmer Divide Observatory: 2009 June - September." *Minor Planet Bull*. **37**, 24-27.

Warner, B.D.; Harris, A.W.; Pravec, P. (2009). "The Asteroid Lightcurve Database." *Icarus* **202**, 134-146. Updated 2020 Aug. *http://www.minorplanet.info/lightcurvedatabase.html*

Wisniewski, W.Z.; Michalowski, T.M.; Harris, A.W.; McMillan, R.S. (1997). "Photometric Observations of 125 Asteroids." *Icarus* **126**, 395-449.

LIGHTCURVE PHOTOMETRY OPPORTUNITIES: 2021 APRIL-JUNE

Brian D. Warner
Center for Solar System Studies / MoreData!
446 Sycamore Ave.
Eaton, CO 80615 USA
brian@MinorPlanetObserver.com

Alan W. Harris
MoreData!
La Cañada, CA 91011-3364 USA

Josef Ďurech
Astronomical Institute
Charles University
18000 Prague, CZECH REPUBLIC
durech@sirrah.troja.mff.cuni.cz

Lance A.M. Benner
Jet Propulsion Laboratory
Pasadena, CA 91109-8099 USA
lance.benner@jpl.nasa.gov

We present lists of asteroid photometry opportunities for objects reaching a favorable apparition and have no or poorly-defined lightcurve parameters. Additional data on these objects will help with shape and spin axis modeling using lightcurve inversion. We also include lists of objects that will or might be radar targets. Lightcurves for these objects can help constrain pole solutions and/or remove rotation period ambiguities that might come from using radar data alone.

We present several lists of asteroids that are prime targets for photometry during the period 2021 April-June.

In the first three sets of tables, "Dec" is the declination and "U" is the quality code of the lightcurve. See the latest asteroid lightcurve data base (LCDB from here on; Warner et al., 2009) documentation for an explanation of the U code:

http://www.minorplanet.info/lightcurvedatabase.html

The ephemeris generator on the CALL web site allows creating custom lists for objects reaching V ≤ 18.0 during any month in the current year and up to five years in the future, e.g., limiting the results by magnitude and declination, family, and more.

http://www.minorplanet.info/PHP/call_OppLCDBQuery.php

We refer you to past articles, e.g., Warner et al. (2021) for more detailed discussions about the individual lists and points of advice regarding observations for objects in each list.

Once you've obtained and analyzed your data, it's important to publish your results. Papers appearing in the *Minor Planet Bulletin* are indexed in the Astrophysical Data System (ADS) and so can be referenced by others in subsequent papers. It's also important to make the data available at least on a personal website or upon request. We urge you to consider submitting your raw data to the ALCDEF database. This can be accessed for uploading and downloading data at

http://www.alcdef.org

The database contains almost 3.8 million observations for 15,000+ objects, making it one of the more useful sources for raw asteroid *time-series* lightcurve data.

Lightcurve/Photometry Opportunities

Objects with U = 3– or 3 are excluded from this list since they will likely appear in the list for shape and spin axis modeling. Those asteroids rated U = 1 should be given higher priority over those rated U = 2 or 2+, but not necessarily over those with no period. On the other hand, d*o not overlook asteroids with* U = 2/2+ *on the assumption that the period is sufficiently established.* Regardless, do not let the existing period influence your analysis since even highly-rated result have been proven wrong at times. Note that the lightcurve amplitude in the tables could be more or less than what's given. Use the listing only as a guide.

An entry in bold italics is a near-Earth asteroid (NEA).

		Brightest				LCDB Data		
Number	Name	Date	Mag	Dec		Period	Amp	U
1669	Dagmar	04 04.9	14.4	-6	>	12	0.15	1
1027	Aesculapia	04 07.0	14.5	-6		13.529	0.09-0.19	2
1340	Yvette	04 08.0	14.7	-7		3.525	0.16	2
2841	Puijo	04 09.4	15.2	+1		3.545	0.03	1+
27225	1999 GB17	04 11.5	15.2	-9		3.853	0.57	2
1796	Riga	04 12.7	14.4	+0		22.226	0.06-0.40	2
163243	***2002 FB3***	***04 12.7***	***14.8***	***+9***		***6.231***	***0.19***	***2***
6785	1990 VA7	04 13.9	15.4	+2		6.417	0.16	2
4362	Carlisle	04 15.2	14.8	-8				
2738	Viracocha	04 19.0	15.4	-13				
15427	Shabas	04 24.7	15.2	-12				
3181	Ahnert	04 24.9	14.6	-14				
4899	Candace	04 30.8	15.2	+7		40.7	0.15	2
6764	Kirillavrov	05 03.1	15.0	-21		4.74	0.07-0.19	2+
5776	1989 UT2	05 03.6	15.5	-16	S	4.341		2
14007	1993 TH14	05 04.9	15.5	-10				
9870	Maehata	05 05.1	15.5	-18				
7309	Shinkawakami	05 09.3	15.1	-19				
11682	Shiwaku	05 09.9	15.5	-15	S	4.019		2
3815	Konig	05 11.7	15.2	-10		6.239	0.14	2
6914	Becquerel	05 14.8	14.6	-22				
5529	Perry	05 16.5	15.5	-26				
14191	1998 XR28	05 19.1	15.5	-23				
13832	1999 XR13	05 20.0	15.1	-9				
3353	Jarvis	05 20.8	14.6	-26		202	0.10-0.50	2+
3648	Raffinetti	05 21.1	15.4	-13				
2779	Mary	05 29.9	15.3	-20		3.36	0.10	2
12375	1994 NO1	06 02.2	15.3	-24	S	39.504		2
11277	Ballard	06 03.4	14.6	-24	>	10	0.25	2-
2359	Debehogne	06 08.3	15.3	-17				
2038	Bistro	06 09.5	14.3	-26		95.667	0.06-0.12	2
8817	Roytraver	06 11.8	15.2	-21		68.79	0.53-0.55	2
12194	1979 KO1	06 15.2	15.0	-24				
34886	2001 VH12	06 17.9	15.3	-49				
4894	Ask	06 18.1	14.4	-23		3.636	0.17-0.23	2+
1834	Palach	06 19.9	14.9	-23		3.139	0.13-0.16	2
450263	***2003 WD158***	***06 20.0***	***14.0***	***-9***				
7851	Azumino	06 21.1	14.8	-29				
3774	Megumi	06 22.6	15.2	-29				
12225	Yanfernandez	06 22.7	15.3	-14				
31498	1999 CX61	06 22.9	15.0	-25				
5042	Colpa	06 23.8	15.3	-25		169.64	0.93	2+
4562	Poleungkuk	06 24.0	15.1	-22		9.477	0.73-0.77	2
3044	Saltykov	06 24.3	15.2	-12		35.357	0.34	2
21313	Xiuyanyu	06 24.7	15.4	-26		4.432		2-
4798	Mercator	06 25.8	14.9	-23				
14665	1999 CC5	06 30.2	15.1	-17		3.009	0.14	2

Low Phase Angle Opportunities

The Low Phase Angle list includes asteroids that reach very low phase angles ($\alpha < 1°$). The "α" column is the minimum solar phase angle for the asteroid. Getting accurate, calibrated measurements (usually V band) at or very near the day of opposition can provide important information for those studying the "opposition effect." Use the on-line query form for the LCDB to get more details about a specific asteroid.

http://www.minorplanet.info/PHP/call_OppLCDBQuery.php

You will have the best chance of success working objects with low amplitude and periods that allow covering at least half a cycle every night. Objects with large amplitudes and/or long periods are much more difficult for phase angle studies since, for proper analysis, the data must be reduced to the average magnitude of the asteroid for each night. This reduction requires that you determine the period and the amplitude of the lightcurve; for long period objects that can be difficult. Refer to Harris et al. (1989) for the details of the analysis procedure.

As an aside, some use the maximum light to find the phase slope parameter (*G*). Even though the results better resemble the behavior of a spherical object of the same albedo, it can produce significantly different values for both *H* and *G* versus when using average light, which is the method used for values listed by the Minor Planet Center.

The International Astronomical Union (IAU) has adopted a new system, H-G_{12}, introduced by Muinonen et al. (2010). It will be some years before H-G_{12} becomes widely used, but not until a discontinuity flaw in the G_{12} function has be resolved. This discontinuity results in false "clusters" or "holes" in the solution density and makes it impossible to draw accurate conclusions.

We strongly encourage obtaining data as close to 0° as possible, then every 1-2° out to 7°, below which the curve tends to be non-linear due to the opposition effect. From 7° out to about 30°, observations at 3-6° intervals should be sufficient. Coverage beyond about 50° is not generally helpful since the H-G system is best defined with data from 0-30°.

It's important to emphasize that all observations should (must) be made using high-quality catalogs to set the comparison star magnitudes. These include ATLAS, Pan-STARRS, SkyMapper, and GAIA2. Catalogs such as CMC-15, APASS, or the MPOSC from *MPO Canopus* should not be used due to significant systematic errors.

Also important is that that there are sufficient data from each observing run such that their location can be found on a combined, phased lightcurve derived from two or more nights obtained *near the same phase angle.* This is so that the lightcurve amplitude isn't significantly different. If necessary, the magnitudes for the given run should be adjusted so that they correspond to mid-light of the combined lightcurve. This goes back to the H-G system being based on average, not maximum or minimum light.

For this table, the asteroid magnitudes are brighter than in others. This is because higher precision is required for this work and the asteroid may be a full magnitude or more fainter when it reaches phase angles out to 20-30°.

Num	Name	Date	α	V	Dec	Period	Amp	U
656	Beagle	04 14.3	0.16	13.8	-09	7.035	0.57-1.20	3
755	Quintilla	04 17.3	0.95	13.3	-08	4.552	0.08-0.45	3
90	Antiope	04 18.7	0.66	12.5	-09	16.509	0.05-0.88	3
127	Johanna	04 23.8	0.22	12.0	-13	12.7988	0.18-0.21	3
509	Iolanda	04 29.4	0.21	12.9	-14	12.306	0.35-0.45	3
210	Isabella	05 04.0	0.49	13.6	-17	6.672	0.09-0.38	3
731	Sorga	05 05.4	0.18	13.8	-16	8.184	0.19-0.72	3
770	Bali	05 07.2	0.15	13.9	-17	5.8190	0.21-0.65	3
397	Vienna	05 11.0	0.27	13.4	-17	15.48	0.16-0.20	3
118	Peitho	05 15.6	0.56	12.5	-20	7.8055	0.11-0.33	3
230	Athamantis	05 22.1	0.15	10.2	-20	24.0055	0.10-0.26	3
95	Arethusa	05 23.1	0.11	12.7	-21	8.705	0.24-0.35	3
128	Nemesis	05 26.8	0.61	11.6	-19	77.81	0.08-0.10	3-
122	Gerda	05 28.1	0.69	12.1	-19	10.685	0.10-0.26	3
378	Holmia	05 29.2	0.93	13.9	-19	4.450	0.10-0.21	3
248	Lameia	05 29.4	0.20	12.7	-22	11.912	0.10-0.17	3
562	Salome	05 29.6	0.27	13.9	-21	6.351	0.17-0.37	3-
425	Cornelia	05 30.1	0.30	13.4	-23	17.505	0.19-0.21	3
503	Evelyn	06 01.6	0.16	13.3	-22	38.780	0.30-0.5	3-
267	Tirza	06 01.7	0.23	13.1	-22	7.648	0.18-0.4	3
184	Dejopeja	06 04.7	0.54	12.6	-24	6.4416	0.22-0.3	3
1303	Luthera	06 05.4	0.46	13.7	-24	5.878	0.05-0.06	3
420	Bertholda	06 08.6	0.72	13.2	-20	11.04	0.24-0.29	3
277	Elvira	06 13.8	0.33	13.7	-22	29.69	0.34-0.59	3
758	Mancunia	06 14.1	0.86	13.4	-20	12.7253	0.15-0.27	3
30	Urania	06 14.7	0.97	10.6	-26	13.686	0.11-0.45	3
895	Helio	06 19.8	0.72	13.5	-21	9.347	0.10-0.23	3
1248	Jugurtha	06 21.2	0.98	13.5	-26	12.910	0.70-1.40	3

Shape/Spin Modeling Opportunities

Those doing work for modeling should contact Josef Ďurech at the email address above. If looking to add lightcurves for objects with existing models, visit the Database of Asteroid Models from Inversion Techniques (DAMIT) web site

https://astro.troja.mff.cuni.cz/projects/damit/

Additional lightcurves could lead to the asteroid being added to or improving one in DAMIT, thus increasing the total number of asteroids with spin axis and shape models.

Included in the list below are objects that:

1. Are rated U = 3– or 3 in the LCDB.
2. Do not have reported pole in the LCDB Summary table.
3. Have at least three entries in the Details table of the LCDB where the lightcurve is rated U ≥ 2.

The caveat for condition #3 is that no check was made to see if the lightcurves are from the same apparition or if the phase angle bisector longitudes differ significantly from the upcoming apparition. The last check is often not possible because the LCDB does not list the approximate date of observations for all details records. Including that information is an on-going project.

Favorable apparitions are in bold text. NEAs are in italics.

		Brightest			LCDB Data		
Num	Name	Date	Mag	Dec	Period	Amp	U
459	Signe	04 01.8	14.5	-1	5.536	0.25-0.54	3
536	Merapi	04 03.8	13.8	+13	8.791	0.23-0.38	3
1591	Baize	04 05.6	14.7	+37	7.794	0.19-0.37	3-
198	Ampella	04 06.1	12.8	-18	10.379	0.11-0.22	3
2150	**Nyctimene**	**04 08.1**	**14.9**	**-10**	**6.131**	**0.56-0.90**	**3**
598	Octavia	04 08.6	14.8	+8	10.89	0.28-0.40	3
81	Terpsichore	04 10.1	13.3	-11	10.943	0.06-0.15	3
318	Magdalena	04 11.3	14.1	+1	42.65	0.06-0.11	3
363	Padua	04 12.7	13.1	-3	8.401	0.08- 0.3	3
973	Aralia	04 12.9	15.0	-21	7.366	0.20-0.25	3
1563	**Noel**	**04 13.0**	**14.4**	**-3**	**3.55**	**0.14-0.18**	**3**
123	Brunhild	04 13.9	12.9	-18	9.873	0.14-0.21	3
656	Beagle	04 14.2	13.7	-9	7.035	0.57-1.20	3
563	Suleika	04 14.3	12.9	+2	5.69	0.13-0.28	3
339	Dorothea	04 14.5	14.0	-2	5.974	0.06-0.10	3
766	Moguntia	04 15.9	14.4	-14	4.816	0.06-0.23	3
3031	**Houston**	**04 17.8**	**14.8**	**-18**	**11.218**	**0.11-0.17**	**3**
541	Deborah	04 18.0	13.9	-18	29.368	0.07-0.10	3
1266	Tone	04 18.0	14.3	-32	15.605	0.06-0.19	3
643	Scheherezade	04 18.4	14.6	-24	14.161	0.23-0.37	3
1153	Wallenbergia	04 20.0	14.6	-17	4.096	0.23-0.33	3
412	Elisabetha	04 21.4	13.0	+8	19.635	0.08-0.20	3
860	Ursina	04 22.3	14.3	-30	9.386	0.15-0.50	3
1509	Esclangona	04 25.0	14.8	-51	3.253	0.11-0.35	3
346	Hermentaria	04 25.8	11.7	-3	28.523	0.07-0.20	3
3385	**Bronnina**	**04 26.4**	**14.7**	**-10**	**2.959**	**0.12-0.35**	**3**
1609	Brenda	04 28.0	14.8	+14	19.776	0.16-0.27	3
481	Emita	05 01.0	13.2	-9	14.412	0.13-0.30	3
5189	***1990 UQ***	***05 01.0***	***14.5***	***+32***	***6.653***	***0.62-1.02***	***3***
987	Wallia	05 04.6	14.3	-27	10.081	0.11-0.36	3
1806	Derice	05 05.0	14.8	-21	3.224	0.07-0.19	3

		Brightest			LCDB Data		
Num	Name	Date	Mag	Dec	Period	Amp	U
3760	Poutanen	05 06.8	15.0	+1	2.956	0.13-0.21	3
307	Nike	05 09.1	14.8	-11	11.857	0.15-0.23	3
1086	Nata	05 10.0	14.3	-29	18.061	0.17-0.18	3-
397	Vienna	05 11.1	13.4	-17	15.48	0.15-0.20	3
1385	Gelria	05 12.0	15.0	-9	4.624	0.08-0.23	3
680	**Genoveva**	**05 14.0**	**12.5**	**-26**	**11.089**	**0.21-0.25**	**3**
1254	Erfordia	05 14.7	14.9	-27	12.287	0.33-0.47	3
1292	Luce	05 17.4	14.4	-21	6.954	0.17-0.26	3
815	Coppelia	05 18.1	14.3	-20	4.421	0.13-0.24	3
917	Lyka	05 18.6	14.7	-27	7.867	0.10-0.26	3
195	Eurykleia	05 18.9	13.2	-28	16.521	0.10-0.24	3
1132	Hollandia	05 19.7	13.6	-26	5.322	0.15-0.35	3
799	Gudula	05 22.7	13.7	-12	14.814	0.27-0.30	3
1308	Halleria	05 23.3	14.9	-28	6.028	0.14-0.17	3
5081	**Sanguin**	**05 27.5**	**14.8**	**-13**	**10.26**	**0.40-0.53**	**3**
909	Ulla	05 27.9	14.4	+4	8.716	0.08-0.24	3
1184	Gaea	05 30.5	14.7	-39	2.871	0.09-0.15	3-
1052	Belgica	05 31.3	15.0	-18	2.71	0.06-0.08	3
929	**Algunde**	**05 31.9**	**13.3**	**-19**	**3.31**	**0.11-0.17**	**3**
503	Evelyn	06 01.6	13.4	-22	38.78	0.30- 0.5	3-
267	**Tirza**	**06 01.7**	**13.2**	**-22**	**7.648**	**0.18- 0.4**	**3**
972	Cohnia	06 02.5	14.3	-28	18.472	0.16-0.21	3
2411	**Zellner**	**06 03.4**	**14.5**	**-20**	**2.975**	**0.31-0.34**	**3**
101	Helena	06 04.0	11.5	-39	23.08	0.09-0.13	3
1303	**Luthera**	**06 05.3**	**13.7**	**-24**	**8.328**	**0.05-0.11**	**3**
5978	**Kaminokuni**	**06 05.6**	**14.8**	**-26**	**7.063**	**0.43-0.50**	**3**
420	Bertholda	06 08.6	13.2	-20	11.04	0.22-0.29	3
456	**Abnoba**	**06 09.5**	**12.1**	**-10**	**18.281**	**0.23-0.32**	**3**
300	Geraldina	06 10.8	14.2	-24	6.842	0.04-0.32	3
1028	Lydina	06 11.0	14.6	-27	11.68	0.22- 0.7	3
1602	Indiana	06 11.7	14.8	-24	2.601	0.12-0.19	3
569	Misa	06 13.1	14.3	-24	11.595	0.09-0.25	3
479	Caprera	06 13.4	14.3	-13	9.454	0.05-0.25	3
1684	**Iguassu**	**06 14.3**	**14.4**	**-21**	**6.416**	**0.15-1.11**	**3**
839	Valborg	06 15.5	13.9	-44	10.366	0.14-0.19	3
619	Triberga	06 16.6	13.5	-1	29.311	0.25-0.45	3
2151	Hadwiger	06 17.1	14.9	-45	5.872	0.07-0.38	3
1967	Menzel	06 17.7	15.0	-27	2.835	0.16-0.39	3
1246	Chaka	06 17.9	13.7	-36	25.462	0.18-0.25	3
1200	Imperatrix	06 18.6	14.6	-17	17.769	0.21-0.25	3
895	Helio	06 19.8	13.5	-21	9.347	0.10-0.23	3
3416	Dorrit	06 19.8	15.0	-73	2.574	0.21-0.27	3
12008	**Kandrup**	**06 19.8**	**13.6**	**+6**	**32.903**	**0.61-0.85**	**3**
1376	Michelle	06 21.6	14.0	-16	5.975	0.03-0.20	3
1867	**Deiphobus**	**06 23.0**	**15.0**	**-31**	**58.66**	**0.10-0.27**	**3-**
2017	Wesson	06 23.3	14.4	-13	3.416	0.38-0.60	3
3996	**Fugaku**	**06 25.6**	**14.8**	**-24**	**7.193**	**0.57-0.86**	**3**
1224	Fantasia	06 28.7	14.4	-19	4.995	0.06-0.47	3
1603	Neva	06 30.2	14.8	-16	6.426	0.16-0.25	3-

Radar-Optical Opportunities

The loss of the Arecibo Observatory in late 2020 leaves a large gap in the study of NEAs and other solar system objects as well as atmospheric research. Since Arecibo is no longer available, we have modified our approach to this listing.

For one, the list of potential radar targets is much smaller since the Goldstone facility, while able to cover more of the sky, achieves a much lower SNR for an asteroid than would Arecibo. This means, broadly speaking, that potential targets must come closer to Earth to achieve useable SNRs.

As before, we will present a list of targets that are within reach of radar, but considering only Goldstone. This allows continued coordination between the optical and radar communities. We will also provide of list that might be called "What Might Have Been", i.e., those objects that would have been considered if Arecibo were still in service. Detailed discussions and ephemerides will not be provided for these objects, unless there is a particular reason to do so.

We hope that this second listing will encourage observations despite being out of Goldstone radar range *for this apparition*. The data can still be important for future Earth encounters that do come within reach of the facilities in operation at that time.

Past radar targets:
http://echo.jpl.nasa.gov/~lance/radar.nea.periods.html

Goldstone targets:
http://echo.jpl.nasa.gov/asteroids/goldstone_asteroid_schedule.html

These lists are based on *known* targets at the time they were prepared. It is very common for newly discovered objects to move into, out of, or up the list and become radar targets on short notice. We recommend that you keep up with the latest discoveries the Minor Planet Center observing tools.

In particular, monitor NEAs and be flexible with your observing program. In some cases, you may have only 1-3 days when the asteroid is within reach of your equipment. Be sure to keep in touch with the radar team (through Benner's email or their Facebook or Twitter accounts) if you get data. The team may not always be observing the target but your initial results may change their plans. In all cases, your efforts are greatly appreciated.

Use the ephemerides below as a guide to your better chances for observing, but remember that photometry may be possible before and/or after the dates in the ephemerides. Note that *geocentric* positions are given. Use these web sites to generate updated and *topocentric* positions:

MPC: *http://www.minorplanetcenter.net/iau/MPEph/MPEph.html*
JPL: *http://ssd.jpl.nasa.gov/?horizons*

In the ephemerides below, "ED" and "SD" are, respectively, the Earth and Sun distances (AU), "V" is the estimated Johnson V magnitude, and "α" is the phase angle. "SE" and "ME" are the great circle distances (in degrees) of the Sun and Moon from the asteroid. "MP" is the lunar phase and "GB" is the galactic latitude. "PHA" indicates that the object is a *potentially hazardous asteroid*, meaning that at some (long distant) time, its orbit might take it very close to Earth.

About YORP Acceleration

Many, if not all, of the targets in this section are near-Earth asteroids. These objects are particularly sensitive to YORP acceleration. YORP (Yarkovsky–O'Keefe–Radzievskii–Paddack) is the asymmetric thermal re-radiation of sunlight that can cause an asteroid's rotation period to increase or decrease. High precision lightcurves at multiple apparitions can be used to model the asteroid's *sidereal* rotation period and see if it's changing.

It usually takes four apparitions to have sufficient data to determine if the asteroid rotation rate is changing under the influence of YORP. This is why observing an asteroid that already has a well-known period remains a valuable use of telescope time. It is even more so when considering the BYORP (binary-YORP) effect among binary asteroids that has stabilized the spin so that acceleration of the primary body is not the same as if it would be if there were no satellite.

To help focus efforts in YORP detection, Table I gives a quick summary of this quarter's radar-optical targets. The family or group for the asteroid is given under the number/name line. Also, underneath the first list will be additional flags such as "PHA" for Potentially Hazardous Asteroid, "NPAR" for a tumbler, and/or "BIN" to indicate the asteroid is a binary (or multiple) system. "BIN?" means that the asteroid is a suspected but not confirmed binary. The period is in hours and, in the case of binary, for the primary. The "Amp" column gives the known range of lightcurve amplitudes. The "App" column gives the number of different

apparitions at which a lightcurve period was reported while the "Last" column gives the year for the last reported period. The "R SNR" column indicates the estimated radar SNR using the tool at

http://www.naic.edu/~eriverav/scripts/index.php

The SNRs were calculated using the current MPCORB absolute magnitude (H), a period of 4 hours (2 hours if $D \leq 200$ m) if it's not known, and the approximate minimum Earth distance during the current quarter. These are estimates only and assume that the radars are fully functional.

If the row is in bold text, the object was found on the radar planning pages listed above. Otherwise, the planning tool at

http://www.minorplanet.info/PHP/call_OppLCDBQuery.php

was used to find known NEAs that were V < 18.0 during the quarter.

Asteroid	Period	Amp	App	Last	R SNR
1997 GL3 NEA PHA	**7.572**	**0.28**	**1**	**1997**	**35**
2004 TP1 NEA PHA	**–**	**–**	**–**	**–**	**15**
(5189) 1990 UQ NEA	**6.676**	**0.62 1.02**	**3**	**2020**	**100**
(494690) 2004 JQ1 NEA	–	–	–	–	13
(450263) 2003 WD158 NEA PHA	**–**	**–**	**–**	**–**	**100**
(441987) 2010 NY65 NEA PHA	**4.9706**	**0.16 0.32**	**5**	**2020**	**30**

Table I. Summary of Goldstone-optical opportunities for the current quarter. Period and amplitude data are from the asteroid lightcurve database (LCDB; Warner et al., 2009). SNR values are *estimates* and are given for relative comparisons among the objects in the list.

Asteroid	Period	Amp	App	Last	R SNR
(142464) 2002 TC9 NEA Apr 01 16.0 +2°	2.320	0.13	1	2017	10
(66400) 2008 JO NEA Apr 21 17.3 30°	–	–	–	–	3
(467351) 2003 KO2 NEA May 01 17.9 +16°	6.48	1.28	1	2016	7
(495615) 2015 PQ291 NEA May 11 15.3 -30°	13.763	0.66	1	2020	5
(408752) 1991 TB2 NEA May 21 15.7 -53°	–	–	–	–	7
(374267) 2005 LW NEA Jun 01 17.2 +15°	–	–	–	–	13
(387505) 1998 KN3 NEA Jun 01 17.1 -20°	–	–	–	–	2
(154330) 2002 VX94 NEA Jun 01 16.2 -72°	8.932	0.65	1	2011	25

Table II. This list includes only those objects that would have been within reach of Arecibo but not Goldstone (assuming SNR > 10 for the latter). The columns are the same as for Table I. In the "R SNR" column, the estimated SNR is for Arecibo.

In Table II, the third line in the first column gives the approximate date when the asteroid is brightest along with the V magnitude and declination at the time.

It's rarely the case, especially for shape/spin axis modeling, that there are too many observations. Remember that the best set for modeling includes data not just from multiple apparitions but from as wide a range of phase angles during each apparition as well.

Unless otherwise said, the estimated diameters given below are based on an albedo of $p_V = 0.20$, the approximate average of the S taxonomic class that dominates the NEA region (Warner et al., 2009).

1997 GL3 (H = 19.1, PHA)

Pravec et al. (1998) reported a period of 7.572 h for this 300-m NEA. The asteroid is favorably placed for the second half of April. The presumed diameter makes it unlikely that the period is < 2 h.

DATE	RA	Dec	ED	SD	V	α	SE	ME	MP	GB
04/10	07 12.5	+25 18	0.07	1.00	16.5	89.7	86	110	-0.04	+16
04/12	08 52.4	+23 09	0.08	1.03	16.1	68.7	107	108	+0.00	+36
04/14	10 00.5	+19 16	0.10	1.06	16.1	54.2	121	101	+0.03	+50
04/16	10 43.0	+15 53	0.12	1.08	16.4	45.2	130	88	+0.13	+58
04/18	11 10.5	+13 20	0.15	1.11	16.7	39.6	135	71	+0.28	+63
04/20	11 29.3	+11 26	0.17	1.14	17.1	36.1	138	52	+0.47	+65
04/22	11 42.9	+09 59	0.20	1.17	17.4	33.8	140	29	+0.68	+66
04/24	11 53.2	+08 51	0.23	1.19	17.7	32.3	141	5	+0.86	+67
04/26	12 01.4	+07 55	0.26	1.22	18.0	31.3	141	23	+0.98	+67
04/28	12 08.0	+07 08	0.29	1.25	18.2	30.7	141	51	-0.99	+68

2004 TP1 (H = 20.7, PHA)

At 220 meters, the period for this NEA is also likely to be $P > 2$ h. The earlier days of the ephemeris are better, mostly because the moon is near new and well away from the asteroid's sky position.

DATE	RA	Dec	ED	SD	V	α	SE	ME	MP	GB
04/07	08 05.5	+59 55	0.06	1.00	17.2	84.9	92	137	-0.24	+32
04/10	09 56.7	+45 39	0.06	1.02	16.6	66.3	111	133	-0.04	+51
04/13	10 52.1	+29 50	0.06	1.04	16.5	50.6	127	119	+0.01	+64
04/16	11 22.2	+17 32	0.08	1.06	16.7	40.2	137	96	+0.13	+67
04/19	11 40.8	+08 54	0.09	1.08	16.9	34.2	143	68	+0.38	+65
04/22	11 53.6	+02 51	0.11	1.10	17.3	31.1	146	35	+0.68	+62
04/25	12 03.1	-01 29	0.13	1.12	17.6	29.7	147	7	+0.93	+59
04/28	12 10.6	-04 43	0.15	1.14	18.0	29.2	147	46	-0.99	+57

(5189) 1990 UQ (H = 17.8)

Warner (2018) reported a period of 6.676 h based on observations in 2017. Follow-up work in 2019 found a period of 6.640 h (Warner and Stephens, 2019). Oey (2020) followed the asteroid in 2017 over a range of phase angles of 60° and greater. Over that time, the amplitude of the lightcurve ranges from 0.75 to 0.92 mag.

This time around, the phase starts at 23° and increases to nearly 90° over the period covered by the ephemeris. This makes it a good project for seeing how the amplitude changes with phase angle. There's also the potential of providing extremely useful data for modeling. The inversion process wants data not only from different viewing aspects but over a good range of phase angles within a given apparition.

DATE	RA	Dec	ED	SD	V	α	SE	ME	MP	GB
04/10	14 59.8	+01 42	0.23	1.21	16.1	22.9	152	134	-0.04	+50
04/13	15 06.5	+03 31	0.20	1.19	15.8	23.5	152	160	+0.01	+50
04/16	15 14.5	+05 46	0.18	1.16	15.5	24.8	151	147	+0.13	+50
04/19	15 24.5	+08 37	0.16	1.14	15.3	27.1	149	117	+0.38	+49
04/22	15 37.6	+12 15	0.13	1.12	15.0	30.7	145	84	+0.68	+48
04/25	15 55.4	+17 02	0.11	1.10	14.7	36.0	140	54	+0.93	+46
04/28	16 21.3	+23 23	0.10	1.07	14.5	43.8	132	43	-0.99	+43
05/01	17 01.6	+31 39	0.08	1.05	14.5	55.0	121	60	-0.79	+36
05/04	18 07.3	+41 06	0.07	1.03	14.6	70.0	106	76	-0.48	+25
05/07	19 48.0	+48 17	0.07	1.01	15.1	87.8	88	76	-0.20	+11

(494690) 2004 JQ1 (H = 20.0)

The LCDB had no rotation period entries for this 300-m NEA, which will be a difficult target because of the large phase angles, relatively small solar elongations, and low galactic latitudes. Given the diameter, the period should be more than 2 hours, but it's wise to expect the unexpected.

DATE	RA	Dec	ED	SD	V	α	SE	ME	MP	GB
05/24	20 09.6	+25 25	0.15	1.06	18.4	67.7	104	98	+0.91	-4
05/25	20 21.5	+25 27	0.14	1.05	18.3	69.8	103	90	+0.97	-6
05/26	20 35.5	+25 25	0.13	1.04	18.2	72.3	101	83	+1.00	-9
05/27	20 51.9	+25 15	0.12	1.04	18.0	75.3	98	76	-1.00	-12
05/28	21 11.3	+24 55	0.11	1.03	18.0	78.8	95	69	-0.96	-16
05/29	21 34.4	+24 18	0.10	1.02	17.9	82.9	92	63	-0.91	-20
05/30	22 01.6	+23 18	0.09	1.01	17.9	87.8	87	56	-0.83	-25
05/31	22 33.2	+21 43	0.08	1.01	17.9	93.7	82	49	-0.73	-31
06/01	23 09.0	+19 27	0.08	1.00	18.1	100.3	75	41	-0.63	-37
06/02	23 47.8	+16 24	0.07	0.99	18.3	107.5	68	33	-0.53	-44

(450263) 2003 WD158 (H = 18.8, PHA)

This NEA has an estimated diameter of about 500 m. There were no previously reported rotation periods in the LCDB. Observations will likely be hampered by the low galactic latitudes, i.e., potentially rich star fields.

DATE	RA	Dec	ED	SD	V	α	SE	ME	MP	GB
06/10	20 40.7	+60 10	0.07	1.01	16.1	89.5	87	85	+0.00	+11
06/15	19 43.5	+27 09	0.05	1.04	14.6	56.9	121	127	+0.19	+2
06/20	19 12.3	-09 16	0.06	1.07	14.0	22.1	157	85	+0.71	-9
06/25	18 53.0	-29 31	0.09	1.11	14.4	9.7	169	6	-1.00	-13
06/30	18 40.1	-39 23	0.13	1.14	15.4	14.4	164	68	-0.68	-15
07/05	18 31.2	-44 34	0.16	1.17	16.2	19.3	158	127	-0.22	-15
07/10	18 25.4	-47 29	0.20	1.20	16.8	22.8	153	156	+0.00	-16
07/15	18 22.0	-49 08	0.25	1.23	17.4	25.3	149	103	+0.25	-16
07/20	18 20.7	-50 01	0.29	1.27	17.9	27.4	145	41	+0.78	-16

(441987) 2010 NY65 (H = 21.5, PHA)

Finding a definitive period for the 160-m 2010 NY65 has proved to be somewhat difficult. Warner (2016) found a period of 4.979 h based on data from 2016 July. A similar period was found about a year later (Warner, 2017). Behrend (2019web), however, found what appeared to be a more convincing solution of 5.195 h. Warner and Stephens (2020) observed the asteroid again in 2019 and 2020. All their previous data sets along with the new data appeared to fit near the original period of 4.979 h and an entirely new solution of about 5.8 h.

The core of the problem is that the periods are nearly commensurate with an Earth day and so *rotational aliasing* comes into play. This is when the number actual rotations over the range of the data set cannot be uniquely defined. To find an unambiguous will likely require a coordinated campaign involving observers from a wide range of longitudes.

DATE	RA	Dec	ED	SD	V	α	SE	ME	MP	GB
06/27	12 47.1	+23 40	0.04	1.01	17.8	91.6	86	123	-0.93	+86
06/28	13 26.9	+22 19	0.05	1.02	17.6	83.5	94	126	-0.86	+81
06/29	14 00.1	+20 42	0.05	1.03	17.6	76.6	101	130	-0.78	+73
06/30	14 27.3	+19 02	0.05	1.03	17.6	70.9	106	134	-0.68	+67
07/01	14 49.4	+17 28	0.06	1.04	17.7	66.2	111	138	-0.59	+61
07/02	15 07.4	+16 04	0.07	1.05	17.8	62.5	114	142	-0.49	+57
07/03	15 22.2	+14 48	0.07	1.05	17.9	59.4	117	146	-0.39	+53
07/04	15 34.6	+13 42	0.08	1.06	18.0	56.9	119	149	-0.30	+50

References

Behrend, R. (2019web). Observatoire de Geneve web site. *http://obswww.unige.ch/~behrend/page_cou.html*

Harris, A.W.; Young, J.W.; Contreiras, L.; Dockweiler, T.; Belkora, L.; Salo, H.; Harris, W.D.; Bowell, E.; Poutanen, M.; Binzel, R.P.; Tholen, D.J.; Wang, S. (1989). "Phase relations of high albedo asteroids: The unusual opposition brightening of 44 Nysa and 64 Angelina." *Icarus* **81**, 365-374.

Muinonen, K.; Belskaya, I.N.; Cellino, A.; Delbò, M.; Levasseur-Regourd, A.-C.; Penttilä, A.; Tedesco, E.F. (2010). "A three-parameter magnitude phase function for asteroids." *Icarus* **209**, 542-555.

Oey, J. (2020). "Lightcurve Analysis of Near-Earth Asteroids in 2017 from BMO and JBL." *Minor Planet Bull.* **47**, 136-140.

Pravec, P.; Wolf, M.; Sarounova, L. (1998). "Lightcurves of 26 Near-Earth Asteroids." *Icarus* **136**, 124-153.

Warner, B.D.; Harris, A.W.; Pravec, P. (2009). "The asteroid lightcurve database." *Icarus* **202**, 134-146.

Warner, B.D. (2016). "Near-Earth Asteroid Lightcurve Analysis at CS3-Palmer Divide Station: 2016 April-July." *Minor Planet Bull*. **43**, 311-319.

Warner, B.D. (2017). "Near-Earth Asteroid Lightcurve at CS3-Palmer Divide Station: 2017 April thru June." *Minor Planet Bull.* **44**, 335-344.

Warner, B.D. (2018). "Near-Earth Asteroid Lightcurve Analysis at CS3-Palmer Divide Station: 2017 October - December." *Minor Planet Bull*. **45**, 138-147.

Warner, B.D.; Stephens, R.D. (2019). "Near-Earth Asteroid Lightcurve Analysis at the Center for Solar System Studies: 2019 January - April." *Minor Planet Bull*. **46**, 304-314.

Warner, B.D.; Stephens, R.D. (2020). "Near-Earth Asteroid Lightcurve Analysis at the Center for Solar System Studies: 2020 April - June." *Minor Planet Bull*. **47**, 290-304.

Warner, B.D.; Harris, A.W.; Durech, J.; Benner, L.A.M. (2021). "Lightcurve Photometry Opportunities: 2021 January-March." *Minor Planet Bull.* **48**, 89-97.

IN THIS ISSUE

This list gives those asteroids in this issue for which physical observations (excluding astrometric only) were made. This includes lightcurves, color index, and H-G determinations, etc. In some cases, no specific results are reported due to a lack of or poor-quality data. The page number is for the first page of the paper mentioning the asteroid. EP is the "go to page" value in the electronic version.

Number	Name	EP	Page
10	Hygiea	68	166
67	Asia	34	132
74	Galatea	34	132
102	Miriam	22	120
284	Amalia	46	144
356	Liguria	34	132
424	Gratia	42	140
570	Kythera	34	132
579	Sidonia	42	140
581	Tauntonia	34	132
589	Croatia	27	125
589	Croatia	34	132
589	Croatia	42	140
605	Juvisia	34	132
635	Vundtia	22	120
665	Sabine	1	99
693	Zerbinetta	42	140
699	Hela	38	136
722	Frieda	27	125
748	Simeisa	66	164
754	Malabar	46	144
791	Ani	42	140
805	Hormuthia	27	125
824	Anastasia	42	140
858	El Djezair	42	140
866	Fatme	27	125
897	Lysistrata	60	158
911	Agamemnon	46	144
982	Franklina	60	158
1024	Hale	42	140
1032	Pafuri	60	158
1063	Aquilegia	52	150
1114	Lorraine	27	125
1156	Kira	46	144
1165	Imprinetta	19	117
1241	Dysona	27	125
1269	Rollandia	4	102
1271	Isergina	42	140
1314	Paula	46	144
1342	Brabantia	22	120
1526	Mikkeli	11	109
1541	Estonia	60	158
1570	Brunonia	52	150
1583	Antilochus	69	167
1590	Tsiolkovskaja	46	144
1615	Bardwell	60	158
1663	van den Bos	42	140
1721	Wells	27	125
1754	Cunningham	66	164
1840	Hus	14	112
2191	Uppsala	60	158
2212	Hephaistos	72	170
2254	Requiem	52	150
2262	Mitidika	17	115
2262	Mitidika	60	158
2263	Shaanxi	60	158
2322	Kitt Peak	60	158
2346	Lilio	22	120
2346	Lilio	46	144
2346	Lilio	52	150
2368	Beltrovata	72	170
2403	Sumava	60	158
2424	Tautenburg	19	117
2456	Palamedes	69	167
2510	Shandong	52	150
2689	Bruxelles	27	125
2819	Ensor	60	158
2912	Lapalma	52	150
2920	Automedon	69	167
3000	Michelangelo	19	117
3001	Michelangelo	27	125
3048	Guangzhou	19	117
3063	Makhaon	69	167
3133	Sendai	19	117
3578	Carestia	60	158
3600	Archimedes	27	125
3709	Polypoites	69	167
3781	Dufek	52	150
3793	Leonteus	69	167
3865	Lindbloom	89	187
3955	Bruckner	17	115
4092	Tyr	38	136
4103	Chahine	60	158
4493	Naitomitsu	25	123
4503	Cleobulus	89	187
4625	Shchedrin	49	147
4717	Kaneko	27	125
4729	Mikhailmil'	60	158
4995	Griffin	27	125
5111	Jacliff	19	117
5445	Williwaw	12	110
5802	Casteldelpiano	27	125
6701	Warhol	19	117
7753	1988 XB	72	170
8078	Carolejordan	27	125
8190	Bouguer	60	158
8256	Shenzhou	46	144
8823	1987 WS3	12	110
8823	1987 WS3	49	147
9144	Hollisjohnson	60	158
10115	1992 SK	72	170
10221	Kubrick	27	125
11894	1991 GW	9	107
15010	1998 QL92	49	147
16559	1991 VA3	17	115
16834	1997 WU22	72	170
17312	7662 P-L	19	117
18418	Ujibe	19	117
18640	1998 EF9	10	108
19120	Doronina	9	107
19755	2000 EH34	49	147
20498	1999 RT1	52	150
21082	Araimasaru	49	147
21088	Chelyabinsk	72	170
21182	1994 EC2	17	115
21182	1994 EC2	52	150
21182	1994 EC2	60	158
21242	1995 WZ41	19	117
21242	1995 WZ41	25	123
21787	1999 SG4	27	125
22056	2000 AU31	89	187
22393	1994 QV	17	115
24038	1999 SL8	19	117
25465	Rajagopalan	89	187
26568	2000 ET49	12	110
26858	Misterogers	27	125
32772	1986 JL	52	150
41331	1999 XB232	10	108
43028	1999 VE23	17	115
46818	1998 MZ24	89	187
49125	1998 SB22	27	125
50713	2000 EZ135	10	108
66272	1999 JW6	72	170
68130	2001 AO17	25	123
68359	2001 OZ13	72	170
69230	Hermes	72	170
69274	1989 UZ1	52	150
137311	1999 TX9	19	117
144411	2004 EW9	72	170
153201	2000 WO107	22	120
153201	2000 WO107	72	170
154302	2002 UQ3	72	170
159402	1999 AP10	72	170
163902	2003 SW222	72	170
183230	2002 TC58	25	123
275714	2000 YH4	72	170
306517	1999 WY	52	150
465749	2009 WO6	72	170
474179	1999 VS6	72	170
482505	2012 TQ78	89	187
	2000 TU28	72	170
	2002 GZ8	72	170
	2003 YJ	72	170
	2013 PY6	89	187
	2013 UX14	72	170
	2018 KF1	82	180
	2020 GF2	82	180
	2020 OH3	82	180
	2020 PD1	89	187
	2020 RA6	82	180
	2020 RZ6	82	180
	2020 ST1	72	170
	2020 TD8	82	180
	2020 TP1	82	180
	2020 UA	2	100
	2020 UQ6	7	105
	2020 UQ6	82	180
	2020 VZ6	82	180
	2020 WU5	6	104
	2020 XX3	82	180

THE MINOR PLANET BULLETIN (ISSN 1052-8091) is the quarterly journal of the Minor Planets Section of the Association of Lunar and Planetary Observers (ALPO, http://www.alpo-astronomy.org). Current and most recent issues of the *MPB* are available on line, free of charge from:

http://www.minorplanet.info/MPB

The Minor Planets Section is directed by its Coordinator, Prof. Frederick Pilcher, 4438 Organ Mesa Loop, Las Cruces, NM 88011 USA (fpilcher35@gmail.com). Dr. Alan W. Harris (MoreData! Inc.; harrisaw@colorado.edu), and Dr. Petr Pravec (Ondrejov Observatory; ppravec@asu.cas.cz) serve as Scientific Advisors. The Asteroid Photometry Coordinator is Brian D. Warner (Center for Solar System Studies), Palmer Divide Observatory, 446 Sycamore Ave., Eaton, CO 80615 USA (brian@MinorPlanetObserver.com).

The Minor Planet Bulletin is edited by Professor Richard P. Binzel, MIT 54-410, 77 Massachusetts Ave, Cambridge, MA 02139 USA (rpb@mit.edu). Brian D. Warner (address above) is Associate Editor, and Dr. David Polishook, Department of Earth and Planetary Sciences, Weizmann Institute of Science (david.polishook@weizmann.ac.il) is Assistant Editor. The *MPB* is produced by Dr. Pedro A. Valdés Sada (psada2@ix.netcom.com). The MPB is distributed by Dr. Melissa Hayes-Gehrke. Direct all subscriptions, contributions, address changes, etc. to:

Dr. Melissa Hayes-Gehrke
UMD Astronomy Department
1113 PSC Bldg 415
College Park, MD 20742 USA
(mhayesge@umd.edu)

Effective with Volume 38, the *Minor Planet Bulletin* is a limited print journal, where print subscriptions are available only to libraries and major institutions for long-term archival purposes. In addition to the free electronic download of the *MPB* noted above, electronic retrieval of all *Minor Planet Bulletin* articles (back to Volume 1, Issue Number 1) is available through the Astrophysical Data System:

http://www.adsabs.harvard.edu/

Authors should submit their manuscripts by electronic mail (rpb@mit.edu). Author instructions and a Microsoft Word template document are available at the web page given above. All materials must arrive by the deadline for each issue. Visual photometry observations, positional observations, any type of observation not covered above, and general information requests should be sent to the Coordinator.

* * * * *

The deadline for the next issue (48-3) is April 15, 2021. The deadline for issue 48-4 is July 15, 2021.